

R/V Mirai Cruise Report

MR13-03

Observational study on the Intraseasonal Variation
over the tropical western Pacific



Tropical Western Pacific
May 31, 2013 – July 6, 2013



Japan Agency for
Marine-Earth Science and Technology
(JAMSTEC)

MR13-03 Cruise Report

--- Contents ---

1. Introduction
2. Cruise summary
3. Cruise track and log
4. List of participants
5. Summary of observations
 - 5.1 GPS radiosonde
 - 5.2 Doppler radar
 - 5.3 Micro rain radar
 - 5.4 Disdrometers
 - 5.5 Lidar observations of clouds and aerosols
 - 5.6 Ceilometer
 - 5.7 Ship-borne sky radiometer
 - 5.8 Surface meteorological observations
 - 5.9 Continuous monitoring of surface seawater
 - 5.10 CTDO profiling
 - 5.11 Salinity of sampled water
 - 5.12 Dissolved oxygen of sampled water
 - 5.13 Thermistor chain to profile temperature in the surface layer
 - 5.14 LADCP
 - 5.15 Shipboard ADCP
 - 5.16 Underway CTD
 - 5.17 XCTD
 - 5.18 Argo-type float
 - 5.19 Distribution and ecology of oceanic *Halobates* and their response to environmental factors
 - 5.20 Underway geophysics

Appendices

- A: Atmospheric profiles by the radiosonde observations
- B: Oceanic profiles by the CTDO observations

1. Introduction

The intraseasonal variation (ISV) in the Tropics is a key issue to be solved, as it influences not only the tropical atmospheric and oceanic variations but also the global climate. While the Madden-Julian Oscillation, one of the well-known ISVs, propagates eastward along the equator, the accompanying northward-moving signals becomes apparent in the boreal summer. This northeastward-propagating mode is so-called boreal summer intraseasonal variation (BSISV). Previous studies pointed that the BSISV strongly modulates the rainfall in Asian summer monsoon season, kicks the onset of Asian summer monsoon, or links to the seasonal march of the Asian summer monsoon such as northward shift of Baiu front. Since the ISVs are phenomena coupled with deep cumulus convections, it is manifested over the warm pool region from the Indian Ocean through the western Pacific Ocean.

Recent studies using reanalysis, satellite data or ground-based operational data revealed various aspects of the large-scale feature of the BSISV, especially over the Indian Ocean. On the other hand, only the limited studies were focusing on the process in the western Pacific, though the mechanism may be different between Indian Ocean and western Pacific. In addition, current general circulation models still fail to simulate the BSISV on its northward-propagating speed, amplitude, etc. It is believed that this deficiency is mainly due to the insufficient cumulus parameterization. Therefore, fine-scale observational data is invaluable to promote our knowledge on the mechanism of the BSISV, especially over the western Pacific.

In 2008, we JAMSTEC conducted the fiend campaign named PALAU2008 during R/V Mirai MR08-02 cruise. The project captured a event of BSISV, and revealed that the large-scale convergence and accompanying shallow convections play important roles to moisten the lower and middle troposphere to promote deep convection in BSISV. For the further analyses, on the other hand, it is desired in the upcoming projects to capture more cases of BSISV, or more detailed process including detailed air-sea interaction process.

To achieve further detailed understanding of BSISV over the western Pacific, we in JAMSTEC organized the project PALAU2013, by joining R/V Mirai MR13-03 cruise, land-based radar observation in Palau Islands, and sounding network over Phillipine, Palau, Micronesia and Guam.

The R/V Mirai MR13-03 cruise consists of two legs. The Leg-2 is principle part of the cruise to stay (12N, 135E) to obtain continuous, fine temporal-resolution data for both atmospheric and oceanic states. The principle component of the observations are the surface meteorological measurement, atmospheric sounding by radiosonde, CTD casting to profile the oceanic thermodynamic status, ADCP current measurement, as well as Doppler radar observation to capture the details of precipitating systems. In addition, profiling floats are deployed in Leg-1 to monitor the finer temporal variation of the oceanic profiles for wider area surrounding the station.

This cruise report summarizes the observed items and preliminary results during this cruise. In the first several sections, basic information such as cruise track, on board personnel list are described. Details of each observation are described in Section 5. Additional information and figures are also attached as Appendices.

*** Remarks ***

This cruise report is a preliminary documentation as of the end of the cruise. The contents may be not updated after the end of the cruise, while the contents may be subject to change without notice. Data on the cruise report may be raw or not processed. Please ask the Chief Scientists for the latest information.

2. Cruise Summary

2.1 Ship

Name	Research Vessel MIRAI
L x B x D	128.6m x 19.0m x 13.2m
Gross Tonnage	8,687 tons
Call Sign	JNSR
Home Port	Mutsu, Aomori Prefecture, Japan

2.2 Cruise Code

MR13-03

2.3 Project Name (Main mission)

Observational Study on the Intreseasonal Variability over the western Pacific

2.4 Undertaking Institute

Japan Agency for Marine-Earth Science and Technology (JAMSTEC)
2-15, Natsushima, Yokosuka, Kanagawa 237-0061, JAPAN

2.5 Chief Scientist

Masaki KATSUMATA
Tropical Climate Variability Research Program,
Research Institute for Global Change, JAMSTEC

2.6 Periods and Ports of Call

May 31: departed Sekinehama, Japan
Jun. 1-2: called Hachinohe, Japan
Jun. 10-12: called Koror, Palau
Jul. 6: arrived Yokohama, Japan

2.7 Research Themes of Sub-missions and Principal Investigators (PIs)

- (1) Research on the precipitating systems and air-sea interactions during the generation of the tropical depression
(PI: Taro SHINODA / Nagoya University)
- (2) Lidar observations of optical characteristics and vertical distribution of aerosols and clouds.
(PI: Nobuo SUGIMOTO / National Institute for Environmental Studies)
- (3) Maritime aerosol optical properties from measurements of ship-borne sky radiometer.
(PI: Kazuma AOKI / Toyama University)
- (4) Distribution and ecology of oceanic Halobates inhabiting tropical area of the western Pacific and their responding system to environmental factors.
(PI: Tetsuo HARADA / Kochi University)
- (5) Standardising the marine geophysics data and its application to the ocean floor geodynamics studies.
(PI: Takeshi MATSUMOTO / University of the Ryukyu)

2.8 Observation Summary

GPS Radiosonde	173 times	Jun. 6 to Jun. 9 / Jun. 12 to Jul. 2
C-band Doppler radar	continuously	Jun. 2 to Jun. 9 / Jun. 12 to Jul. 5
Micro rain radar	continuously	Jun. 2 to Jun. 9 / Jun. 12 to Jul. 5
Disdrometers	continuously	Jun. 2 to Jun. 9 / Jun. 12 to Jul. 5
Mie-scattering Lidar	continuously	Jun. 2 to Jun. 9 / Jun. 12 to Jul. 5
Ceilometer	continuously	Jun. 2 to Jun. 9 / Jun. 12 to Jul. 5
Sky Radiometer	continuously	Jun. 2 to Jun. 9 / Jun. 12 to Jul. 5
Surface Meteorology	continuously	Jun. 2 to Jun. 9 / Jun. 12 to Jul. 5
Sea surface water monitoring	continuously	Jun. 2 to Jun. 9 / Jun. 12 to Jul. 5
CTDO profiling	141 profiles	Jun. 7 to Jun. 9 / Jun. 13 to Jun.30
Sea water sampling	20 casts	Jun. 7 to Jun. 9 / Jun. 13 to Jun.30
Thermistor chain	continuously	Jun. 13 to Jun. 30
LADCP	141 profiles	Jun. 7 to Jun. 9 / Jun. 13 to Jun. 30
Shipboard ADCP	continuously	Jun. 2 to Jun. 9 / Jun. 12 to Jul. 5
Underway CTD	42 times	Jun. 4 to Jun. 8 / Jun. 24 to Jun. 30
Deploying Argo-type float	3 times	Jun. 7 to Jun. 9
Sea skater sampling	9 times	Jun. 13 to Jun. 29
Gravity/Magnetic force	continuously	Jun. 2 to Jun. 9 / Jun. 12 to Jul. 5
Topography	continuously	Jun. 2 to Jun. 9 / Jun. 12 to Jul. 5

2.9 Overview

In order to investigate the atmospheric and oceanic variations in the tropical western Pacific and their role in the intraseasonal variation, the intensive observations by using R/V Mirai were carried out. This cruise was a component of the international field campaign named PALAU2013.

The main part of the cruise was dedicated to perform stationary observation at (12N, 135E) to obtain high-resolution time series of the oceanic and atmospheric variations. R/V Mirai was at the station for 18 days from Jun. 13 to Jun. 30 (in Leg-2). Before arriving the station, she cruised almost meridionally from Japan to Palau (in Leg-1).

During the cruise, we witnessed the formation of the typhoon west of R/V Mirai; TS1303 “Yagi” in Leg-1, TS1304 “Leepi” in the beginning of Leg-2, and TS1306 “Rumbia” in the latter half of Leg-2. The precipitating system and their oceanic and atmospheric environments for these events were well captured in detail. The sudden northward-extension of the precipitating area was also captured in the very end of the stationary observation period. The oceanic data also shows interesting features; diurnal cycle, drop of saline in the surface layer (< 50 dbar) from Jun.23, very warm (> 30 deg.C) and low-saline (< 34 PSU) surface water, etc.

These observed results will be analyzed further, with combining the data from other islands and platforms, including profiling floats which were deployed in Leg-1. The further analyses will be performed to engrave the detail of the processes to spawn the active organized precipitating systems such as BSISV, tropical depression, etc.

2.10 Acknowledgments

We would like to express our sincere thanks to Captain Y. Tsutsumi and his crew for their skillful ship operation. Special thanks are extended to the technical staff of Global Ocean Development Inc. and Marine Works Japan, Ltd. for their continuous and skillful support to conduct the observations. Supports from collaborators in the project PALAU2013 are acknowledged.

3. Cruise Track and Log

3.1 Cruise Track

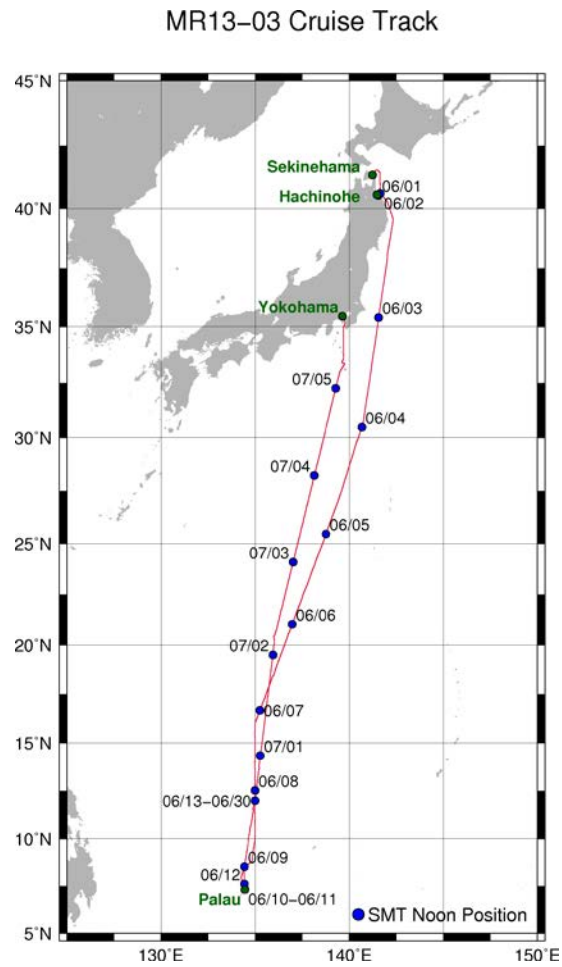


Fig. 3.1-1: Cruise track for Leg-1 and Leg-2. Black dots are for the position at local (SMT) noon.

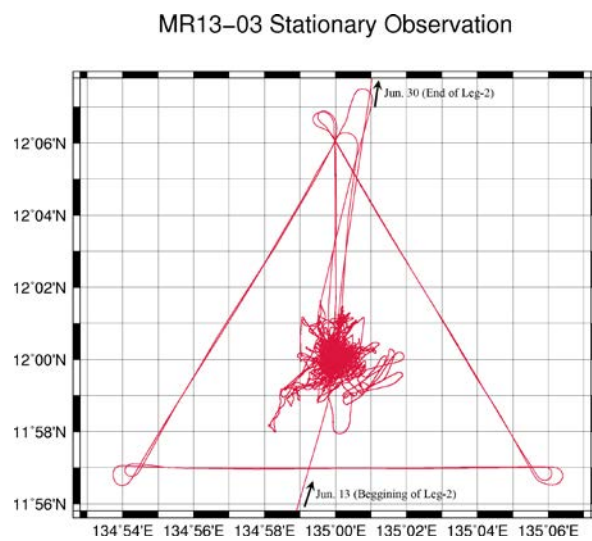


Fig. 3.1-2: Cruise track around the station (12N, 135E) for Leg-2.

3.2 Cruise Log

Date	UTC/SMT	Position and Events
May 31	0700/1600	Departure from Sekinehama
Jun 1	0000/0900	Arrival at Hachinohe
	0550/1450	Departure from Hachinohe
2	2120/0620	Arrival at Hachinohe
	0200/1100	Departure from Hachinohe
3	0530/1430	Start of surface seawater measurement
	1330/2230	Start of Doppler Radar observation
4	2359/0859	(31-01N, 140-48E) UCTD (p1c1; dummy, 200m)
	0106/1006	(30-49N, 140-46E) UCTD (u001c1; 200m)
5	0140/1040	(30-43N, 140-45E) UCTD (u002c1; 200m)
	0208/1108	(30-39N, 140-44E) UCTD (u002c2; 200m)
6	0237/1137	(30-34N, 140-42E) UCTD (u002c3; 200m)
	0002/0902	(25-59N, 138-59E) UCTD (u003c1; 200m)
7	0038/0938	(25-53N, 138-56E) UCTD (u003c2; 200m)
	0109/1009	(25-48N, 138-54E) UCTD (u003c3; 200m)
8	0140/1040	(25-43N, 138-52E) UCTD (u004c1; 500m)
	1003/1903	(24-01N, 138-10E) Sea skater collection (#001-1)
9	1031/1931	(23-59N, 138-10E) Sea skater collection (#001-2)
	1052/1952	(23-59N, 138-10E) Sea skater collection (#001-3)
10	2330/0830	(21-38N, 137-12E) Radiosonde (#001)
	0029/0929	(21-27N, 137-08E) UCTD (u005c1; 500m)
11	0114/1014	(21-20N, 137-05E) UCTD (u005c2; 500m)
	0158/1058	(21-12N, 137-02E) UCTD (u005c3; 500m)
12	0530/1430	(20-35N, 136-47E) Radiosonde (#002)
	1130/2030	(19-30N, 136-22E) Radiosonde (#003)
13	1730/0230	(18-26N, 135-57E) Radiosonde (#004)
	2335/0835	(17-20N, 135-32E) Radiosonde (#005)
14	0530/1430	(16-13N, 135-04E) Radiosonde (#006)
	0646/1546	(16-00N, 135-00E) CTD (N01M01; 500m), with sampling seawater
15	0725/1625	(16-00N, 135-00E) ARGO-type float (#1)
	1130/2030	(15-12N, 135-00E) Radiosonde (#007)
16	1159/2059	(15-06N, 135-00E) UCTD (p2c1; dummy, 200m)
	1222/2122	(15-02N, 135-00E) UCTD (u006c1; 200m)
17	1730/0230	(14-02N, 134-59E) Radiosonde (#008)
	2328/0828	(13-00N, 135-00E) Radiosonde (#009)
18	2331/0831	(13-00N, 135-00E) CTD (N02M01; 1000m), with sampling seawater
	0022/0922	(13-00N, 135-00E) ARGO-type float (#2)
19	0030/0930	(12-59N, 135-00E) UCTD (u007c1; 1000m)
	0530/1430	(12-08N, 135-00E) Radiosonde (#010)
20	1130/2030	(10-53N, 135-00E) Radiosonde (#011)
	1605/0105	(10-00N, 134-59E) CTD (N03M01; 500m), with sampling seawater
21	1639/0139	(09-59N, 134-59E) ARGO-type float (#3)
	1720/0220	(09-54N, 135-00E) Radiosonde (#012)
22	2331/0831	(08-52N, 134-51E) Radiosonde (#013)
	0530/1430	(08-11N, 134-20E) Radiosonde (#014)
23	0607/1507	(08-06N, 134-17E) Test of 3-dimensional magnetometer
	0844/1744	(07-46N, 134-18E) XCTD
24	1130/2030	(07-45N, 134-18E) Radiosonde (#015)
	1830/0230	(07-45N, 134-18E) Radiosonde (#016)
25	2130/0630	Stop of Doppler Radar observation
	2130/0630	Stop of surface seawater measurement
26	0110/1010	Arrival at Koror
27	0100/1000	Departure from Koror
	0430/1330	Start of surface seawater measurement
28	0550/1450	Start of Doppler Radar observation
	1130/2030	(09-24N, 134-34E) Radiosonde (#017)

	1430/2330	(09-56N, 134-37E)	Radiosonde (#018)
	1730/0230	(10-29N, 134-44E)	Radiosonde (#019)
	2030/0530	(11-00N, 134-50E)	Radiosonde (#020)
	2330/0830	(11-33N, 134-54E)	Radiosonde (#021)
13	0230/1130	(12-00N, 135-00E)	Radiosonde (#022)
	0530/1430	(12-00N, 135-00E)	Radiosonde (#023)
	0535/1435	(12-00N, 135-00E)	CTD (12M001; 500m)
	0735/1635	Deployment of Thermistor Chain and Sea Snake	
	0830/1730	(12-00N, 135-00E)	Radiosonde (#024)
	0838/1738	(12-00N, 135-00E)	CTD (12M002; 500m)
	1130/2030	(12-00N, 135-00E)	Radiosonde (#025)
	1137/2037	(12-00N, 135-00E)	CTD (12M003; 500m)
	1217/2117	(12-00N, 135-00E)	Sea skater collection (#002-1)
	1238/2138	(11-59N, 135-00E)	Sea skater collection (#002-2)
	1259/2159	(11-59N, 135-00E)	Sea skater collection (#002-3)
	1430/2330	(12-00N, 135-00E)	Radiosonde (#026)
	1436/2336	(12-00N, 135-00E)	CTD (12M004; 500m)
	1730/0230	(12-00N, 135-00E)	Radiosonde (#027)
	1736/0236	(12-00N, 135-00E)	CTD (12M005; 500m)
	2030/0530	(12-00N, 135-00E)	Radiosonde (#028)
	2038/0538	(12-00N, 135-00E)	CTD (12M006; 500m)
	2330/0830	(12-00N, 135-01E)	Radiosonde (#029)
	2336/0836	(12-00N, 135-01E)	CTD (12M007; 1000m), with sampling seawater
14	0105/1005	Recovery of Thermistor Chain and Sea Snake	
	0230/1130	(12-00N, 135-00E)	Radiosonde (#030)
	0234/1134	(12-00N, 135-00E)	CTD (12M008; 500m)
	0530/1430	(11-59N, 135-00E)	Radiosonde (#031)
	0535/1435	(11-59N, 135-00E)	CTD (12M009; 500m)
	0735/1635	Deployment of Thermistor Chain and Sea Snake	
	0830/1730	(11-59N, 134-59E)	Radiosonde (#032)
	0837/1737	(11-59N, 134-59E)	CTD (12M010; 500m)
	1117/2017	(11-59N, 134-59E)	Radiosonde (#033)
	1151/2051	(11-58N, 134-58E)	Radiosonde (#034)
	1157/2057	(11-58N, 134-58E)	CTD (12M011; 500m)
	1433/2333	(11-59N, 134-59E)	Radiosonde (#035)
	1440/2340	(11-59N, 134-59E)	CTD (12M012; 500m)
	1730/0230	(12-00N, 135-00E)	Radiosonde (#036)
	1738/0238	(12-00N, 135-00E)	CTD (12M013; 500m)
	2030/0530	(12-00N, 135-00E)	Radiosonde (#037)
	2037/0537	(12-00N, 135-00E)	CTD (12M014; 500m)
	2330/0830	(12-00N, 135-00E)	Radiosonde (#038)
	2335/0835	(12-00N, 135-00E)	CTD (12M015; 1000m), with sampling seawater
15	0230/1130	(12-00N, 135-00E)	Radiosonde (#039)
	0235/1135	(12-00N, 135-00E)	CTD (12M016; 500m)
	0530/1430	(12-00N, 135-00E)	Radiosonde (#040)
	0546/1446	(12-00N, 135-00E)	Radiosonde (#041)
	0551/1451	(12-00N, 135-00E)	CTD (12M017; 500m)
	0630/1530	Recovery of Thermistor Chain and Sea Snake	
	0708/1608	Deployment of Thermistor Chain and Sea Snake	
	0831/1731	(12-01N, 135-00E)	Radiosonde (#042)
	0837/1737	(12-01N, 135-00E)	CTD (12M018; 500m)
	1130/2030	(12-01N, 135-00E)	Radiosonde (#043)
	1135/2035	(12-01N, 135-00E)	CTD (12M019; 500m)
	1209/2109	(12-01N, 135-00E)	Sea skater collection (#003-1)
	1231/2131	(12-00N, 135-00E)	Sea skater collection (#003-2)
	1254/2154	(12-00N, 135-00E)	Sea skater collection (#003-3)
	1437/2337	(12-00N, 135-00E)	Radiosonde (#044)
	1446/2346	(12-00N, 135-00E)	CTD (12M020; 500m)
	1730/0230	(12-00N, 135-00E)	Radiosonde (#045)
	1736/0236	(12-00N, 135-00E)	CTD (12M021; 500m)
	2030/0530	(11-59N, 134-59E)	Radiosonde (#046)

	2035/0535	(11-59N, 134-59E)	CTD (12M022; 500m)
	2102/0602	(11-59N, 135-00E)	Radiosonde (#047)
	2330/0830	(12-00N, 135-00E)	Radiosonde (#048)
	2336/0836	(12-00N, 135-00E)	CTD (12M023; 1000m), with sampling seawater
16	0048/0948	Recovery of Sea Snake	
	0230/1130	(12-00N, 135-00E)	Radiosonde (#049)
	0236/1136	(12-00N, 135-00E)	CTD (12M024; 500m)
	0530/1430	(12-00N, 135-00E)	Radiosonde (#050)
	0547/1447	(12-00N, 135-00E)	Radiosonde (#051)
	0550/1450	(12-00N, 135-00E)	CTD (12M025; 500m)
	0829/1729	(12-00N, 135-00E)	Radiosonde (#052)
	0835/1735	(12-00N, 135-00E)	CTD (12M026; 500m)
	1130/2030	(12-00N, 134-59E)	Radiosonde (#053)
	1138/2038	(12-00N, 134-59E)	CTD (12M027; 500m)
	1430/2330	(12-00N, 135-01E)	Radiosonde (#054)
	1437/2337	(12-00N, 135-01E)	CTD (12M028; 500m)
	1731/0231	(12-00N, 135-01E)	Radiosonde (#055)
	1738/0238	(12-00N, 135-01E)	CTD (12M029; 500m)
	2030/0530	(12-00N, 135-00E)	Radiosonde (#056)
	2035/0535	(12-00N, 135-00E)	CTD (12M030; 500m)
	2330/0830	(12-00N, 135-00E)	Radiosonde (#057)
	2336/0836	(12-00N, 135-00E)	CTD (12M031; 1000m), with sampling seawater
17	0124/1024	Deployment of Sea Snake	
	0230/1130	(11-59N, 135-00E)	Radiosonde (#058)
	0236/1136	(11-59N, 135-00E)	CTD (12M032; 500m)
	0530/1430	(12-00N, 135-00E)	Radiosonde (#059)
	0535/1435	(12-00N, 135-00E)	CTD (12M033; 500m)
	0830/1730	(12-00N, 135-00E)	Radiosonde (#060)
	0837/1737	(12-00N, 135-00E)	CTD (12M034; 500m)
	1130/2030	(12-01N, 135-00E)	Radiosonde (#061)
	1136/2036	(12-01N, 135-00E)	CTD (12M035; 500m)
	1211/2111	(12-01N, 135-00E)	Sea skater collection (#004-1)
	1232/2132	(12-00N, 135-00E)	Sea skater collection (#004-2)
	1252/2152	(12-00N, 134-59E)	Sea skater collection (#004-3)
	1430/2330	(12-00N, 134-59E)	Radiosonde (#062)
	1440/2340	(12-00N, 134-59E)	CTD (12M036; 500m)
	1450/2350	(12-00N, 134-59E)	Radiosonde (#063)
	1730/0230	(12-00N, 135-00E)	Radiosonde (#064)
	1736/0236	(12-00N, 135-00E)	CTD (12M037; 500m)
	2030/0530	(12-00N, 135-00E)	Radiosonde (#065)
	2107/0607	(12-00N, 135-00E)	CTD (12M038; 500m)
	2330/0830	(12-00N, 135-00E)	Radiosonde (#066)
18	0000/0900	(12-00N, 135-00E)	CTD (12M039; 1000m), with sampling seawater
	0230/1130	(12-00N, 135-00E)	Radiosonde (#067)
	0235/1135	(12-00N, 135-00E)	CTD (12M040; 500m)
	0530/1430	(12-00N, 135-00E)	Radiosonde (#068)
	0830/1730	(12-00N, 135-00E)	Radiosonde (#069)
	0837/1737	(12-00N, 135-00E)	CTD (12M042; 500m)
	1130/2030	(11-59N, 135-00E)	Radiosonde (#070)
	1136/2036	(11-59N, 135-01E)	CTD (12M043; 500m)
	1430/2330	(11-59N, 135-00E)	Radiosonde (#071)
	1437/2337	(11-59N, 135-00E)	CTD (12M044; 500m)
	1730/0230	(12-00N, 135-01E)	Radiosonde (#072)
	1736/0236	(11-59N, 135-01E)	CTD (12M045; 500m)
	2030/0530	(11-59N, 135-01E)	Radiosonde (#073)
	2037/0537	(11-59N, 135-01E)	CTD (12M046; 500m)
	2330/0830	(12-00N, 135-00E)	Radiosonde (#074)
	2337/0837	(12-00N, 135-00E)	CTD (12M047; 1000m), with sampling seawater
19	0230/1130	(11-59N, 134-59E)	Radiosonde (#075)
	0236/1136	(11-59N, 134-59E)	CTD (12M048; 500m)
	0530/1430	(12-00N, 135-00E)	Radiosonde (#076)

	0538/1438	(11-59N, 135-00E)	CTD (12M049; 500m)
	0830/1730	(12-00N, 135-00E)	Radiosonde (#077)
	0836/1736	(12-01N, 135-00E)	CTD (12M050; 500m)
	1130/2030	(12-01N, 135-00E)	Radiosonde (#078)
	1136/2036	(12-01N, 135-00E)	CTD (12M051; 500m)
	1213/2113	(12-01N, 135-00E)	Sea skater collection (#005-1)
	1234/2134	(12-00N, 134-59E)	Sea skater collection (#005-2)
	1254/2154	(12-00N, 134-59E)	Sea skater collection (#005-3)
	1430/2330	(12-00N, 134-59E)	Radiosonde (#079)
	1436/2336	(11-59N, 134-59E)	CTD (12M052; 500m)
	1730/0230	(12-00N, 135-00E)	Radiosonde (#080)
	1736/0236	(12-00N, 135-00E)	CTD (12M053; 500m)
	2030/0530	(12-00N, 135-00E)	Radiosonde (#081)
	2036/0536	(12-00N, 135-00E)	CTD (12M054; 500m)
	2330/0830	(12-00N, 135-00E)	Radiosonde (#082)
	2336/0836	(12-00N, 135-00E)	CTD (12M055; 1000m), with sampling seawater
20	0230/1130	(12-00N, 135-00E)	Radiosonde (#083)
	0235/1135	(12-00N, 135-00E)	CTD (12M056; 500m)
	0530/1430	(12-00N, 135-00E)	Radiosonde (#084)
	0535/1435	(12-00N, 135-00E)	CTD (12M057; 500m)
	0830/1730	(12-00N, 135-00E)	Radiosonde (#085)
	0836/1736	(12-00N, 135-00E)	CTD (12M058; 500m)
	1144/2044	(12-00N, 135-00E)	Radiosonde (#086)
	1151/2051	(12-00N, 135-00E)	CTD (12M059; 500m)
	1423/2323	(12-00N, 135-00E)	Radiosonde (#087)
	1434/2334	(12-00N, 135-00E)	CTD (12M060; 500m)
	1738/0238	(12-00N, 135-00E)	Radiosonde (#088)
	1743/0243	(12-00N, 135-00E)	CTD (12M061; 500m)
	2030/0530	(12-00N, 135-00E)	Radiosonde (#089)
	2036/0536	(12-00N, 135-00E)	CTD (12M062; 500m)
	2330/0830	(12-00N, 135-00E)	Radiosonde (#090)
	2335/0835	(12-00N, 135-00E)	CTD (12M063; 1000m), with sampling seawater
21	0230/1130	(12-00N, 135-00E)	Radiosonde (#091)
	0236/1136	(12-00N, 135-00E)	CTD (12M064; 500m)
	0345/1245		Recovery of Sea Snake
	0420/1320		Deployment of Sea Snake
	0530/1430	(12-00N, 135-00E)	Radiosonde (#092)
	0535/1435	(12-00N, 135-00E)	CTD (12M065; 500m)
	0830/1730	(12-00N, 135-00E)	Radiosonde (#093)
	0837/1737	(12-00N, 135-00E)	CTD (12M066; 500m)
	1130/2030	(12-01N, 135-00E)	Radiosonde (#094)
	1136/2036	(12-01N, 135-00E)	CTD (12M067; 500m)
	1210/2110	(12-01N, 135-00E)	Sea skater collection (#006-1)
	1232/2132	(12-00N, 135-00E)	Sea skater collection (#006-2)
	1252/2152	(11-59N, 135-00E)	Sea skater collection (#006-3)
	1430/2330	(12-00N, 135-00E)	Radiosonde (#095)
	1436/2336	(12-00N, 135-00E)	CTD (12M068; 500m)
	1730/0230	(12-00N, 135-00E)	Radiosonde (#096)
	1738/0238	(12-00N, 135-00E)	CTD (12M069; 500m)
	1749/0249	(12-00N, 135-00E)	Radiosonde (#097)
	2030/0530	(12-00N, 135-00E)	Radiosonde (#098)
	2036/0536	(12-00N, 135-00E)	CTD (12M070; 500m)
	2331/0831	(12-00N, 135-00E)	Radiosonde (#099)
	2336/0836	(12-00N, 135-00E)	CTD (12M071; 1000m), with sampling seawater
22	0230/1130	(12-00N, 135-00E)	Radiosonde (#100)
	0237/1137	(12-00N, 135-00E)	CTD (12M072; 500m)
	0530/1430	(12-00N, 135-00E)	Radiosonde (#101)
	0536/1436	(12-00N, 135-00E)	CTD (12M073; 500m)
	0830/1730	(12-00N, 135-00E)	Radiosonde (#102)
	0835/1735	(12-00N, 135-00E)	CTD (12M074; 500m)
	1130/2030	(12-00N, 135-00E)	Radiosonde (#103)

	1136/2036	(12-00N, 135-00E)	CTD (12M075; 500m)
	1430/2330	(12-00N, 135-00E)	Radiosonde (#104)
	1436/2336	(12-00N, 135-00E)	CTD (12M076; 500m)
	1722/0222	(12-00N, 135-00E)	Radiosonde (#105)
	1729/0229	(12-00N, 135-00E)	CTD (12M077; 500m)
	2030/0530	(12-00N, 135-00E)	Radiosonde (#106)
	2038/0538	(12-01N, 135-00E)	CTD (12M078; 500m)
	2330/0830	(12-00N, 135-00E)	Radiosonde (#107)
	2337/0837	(12-00N, 135-00E)	CTD (12M079; 1000m), with sampling seawater
23	0230/1130	(12-00N, 135-00E)	Radiosonde (#108)
	0233/1133	(12-00N, 135-00E)	CTD (12M080; 500m)
	0530/1430	(12-00N, 135-00E)	Radiosonde (#109)
	0534/1434	(12-00N, 135-00E)	CTD (12M081; 500m)
	0830/1730	(12-00N, 135-00E)	Radiosonde (#110)
	0834/1734	(12-00N, 135-00E)	CTD (12M082; 500m)
	1130/2030	(12-01N, 134-59E)	Radiosonde (#111)
	1135/2035	(12-01N, 134-59E)	CTD (12M083; 500m)
	1214/2114	(12-01N, 134-59E)	Sea skater collection (#007-1)
	1235/2135	(12-00N, 135-00E)	Sea skater collection (#007-2)
	1256/2156	(12-00N, 135-00E)	Sea skater collection (#007-3)
	1430/2330	(12-00N, 135-00E)	Radiosonde (#112)
	1435/2335	(12-00N, 135-00E)	CTD (12M084; 500m)
	1730/0230	(12-00N, 135-00E)	Radiosonde (#113)
	1735/0235	(12-00N, 135-00E)	CTD (12M085; 500m)
	2030/0530	(12-00N, 135-00E)	Radiosonde (#114)
	2035/0535	(12-00N, 135-00E)	CTD (12M086; 500m)
	2330/0830	(12-00N, 135-00E)	Radiosonde (#115)
	2337/0837	(12-00N, 135-00E)	CTD (12M087; 1000m), with sampling seawater
24	0230/1130	(12-00N, 135-00E)	Radiosonde (#116)
	0237/1137	(12-00N, 135-00E)	CTD (12M088; 500m)
	0530/1430	(12-00N, 135-00E)	Radiosonde (#117)
	0535/1435	(12-00N, 135-00E)	CTD (12M089; 500m)
	0612/1512	(12-00N, 135-00E)	UCTD (u008c1; 500m)
	0830/1730	(12-00N, 135-00E)	Radiosonde (#118)
	0835/1735	(12-00N, 135-00E)	CTD (12M090; 500m)
	1130/2030	(12-00N, 135-00E)	Radiosonde (#119)
	1134/2034	(12-00N, 135-00E)	CTD (12M091; 500m)
	1430/2330	(12-00N, 135-00E)	Radiosonde (#120)
	1435/2335	(12-00N, 135-00E)	CTD (12M092; 500m)
	1730/0230	(12-00N, 135-00E)	Radiosonde (#121)
	1735/0235	(12-00N, 135-00E)	CTD (12M093; 500m)
	2030/0530	(12-00N, 135-00E)	Radiosonde (#122)
	2036/0536	(12-00N, 135-00E)	CTD (12M094; 500m)
	2330/0830	(12-00N, 135-00E)	Radiosonde (#123)
	2337/0837	(12-00N, 135-00E)	CTD (12M095; 1000m), with sampling seawater
25	0230/1130	(12-00N, 135-00E)	Radiosonde (#124)
	0237/1137	(12-01N, 135-00E)	CTD (12M096; 500m)
	0530/1430	(12-00N, 135-00E)	Radiosonde (#125)
	0536/1436	(12-00N, 135-00E)	CTD (12M097; 500m), with UCTD (u009c1)
	0830/1730	(12-00N, 135-00E)	Radiosonde (#126)
	0837/1737	(12-00N, 135-00E)	CTD (12M098; 500m)
	1130/2030	(12-01N, 135-00E)	Radiosonde (#127)
	1135/2035	(12-01N, 135-00E)	CTD (12M099; 500m)
	1210/2110	(12-01N, 135-00E)	Sea skater collection (#008-1)
	1231/2131	(12-01N, 135-00E)	Sea skater collection (#008-2)
	1252/2152	(12-00N, 135-00E)	Sea skater collection (#008-3)
	1430/2330	(12-00N, 135-00E)	Radiosonde (#128)
	1436/2336	(12-00N, 135-00E)	CTD (12M100; 500m)
	1730/0230	(12-00N, 135-00E)	Radiosonde (#129)
	1734/0234	(12-00N, 135-00E)	CTD (12M101; 500m)
	2031/0531	(12-00N, 135-00E)	Radiosonde (#130)

	2038/0538	(12-00N, 135-00E)	CTD (12M102; 500m)
	2330/0830	(12-00N, 135-00E)	Radiosonde (#131)
	2337/0837	(12-00N, 135-00E)	CTD (12M103; 1000m), with sampling seawater
26	0230/1130	(12-00N, 135-00E)	Radiosonde (#132)
	0234/1134	(12-00N, 135-00E)	CTD (12M104; 500m)
	0530/1430	(12-00N, 135-00E)	Radiosonde (#133)
	0536/1436	(12-00N, 135-00E)	CTD (12M105; 500m)
	0612/1512	(12-00N, 135-00E)	UCTD (u010c1; 500m)
	0630/1530	(12-00N, 135-00E)	UCTD (u010c2; 500m)
	0830/1730	(12-00N, 135-00E)	Radiosonde (#134)
	0836/1736	(12-00N, 135-00E)	CTD (12M106; 500m)
	1130/2030	(12-00N, 135-00E)	Radiosonde (#135)
	1137/2037	(12-00N, 135-00E)	CTD (12M107; 500m)
	1212/2112	(12-00N, 135-00E)	UCTD (u011c1; 500m)
	1234/2134	(12-00N, 135-00E)	UCTD (u011c2; 500m)
	1430/2330	(12-00N, 135-00E)	Radiosonde (#136)
	1439/2339	(12-00N, 135-00E)	CTD (12M108; 500m)
	1730/0230	(12-00N, 135-00E)	Radiosonde (#137)
	1734/0234	(12-00N, 135-00E)	CTD (12M109; 500m)
	2030/0530	(12-00N, 135-00E)	Radiosonde (#138)
	2036/0536	(12-00N, 135-00E)	CTD (12M110; 500m)
	2330/0830	(12-00N, 135-00E)	Radiosonde (#139)
	2339/0839	(12-00N, 135-00E)	CTD (12M111; 1000m), with sampling seawater
27	0231/1131	(12-00N, 135-00E)	Radiosonde (#140)
	0237/1137	(12-01N, 135-00E)	CTD (12M112; 500m)
	0530/1430	(12-00N, 135-00E)	Radiosonde (#141)
	0536/1436	(12-00N, 135-00E)	CTD (12M113; 500m), with UCTD (u012c1)
	0830/1730	(12-00N, 135-00E)	Radiosonde (#142)
	0835/1735	(12-00N, 135-00E)	CTD (12M114; 500m), with UCTD (u013c1)
	1130/2030	(12-01N, 134-59E)	Radiosonde (#143)
	1135/2035	(12-01N, 134-59E)	CTD (12M115; 500m)
	1209/2109	(12-01N, 134-59E)	Sea skater collection (#009-1)
	1230/2130	(12-01N, 134-59E)	Sea skater collection (#009-2)
	1253/2153	(12-00N, 134-59E)	Sea skater collection (#009-3)
	1430/2330	(12-00N, 135-00E)	Radiosonde (#144)
	1435/2335	(12-00N, 135-00E)	CTD (12M116; 500m)
	1730/0230	(12-00N, 135-00E)	Radiosonde (#145)
	1737/0237	(12-00N, 135-00E)	CTD (12M117; 500m)
	2030/0530	(12-00N, 135-00E)	Radiosonde (#146)
	2036/0536	(12-00N, 135-00E)	CTD (12M118; 500m)
	2330/0830	(12-00N, 135-00E)	Radiosonde (#147)
	2337/0837	(12-00N, 135-00E)	CTD (12M119; 1000m), with sampling seawater
28	0230/1130	(12-00N, 135-00E)	Radiosonde (#148)
	0237/1137	(12-00N, 135-00E)	CTD (12M120; 500m)
	0530/1430	(12-00N, 135-00E)	Radiosonde (#149)
	0536/1436	(12-00N, 135-00E)	CTD (12M121; 500m)
	0610/1510	(12-00N, 135-00E)	UCTD (u014c1; 500m)
	0628/1528	(12-00N, 135-00E)	UCTD (u014c2; 500m)
	0830/1730	(12-00N, 135-00E)	Radiosonde (#150)
	0835/1735	(12-00N, 135-00E)	CTD (12M122; 500m)
	1130/2030	(12-00N, 135-00E)	Radiosonde (#151)
	1136/2036	(12-00N, 135-00E)	CTD (12M123; 500m)
	1210/2110	(12-00N, 135-00E)	UCTD (p3c1; 500m)
	1228/2128	(12-00N, 135-00E)	UCTD (u015c1; 500m)
	1246/2146	(12-00N, 135-00E)	UCTD (u015c2; 500m)
	1430/2330	(12-00N, 135-00E)	Radiosonde (#152)
	1436/2336	(12-00N, 135-00E)	CTD (12M124; 500m)
	1730/0230	(12-00N, 135-00E)	Radiosonde (#153)
	1737/0237	(11-59N, 135-00E)	CTD (12M125; 500m)
	2030/0530	(12-00N, 135-00E)	Radiosonde (#154)
	2036/0536	(12-00N, 135-00E)	CTD (12M126; 500m)

		2330/0830	(12-00N, 135-00E)	Radiosonde (#155)
		2337/0837	(12-00N, 135-00E)	CTD (12M127; 1000m), with sampling seawater
29		0230/1130	(12-00N, 135-00E)	Radiosonde (#156)
		0236/1136	(12-00N, 135-00E)	CTD (12M128; 500m)
		0530/1430	(12-00N, 135-00E)	Radiosonde (#157)
		0536/1436	(12-00N, 135-00E)	CTD (12M129; 500m)
		0830/1730	(12-00N, 135-00E)	Radiosonde (#158)
		0835/1735	(12-00N, 135-00E)	CTD (12M130; 500m)
		1130/2030	(12-01N, 135-00E)	Radiosonde (#159)
		1136/2036	(12-01N, 135-00E)	CTD (12M131; 500m)
		1210/2110	(12-01N, 135-00E)	Sea skater collection (#010-1)
		1232/2132	(12-01N, 135-00E)	Sea skater collection (#010-2)
		1253/2153	(12-00N, 135-00E)	Sea skater collection (#010-3)
		1430/2330	(12-00N, 135-00E)	Radiosonde (#160)
		1436/2336	(12-00N, 135-00E)	CTD (12M132; 500m)
		1730/0230	(12-00N, 135-00E)	Radiosonde (#161)
		1737/0237	(12-00N, 135-00E)	CTD (12M133; 500m)
		2030/0530	(12-00N, 135-00E)	Radiosonde (#162)
		2036/0536	(12-00N, 135-00E)	CTD (12M134; 500m)
		2330/0830	(12-00N, 135-00E)	Radiosonde (#163)
		2336/0836	(12-00N, 135-00E)	CTD (12M135; 1000m), with sampling seawater
30		0101/1001	Recovery of Thermistor Chain and Sea Snake	
		0230/1130	(12-00N, 135-00E)	Radiosonde (#164)
		0237/1137	(12-01N, 135-00E)	CTD (12M136; 500m)
		0355/1255	(12-06N, 135-00E)	UCTD (u101c1; 250m)
		0428/1328	(12-01N, 134-57E)	UCTD (u101c2; 250m)
		0516/1416	(11-57N, 134-55E)	UCTD (u101c3; 250m)
		0530/1430	(11-57N, 134-57E)	Radiosonde (#165)
		0549/1449	(11-57N, 135-00E)	UCTD (u101c4; 250m)
		0632/1532	(11-57N, 135-05E)	UCTD (u101c5; 250m)
		0701/1601	(12-01N, 135-03E)	UCTD (u101c6; 250m)
		0743/1643	(12-06N, 135-00E)	UCTD (u101c7; 250m)
		0830/1730	(12-00N, 135-00E)	Radiosonde (#166)
		0836/1736	(12-00N, 135-00E)	CTD (12M137; 500m)
		0947/1847	(12-06N, 135-00E)	UCTD (u102c1; 250m)
		1019/1919	(12-01N, 134-57E)	UCTD (u102c2; 250m)
		1100/2000	(11-57N, 134-55E)	UCTD (u102c3; 250m)
		1130/2030	(11-57N, 134-59E)	Radiosonde (#167)
		1134/2034	(11-57N, 135-00E)	UCTD (u102c4; 250m)
		1221/2121	(11-57N, 135-05E)	UCTD (u102c5; 250m)
		1250/2150	(12-02N, 135-03E)	UCTD (u102c6; 250m)
		1335/2235	(12-06N, 135-00E)	UCTD (u102c7; 250m)
		1430/2330	(12-00N, 135-00E)	Radiosonde (#168)
		1435/2335	(12-00N, 135-00E)	CTD (12M138; 500m)
		1736/0236	(12-28N, 135-05E)	Radiosonde (#169)
		2021/0521	(12-59N, 135-06E)	Radiosonde (#170)
		2330/0830	(13-38N, 135-13E)	Radiosonde (#171)
Jul	1	0230/1130	(14-15N, 135-16E)	Radiosonde (#172)
		0530/1430	(14-50N, 135-22E)	Radiosonde (#173)
		0830/1730	(15-28N, 135-26E)	Radiosonde (#174)
		1130/2030	(16-06N, 135-31E)	Radiosonde (#175)
		1727/0227	(17-26N, 135-41E)	Radiosonde (#176)
		2330/0830	(18-45N, 135-51E)	Radiosonde (#177)
	2	0530/1430	(20-02N, 136-01E)	Radiosonde (#178)
	5	0010/0910	Stop of Doppler Radar observation	
		0030/0930	Stop of surface seawater measurement	
		0401/1301	(22-26N, 139-20E)	Test of 3-dimensional magnetometer
	6	0140/1040	Arrival at Yokohama	

4. List of Participants

4.1 Participants (on board)

Name	Affiliation	*Theme No.	Period on board
Masaki KATSUMATA	JAMSTEC	M	Leg-1 + 2
Satoru YOKOI	JAMSTEC	M	Leg-1 + 2
Takuya HASEGAWA	JAMSTEC	M	Leg-1
Qoosaku MOTTEKI	JAMSTEC	M	Leg-1
Ayumi MASUDA	JAMSTEC	M	Leg-1 + 2
Hiroaki YOSHIOKA	JAMSTEC	M	Leg-1 + 2
Satoki TSUJINO	Nagoya Univ.	1	Leg-1 + 2
Tetsuo HARADA	Kochi Univ.	4	Leg-1
Takero SEKIMOTO	Kochi Univ.	4	Leg-1 + 2
Kazuho YOSHIDA	Global Ocean Development Inc. (GODI)	T	Leg-1 + 2
Wataru TOKUNAGA	GODI	T	Leg-1
Souichiro SUEYOSHI	GODI	T	Leg-2
Kouichi INAGAKI	GODI	T	Leg-1 + 2
Hiroshi MATSUNAGA	Marine Works Japan Ltd. (MWJ)	T	Leg-1 + 2
Hiroki USHIROMURA	MWJ	T	Leg-1 + 2
Misato KUWAHARA	MWJ	T	Leg-1 + 2
Shinsuke TOYODA	MWJ	T	Leg-2
Rei ITO	MWJ	T	Leg-2
Hideki YAMAMOTO	MWJ	T	Leg-2
Masahiro ORUI	MWJ	T	Leg-2
Sonoka WAKATSUKI	MWJ	T	Leg-2

* Theme number corresponds to that shown in Section 2.7.
M and T means main mission and technical staff, respectively.

4.2 Participants (not on board)

Name	Affiliation	*Theme No.
Ryuichi SHIROOKA	JAMSTEC	M
Taro SHINODA	Nagoya Univ.	1
Nobuo SUGIMOTO	NIES	2
Kazuma AOKI	Toyama Univ.	3
Takeshi MATSUMOTO	Ryukyu Univ.	5

4.3 Ship Crew

Yoshiharu TSUTSUMI	Master	Leg-1 + 2
Takeshi ISOHI	Chief Officer	Leg-1 + 2
Kan MATSUURA	First Officer	Leg-1 + 2
Nobuo FUKAURA	Second Officer	Leg-1 + 2
Takahiro NOGUCHI	Third Officer	Leg-1 + 2
Hiroki KOBAYASHI	Jr. Third Officer	Leg-2
Ryo SAKATA	Chief Engineer	Leg-1 + 2
Hiroyuki TOHKEN	First Engineer	Leg-1 + 2
Naoto MIYAZAKI	Second Engineer	Leg-1 + 2
Yusuke KIMOTO	Third Engineer	Leg-1 + 2
Ryo KIMURA	Technical Officer	Leg-1 + 2
Kazuyoshi KUDO	Boatswain	Leg-1 + 2
Tsuyoshi SATOH	Able Seaman	Leg-1 + 2
Tsuyoshi MONZAWA	Able Seaman	Leg-1 + 2
Masashige OKADA	Able Seaman	Leg-1 + 2
Shuji KOMATA	Able Seaman	Leg-1 + 2
Masaya TANIKAWA	Ordinary Seaman	Leg-1 + 2
Hideaki TAMOTSU	Ordinary Seaman	Leg-1 + 2
Kotaro SAKAI	Ordinary Seaman	Leg-1 + 2
Ryosuke HIRATSUKA	Ordinary Seaman	Leg-1 + 2
Akiya CHISHIMA	Ordinary Seaman	Leg-1 + 2
Tetsuya SAKAMOTO	Ordinary Seaman	Leg-1 + 2
Yoshihiro SUGIMOTO	No.1 Oiler	Leg-1 + 2
Nobuo BOSHITA	Oiler	Leg-1 + 2
Masato SHIRAKURA	Oiler	Leg-1 + 2
Daisuke TANIGUCHI	Oiler	Leg-1 + 2
Keisuke YOSHIDA	Ordinary Oiler	Leg-1 + 2
Hiroshi IKUTA	Ordinary Oiler	Leg-1 + 2
Hitoshi OTA	Chief Steward	Leg-1 + 2
Tamotsu UEMURA	Cook	Leg-1 + 2
Sakae HOSHIKUMA	Cook	Leg-1 + 2
Tsuneaki YOSHINAGA	Cook	Leg-1 + 2
Shohei MARUYAMA	Steward	Leg-1 + 2

5. Summary of Observations

5.1 GPS Radiosonde

(1) Personnel

Masaki KATSUMATA	(JAMSTEC)	- Principal Investigator
Satoru YOKOI	(JAMSTEC)	
Qoosaku MOTOKI	(JAMSTEC)	
Ayumi MASUDA	(JAMSTEC)	
Hiroaki YOSHIOKA	(JAMSTEC)	
Satoki TSUJINO	(Nagoya Univ.)	
Ryuichi SHIROOKA	(JAMSTEC)	(not on board)
Kazuho YOSHIDA	(GODI)	- Operation Leader
Souichiro SUEYOSHI	(GODI)	
Wataru TOKUNAGA	(GODI)	
Kouichi INAGAKI	(GODI)	
Ryo KIMURA	(MIRAI Crew)	

(2) Objectives

To obtain atmospheric profile of temperature, humidity, and wind speed/direction, and their temporal variations

(3) Methods

Atmospheric sounding by radiosonde by using system by Vaisala Oyj was carried out. The GPS radiosonde sensor (RS92-SGPD) was launched with the balloons (Totex TA-200/350). The on-board system to calibrate, to launch, to log the data and to process the data, consists of processor (Vaisala, SPS-311), processing and recording software (DigiCORA III, ver.3.64), GPS antenna (GA20), UHF antenna (RB21), ground check kit (GC25), and balloon launcher (ASAP). In the "ground-check" process, the pressure sensor (Vaisala PTB-330) was also utilized as the standard. In case the relative wind to the ship (launcher) is not appropriate for the launch, the handy launch was selected.

The radiosondes were launched every 3 hours from 12UTC on Jun. 12, 2013, to 12UTC on Jul. 01, 2013, when the vessel was at or around the station (12N, 135E). During the period, the launch at the local noon (03UTC) utilized larger balloon (TA-350), while other launch utilized smaller one (TA-200). In addition, the 6-hourly launch was conducted in Leg-1 (from 00UTC on Jun.06, 2013, to 18UTC on Jun.09, 2013) and in Leg-2 (12UTC on Jul. 01, 2013, to 06UTC on Jul. 02, 2013). In total, 173 soundings were carried out, as listed in Table 5.1-1.

(4) Preliminary Results

The results from Vaisala system are shown in the figures. Figure 5.1-1 is the time-height cross sections during the stationary observation period at (12N, 135E) for equivalent potential temperature, relative humidity, zonal and meridional wind components. Several basic parameters are derived from sounding data as in Fig. 5.1-2, including convective available potential energy (CAPE), convective inhibition (CIN) and total precipitable water vapor (TPW). Each vertical profiles of temperature and dew point temperature on the thermodynamic chart with wind profiles are attached in Appendix-A.

(5) Data archive

Data were sent to the world meteorological community via Global Telecommunication System (GTS) through the Japan Meteorological Agency, immediately after each observation. Raw data is recorded in Vaisala original binary format during both ascent and descent. The ASCII data is also available. These raw datasets will be submitted to JAMSTEC Data Management Group (DMG). The corrected datasets will be available from Mirai website at <http://www.jamstec.go.jp/cruisedata/mirai/e/>.

Table 5.1-1: Radiosonde launch log, with surface values and maximum height.

ID	Nominal Time YYYYMMDDhh	Launched Location		Surface Values					Max. Height m	Cloud	
		Lat.	Lon.	P	T	RH	WD	WS		Am.	Type
		deg.N	deg.E	hPa	deg.C	%	deg	m/s			
Leg-1											
RS001	2013060600	21.716	137.234	1011.1	28.6	82	141	6.6	24423	5	Cu, As, Ac, Cc
RS002	2013060606	22.665	136.832	1009.4	28.0	79	173	5.6	21021	9	Cu,As
RS003	2013060612	19.561	136.394	1009.2	27.6	83	159	4.0	24886	-	-
RS004	2013060618	18.489	135.993	1006.8	27.9	80	138	9.4	22945	-	-
RS005	2013060700	17.422	135.557	1007.4	27.6	89	103	5.1	24040	9	Cb,Cu
RS006	2013060706	16.242	135.097	1005.1	29.2	78	147	9.8	24527	8	Cu,Sc,As
RS007	2013060712	15.265	135.001	1006.2	27.8	86	134	10.6	23708	-	-
RS008	2013060718	14.097	135.005	1004.4	28.2	87	143	7.0	17883	-	-
RS009	2013060800	13.065	135.002	1006.2	29.2	80	163	7.7	24648	9	Cb,Cu,As
RS010	2013060806	12.122	135.002	1004.1	28.2	84	196	6.4	24213	5	Cu,As
RS011	2013060812	10.962	134.999	1006.5	26.5	87	221	6.5	18442	-	-
RS012	2013061818	9.930	134.993	1005.0	26.5	92	270	2.0	17992	-	-
RS013	2013060900	8.906	134.858	1006.5	26.0	87	90	0.6	20864	10	Ns
RS014	2013060906	8.251	134.330	1004.9	27.7	80	355	1.2	17020	10	Cu, Ns
RS015	2013060912	7.748	134.301	1005.0	27.8	83	45	6.9	23152	8	As?
RS016	2013060918	7.757	134.295	1003.3	28.5	84	103	7.9	24630	10	Cu, Sc
Leg-2											
RS017	2013061212	9.378	134.559	1004.0	28.8	85	116	7.4	24919	-	-
RS018	2013061215	9.894	134.649	1005.0	27.8	81	123	6.6	23355	1	-
RS019	2013061218	10.428	134.733	1003.5	26.9	82	91	12.6	24027	3	-
RS020	2013061221	10.980	134.827	1003.7	28.6	82	100	8.9	21851	7	Cu,Ci,As
RS021	2013061300	11.492	134.914	1004.8	29.0	82	113	8.0	24694	5	Cu,Cb
RS022	2013061303	12.001	135.000	1004.4	29.3	80	102	8.8	26190	4	Cu,Ci,As
RS023	2013061306	12.000	135.001	1003.1	29.5	80	100	8.6	24543	6	Cu,Ci
RS024	2013061309	11.995	135.008	1003.5	29.3	79	86	9.3	24837	3	Cu,Ci
RS025	2013061312	11.999	134.998	1004.7	28.6	86	87	9.4	23637	-	-
RS026	2013061315	11.981	134.997	1005.0	28.7	86	72	7.1	23284	-	-
RS027	2013061318	11.999	135.008	1003.6	28.8	81	67	9.9	25377	-	-
RS028	2013061321	12.008	135.002	1003.9	27.9	87	55	7.8	24014	8	Cu,Cb,Ci
RS029	2013061400	12.005	135.016	1005.1	28.7	83	98	7.6	22761	3	Cu,Cb,As
RS030	2013061403	11.996	135.002	1004.0	27.6	86	80	5.9	25619	5	Ns,Cu,Ac,As,St
RS031	2013061406	11.992	134.997	1003.3	28.5	85	66	6.9	24207	6	Cu,Ac
RS032	2013061409	11.991	134.987	1003.6	28.5	83	71	8.5	25171	8	Cu,As,Ac
RS033	no valid data										
RS034	2013061412	11.981	134.976	1005.3	26.0	92	68	11.9	18135	-	-
RS035	2013061415	11.987	134.978	1005.0	26.4	89	90	13.1	18172	-	-
RS036	2013061418	12.001	135.001	1004.1	26.6	91	119	13.0	4807	-	-
RS037	2013061421	11.997	134.997	1004.0	27.3	86	112	12.7	23696	10	Cu,As
RS038	2013061500	11.999	134.998	1004.7	26.9	88	128	12.0	5422	10	Cu,As
RS039	2013061503	12.003	135.007	1005.0	28.1	85	131	10.7	27411	10	Sc,Cu,As
RS040	no valid data										
RS041	2013061506	11.999	135.005	1003.3	27.6	88	129	10.9	24334	10	Ns,Cu
RS042	2013061509	12.005	135.007	1003.7	28.6	82	122	11.4	21064	10	Cu,As,St
RS043	2013061512	12.021	135.006	1005.7	28.8	83	129	10.0	21966	-	-
RS044	2013061515	11.996	135.005	1006.0	26.8	90	163	11.0	18286	-	-
RS045	2013061518	12.001	135.001	1004.3	26.7	88	129	12.1	20487	-	-
RS046	2013061521	11.988	134.988	1004.7	28.2	82	138	10.3	1057	-	-

RS047	2013061521	11.988	134.991	1005.2	28.0	85	151	8.4	23156	10	Cu,Cb,As
RS048	2013061600	11.996	134.998	1005.9	28.4	81	138	11.8	25110	9	Cu,Cb,As
RS049	2013061603	11.993	134.993	1005.9	27.3	85	151	11.9	24642	9	Cu,Cb,As
RS050	no valid data										
RS051	2013061606	12.001	135.004	1003.2	28.8	80	137	7.8	24048	10	As,Cu
RS052	2013061609	11.999	135.000	1004.4	28.5	76	153	8.7	25156	10	Cu,As
RS053	2013061612	11.994	134.991	1005.7	28.6	79	150	9.0	24493	-	-
RS054	2013061615	11.996	135.012	1004.5	28.6	79	143	6.6	23943	-	-
RS055	2013061618	11.998	135.011	1003.3	28.5	29	138	5.2	24491	-	-
RS056	2013061621	12.003	135.010	1004.2	28.1	80	176	5.6	22606	8	Cu,Cb,As
RS057	2013061700	11.996	134.999	1004.8	29.2	76	142	9.0	25819	4	Cu,Ci,Cc,Cs
RS058	2013061703	11.984	134.998	1004.0	28.1	86	151	5.7	28436	5	Cu,Ac,Cb,Ci,Sc
RS059	2013061706	12.003	135.006	1002.7	29.1	77	138	9.2	23101	6	Cu,Cs,Ci,Ac
RS060	2013061709	12.013	135.006	1003.4	28.9	78	128	10.2	24780	8	Ns,Cu
RS061	2013061712	12.018	135.010	1004.2	28.6	82	135	10.8	22547	5	As
RS062	no valid data										
RS063	2013061715	11.999	134.983	1004.3	28.5	82	165	10.3	23231	-	-
RS064	2013061718	12.000	135.005	1003.2	28.0	85	164	10.6	24009	-	-
RS065	2013061721	12.002	134.999	1003.7	28.1	78	195	9.0	23233	6	Cu,Ac,Ci
RS066	2013061800	11.999	134.999	1004.8	28.7	76	178	7.7	24565	4	Cu,Ci,Cs
RS067	2013061803	12.000	134.994	1004.5	29.1	77	173	7.2	28213	4	Cu,As,Ci
RS068	2013061806	12.003	135.010	1004.1	30.7	73	168	6.5	22758	4	Cu,Cs,Ci,As
RS069	2013061809	11.997	135.009	1004.1	28.9	78	132	8.6	25528	3	Cs,Cu
RS070	2013061812	11.984	135.004	1005.9	28.9	84	121	9.0	23353	-	-
RS071	2013061815	11.985	135.012	1006.6	28.8	81	148	7.3	23751	-	As,Ac
RS072	2013061818	11.999	135.017	1005.2	28.8	77	139	5.0	22858	-	-
RS073	2013061821	11.988	135.017	1006.0	29.0	80	129	6.9	24539	7	Cu,As,Cs
RS074	2013061900	12.001	135.003	1007.6	29.2	79	118	5.5	24913	6	Cu,As,Ci
RS075	2013061903	11.985	134.978	1007.2	29.3	79	147	5.3	28570	6	Cu,Cs
RS076	2013061906	12.004	135.009	1006.3	28.5	81	184	3.0	26540	10	Cu,As,Ac,St
RS077	2013061909	12.016	135.007	1006.4	29.1	80	137	6.1	23165	10	Cu,As,St,Cs
RS078	2013061912	12.019	135.007	1009.0	28.4	85	152	5.3	23229	-	As,Cs
RS079	2013061915	11.996	134.988	1008.8	28.5	79	138	4.4	23397	8	Cs
RS080	2013061918	12.002	134.998	1007.1	28.2	83	119	4.0	25091	2	-
RS081	2013061921	12.006	135.008	1007.3	28.2	84	107	5.1	25069	7	Cu,As,Ci
RS082	2013062000	12.000	134.998	1009.0	29.0	79	117	6.0	20562	4	Cu,Cs,Cc
RS083	2013062003	11.999	135.005	1008.4	29.4	78	106	6.6	26946	2	Cu,As,Ci
RS084	2013062006	12.005	135.002	1006.2	29.3	77	107	8.6	24945	5	Ci,Cu
RS085	2013062009	12.000	135.000	1006.0	29.3	79	94	7.4	25242	3	Cb,Cu,Cs
RS086	2013062012	11.997	134.998	1008.6	29.2	77	79	9.0	26012	8	Cs
RS087	2013062015	11.997	135.004	1008.8	29.1	80	84	5.7	25289	9	Cu
RS088	2013062018	11.997	135.002	1007.4	27.2	87	88	6.3	24615	-	-
RS089	2013062021	12.000	135.000	1007.9	28.7	81	98	6.5	24642	6	Cu,Ci
RS090	2013062100	12.004	135.001	1008.8	29.0	80	102	5.1	23866	2	Cu,Cc,Cs,Ci
RS091	2013062103	11.998	134.999	1008.6	28.8	80	133	3.1	29352	4	Cu,Cc,Ci
RS092	2013062106	11.997	134.999	1007.0	29.2	79	101	8.6	24995	6	Cu,Cs,Ci
RS093	2013062109	12.011	135.003	1006.8	29.2	76	114	7.2	25043	6	Cu,Cs
RS094	2013062112	12.020	135.005	1008.2	28.7	83	107	7.5	23847	5	Ci,Cu
RS095	2013062115	11.992	134.998	1008.6	29.0	82	111	6.3	24025	5	Cu
RS096	no valid data										
RS097	2013062118	11.997	135.000	1006.7	28.8	83	107	5.6	23827	2	Cu,As,Sc
RS098	2013062121	12.011	235.005	1006.7	28.5	85	82	6.3	22686	3	Cu,As
RS099	2013062200	11.999	135.001	1008.2	28.5	80	88	4.2	24694	4	Cu,As
RS100	2013062203	12.001	134.998	1007.8	28.8	84	69	8.2	26979	6	Cu,As,Cs
RS101	2013062206	11.999	135.000	1006.7	29.2	79	93	6.5	24056	8	Cs,Cu
RS102	2013062209	12.002	135.002	1006.4	29.1	81	102	5.0	21907	7	Cu,Ci,Cs
RS103	2013062212	12.003	135.004	1008.0	28.6	85	64	5.6	24952	3	Cu,As
RS104	2013062215	12.005	135.002	1008.5	28.9	80	108	6.3	24575	-	Cu
RS105	2013062218	12.001	134.998	1007.8	28.8	81	112	5.4	21965	7	Nb, Ns, Sc, Cu
RS106	2013062221	12.005	135.001	1007.9	27.7	85	75	8.4	24561	10	Cu,Cb,St,As
RS107	2013062300	12.002	135.000	1009.5	28.9	80	91	6.7	23881	2	Cu,Cb,Cs
RS108	2013062303	11.998	134.999	1008.5	29.1	82	110	4.8	27598	4	Cu,Cb
RS109	2013062306	12.001	134.999	1006.8	29.2	79	87	7.0	24540	0	Cu
RS110	2013062309	12.001	134.998	1006.9	29.4	78	64	7.6	24564	2	Cu
RS111	2013062312	12.017	134.991	1008.3	29.1	78	71	7.8	25107	2	Cu
RS112	2013062315	12.002	134.998	1008.9	28.9	78	61	8.5	24108	2	Cu

RS113	2013062318	12.000	134.999	1007.4	28.8	78	59	8.7	23532	3	Cu,As
RS114	2013062321	12.001	134.998	1007.5	28.9	77	65	9.0	24497	6	Cu,Cc,Cs,As
RS115	2013062400	12.000	134.999	1008.2	28.9	78	48	10.3	24135	7	Cu,As
RS116	2013062403	11.999	135.001	1008.0	29.8	78	63	9.8	22686	5	Cu,Cb,Ac
RS117	2013062406	12.001	135.000	1007.3	28.9	78	73	6.1	25451	5	Cu,As
RS118	2013062409	12.001	134.997	1007.3	27.9	83	89	9.7	25002	10	Cu,As,Cs
RS119	2013062412	12.001	134.999	1008.2	28.7	83	79	9.3	23735	1	Cu
RS120	2013062415	12.001	134.997	1009.1	29.0	82	86	10.1	24872	3	Cu
RS121	2013062418	12.001	134.998	1007.6	28.4	86	71	9.8	25247	3	Cu,As
RS122	2013062421	12.000	134.997	1007.5	28.4	86	69	10.9	24460	4	Cs,Cu
RS123	2013062500	12.000	135.000	1008.2	29.1	81	74	10.9	24748	5	Cu
RS124	2013062503	12.002	134.999	1008.1	29.4	79	91	8.4	27570	4	Cu,Ci
RS125	2013062506	12.000	135.000	1006.8	28.9	83	99	7.6	25714	4	Cu,Ci
RS126	2013062509	12.000	135.000	1006.6	28.8	85	121	8.2	24153	6	Ns,Cs,Cu
RS127	2013062512	12.019	135.003	1007.8	28.9	81	131	6.7	24199	2	Cu
RS128	2013062515	12.000	135.006	1008.5	28.8	82	151	4.3	21696	4	Cu,Cc
RS129	2013062518	12.000	135.000	1007.3	27.7	83	59	2.3	25174	9	Nb,As,Cu
RS130	2013062521	12.001	135.001	1007.4	26.4	91	57	1.8	22945	8	Cu,As,Cs
RS131	2013062600	11.999	135.000	1008.2	27.8	83	100	2.1	22678	8	Cu,Ac,As
RS132	2013062603	11.998	134.999	1007.7	28.3	79	103	3.0	29076	8	Cu,As,Ci
RS133	2013062606	12.000	134.999	1006.6	28.4	80	119	3.8	24986	10	Cu
RS134	2013062609	12.000	134.998	1006.2	28.3	81	133	5.9	25779	10	Cs,Cc,Ac,Cu
RS135	2013062612	12.001	134.999	1007.2	27.7	87	178	4.8	24736	4	Cu,As
RS136	2013962615	11.999	135.000	1007.6	27.5	87	197	2.4	23423	3	Cu
RS137	2013062618	12.002	135.001	1005.8	27.6	81	250	0.5	23980	9	Cu,Ac
RS138	2013062621	12.007	134.999	1005.6	28.0	81	75	3.9	21970	8	Cu,As,Cs,
RS139	2013062700	12.000	134.999	1005.9	28.7	77	77	5.5	25052	8	Cu,Cc,Cs
RS140	2013062703	12.003	134.997	1005.6	27.3	83	58	5.4	28784	7	Cu,Ns,Ac
RS141	2013062706	12.000	135.000	1003.9	28.0	85	87	5.5	25381	9	As,Cu
RS142	2013062709	12.002	134.999	1004.3	28.2	79	99	7.5	16131	5	Cu,Ac,Ci
RS143	2013062712	12.017	134.992	1005.8	28.7	80	118	9.1	24981	0	-
RS144	2013062715	12.000	134.994	1006.4	28.1	82	112	7.8	22209	4	Cu
RS145	2013062718	12.001	135.000	1004.4	28.6	77	157	7.6	23811	9	As,Cu
RS146	2013062721	12.001	134.999	1005.3	28.6	79	124	5.1	24552	10	As,Cu
RS147	2013062800	12.002	134.998	1006.2	28.8	79	129	6.1	24179	8	As,Cs,Cu
RS148	2013062803	11.999	135.000	1006.3	29.4	77	137	5.6	27645	9	Cu,As
RS149	2013062806	12.002	135.001	1005.8	27.9	82	168	5.8	24349	7	Cu,As
RS150	2013062809	12.000	134.999	1005.0	28.4	83	119	6.6	24746	8	Cu,As
RS151	2013062812	12.005	134.999	1006.4	28.7	80	140	7.2	24977	0	-
RS152	2013062815	11.999	135.004	1006.7	28.8	80	142	6.3	24253	3	Cu,Cs
RS153	2013062818	11.998	135.000	1006.0	28.6	82	139	5.9	25289	4	Ns,Cu,As
RS154	2013062821	12.001	135.010	1007.1	28.4	80	140	7.2	25365	8	Cu,Ac,As
RS155	2013062900	12.006	135.009	1008.4	29.1	79	118	6.2	24233	2	Cu,Cc
RS156	2013062903	11.996	134.999	1007.8	29.1	80	131	4.9	27992	1	Cu, Cs, Cc
RS157	2013062906	12.000	135.000	1007.1	29.3	78	119	5.4	24319	5	Cu
RS158	2013062909	12.003	135.000	1007.4	29.2	77	105	4.6	25676	5	Cu,Ci
RS159	2013062912	12.018	135.004	1009.2	29.1	78	100	5.2	24168	0	-
RS160	2013062915	12.002	135.003	1009.4	28.9	81	115	3.2	23893	1	Cu
RS161	2013062918	12.004	135.001	1008.1	28.6	82	65	3.3	23997	2	Cu,As
RS162	2013062921	12.002	135.000	1007.8	28.7	78	44	1.7	19592	3	Cu,As
RS163	2013063000	12.004	135.002	1008.3	29.1	79	47	5.5	24582	2	Cu
RS164	2013063003	12.010	134.992	1007.4	29.4	79	60	4.3	26818	2	Cu
RS165	2013063006	11.942	134.901	1006.3	29.2	82	37	5.5	24223	5	Cu,Ac
RS166	2013063009	12.043	135.000	1006.1	29.3	82	46	5.9	25773	5	Cu,Ci,Ac,As,Cb
RS167	2013063012	11.951	134.915	1007.5	29.0	84	79	6.3	24024	-	-
RS168	2013063015	12.024	134.997	1007.3	28.9	84	68	6.3	22950	-	As?
RS169	2013063018	12.419	135.058	1005.7	27.1	79	22	4.5	19302		Nb,As,Cu
RS170	2013063021	12.968	135.120	1006.0	27.7	83	148	5.6	23872	10	Ns,Nb,Sc,St
RS171	2013070100	13.561	135.194	1007.3	28.2	85	61	3.2	23994	7	Cu,As,Cs
RS172	2013070103	14.149	135.254	1007.0	28.9	82	74	5.5	27322	10	Ci,Cs,Cu
RS173	2013070106	14.780	135.341	1005.6	29.2	77	96	7.7	25565	1	Ci,Cs,As,Cu,Cb
RS174	2013070109	15.365	135.421	1006.1	29.6	74	99	7.3	23914	7	Ci,Cu,As
RS175	2013070112	16.006	135.501	1007.3	29.1	80	110	8.3	23244	0	-
RS176	2013070118	17.378	135.674	1007.2	28.5	82	113	5.8	5736	10	-
RS177	2013070200	18.648	135.837	1009.9	28.7	80	93	4.6	22990	3	Cu,As,Cs
RS178	2013070206	19.961	135.997	1007.8	29.3	79	57	6.5	23337	2	Cu,As,Cs

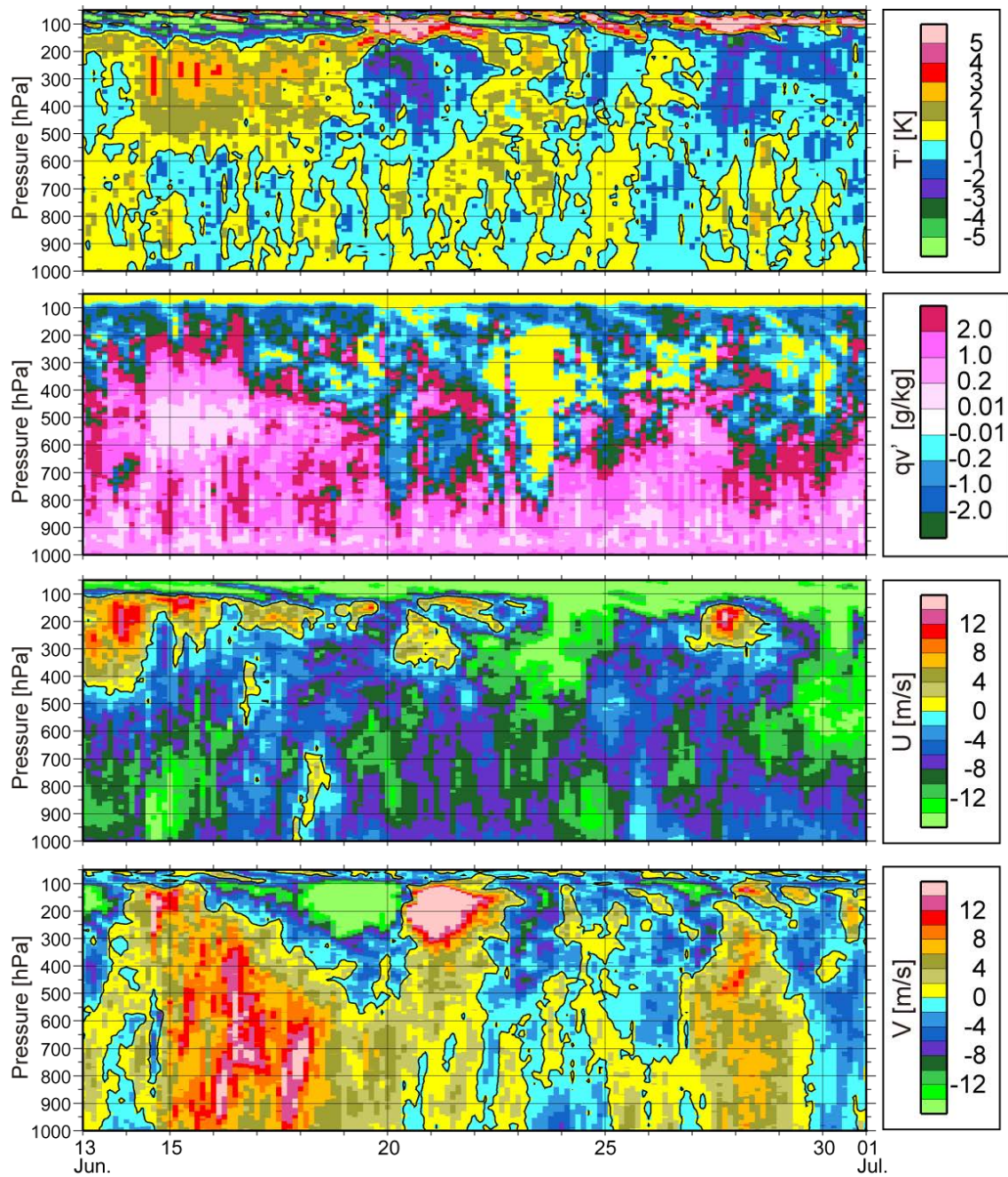


Fig. 5.1-1: Time-height cross sections of observed parameters at (12N, 135E); (a) temperature, in anomaly to the period-averaged value at each pressure level, (b) water vapor mixing ratio, in anomaly to the period-averaged value at each pressure level, (c) zonal wind (absolute value), and (d) meridional wind (absolute value).

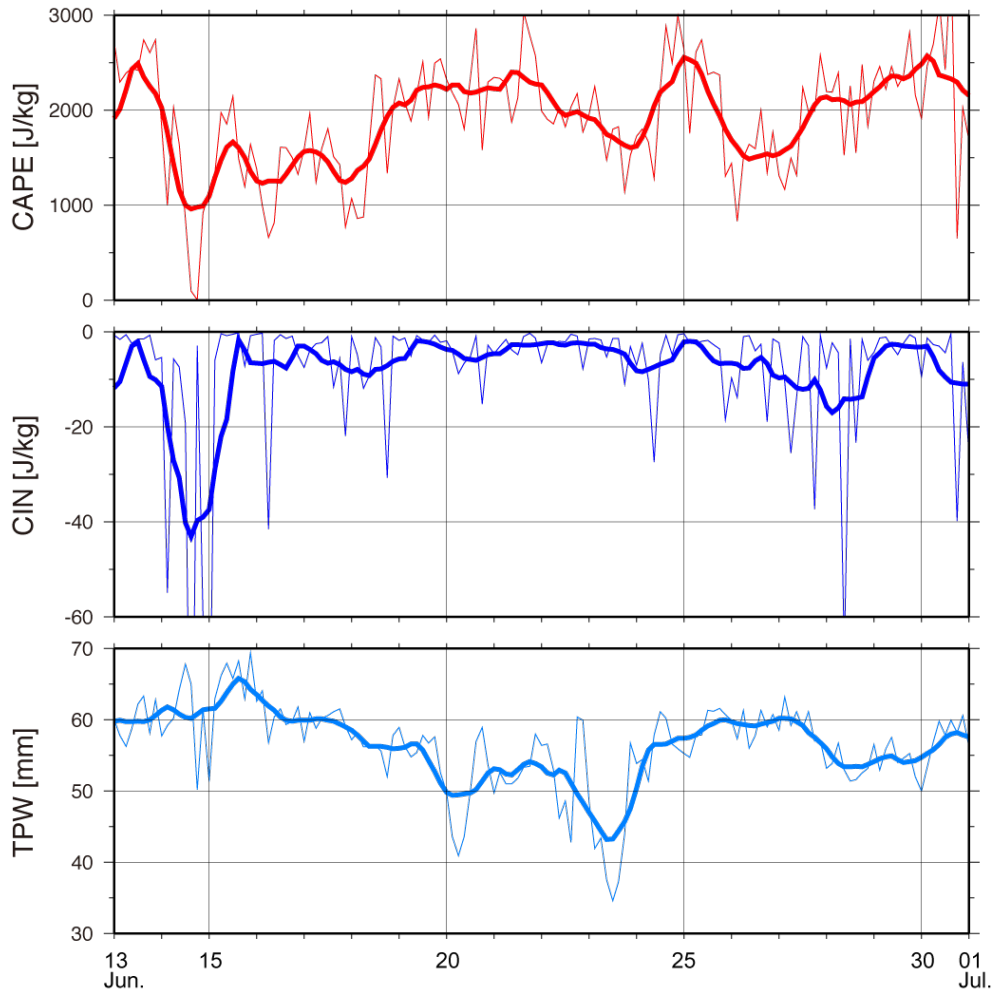


Fig. 5.1-2: Time series of the parameters derived from the radiosonde observations; (a) CAPE, (b) CIN, and (c) precipitable water. The thin lines are from the 3-hourly snapshots, while the thick lines are the running mean for 25 hours.

5.2 Doppler Radar

(1) Personnel

Masaki KATSUMATA	(JAMSTEC)	- Principal Investigator
Satoru YOKOI	(JAMSTEC)	
Qoosaku MOTTEKI	(JAMSTEC)	
Ayumi MASUDA	(JAMSTEC)	
Hiroaki YOSHIOKA	(JAMSTEC)	
Satoki TSUJINO	(Nagoya Univ.)	
Ryuichi SHIROOKA	(JAMSTEC)	(not on board)
Kazuho YOSHIDA	(GODI)	- Operation Leader
Souichiro SUEYOSHI	(GODI)	
Wataru TOKUNAGA	(GODI)	
Kouichi INAGAKI	(GODI)	
Ryo KIMURA	(MIRAI Crew)	

(2) Objective

The objective of the Doppler radar observation in this cruise is to investigate three dimensional rainfall and kinematic structures of precipitation systems and their temporal and special variations in the tropical and subtropical western Pacific, especially at around (12N, 135E).

(3) Method

The Doppler radar on board of Mirai is used. The specification of the radar is:

Frequency:	5290 MHz
Beam Width:	less than 1.5 degrees
Output Power:	250 kW (Peak Power)
Signal Processor:	RVP-7 (Vaisala Inc. Sigmet Product Line, U.S.A.)
Inertial Navigation Unit:	PHINS (Ixsea S.A.S., France)
Application Software:	IRIS/Open (Vaisala Inc. Sigmet Product Line, U.S.A.)

Parameters of the radar are checked and calibrated at the beginning and the end of the intensive observation. Meanwhile, daily checking is performed for (1) frequency, (2) mean output power, (3) pulse width, and (4) PRF (pulse repetition frequency).

During the cruise, the volume scan consisting of 21 PPIs (Plan Position Indicator) is conducted every 10 minutes. A dual PRF mode with the maximum range of 160 km is used for the volume scan. Meanwhile, a surveillance PPI scan is performed every 30 minutes in a single PRF mode with the maximum range of 300 km. At the same time, RHI (Range Height Indicator) scans of the dual PRF mode are also operated whenever detailed vertical structures are necessary in certain azimuth directions. Detailed information for each observational mode is listed in Table 5.2-1. The Doppler radar observation is from Jun. 3 to Jun. 9 during the Leg 1, and from Jun. 12 to Jul. 4 during the Leg 2.

Table 5.2-1 Parameters for each observational mode

	Surveillance PPI	Volume Scan	RHI
Pulse Width	2 (microsec)	0.5 (microsec)	0.5 (microsec)
Scan Speed	18 (deg/sec)	18 (deg/sec)	Automatically determined
PRF	260 (Hz)	900/720 (Hz)	900 (Hz)
Sweep Integration	32 samples	50 samples	32 samples
Ray Spacing	1.0 (deg)	1.0 (deg)	0.2 (deg)
Bin Spacing	250 (m)	250 (m)	250 (m)
Elevation Angle	0.5	0.5, 1.0, 1.8, 2.6, 3.4, 4.2, 5.0, 5.8, 6.7, 7.7, 8.9, 10.3, 12.3, 14.5, 17.1, 20.0, 23.3, 27.0, 31.0, 35.4, 40.0	0.0 to 60.0
Azimuth	Full Circle	Full Circle	Optional
Range	300 (km)	160 (km)	160 (km)

(4) Preliminary results

Figure 5.2-1 shows the time series of the derived parameters from the volume scans during the period when Mirai was staying at or near (12N, 135E). There are interesting features in the figures. Regarding the typhoon formation, for example, large areal coverage, large portion of stratiform area, and continuous rain was observed in Jun.14 to 16 when the typhoon “Leepi” was formed, while the smaller areal coverage and intermittent rain was observed in Jun. 24 to 26 when the typhoon “Rumbia” was formed. On the other hand, the largest rain rate was observed in Jun. 30. In the day, areal coverage was smaller than event in Jun. 14 but most of the rain was from convective portion where generally the radar reflectivity is strong. The further detailed analyses will be studied soon.

(5) Data archive

All data of the Doppler radar observation during this cruise will be submitted to the JAMSTEC Data Management Group (DMG).

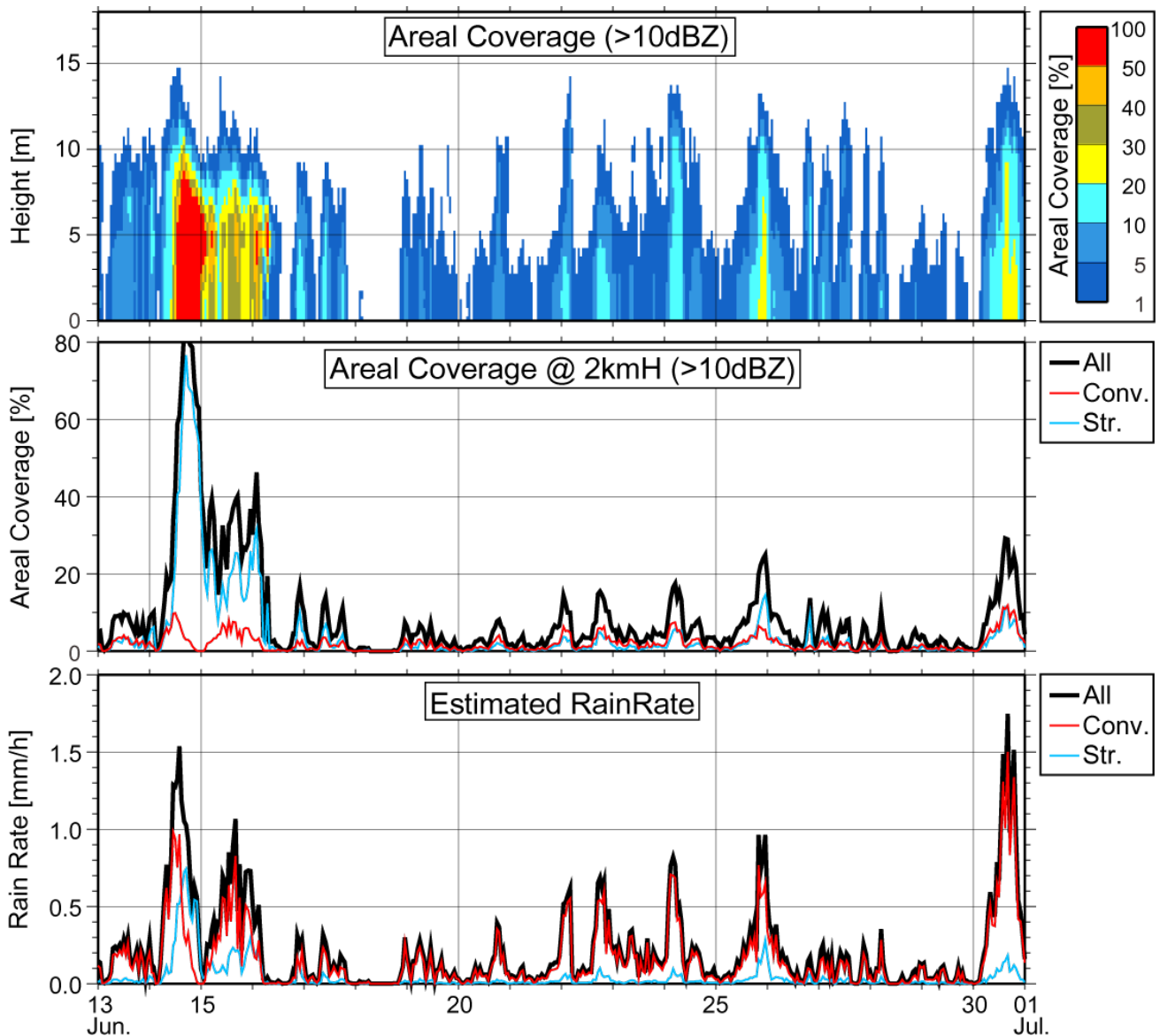


Fig. 5.2-1: Time series of the derived parameters from the Doppler radar data for stationary observation period; (top) vertical profile of the areal coverage of the radar echo greater than 10 dBZ; (middle) areal coverage of the radar echo greater than 10 dBZ; (bottom) estimated rain rate averaged for observed area. The middle and bottom panel shows values for all echo (black), convective portion (red) and stratiform portion (blue), while top panel shows values for all echo. All values are calculated within 100 km in range distance from radar.

5.3 Micro Rain Radar

(1) Personnel

Masaki KATSUMATA (JAMSTEC) - Principal Investigator

(2) Objectives

The micro rain radar (MRR) is a compact vertically-pointing Doppler radar, to detect vertical profiles of rain drop size distribution. The objective of this observation is to understand detailed vertical structure of the precipitating systems.

(3) Methods

The MRR-2 (METEK GmbH) was utilized. The specifications are in Table 5.3-1. The antenna unit was installed at the starboard side of the anti-rolling systems (see Fig. 5.3-1), and wired to the junction box and laptop PC inside the vessel.

The data was averaged and stored every one minute. The vertical profile of each parameter was obtained every 200 meters in range distance (i.e. height) up to 6200 meters, i.e. well beyond the melting layer. The recorded parameters were; Drop size distribution, radar reflectivity, path-integrated attenuation, rain rate, liquid water content and fall velocity.

Fig. 5.3-1: Photo of the antenna unit of MRR (designated by broken circle).



Table 5.3-1: Specifications of the MRR-2.

Transmitter power	50 mW
Operating mode	FM-CW
Frequency	24.230 GHz (modulation 1.5 to 15 MHz)
3dB beam width	1.5 degrees
Spurious emission	< -80 dBm / MHz
Antenna Diameter	600 mm
Gain	40.1 dBi

(4) Preliminary Results

Figure 5.3-2 displays an example of the time-height cross section for one day. The temporal variation reasonably corresponds to the rainrall measured by the Mirai Surface Met sensors (see Section 5.8), disdrometers (see Section 5.4), etc.

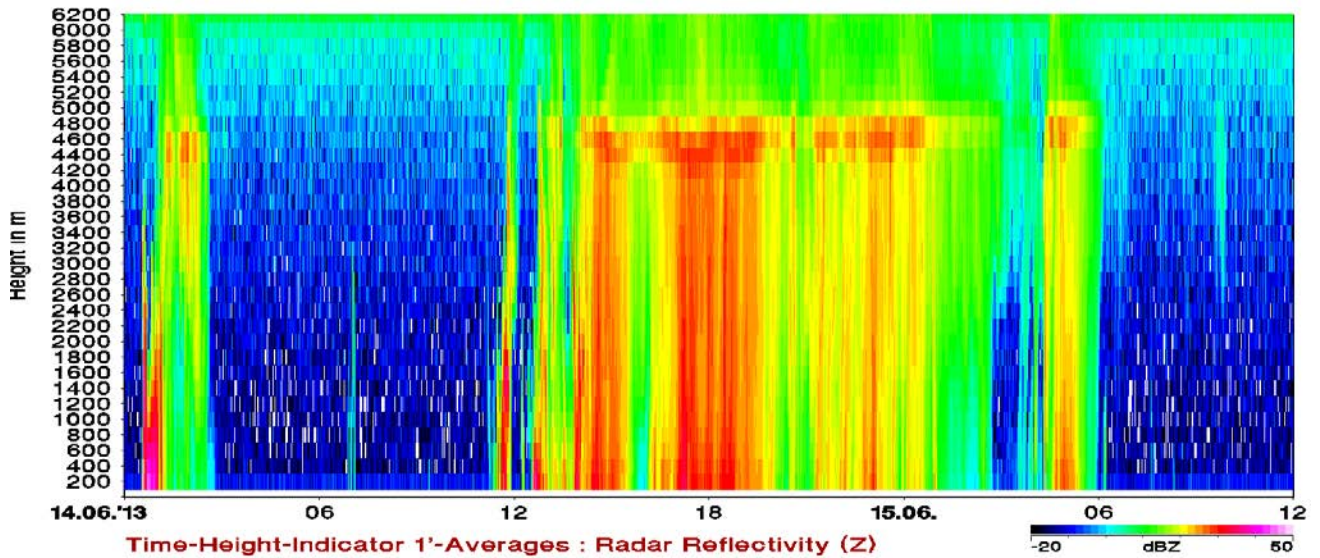


Fig. 5.3-2: An example of the time-height cross section of the radar reflectivity, from 00UTC on Jun. 14 to 12UTC on Jun.15 (36 hours).

(5) Data Archive

All data obtained during this cruise will be submitted to the JAMSTEC Data Management Gropup (DMG).

5.4 Disdrometers

(1) Personnel

Masaki KATSUMATA (JAMSTEC) - Principal Investigator

(2) Objectives

The disdrometer can continuously obtain size distribution of raindrops. The objective of this observation is (a) to reveal microphysical characteristics of the rainfall, depends on the type, temporal stage, etc. of the precipitating clouds, (b) to retrieve the coefficient to convert radar reflectivity (especially from Doppler radar in Section 5.2) to the rainfall amount, and (c) to validate the algorithms and the product of the satellite-borne precipitation radars; TRMM/PR and GPM/DPR.

(3) Methods

Three different types of disdrometers are utilized to obtain better reasonable and accurate value on the moving vessel. All three, and one optical rain gauge, are installed in one place, the starboard side on the roof of the anti-rolling system of R/V Mirai, as in Fig. 5.4-1. The details of the sensors are described below. All the sensors archive data every one minute.

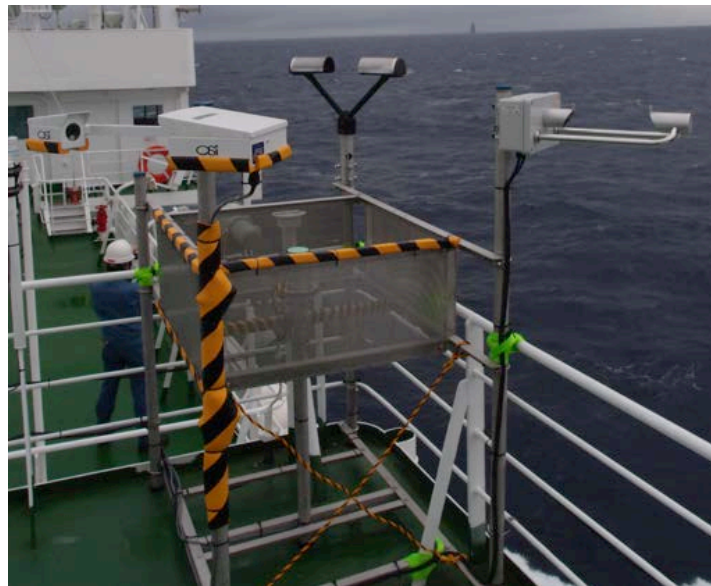


Fig. 5.4-1: The disdrometers, installed on the roof of the anti-rolling tank.

(3-1) Joss-Waldvogel type disdrometer

The “Joss-Waldvogel-type” disdrometer system (RD-80, Disdromet Inc.) (hereafter JW) equipped a microphone on the top of the sensor unit. When a raindrop hit the microphone, the magnitude of induced sound is converted to the size of raindrops. The logging program “DISDRODATA” determines the size as one of the 20 categories as in Table 5.4-1, and accumulates the number of raindrops at each category. The rainfall amount could be also retrieved from the obtained drop size distribution. The number of raindrops in each category, and converted rainfall amount, are recorded every one minute.

(3-2) Laser Precipitation Monitor (LPM) optical disdrometer

The “Laser Precipitation Monitor (LPM)” (Adolf Thies GmbH & Co) is an optical disdrometer. The instrument consists of the transmitter unit which emit the infrared laser, and the receiver unit which detects the intensity of the laser come thru the certain path length in the air. When a precipitating particle fall thru the laser, the received intensity of the laser is reduced. The receiver unit detect the magnitude and the duration of the reduction and then convert them onto particle size and fall speed. The sampling volume, i.e. the size of the laser beam “sheet”, is 20 mm (W) x 228 mm (D) x 0.75 mm (H).

The number of particles are categorized by the detected size and fall speed and counted every minutes. The categories are shown in Table 5.4-2.

(3-3) “Parsivel” optical disdrometer

The “Parsivel” (Adolf Thies GmbH & Co) is another optical disdrometer. The principle is same as the LPM. The sampling volume, i.e. the size of the laser beam “sheet”, is 30 mm (W) x 180 mm (D). The categories are shown in Table 5.4-3.

(3-4) Optical rain gauge

The optical rain gauge, which detect scintillation of the laser by falling raindrops, is installed beside the above three disdrometers to measure the exact rainfall. The ORG-815DR (Optical Scientific Inc.) is utilized with the controlling and recording software (manufactured by Sankosha Co.).

(4) Preliminary Results

Examples of the obtained data are displayed in Fig. 5.4-2. The further analyses for the rainfall amount, drop-size-distribution parameters, etc., will be in future work.

(5) Data Archive

All data obtained during this cruise will be submitted to the JAMSTEC Data Management Group (DMG).

(6) Acknowledgment

The Joss-Waldvogel-type disdrometer is kindly provided by Hydrologic and Atmospheric Research Center (HyARC), Nagoya University. The Parsivel disdrometer and the optical rain gauge are kindly provided by National Institute for Information and Communication Technology (NICT). The operations are supported by Japan Aerospace Exploration Agency (JAXA) Precipitation Measurement Mission (PMM).

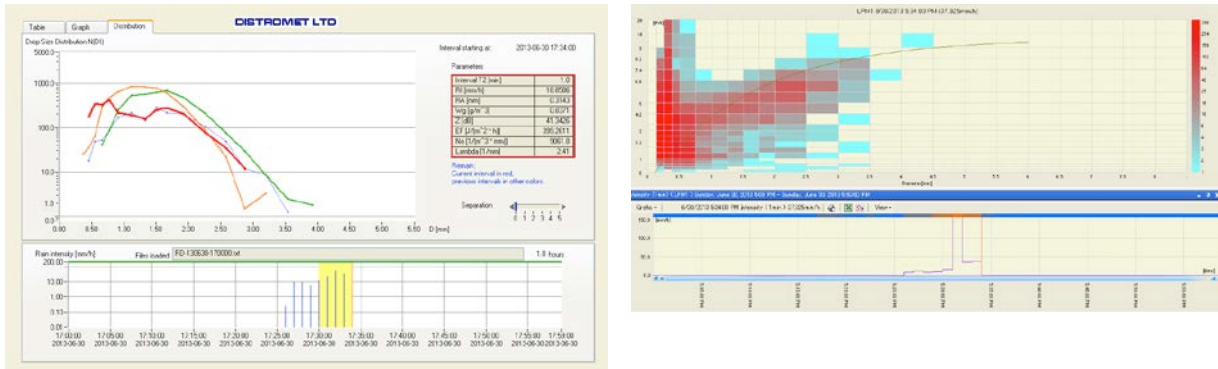


Fig. 5.4-2: Example of the obtained data. (left) Drop size distribution obtained by Joss-Waldvogel-type disdrometer. (right) Histogram of the number of drops categorized by detected drop size and falling speed, obtained by LPM. Both data are at 1734UTC on Jun.29, 2013.

Table 5.4-1: Category number and corresponding size of the raindrop for JW disdrometer.

Category	Corresponding size range [mm]
1	0.313 - 0.405
2	0.405 - 0.505
3	0.505 - 0.696
4	0.696 - 0.715
5	0.715 - 0.827
6	0.827 - 0.999
7	0.999 - 1.232
8	1.232 - 1.429
9	1.429 - 1.582
10	1.582 - 1.748
11	1.748 - 2.077
12	2.077 - 2.441
13	2.441 - 2.727
14	2.727 - 3.011
15	3.011 - 3.385
16	3.385 - 3.704
17	3.704 - 4.127
18	4.127 - 4.573
19	4.573 - 5.145
20	5.145 or larger

Table 5.4-2: Categories of the size and the fall speed for LPM.

Particle Size			Fall Speed		
Class	Diameter [mm]	Class width [mm]	Class	Speed [m/s]	Class width [m/s]
1	≥ 0.125	0.125	1	≥ 0.000	0.200
2	≥ 0.250	0.125	2	≥ 0.200	0.200
3	≥ 0.375	0.125	3	≥ 0.400	0.200
4	≥ 0.500	0.250	4	≥ 0.600	0.200
5	≥ 0.750	0.250	5	≥ 0.800	0.200
6	≥ 1.000	0.250	6	≥ 1.000	0.400
7	≥ 1.250	0.250	7	≥ 1.400	0.400
8	≥ 1.500	0.250	8	≥ 1.800	0.400
9	≥ 1.750	0.250	9	≥ 2.200	0.400
10	≥ 2.000	0.500	10	≥ 2.600	0.400
11	≥ 2.500	0.500	11	≥ 3.000	0.800
12	≥ 3.000	0.500	12	≥ 3.400	0.800
13	≥ 3.500	0.500	13	≥ 4.200	0.800
14	≥ 4.000	0.500	14	≥ 5.000	0.800
15	≥ 4.500	0.500	15	≥ 5.800	0.800
16	≥ 5.000	0.500	16	≥ 6.600	0.800
17	≥ 5.500	0.500	17	≥ 7.400	0.800
18	≥ 6.000	0.500	18	≥ 8.200	0.800
19	≥ 6.500	0.500	19	≥ 9.000	1.000
20	≥ 7.000	0.500	20	≥ 10.000	10.000
21	≥ 7.500	0.500			
22	≥ 8.000	unlimited			

Table 5.4-3: Categories of the size and the fall speed for Parsivel.

Particle Size			Fall Speed		
Class	Average Diameter [mm]	Class spread [mm]	Class	Average Speed [m/s]	Class Spread [m/s]
1	0.062	0.125	1	0.050	0.100
2	0.187	0.125	2	0.150	0.100
3	0.312	0.125	3	0.250	0.100
4	0.437	0.125	4	0.350	0.100
5	0.562	0.125	5	0.450	0.100
6	0.687	0.125	6	0.550	0.100
7	0.812	0.125	7	0.650	0.100
8	0.937	0.125	8	0.750	0.100
9	1.062	0.125	9	0.850	0.100
10	1.187	0.125	10	0.950	0.100
11	1.375	0.250	11	1.100	0.200
12	1.625	0.250	12	1.300	0.200
13	1.875	0.250	13	1.500	0.200
14	2.125	0.250	14	1.700	0.200
15	2.375	0.250	15	1.900	0.200
16	2.750	0.500	16	2.200	0.400
17	3.250	0.500	17	2.600	0.400
18	3.750	0.500	18	3.000	0.400
19	4.250	0.500	19	3.400	0.400
20	4.750	0.500	20	3.800	0.400
21	5.500	1.000	21	4.400	0.800
22	6.500	1.000	22	5.200	0.800
23	7.500	1.000	23	6.000	0.800
24	8.500	1.000	24	6.800	0.800
25	9.500	1.000	25	7.600	0.800
26	11.000	2.000	26	8.800	1.600
27	13.000	2.000	27	10.400	1.600
28	15.000	2.000	28	12.000	1.600
29	17.000	2.000	29	13.600	1.600
30	19.000	2.000	30	15.200	1.600
31	21.500	3.000	31	17.600	3.200
32	24.500	3.000	32	20.800	3.200

5.5 Lidar Observations of Clouds and Aerosols

(1) Personnel

Nobuo Sugimoto	(National Institute for Environmental Studies; NIES)	*not on board
Ichiro Matsui	(NIES)	*not on board
Atsushi Shimizu	(NIES)	*not on board
Tomoaki Nishizawa	(NIES)	*not on board

(2) Objectives

Objectives of the observations in this cruise is to study distribution and optical characteristics of ice/water clouds and marine aerosols using a two-wavelength lidar.

(3) Measured parameters

- Vertical profiles of backscattering coefficient at 532 nm
- Vertical profiles of backscattering coefficient at 1064 nm
- Depolarization ratio at 532 nm

(4) Method

Vertical profiles of aerosols and clouds were measured with a two-wavelength lidar. The lidar employs a Nd:YAG laser as a light source which generates the fundamental output at 1064 nm and the second harmonic at 532 nm. Transmitted laser energy is typically 100 mJ per pulse at 1064 nm and 50 mJ per pulse at 532 nm. The pulse repetition rate is 10 Hz. The receiver telescope has a diameter of 20 cm. The receiver has three detection channels to receive the lidar signals at 1064 nm and the parallel and perpendicular polarization components at 532 nm. An analog-mode avalanche photo diode (APD) is used as a detector for 1064 nm, and photomultiplier tubes (PMTs) are used for 532 nm. The detected signals are recorded with a digital oscilloscope and stored on a hard disk with a computer. The lidar system was installed in the radiosonde container on the compass deck. The container has a glass window on the roof, and the lidar was operated continuously regardless of weather.

(5) Results

Data obtained in this cruise has not been analyzed.

(6) Data archive

The raw and processed data (shown as below) will be archived in NIES and will be submitted to JAMSTEC.

- raw data

lidar signal at 532 nm

lidar signal at 1064 nm

depolarization ratio at 532 nm

temporal resolution 15 min.

vertical resolution 6 m.

- processed data

cloud base height, apparent cloud top height

phase of clouds (ice/water)

cloud fraction

boundary layer height (aerosol layer upper boundary height)

backscatter coefficient of aerosols

particle depolarization ratio of aerosols

5.6 Ceilometer

(1) Personnel

Masaki KATSUMATA (JAMSTEC) *Principal Investigator
Kazuho YOSHIDA (Global Ocean Development Inc., GODI)
Koichi INAGAKI (GODI)
Wataru TOKUNAGA (GODI)
Souichiro SUEYOSHI (GODI)
Ryo KIMURA (MIRAI Crew)

(2) Objectives

The information of cloud base height and the liquid water amount around cloud base is important to understand the process on formation of the cloud. As one of the methods to measure them, the ceilometer observation was carried out.

(3) Parameters

1. Cloud base height [m].
2. Backscatter profile, sensitivity and range normalized at 10 m resolution.
3. Estimated cloud amount [oktas] and height [m]; Sky Condition Algorithm.

(4) Methods

We measured cloud base height and backscatter profile using ceilometer (CL51, VAISALA, Finland) throughout the MR13-03 cruise.

Major parameters for the measurement configuration are as follows;

Laser source:	Indium Gallium Arsenide (InGaAs) Diode Laser
Transmitting center wavelength:	910±10 nm at 25 degC
Transmitting average power:	19.5 mW
Repetition rate:	6.5 kHz
Detector:	Silicon avalanche photodiode (APD)
Measurement range:	0 ~ 15 km 0 ~ 13 km (Cloud detection)
Resolution:	10 meter in full range
Sampling rate:	36 sec
Sky Condition	0, 1, 3, 5, 7, 8 oktas (9: Vertical Visibility) (0: Sky Clear, 1:Few, 3:Scattered, 5-7: Broken, 8: Overcast)

On the archive dataset, cloud base height and backscatter profile are recorded with the resolution of 10 m (33 ft).

(5) Preliminary results

Fig.5.6-1 shows the time series plot of the lowest, second and third cloud base height during the cruise.

(6) Data archives

The raw data obtained during this cruise will be submitted to the Data Management Group (DMG) in JAMSTEC.

(7) Remarks

- 1) The following period, data acquisition was suspended in the territorial waters.
21:30UTC 9 Jun. 2013 to 5:50UTC 12 Jun. 2013 (Republic of Palau)

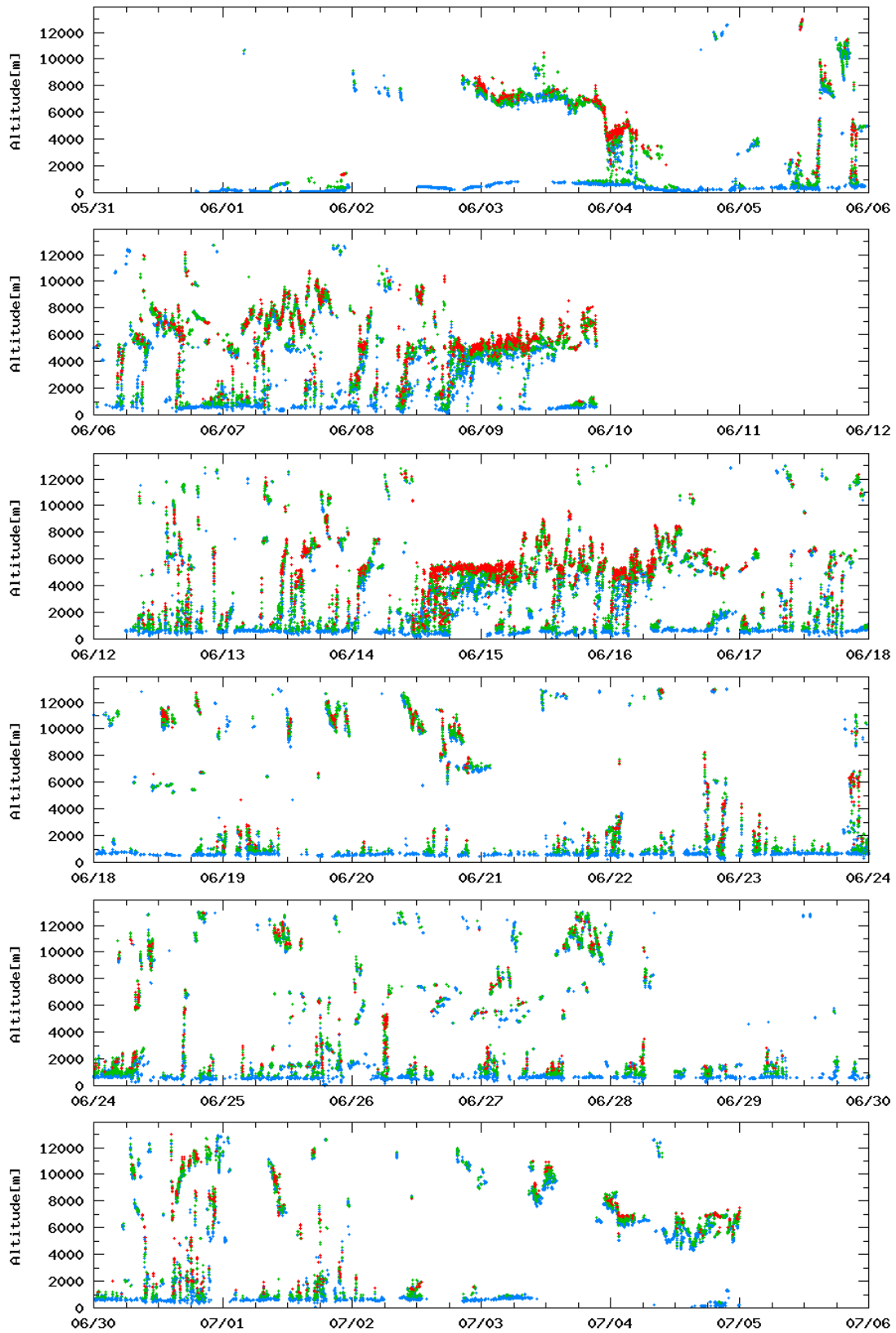


Fig. 5.6-1 First (Blue), 2nd (Green) and 3rd (Red) lowest cloud base height during the cruise.

5.7. Aerosol optical characteristics measured by Ship-borne Sky radiometer

(1) Personnel

Kazuma Aoki (University of Toyama)- Principal Investigator (not on board)

Tadahiro Hayasaka (Tohoku University) - Co-Investigator (not onboard)

(Sky radiometer operation was supported by Global Ocean Development Inc.)

(2) Objectives

Objective of this observation is to study distribution and optical characteristics of marine aerosols by using a ship-borne sky radiometer (POM-01 MKII: PREDE Co. Ltd., Japan). Furthermore, collections of the data for calibration and validation to the remote sensing data were performed simultaneously.

(3) Methods and Instruments

The sky radiometer measures the direct solar irradiance and the solar aureole radiance distribution with seven interference filters (0.34, 0.4, 0.5, 0.675, 0.87, 0.94, and 1.02 μm). Analysis of these data was performed by SKYRAD.pack version 4.2 developed by Nakajima *et al.* 1996.

@ Measured parameters

- Aerosol optical thickness at five wavelengths (400, 500, 675, 870 and 1020 nm)
- Ångström exponent
- Single scattering albedo at five wavelengths
- Size distribution of volume (0.01 μm – 20 μm)

GPS provides the position with longitude and latitude and heading direction of the vessel, and azimuth and elevation angle of the sun. Horizon sensor provides rolling and pitching angles.

(4) Preliminary results

Only data collection were performed onboard. At the time of writing, the data obtained in this cruise are under post-cruise processing at University of Toyama.

(5) Data archives

Aerosol optical data are to be archived at University of Toyama (K.Aoki, SKYNET/SKY: <http://skyrad.sci.u-toyama.ac.jp/>) after the quality check and will be submitted to JAMSTEC.

5.8 Surface Meteorological Observations

(1) Personnel

Masaki KATSUMATA (JAMSTEC) * Principal Investigator
Kazuho YOSHIDA (Global Ocean Development Inc., GODI)
Koichi INAGAKI (GODI)
Wataru TOKUNAGA (GODI)
Souichiro SUEYOSHI (GODI)
Ryo KIMURA (Mirai Crew)

(2) Objectives

Surface meteorological parameters are observed as a basic dataset of the meteorology. These parameters provide the temporal variation of the meteorological condition surrounding the ship.

(3) Methods

Surface meteorological parameters were observed throughout the MR13-03 cruise. The observation was carried out following periods,

Leg1: 7:00 UTC 31 May, 2013 to 21:30 UTC 9 June, 2013

Leg2: 5:50 UTC 12 June, 2013 to **:**:** UTC 6 July, 2013

During this cruise, we used two systems for the observation.

i. MIRAI Surface Meteorological observation (SMet) system

Instruments of SMet system are listed in Table 5.8-1 and measured parameters are listed in Table 5.8-2. Data were collected and processed by KOAC-7800 weather data processor made by Koshin-Denki, Japan. The data set consists of 6-second averaged data.

ii. Shipboard Oceanographic and Atmospheric Radiation (SOAR) measurement system

SOAR system designed by BNL (Brookhaven National Laboratory, USA) consists of major five parts.

- a) Portable Radiation Package (PRP) designed by BNL – short and long wave downward radiation.
- b) Zeno Meteorological (Zeno/Met) system designed by BNL – wind, air temperature, relative humidity, pressure, and rainfall measurement.
- c) “SeaSnake” the floating thermistor designed by BNL – skin sea surface temperature (SSST) measurement.
- d) Photosynthetically Available Radiation (PAR) sensor manufactured by Biospherical Instruments Inc (USA) – PAR measurement
- e) Scientific Computer System (SCS) developed by NOAA (National Oceanic and Atmospheric Administration, USA) – centralized data acquisition and logging of all data sets.

SCS recorded PRP data every 6 seconds, Zeno/Met data every 10 seconds and SeaSnake data every second. PAR data was recorded every 3 seconds. Instruments and their locations are listed in Table 5.8-3 and measured parameters are listed in Table 5.8-4.

SeaSnake has two thermistor probes and output voltage was converted to SSST by Steinhart-Hart equation with following coefficients led from the calibration data.

Sensor	a	b	c
T02-005 Sensor:	8.10910e-04	-2.11601e-04	-7.11351e-08
T02-100 Sensor:	8.32296e-04	-2.08699e-04	-7.87005e-08
T03-005 Sensor:	8.08796e-04	-2.11595e-04	-7.23218e-08
T03-100 Sensor:	7.95085e-04	-2.14805e-04	-6.77238e-08

$$y = a + b * x + c * x**3$$

$$x = \log (1 / ((Vref / V - 1) * R2 - R1))$$

$$T = 1 / y - 273.15$$

Vref = 2500[mV], R1=249000[Ω], R2=1000[Ω]
T: Temperature [degC], V: Sensor output voltage [mV]

For the quality control as post processing, we checked the following sensors, before and after the cruise.

- i. Young Rain gauge (SMet and SOAR)
Inspect of the linearity of output value from the rain gauge sensor to change Input value by adding fixed quantity of test water.
- ii. Barometer (SMet and SOAR)
Comparison with the portable barometer value, PTB220, VAISALA
- iii. Thermometer (air temperature and relative humidity) (SMet and SOAR)
Comparison with the portable thermometer value, HMP41/45, VAISALA
- iv. SeaSnake SSST
SeaSnake thermistor probe was calibrated by the bath equipped with SBE-3 plus, Sea-Bird Electronics, Inc.

(4) Preliminary results

Figure 5.8-1 shows the time series of the following parameters;

- Wind (SMet)
- Air temperature (SOAR)
- Relative humidity (SOAR)
- Precipitation (SOAR, rain gauge)
- Short/long wave radiation (SOAR)
- Barometric Pressure (SMet)
- Sea surface temperature (SMet)
- Significant wave height (SMet)

Figure 5.8-2 shows the time series of SSST compared to sea surface temperature (TSG).

(5) Data archives

These meteorological data will be submitted to the Data Management Group (DMG) of JAMSTEC just after the cruise.

(6) Remarks

1. The following period, data acquisition was suspended in the territorial waters.
21:30UTC 9 Jun. 2013 to 5:50UTC 12 Jun. 2013 (Republic of Palau)

2. The following periods, SST data was available.
 5:29UTC 02 Jun. 2013 - 21:30UTC 9 Jun.. 2013
 5:50UTC 12 Jun. 2013 - 0:27UTC 5 Jul. 2013

3. The following periods, SeaSnake SSST data was available.
 [T02-005 & T02-100 sensor]
 7:35UTC 13 Jun. 2013 - 1:04UTC 14 Jun. 2013
 7:37UTC 14 Jun. 2013 - 6:23UTC 15 Jun. 2013
 7:33UTC 15 Jun. 2013 - 19:46UTC 15 Jun. 2013

 [T03-005 & T03-100 sensor]
 1:24UTC 17 Jun. 2013 - 3:47UTC 21 Jun. 2013
 4:35UTC 21 Jun. 2013 - 0:44UTC 30 Jun. 2013

4. The following time, increasing of SMet capacitive rain gauge data were invalid
 4:21UTC 2 Jun. 2013
 6:56UTC 20 Jun. 2013
 7:11UTC 20 Jun. 2013
 1:54UTC 29 Jun. 2013
 17:21UTC 3 Jul. 2013

Table 5.8-1: Instruments and installation locations of MIRAI Surface Meteorological observation system

Sensors	Type	Manufacturer	Location (altitude from surface)
Anemometer	KE-500	Koshin Denki, Japan	foremast (24 m)
Tair/RH	HMP155	Vaisala, Finland with	
43408 Gill aspirated radiation shield		R.M. Young, USA	compass deck (21 m) starboard side and port side
Thermometer: SST	RFN1-0	Koshin Denki, Japan	4th deck (-1m, inlet -5m)
Barometer	Model-370	Setra System, USA	captain deck (13 m) weather observation room
Rain gauge	50202	R. M. Young, USA	compass deck (19 m)
Optical rain gauge	ORG-815DS	Osi, USA	compass deck (19 m)
Radiometer (short wave)	MS-802	Eko Seiki, Japan	radar mast (28 m)
Radiometer (long wave)	MS-202	Eko Seiki, Japan	radar mast (28 m)
Wave height meter	WM-2	Tsurumi-seiki, Japan	bow (10 m)

Table 5.8-2: Parameters of MIRAI Surface Meteorological observation system

Parameter	Units	Remarks
1 Latitude	degree	
2 Longitude	degree	
3 Ship's speed	knot	Mirai log, DS-30 Furuno
4 Ship's heading	degree	Mirai gyro, TG-6000, Tokimec
5 Relative wind speed	m/s	6sec./10min. averaged
6 Relative wind direction	degree	6sec./10min. averaged
7 True wind speed	m/s	6sec./10min. averaged

8 True wind direction	degree	6sec./10min. averaged
9 Barometric pressure	hPa	adjusted to sea surface level 6sec. averaged
10 Air temperature (starboard side)	degC	6sec. averaged
11 Air temperature (port side)	degC	6sec. averaged
12 Dewpoint temperature (starboard side)	degC	6sec. averaged
13 Dewpoint temperature (port side)	degC	6sec. averaged
14 Relative humidity (starboard side)	%	6sec. averaged
15 Relative humidity (port side)	%	6sec. averaged
16 Sea surface temperature	degC	6sec. averaged
17 Rain rate (optical rain gauge)	mm/hr	hourly accumulation
18 Rain rate (capacitive rain gauge)	mm/hr	hourly accumulation
19 Down welling shortwave radiation	W/m2	6sec. averaged
20 Down welling infra-red radiation	W/m2	6sec. averaged
21 Significant wave height (bow)	m	hourly
22 Significant wave height (aft)	m	hourly
23 Significant wave period (bow)	second	hourly
24 Significant wave period (aft)	second	hourly

Table 5.8-3: Instruments and installation locations of SOAR system

<u>Sensors (Zeno/Met)</u>	<u>Type</u>	<u>Manufacturer</u>	<u>Location (altitude from surface)</u>
Anemometer	05106	R.M. Young, USA	foremast (25 m)
Tair/RH with 43408 Gill aspirated radiation shield	HMP45A	Vaisala, Finland R.M. Young, USA	foremast (23 m)
Barometer with 61002 Gill pressure port	61302V	R.M. Young, USA R.M. Young, USA	foremast (23 m)
Rain gauge	50202	R.M. Young, USA	foremast (24 m)
Optical rain gauge	ORG-815DA	Osi, USA	foremast (24 m)
<u>Sensors (PRP)</u>	<u>Type</u>	<u>Manufacturer</u>	<u>Location (altitude from surface)</u>
Radiometer (short wave)	PSP	Epply Labs, USA	foremast (25 m)
Radiometer (long wave)	PIR	Epply Labs, USA	foremast (25 m)
Fast rotating shadowband radiometer		Yankee, USA	foremast (25 m)
<u>Sensor (PAR)</u>	<u>Type</u>	<u>Manufacturer</u>	<u>Location (altitude from surface)</u>
PAR sensor	PUV-510	Biospherical Instrum -ents Inc., USA	Navigation deck (18m)
<u>Sensors (SeaSnake)</u>	<u>Type</u>	<u>Manufacturer</u>	<u>Location (altitude from surface)</u>
Thermistor	107	Campbell Scientific, USA	bow, 5m extension (0 m)

Table 5.8-4: Parameters of SOAR system

Parameter	Units	Remarks
1 Latitude	degree	
2 Longitude	degree	
3 SOG	knot	
4 COG	degree	
5 Relative wind speed	m/s	
6 Relative wind direction	degree	
7 Barometric pressure	hPa	
8 Air temperature	degC	
9 Relative humidity	%	
10 Rain rate (optical rain gauge)	mm/hr	
11 Precipitation (capacitive rain gauge)	mm	reset at 50 mm
12 Down welling shortwave radiation	W/m ²	
13 Down welling infra-red radiation	W/m ²	
14 Defuse irradiance	W/m ²	
15 "SeaSnake" raw data	mV	
16 SSST (SeaSnake)	degC	
17 PAR	microE/cm ² /sec	

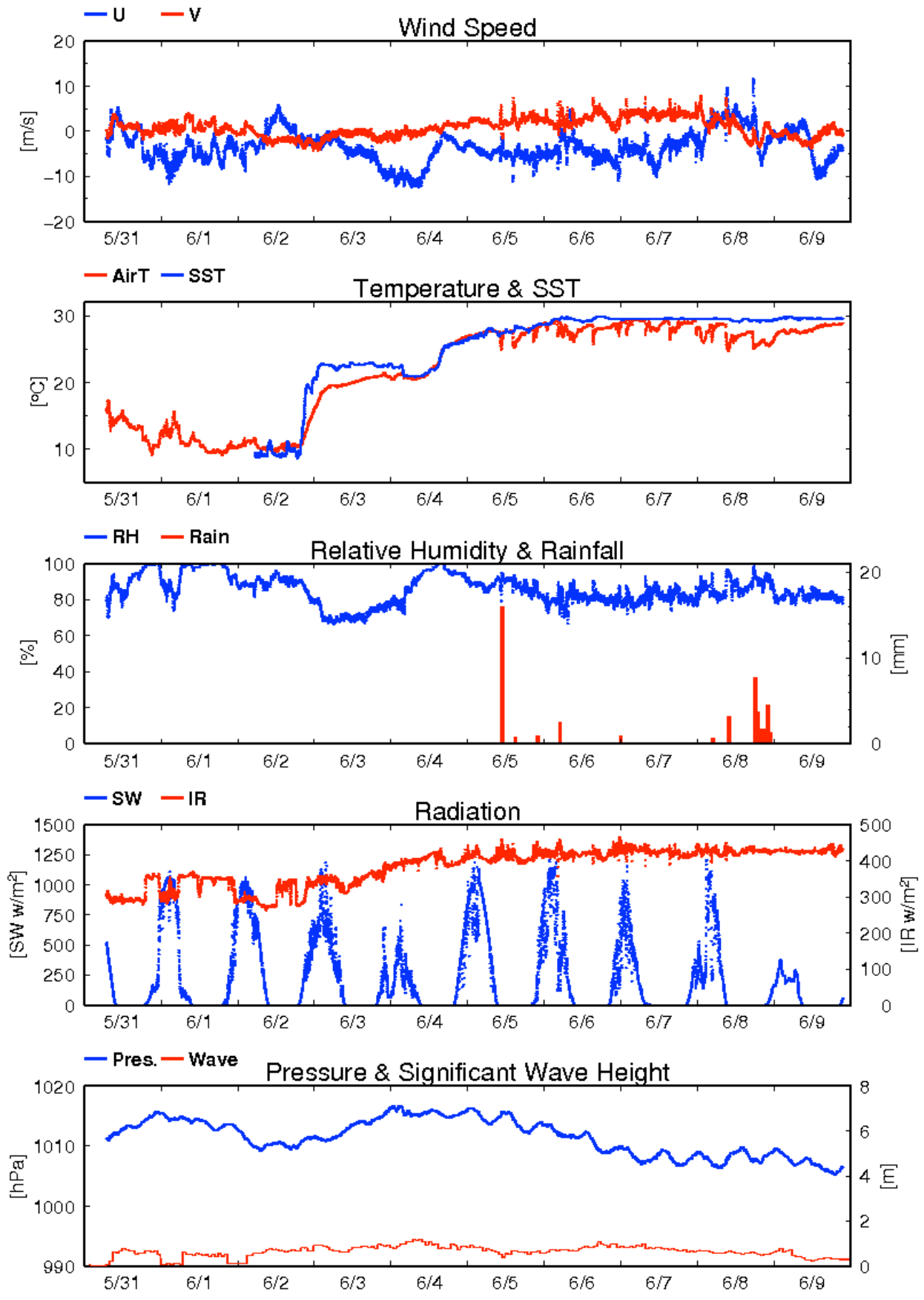


Fig. 5.8-1 Time series of surface meteorological parameters during the cruise

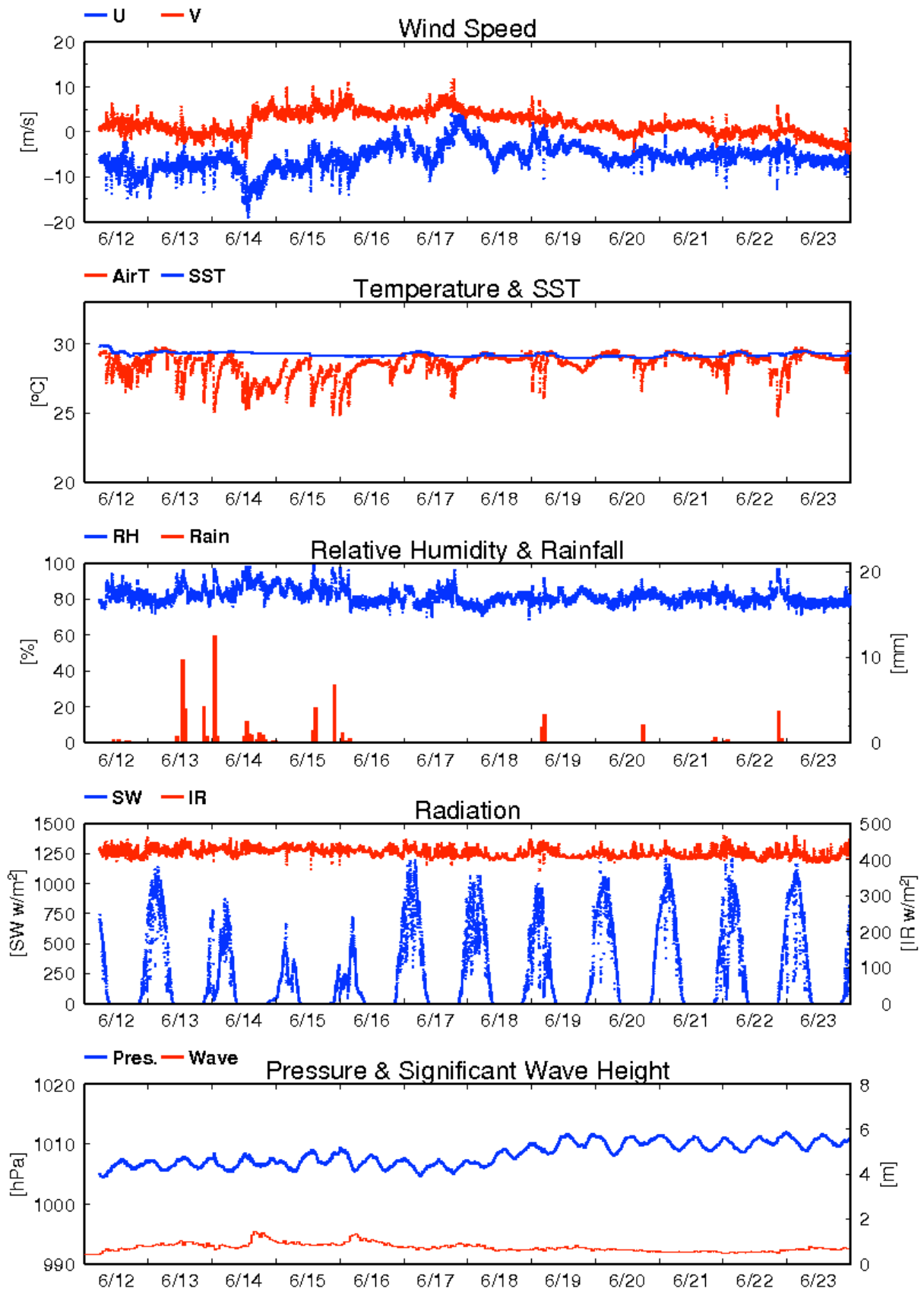


Fig. 5.8-1 (Continued)

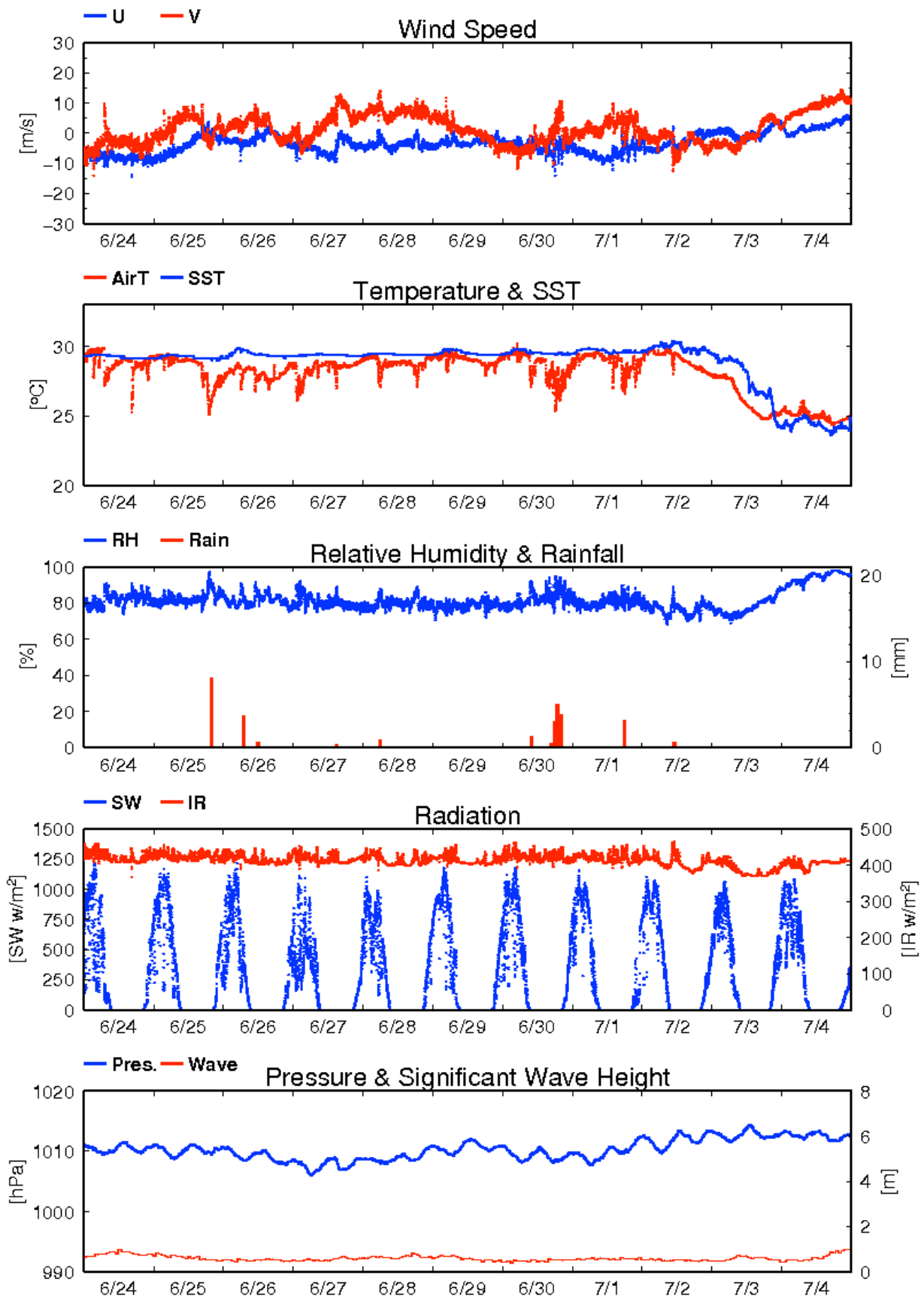


Fig. 5.8-1 (Continued)

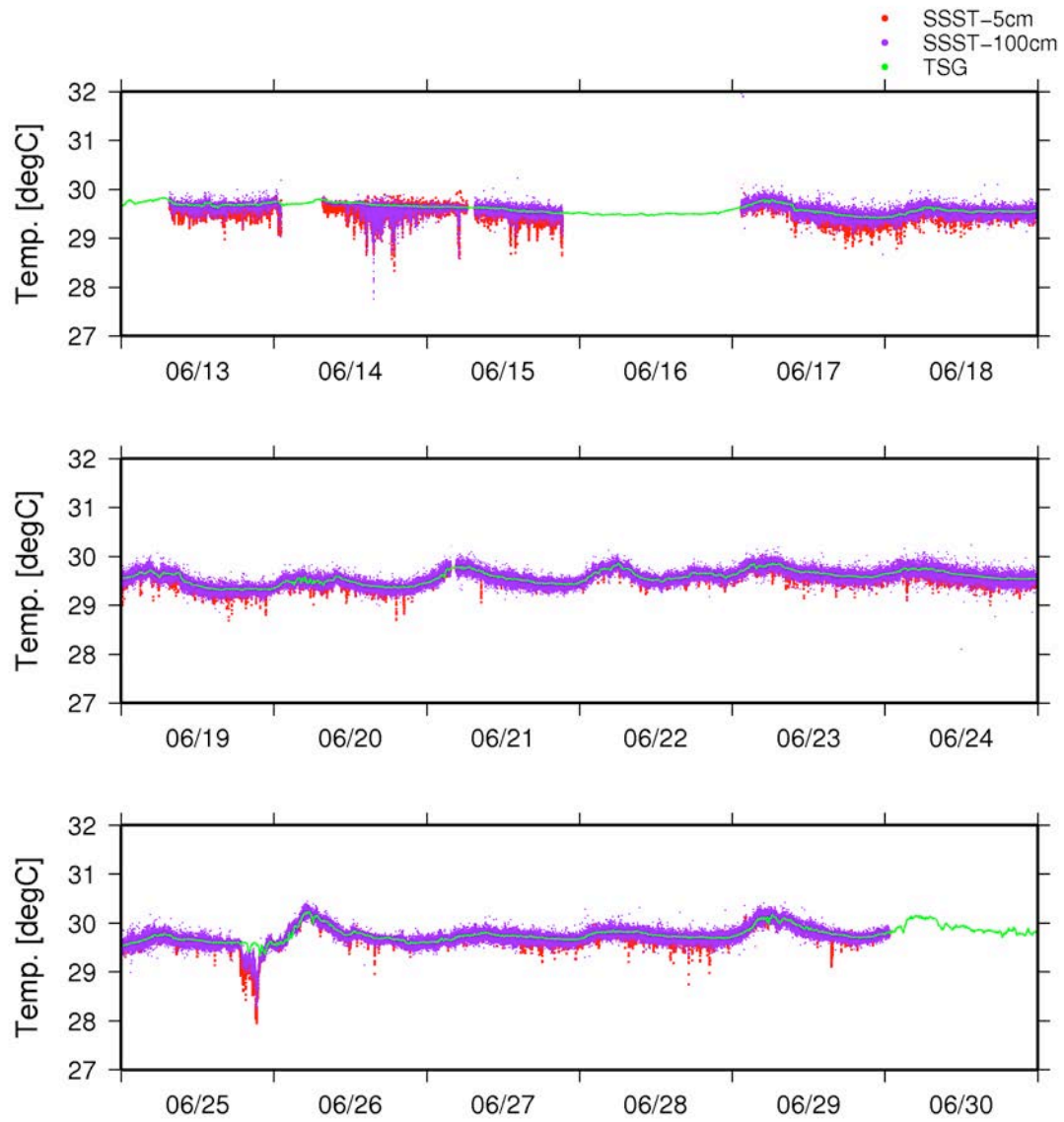


Fig. 5.8-2 Time series of and Skin Sea Surface Temperature(SSST) and Sea Surface Temperature (TSG) during Leg2 cruise.

5.9 Continuous monitoring of surface seawater

(1) Personnel (*: Leg-1, **: Leg-2, ***: Leg-1+2)

Masaki KATSUMATA*** (JAMSTEC) - Principal Investigator
Hideki YAMAMOTO** (MWJ)
Misato KUWAHARA*** (MWJ) - Operation Leader (Leg-1+2)

(2) Objective

Our purpose is to obtain salinity, temperature, dissolved oxygen, and fluorescence data continuously in near-sea surface water.

(3) Instruments and Methods

The Continuous Sea Surface Water Monitoring System (Marine Works Japan Co. Ltd.) has four sensors and automatically measures salinity, temperature, dissolved oxygen and fluorescence in near-sea surface water every one minute. This system is located in the “*sea surface monitoring laboratory*” and connected to shipboard LAN-system. Measured data, time, and location of the ship were stored in a data management PC. The near-surface water was continuously pumped up to the laboratory from about 4 m water depth and flowed into the system through a vinyl-chloride pipe. The flow rate of the surface seawater was adjusted to be $4.5 \text{ dm}^3 \text{ min}^{-1}$. Specifications of the each sensor in this system are listed below.

a. Instruments

Software

Seamoni-kun Ver.1.40

Sensors

Specifications of the each sensor in this system are listed below.

Temperature and Conductivity sensor

Model: SBE-45, SEA-BIRD ELECTRONICS, INC.
Serial number: 4557820-0319
Measurement range: Temperature -5 to +35 °C
Conductivity 0 to 7 S m⁻¹
Initial accuracy: Temperature 0.002 °C
Conductivity 0.0003 S m⁻¹
Typical stability (per month): Temperature 0.0002 °C
Conductivity 0.0003 S m⁻¹
Resolution: Temperatures 0.0001 °C
Conductivity 0.00001 S m⁻¹

Bottom of ship thermometer

Model: SBE 38, SEA-BIRD ELECTRONICS, INC.
Serial number: 3852788-0457
Measurement range: -5 to +35 °C
Initial accuracy: ±0.001 °C
Typical stability (per 6 month): 0.001 °C
Resolution: 0.00025 °C

Dissolved oxygen sensor

Model: OPTODE 3835, AANDERAA Instruments.
 Serial number: 1519
 Measuring range: 0 - 500 $\mu\text{mol dm}^{-3}$
 Resolution: $<1 \mu\text{mol dm}^{-3}$
 Accuracy: $<8 \mu\text{mol dm}^{-3}$ or 5% whichever is greater
 Settling time: $<25 \text{ s}$

Fluorometer

Model: C3, TURNER DESIGNS
 Serial number: 2300384

(4) Preliminary Result

Start date and time and End one of monitoring are shown in Table 5.9-1.

Table 5.9-1 Events list of the surface seawater monitoring during MR13-03

System Date [UTC]	System Time [UTC]	Events	Remarks
2013/06/02	06:30	All the measurements started and data was available.	Leg 1 start.
2013/06/09	21:30	All the measurements stopped.	Leg 1 end.
2013/06/12	06:10	All the measurements started and data was available.	Leg 2 start.
2013/07/5	00:00	All the measurements stopped.	Leg 2 end.

We took the surface water samples to compare sensor data with bottle data of salinity and dissolved oxygen and fluorescence.

The results are shown in Fig.5.9 -1~3. All the salinity samples were analyzed by the Guideline 8400B “AUTOSAL”, and dissolve oxygen samples were analyzed by Winkler method, and fluorescence were measured by Turner Design 10-AU-005. The figure plotted only data flag 1. It is excluded Questionable data of flag 3.

The water sample quality flag definitions are given in Table 5.9-2.(cf. WHP Data Reporting Requirements)

Table 5.9-2 Water sample quality flag difinitions

Flag Value	Difinition
1	Sample for this measurement was drawn from water bottle but analysis not received
2	Acceptable measurement.
3	Questionable measurement.
4	Bad measurement
5	Not reported.
6	Mean of replicate measurements.
7	Manual chromatographic peak measurement
8	Irregular digital chromatographic peak integration.
9	Sample not drawn for this measurement from this bottle.

(5) Chlorophyll a measurements of bottle data by fluorometric determination

a. sample list

Bottle sample was took from water sampling line of this equipment with silicon tube tip of PFA. Sampling date and time ,flag and remarks were listed in table 5.9-3.

Table 5.9-3. List of sampling date ,time ,flag and remarks.

seq.	Sampling date and time(UTC)	Flag	Remarks
1	2013/06/03 06:47	3	see ※ the marginal space.
2	2013/06/04 02:34	3	see ※ the marginal space.
3	2013/06/05 04:52	3	see ※ the marginal space.
4	2013/06/06 02:44	3	see ※ the marginal space.
5	2013/06/07 02:34	3	see ※ the marginal space.
6	2013/06/08 02:20	3	see ※ the marginal space.
7	2013/06/09 02:46	3	see ※ the marginal space.
8	2013/06/13 00:13	3	see ※ the marginal space.
9	2013/06/13 23:43	3	see ※ the marginal space.
10	2013/06/14 23:41	3	see ※ the marginal space.
11	2013/06/15 23:45	3	see ※ the marginal space.
12	2013/06/16 23:41	1	
13	2013/06/17 23:49	1	
14	2013/06/18 23:44	1	
15	2013/06/19 23:41	1	
16	2013/06/20 23:43	1	
17	2013/06/21 23:44	1	
18	2013/06/22 23:43	1	
19	2013/06/23 23:46	1	
20	2013/06/24 23:42	1	
21	2013/06/25 23:46	1	
22	2013/06/26 23:44	1	
23	2013/06/27 23:45	1	
24	2013/06/28 23:42	1	
25	2013/06/29 23:44	1	
26	2013/06/30 23:52	1	
27	2013/07/01 23:44	1	
28	2013/07/02 23:41	1	

※ 11data as flag 3, 2013/06/03 06:47 ~ 2013/06/15 23:45, using filtered seawater was contaminated. It was not acceptable concentration of high Chlorophyll a. These samples collected in this range has a

possibility of having estimated highly 0.00 - 0.02 ug/l.

b. Instruments and Methods

Water samples (0.5L) for total chlorophyll *a* were filtered (<0.02 MPa) through 25mm-diameter Whatman GF/F filter. Phytoplankton pigments retained on the filters were immediately extracted in a polypropylene tube with 7 ml of N,N-dimethylformamide (Suzuki and Ishimaru, 1990). Those tubes were stored at -20°C under the dark condition to extract chlorophyll *a* for 24 hours or more.

Fluorescences of each sample were measured by Turner Design fluorometer (10-AU-005), which was calibrated against a pure chlorophyll *a* (Sigma-Aldrich Co.). We applied fluorometric determination for the samples of total chl-*a*: “Non-acidification method” (Welschmeyer, 1994). Analytical conditions of each method were listed in table 5.9-4.

Table 5.9-4 Analytical conditions of “Non-acidification method”

item	Wave length, type
Excitation filter (nm)	436
Emission filter (nm)	680
Lamp	Blue Mercury Vapor

(6) Data archive

These data obtained in this cruise will be submitted to the Data Management Group (DMG) of JAMSTEC, and will be opened to the public via “R/V Mirai Data Web Page” in JAMSTEC home page.

(7) Reference

Suzuki, R., and T. Ishimaru (1990), An improved method for the determination of phytoplankton chlorophyll using N, N-dimethylformamide, *J. Oceanogr. Soc. Japan*, 46, 190-194.

Welschmeyer, N. A. (1994), Fluorometric analysis of chlorophyll *a* in the presence of chlorophyll *b* and pheopigments. *Limnol. Oceanogr.* 39, 1985-1992.

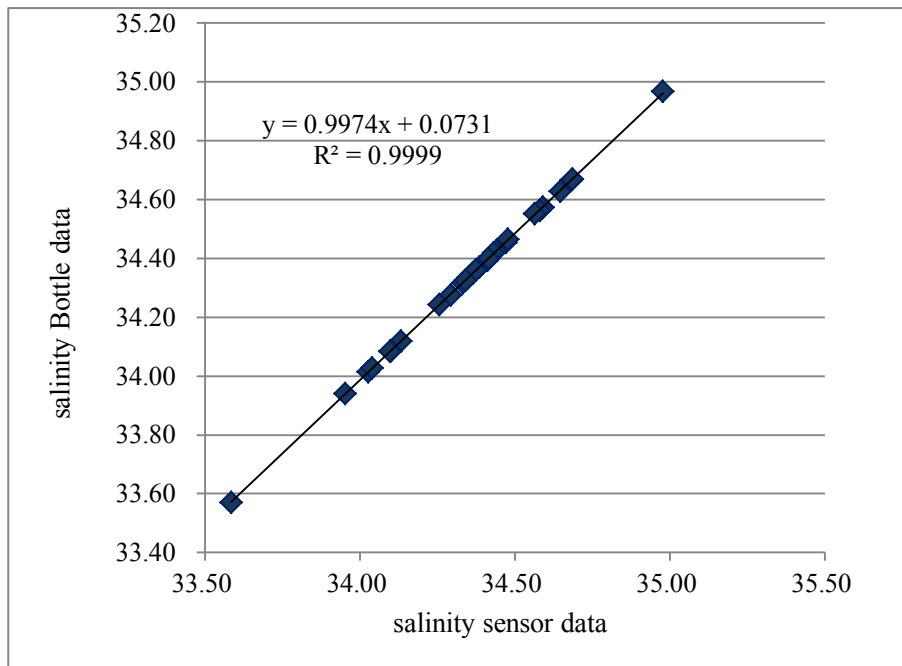


Fig.5.9-1 Correlation of salinity between sensor data and bottle data.

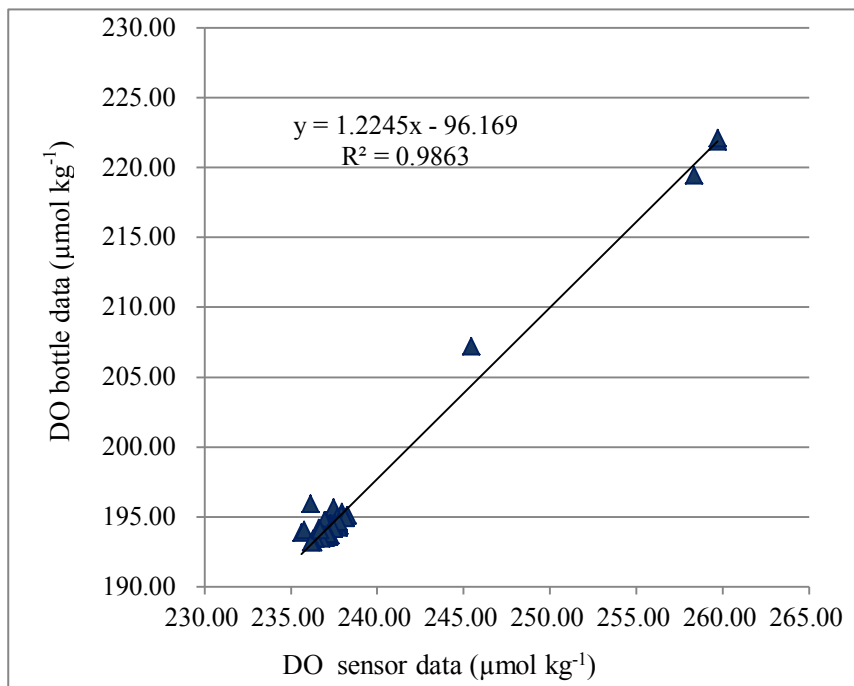


Fig.5.9-2 Correlation of dissolved oxygen between sensor data and bottle data.

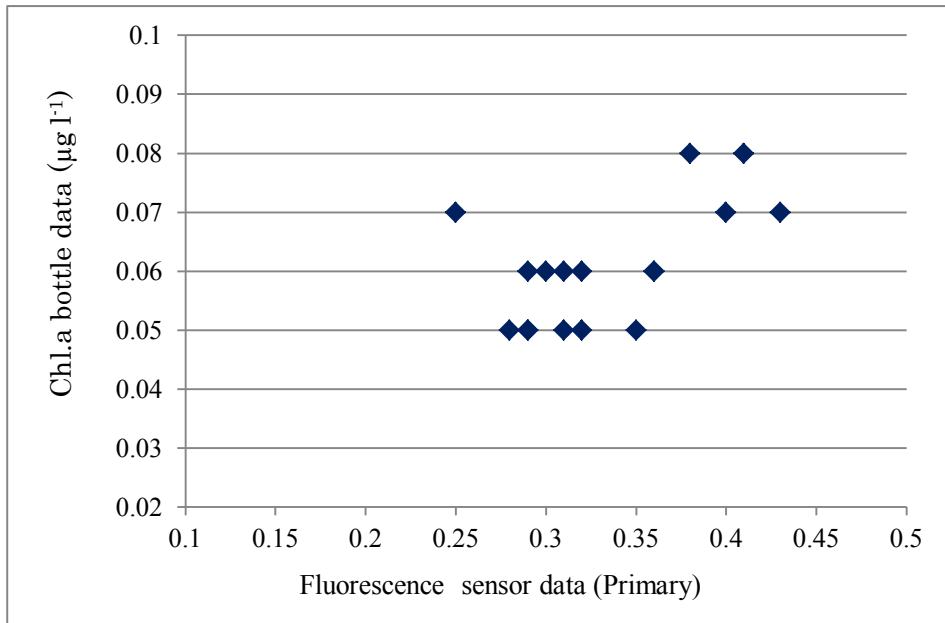


Fig.5.9-3 Correlation of fluorescence between sensor data and bottle data.
 (It was excluded Questionable of 11 data from plotting in fig..)

5.10 CTDO profiling

(1) Personnel (*: Leg-1, **: Leg-2, ***: Leg-1+2)

Masaki Katsumata *** (JAMSTEC) *Principal Investigator (Leg-1+2)
Rei Ito** (MWJ) *Operation Leader (Leg-2)
Hiroshi Matsunaga*** (MWJ) *Operation Leader (Leg-1)
Shinsuke Toyoda** (MWJ)
Hiroki Ushiromura*** (MWJ)
Masahiro Orui** (MWJ)
Sonoka Wakatsuki** (MWJ)

(2) Objective

Investigation of oceanic structure and water sampling.

(3) Parameters

Temperature (Primary and Secondary)
Conductivity (Primary and Secondary)
Pressure
Dissolved Oxygen (Primary and Secondary)
Fluorescence

(4) Methods

CTD/Carousel Water Sampling System, which is a 36-position Carousel water sampler (CWS) with Sea-Bird Electronics, Inc. CTD (SBE9plus), was used during this cruise. 12-liter Niskin Bottles were used for sampling seawater. The sensors attached on the CTD were temperature (Primary and Secondary), conductivity (Primary and Secondary), pressure, dissolved oxygen (Primary and Secondary) and fluorescence. Salinity was calculated by measured values of pressure, conductivity and temperature. The CTD/CWS was deployed from starboard on working deck.

The CTD raw data were acquired on real time using the Seasave-Win32 (ver.7.22.5) provided by Sea-Bird Electronics, Inc. and stored on the hard disk of the personal computer. Seawater was sampled during the up cast by sending fire commands from the personal computer. We usually stop for 60 seconds to stabilize then fire.

140 casts of CTD measurements were conducted (Table 5.10.1).

Data processing procedures and used utilities of SBE Data Processing-Win32 (ver.7.22.5a) and SEASOFT were as follows:

(The process in order)

DATCNV: Convert the binary raw data to engineering unit data. DATCNV also extracts bottle information where scans were marked with the bottle confirm bit during acquisition. The duration was set to 3.0 seconds, and the offset was set to 0.0 seconds.

BOTTLESUM: Create a summary of the bottle data. The data were averaged over 3.0 seconds.

ALIGNCTD: Convert the time-sequence of sensor outputs into the pressure sequence to ensure that all calculations were made using measurements from the same parcel of water. Dissolved oxygen data are systematically delayed with respect to depth mainly because of the long time constant of the dissolved oxygen sensor and of an additional delay from the transit time of water in the pumped plumbing line. This delay was compensated by 5 seconds advancing dissolved oxygen sensor output (dissolved oxygen voltage) relative to the temperature data.

WILDEDIT: Mark extreme outliers in the data files. The first pass of WILDEDIT obtained an accurate estimate of the true standard deviation of the data. The data were read in blocks of 1000 scans. Data greater than 10 standard deviations were flagged. The second pass computed a standard deviation over the same 1000 scans excluding the flagged values. Values greater than 20 standard deviations were marked bad. This process was applied to pressure, depth, temperature, conductivity and dissolved oxygen voltage.

CELLTM: Remove conductivity cell thermal mass effects from the measured conductivity. Typical values used were thermal anomaly amplitude $\alpha = 0.03$ and the time constant $1/\beta = 7.0$.

FILTER: Perform a low pass filter on pressure with a time constant of 0.15 second. In order to produce zero phase lag (no time shift) the filter runs forward first then backward

WFILTER: Perform a median filter to remove spikes in the fluorescence data. A median value was determined by 49 scans of the window.

SECTIONU (original module of SECTION): Select a time span of data based on scan number in order to reduce a file size. The minimum number was set to be the starting time when the CTD package was beneath the sea-surface after activation of the pump. The maximum number of was set to be the end time when the package came up from the surface.

LOOPEDIT: Mark scans where the CTD was moving less than the minimum velocity of 0.0 m/s (traveling backwards due to ship roll).

DERIVE: Compute dissolved oxygen (SBE43).

BINAVG: Average the data into 1-dbar pressure bins.

BOTTOMCUT (original module): Deletes discontinuous scan bottom data, if it's created by BINAVG.

DERIVE: Compute salinity, potential temperature, and sigma-theta.

SPLIT: Separate the data from an input .cnv file into down cast and up cast files.

Configuration file:

MR1303A.xmlcon: N01M01 - 12M040
MR1303B.xmlcon: 12M042 - 12M048
MR1303C.xmlcon: 12M049 - 12M082
MR1303D.xmlcon: 12M083 - 12M104
MR1303E.xmlcon: 12M105 - 12M138

Specifications of the sensors are listed below.

CTD: SBE911plus CTD system

Under water unit:

SBE9plus (S/N 09P27443-0677, Sea-Bird Electronics, Inc.)

Pressure sensor: Digiquartz pressure sensor (S/N 79511)

Calibrated Date: 07 May 2013

Temperature sensors:

Primary: SBE03-04/F (S/N 031525, Sea-Bird Electronics, Inc.)

Calibrated Date: 31 Aug. 2012

Secondary: SBE03Plus (S/N 03P2730, Sea-Bird Electronics, Inc.)

Calibrated Date: 18 Apr. 2012

Conductivity sensors:

Primary: SBE04C (S/N 042240, Sea-Bird Electronics, Inc.)

Calibrated Date: 26 Jun. 2012

Secondary: SBE04-04/0 (S/N 041172, Sea-Bird Electronics, Inc.)

Calibrated Date: 18 Aug. 2012

Dissolved Oxygen sensor:

Primary: SBE43 (S/N 430205, Sea-Bird Electronics, Inc.)

Calibrated Date: 08 Dec. 2012

Secondary: SBE43 (S/N 43221, Sea-Bird Electronics, Inc.)

Calibrated Date: 19 Oct. 2012

Fluorescence:

Chlorophyll Fluorometer (S/N 3054, Seapoint Sensors, Inc.)

Gain setting: 30X, 0-5 µg/l

Calibrated Date: None
Offset : 0.000
Used Cast: from N01M01 to 12M082

Chlorophyll Fluorometer (S/N 2936, Seapoint Sensors, Inc.)
Gain setting: 30X, 0-5 µg/l
Calibrated Date: None
Offset : 0.000
Used Cast: from 12M083 to 12M138

Carousel water sampler:
SBE32 (S/N 3227443-0391, Sea-Bird Electronics, Inc.)

Deck unit: SBE11plus (S/N 11P9833-0344, Sea-Bird Electronics, Inc.)

(5) Preliminary Results

During this cruise, 140casts of CTD observation were carried out. Date, time and locations of the CTD casts are listed in Table 5.10.1.

The time series contours of primary temperature, salinity, dissolved oxygen and fluorescence with pressure are shown in Fig. 5.10.1. Vertical profile (down cast) of primary temperature, salinity and dissolved oxygen with pressure are shown in the appendix.

In some casts, we judged noise or spike in the data. These were as follows.

- 12M014: Primary dissolved oxygen down 91 dbar - down 336 dbar (bad data)
- 12M034: Primary dissolved oxygen down 339 dbar - down 357 dbar (bad data)
- 12M053: Primary dissolved oxygen down 276 dbar - down 280 dbar (spike)
- 12M082: Primary dissolved oxygen down 227 dbar - 228 dbar (spike)
- 12M086: Primary dissolved oxygen down 87 dbar - down 276dbar (bad data)
- 12M107: Primary dissolved oxygen down 156 dbar - down 159 dbar (bad data)
- 12M134: Primary dissolved oxygen down 144 dbar - 145 dbar (spike)

(6) Remarks

Station of 12M041 was canceled by winch trouble.

CTD secondary temperature, secondary conductivity, secondary salinity, secondary dissolved oxygen voltage and secondary oxygen were shifted from up cast 492 - up cast 504 dbar in station of 12M119.

CTD fluorescence data was shifted from down cast surface to up to about 100 dbar from 12M003 to 12M007, 12M009 to 12M040, 12M042, 12M044 to 12M079 and 12M081 to 12M082. Therefore we exchanged fluorescence sensor from 12M083 to 12M138. So fluorescence data from 12M003 to 12M082 indicate to use up cast data.

(7) Data archive

All raw and processed data will be submitted to the Data Management Group (DMG), JAMSTEC, and will be opened to public via "R/V MIRAI Data Web Page" in JAMSTEC home page.

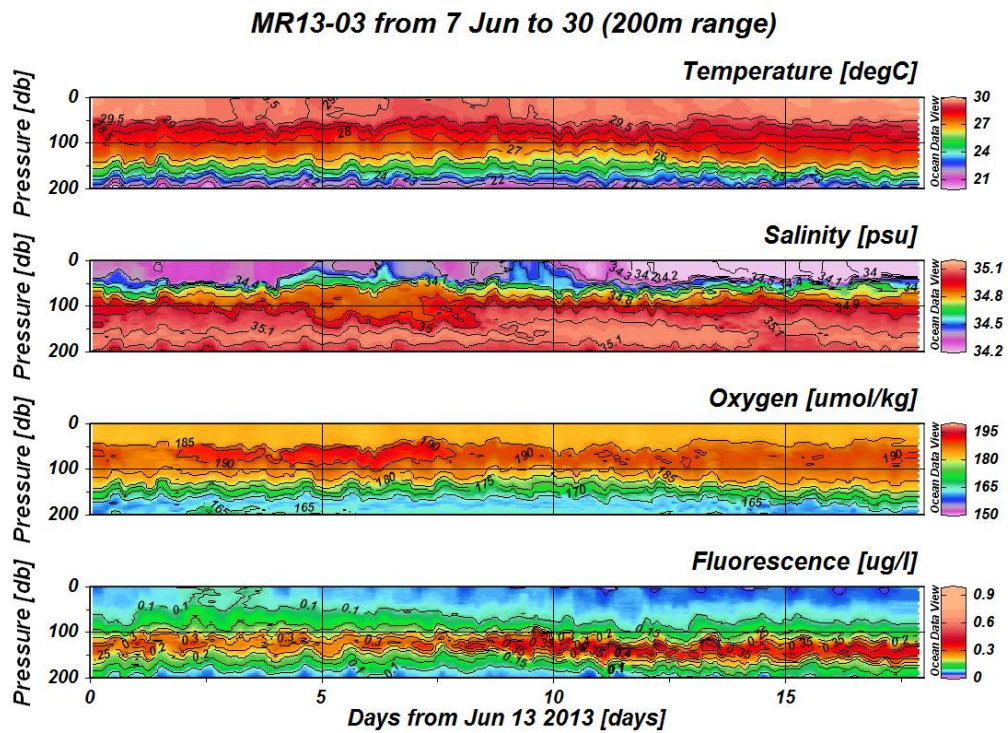
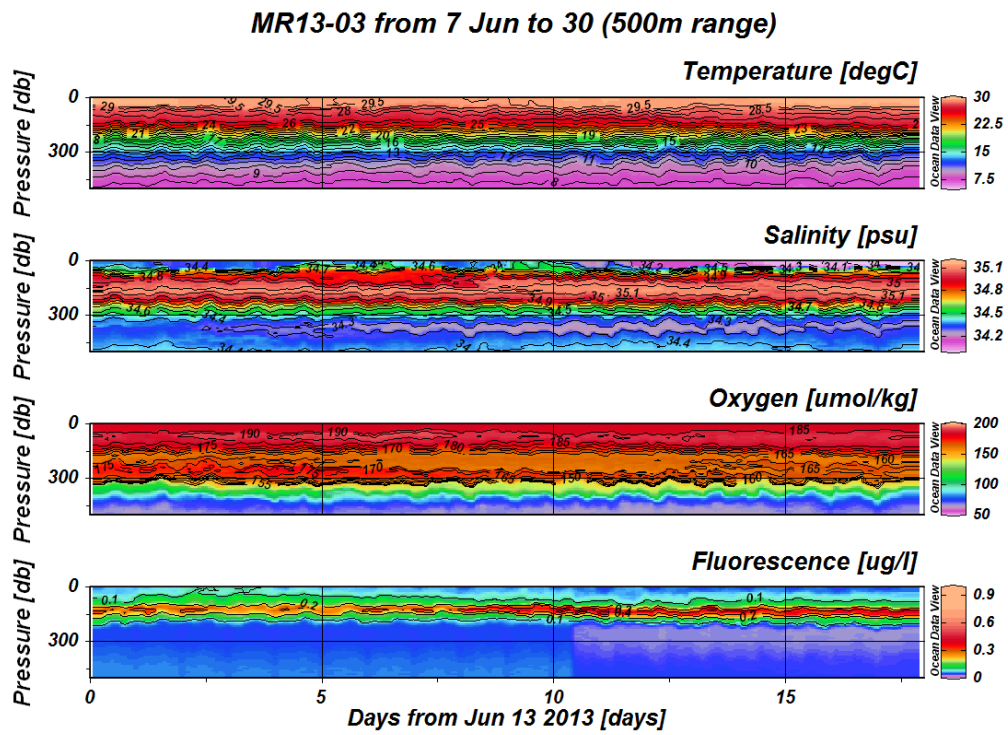


Fig. 5.10.1 the time series contours shows temperature, salinity, dissolved oxygen and fluorescence.

Upper shows 500m range and lower shows 200m range, respectively. (Fluorescence data from 12M003 to 12M082 stations used up cast data. Other than stations used down cast data.)

Table 5.10-1 MR13-03 CTD cast table

Stnnbr	Castno	Date(UTC)	Time(UTC)		Bottom Position		Depth	Wire Out	HT Above Bottom	Max Depth	Max Pressure	CTD Filename	Remark
		(mmddy)	Start	End	Latitude	Longitude							
N01	1	060713	06:51	07:17	15-59.96N	135-00.08E	4672.0	498.9	-	501.4	505.0	N01M01	Water sampling cast
N02	1	060713	23:37	00:13	13-00.06N	135-00.12E	5260.0	1000.1	-	999.8	1008.0	N02M01	Water sampling cast
N03	1	060813	16:10	16:32	10-00.02N	135-00.04E	4189.0	498.7	-	500.5	504.0	N03M01	Water sampling cast
12	1	061313	05:40	06:02	12-00.06N	134-59.82E	4615.0	499.0	-	500.5	504.0	12M001	Start fixed observation
12	2	061313	08:42	09:04	11-59.82N	135-00.03E	4604.0	501.4	-	502.5	506.0	12M002	
12	3	061313	11:42	12:03	11-59.78N	134-59.94E	4611.0	501.2	-	501.5	505.0	12M003	
12	4	061313	14:42	15:03	11-59.48N	134-59.85E	4620.0	501.1	-	501.5	505.0	12M004	
12	5	061313	17:42	18:04	11-59.64N	135-00.52E	4572.0	500.7	-	501.5	505.0	12M005	
12	6	061313	20:42	21:05	12-00.25N	135-00.19E	4604.0	499.0	-	501.5	505.0	12M006	
12	7	061313	23:41	00:40	12-00.23N	135-00.82E	4558.0	1000.1	-	1000.8	1009.0	12M007	Water sampling cast
12	8	061413	02:38	03:00	11-59.80N	135-00.14E	4604.0	500.7	-	502.5	506.0	12M008	
12	9	061413	05:42	06:04	11-59.40N	134-59.60E	4620.0	499.6	-	500.5	504.0	12M009	
12	10	061413	08:43	09:05	11-59.21N	134-59.03E	4609.0	499.6	-	501.5	505.0	12M010	
12	11	061413	12:02	12:22	11-58.10N	134-58.20E	4580.0	502.2	-	501.5	505.0	12M011	
12	12	061413	14:47	15:09	11-58.75N	134-58.70E	4605.0	499.2	-	500.5	504.0	12M012	
12	13	061413	17:44	18:07	11-59.69N	134-59.75E	4617.0	499.6	-	500.5	504.0	12M013	
12	14	061413	20:44	21:07	11-59.77N	134-59.56E	4618.0	500.3	-	502.5	506.0	12M014	
12	15	061413	23:40	00:37	11-59.94N	134-59.74E	4618.0	1003.3	-	1002.8	1011.0	12M015	Water sampling cast
12	16	061513	02:40	03:00	12-00.47N	135-00.37E	4614.0	498.9	-	500.5	504.0	12M016	
12	17	061513	05:56	06:18	11-59.92N	135-00.21E	4591.0	500.0	-	501.5	505.0	12M017	
12	18	061513	08:42	09:04	12-00.57N	135-00.22E	4607.0	499.6	-	501.5	505.0	12M018	
12	19	061513	11:40	11:59	12-01.10N	135-00.07E	4626.0	502.5	-	502.5	506.0	12M019	
12	20	061513	14:51	15:13	11-59.89N	135-00.49E	4579.0	499.0	-	501.5	505.0	12M020	
12	21	061513	17:42	18:04	11-59.98N	134-59.84E	4614.0	499.2	-	500.5	504.0	12M021	
12	22	061513	20:41	21:04	11-59.26N	134-59.51E	4623.0	500.7	-	500.5	504.0	12M022	
12	23	061513	23:41	00:38	11-59.89N	135-00.28E	4582.0	1007.9	-	1001.8	1010.0	12M023	Water sampling cast
12	24	061613	02:40	03:01	11-59.69N	135-00.13E	4603.0	500.3	-	500.5	504.0	12M024	
12	25	061613	05:54	06:15	12-00.15N	135-00.47E	4589.0	501.1	-	501.5	505.0	12M025	
12	26	061613	08:40	09:02	11-59.99N	135-00.19E	4589.0	499.6	-	500.5	504.0	12M026	

12	27	061613	11:42	12:02	11-59.46N	134-59.42E	4621.0	501.2	-	501.5	505.0	12M027	
12	28	061613	14:42	15:03	11-59.71N	135-00.78E	4552.0	499.6	-	500.5	504.0	12M028	
12	29	061613	17:43	18:05	11-59.59N	135-00.72E	4531.0	500.0	-	502.5	506.0	12M029	
12	30	061613	20:41	21:04	11-59.72N	135-00.36E	4585.0	499.2	-	501.5	505.0	12M030	
12	31	061613	23:40	00:40	11-59.54N	134-59.91E	4615.0	1001.8	-	1001.8	1010.0	12M031	Water sampling cast
12	32	061713	02:41	03:02	11-59.31N	135-00.18E	4613.0	500.1	-	500.5	504.0	12M032	
12	33	061713	05:40	06:01	11-59.85N	134-59.85E	4614.0	499.8	-	500.5	504.0	12M033	
12	34	061713	08:42	09:04	12-00.36N	134-59.81E	4618.0	501.6	-	501.5	505.0	12M034	
12	35	061713	11:41	12:01	12-00.82N	135-00.10E	4619.0	501.8	-	502.5	506.0	12M035	
12	36	061713	14:45	15:06	12-00.04N	134-58.99E	4606.0	500.9	-	502.5	506.0	12M036	
12	37	061713	17:41	18:03	12-00.03N	134-59.77E	4619.0	500.0	-	501.5	505.0	12M037	
12	38	061713	21:13	21:36	12-00.15N	134-59.84E	4617.0	499.0	-	500.5	504.0	12M038	
12	39	061813	00:05	01:12	11-59.93N	135-00.15E	4601.0	1003.8	-	1001.8	1010.0	12M039	Water sampling cast
12	40	061813	02:40	03:01	12-00.09N	135-00.15E	4602.0	501.1	-	501.5	505.0	12M040	
12	42	061813	08:42	09:06	11-59.53N	135-00.59E	4575.0	504.0	-	501.5	505.0	12M042	
12	43	061813	11:40	12:01	11-59.07N	135-00.59E	4601.0	504.2	-	501.5	505.0	12M043	
12	44	061813	14:41	15:03	11-58.75N	135-00.35E	4603.0	501.6	-	502.5	506.0	12M044	
12	45	061813	17:42	18:03	11-59.27N	135-00.71E	4582.0	499.4	-	500.5	504.0	12M045	
12	46	061813	20:43	21:06	11-59.10N	135-00.76E	4402.0	500.5	-	502.5	506.0	12M046	
12	47	061813	23:43	00:49	11-59.68N	135-00.17E	4602.0	1000.0	-	1001.8	1010.0	12M047	Water sampling cast
12	48	061913	02:41	03:02	11-59.27N	134-59.04E	4614.0	501.1	-	502.5	506.0	12M048	
12	49	061913	05:43	06:04	11-59.45N	135-00.03E	4620.0	500.1	-	500.5	504.0	12M049	
12	50	061913	08:42	09:03	12-00.52N	134-59.72E	4617.0	500.0	-	501.5	505.0	12M050	
12	51	061913	11:41	12:02	12-01.06N	134-59.83E	4628.0	500.9	-	501.5	505.0	12M051	
12	52	061913	14:42	15:02	11-59.91N	134-59.16E	4616.0	502.2	-	500.5	504.0	12M052	
12	53	061913	17:41	18:02	12-00.04N	134-59.87E	4623.0	501.4	-	501.5	505.0	12M053	
12	54	061913	20:42	21:05	12-00.27N	135-00.37E	4592.0	500.9	-	501.5	505.0	12M054	
12	55	061913	23:41	00:40	11-59.95N	134-59.66E	4618.0	1003.1	-	1000.8	1009.0	12M055	Water sampling cast
12	56	062013	02:39	03:00	12-00.16N	135-00.41E	4584.0	502.0	-	500.5	504.0	12M056	
12	57	062013	05:40	06:01	11-59.94N	135-00.08E	4602.0	503.4	-	501.5	505.0	12M057	
12	58	062013	08:41	09:03	11-59.61N	135-00.19E	4593.0	500.3	-	501.5	505.0	12M058	
12	59	062013	11:56	12:16	11-59.78N	134-59.90E	4611.0	500.9	-	501.5	505.0	12M059	
12	60	062013	14:40	15:01	12-00.05N	135-00.07E	4610.0	500.9	-	502.5	506.0	12M060	
12	61	062013	17:48	18:09	11-59.50N	135-00.01E	4617.0	500.0	-	500.5	504.0	12M061	

12	62	062013	20:42	21:04	11-59.55N	134-59.86E	4623.0	500.5	-	502.5	506.0	12M062	
12	63	062013	23:41	00:40	11-59.80N	134-59.88E	4615.0	1002.3	-	1000.8	1009.0	12M063	Water sampling cast
12	64	062113	02:41	03:02	11-59.80N	134-59.87E	4618.0	502.3	-	502.5	506.0	12M064	
12	65	062113	05:39	05:59	11-59.90N	134-59.96E	4609.0	499.6	-	500.5	504.0	12M065	
12	66	062113	08:42	09:02	12-00.24N	134-59.81E	4619.0	501.2	-	501.5	505.0	12M066	
12	67	062113	11:41	12:01	12-00.87N	134-59.96E	4623.0	501.6	-	501.5	505.0	12M067	
12	68	062113	14:42	15:03	11-59.76N	134-59.81E	4619.0	500.3	-	501.5	505.0	12M068	
12	69	062113	17:45	18:06	12-00.06N	134-59.91E	4618.0	502.9	-	502.5	506.0	12M069	
12	70	062113	20:40	21:02	12-00.41N	134-59.93E	4618.0	500.5	-	501.5	505.0	12M070	
12	71	062113	23:42	00:40	11-59.66N	134-59.82E	4618.0	1000.9	-	1000.8	1009.0	12M071	Water sampling cast
12	72	062213	02:42	03:02	12-00.43N	134-59.86E	4618.0	503.3	-	502.5	506.0	12M072	
12	73	062213	05:40	06:01	12-00.01N	134-59.89E	4614.0	498.3	-	500.5	504.0	12M073	
12	74	062213	08:40	09:01	11-59.97N	134-59.98E	4614.0	500.3	-	501.5	505.0	12M074	
12	75	062213	11:40	12:00	11-59.99N	135-00.17E	4595.0	502.3	-	502.5	506.0	12M075	
12	76	062213	14:42	15:02	12-00.01N	134-59.87E	4619.0	500.3	-	500.5	504.0	12M076	
12	77	062213	17:33	17:54	12-00.11N	134-59.91E	4611.0	500.0	-	500.5	504.0	12M077	
12	78	062213	20:41	21:03	12-00.59N	134-59.89E	4622.0	499.8	-	502.5	506.0	12M078	
12	79	062213	23:42	00:40	12-00.26N	134-59.95E	4612.0	1002.3	-	1001.8	1010.0	12M079	Water sampling cast
12	80	062313	02:38	02:58	12-00.22N	134-59.99E	4609.0	501.4	-	502.5	506.0	12M080	
12	81	062313	05:38	05:58	12-00.09N	135-00.04E	4608.0	499.4	-	500.5	504.0	12M081	
12	82	062313	08:40	09:02	12-00.16N	134-59.88E	4613.0	501.4	-	500.5	504.0	12M082	
12	83	062313	11:41	12:03	12-00.83N	134-59.29E	4604.0	500.9	-	501.5	505.0	12M083	Exchanged fluorescence sensor
12	84	062313	14:40	15:00	11-59.87N	134-59.63E	4620.0	500.5	-	501.5	505.0	12M084	
12	85	062313	17:40	18:01	12-00.07N	134-59.74E	4622.0	500.5	-	500.5	504.0	12M085	
12	86	062313	20:41	21:03	12-00.06N	134-59.68E	4618.0	498.3	-	500.5	504.0	12M086	
12	87	062313	23:43	00:44	12-00.01N	134-59.69E	4623.0	1000.7	-	1000.8	1009.0	12M087	Water sampling cast
12	88	062413	02:42	03:04	12-00.32N	135-00.00E	4615.0	500.5	-	501.5	505.0	12M088	
12	89	062413	05:39	06:01	12-00.06N	134-59.93E	4613.0	499.8	-	501.5	505.0	12M089	
12	90	062413	08:41	09:02	11-59.89N	134-59.68E	4618.0	499.8	-	502.5	506.0	12M090	
12	91	062413	11:40	12:01	11-59.97N	134-59.63E	4620.0	502.7	-	501.5	505.0	12M091	
12	92	062413	14:40	15:01	12-00.04N	134-59.73E	4617.0	501.6	-	501.5	505.0	12M092	
12	93	062413	17:40	18:00	12-00.20N	134-59.77E	4617.0	503.8	-	502.5	506.0	12M093	
12	94	062413	20:42	21:05	12-00.24N	134-59.56E	4620.0	499.0	-	501.5	505.0	12M094	

12	95	062413	23:42	00:43	12-00.33N	134-59.75E	4618.0	1001.6	-	1001.8	1010.0	12M095	Water sampling cast
12	96	062513	02:42	03:03	12-00.75N	134-59.75E	4622.0	500.5	-	500.5	504.0	12M096	
12	97	062513	05:41	06:07	12-00.12N	134-59.95E	4610.0	501.8	-	502.5	506.0	12M097	
12	98	062513	08:43	09:04	12-00.05N	134-59.89E	4613.0	500.5	-	501.5	505.0	12M098	
12	99	062513	11:41	12:02	12-01.05N	135-00.08E	4624.0	500.9	-	502.5	506.0	12M099	
12	100	062513	14:41	15:02	11-59.76N	134-59.98E	4619.0	500.7	-	502.5	506.0	12M100	
12	101	062513	17:39	18:00	12-00.17N	135-00.15E	4607.0	501.1	-	501.5	505.0	12M101	
12	102	062513	20:42	21:03	12-00.38N	135-00.05E	4616.0	500.5	-	500.5	504.0	12M102	
12	103	062513	23:43	00:45	11-59.99N	134-59.95E	4610.0	1002.7	-	1000.8	1009.0	12M103	Water sampling cast
12	104	062613	02:38	02:59	12-00.40N	135-00.10E	4611.0	503.3	-	500.5	504.0	12M104	
12	105	062613	05:40	06:00	12-00.02N	134-59.97E	4609.0	502.5	-	502.5	506.0	12M105	
12	106	062613	08:42	09:02	12-00.04N	134-59.80E	4618.0	501.4	-	500.5	504.0	12M106	
12	107	062613	11:42	12:02	11-59.90N	134-59.50E	4619.0	501.6	-	501.5	505.0	12M107	
12	108	062613	14:44	15:04	11-59.89N	134-59.77E	4624.0	501.1	-	501.5	505.0	12M108	
12	109	062613	17:39	18:00	12-00.26N	134-59.78E	4620.0	500.3	-	500.5	504.0	12M109	
12	110	062613	20:41	21:03	12-00.47N	134-59.84E	4619.0	500.1	-	500.5	504.0	12M110	
12	111	062613	23:44	00:44	12-00.11N	134-59.70E	4620.0	1001.8	-	1000.8	1009.0	12M111	Water sampling cast
12	112	062713	02:42	03:02	12-00.50N	134-59.67E	4618.0	500.9	-	501.5	505.0	12M112	
12	113	062713	05:40	06:06	12-00.17N	134-59.79E	4629.0	503.6	-	501.5	505.0	12M113	
12	114	062713	08:41	09:08	12-00.22N	134-59.66E	4619.0	501.1	-	502.5	506.0	12M114	
12	115	062713	11:40	12:00	12-01.08N	134-59.14E	4585.0	500.3	-	501.5	505.0	12M115	
12	116	062713	14:40	15:00	12-00.05N	134-59.78E	4628.0	499.6	-	501.5	505.0	12M116	
12	117	062713	17:41	18:03	11-59.88N	134-59.95E	4610.0	500.0	-	501.5	505.0	12M117	
12	118	062713	20:42	21:03	12-00.10N	134-59.84E	4617.0	500.3	-	501.5	505.0	12M118	
12	119	062713	23:42	00:41	12-00.21N	134-59.88E	4618.0	1006.0	-	1000.8	1009.0	12M119	Water sampling cast
12	120	062813	02:42	03:02	12-00.33N	135-00.07E	4614.0	502.3	-	501.5	505.0	12M120	
12	121	062813	05:40	06:00	12-00.21N	134-59.97E	4614.0	500.3	-	501.5	505.0	12M121	
12	122	062813	08:41	09:01	12-00.03N	134-59.88E	4616.0	501.1	-	501.5	505.0	12M122	
12	123	062813	11:41	12:01	12-00.25N	134-59.61E	4622.0	500.0	-	501.5	505.0	12M123	
12	124	062813	14:41	15:01	11-59.78N	134-59.97E	4611.0	499.6	-	500.5	504.0	12M124	
12	125	062813	17:41	18:01	11-59.46N	134-59.94E	4616.0	501.2	-	502.5	506.0	12M125	
12	126	062813	20:42	21:03	11-59.54N	135-00.32E	4583.0	499.2	-	501.5	505.0	12M126	
12	127	062813	23:42	00:42	11-59.77N	135-00.02E	4605.0	1000.7	-	1000.8	1009.0	12M127	Water sampling cast
12	128	062913	02:41	03:02	12-00.13N	134-59.70E	4624.0	501.2	-	500.5	504.0	12M128	

12	129	062913	05:40	06:00	12-00.07N	134-59.84E	4615.0	500.9	-	501.5	505.0	12M129	
12	130	062913	08:41	09:02	12-00.21N	134-59.92E	4614.0	500.5	-	500.5	504.0	12M130	
12	131	062913	11:41	12:01	12-01.16N	135-00.14E	4625.0	502.0	-	500.5	504.0	12M131	
12	132	062913	14:41	15:02	12-00.21N	135-00.15E	4605.0	500.9	-	501.5	505.0	12M132	
12	133	062913	17:41	18:02	12-00.24N	135-00.13E	4615.0	500.9	-	500.5	504.0	12M133	
12	134	062913	20:42	21:03	12-00.36N	134-59.82E	4619.0	500.7	-	500.5	504.0	12M134	
12	135	062913	23:42	00:40	12-00.48N	134-59.96E	4615.0	1003.6	-	999.8	1008.0	12M135	Water sampling cast
12	136	063013	02:42	03:03	12-00.75N	134-59.54E	4629.0	504.7	-	500.5	504.0	12M136	
12	137	063013	08:41	09:01	12-00.19N	135-00.14E	4608.0	500.5	-	501.5	505.0	12M137	
12	138	063013	14:41	15:02	12-00.11N	135-00.06E	4613.0	500.5	-	501.5	505.0	12M138	End fixed observation

5.11 Salinity of sampled water

(1) Personnel

Masaki Katsumata (JAMSTEC) - Principal Investigator
Hiroki Ushiomura (MWJ) - Operation Leader
Sonoka Wakatsuki (MWJ)

(2) Objective

To provide a calibration for the measurement of salinity of bottle water collected on the CTD casts and The Continuous Sea Surface Water Monitoring System (TSG).

(3) Method

a. Salinity Sample Collection

Seawater samples were collected with 12 liter Niskin-X bottles and TSG. The salinity sample bottle of the 250ml brown glass bottle with screw cap was used for collecting the sample water. Each bottle was rinsed 3 times with the sample water, and was filled with sample water to the bottle shoulder. All of sample bottle were sealed with a plastic cone and a screw cap because we took into consideration the possibility of storage for about a month. The cone was rinsed 3 times with the sample seawater before its use. Each bottle was stored for more than 23 hours in the laboratory before the salinity measurement.

The kind and number of samples taken are shown as follows ;

Table 5.11-1 Kind and number of samples

Kind of Samples	Number of Samples
Samples for CTD	40
Samples for TSG	29
Total	69

b. Instruments and Method

The salinity analysis was carried out on R/V MIRAI during the cruise of MR13-03 using the salinometer (Model 8400B “AUTOSAL” ; Guildline Instruments Ltd.: S/N 62556) with an additional peristaltic-type intake pump (Ocean Scientific International, Ltd.). A pair of precision digital thermometers (Model 9540 ; Guildline Instruments Ltd.) were used. The thermometer monitored the ambient temperature and the other monitored a bath temperature.

The specifications of the AUTOSAL salinometer and thermometer are shown as follows ;

Salinometer (Model 8400B “AUTOSAL” ; Guildline Instruments Ltd.)

Measurement Range : 0.005 to 42 (PSU)

Accuracy : Better than ± 0.002 (PSU) over 24 hours
without re-standardization

Maximum Resolution : Better than ± 0.0002 (PSU) at 35 (PSU)

Thermometer (Model 9540 ; Guildline Instruments Ltd.)
 Measurement Range : -40 to +180 deg C
 Resolution : 0.001
 Limits of error \pm deg C : 0.01 (24 hours @ 23 deg C \pm 1 deg C)
 Repeatability : \pm 2 least significant digits

The measurement system was almost the same as Aoyama *et al.* (2002). The salinometer was operated in the air-conditioned ship's laboratory at a bath temperature of 24 deg C. The ambient temperature varied from approximately 22 deg C to 24 deg C, while the bath temperature was very stable and varied within \pm 0.004 deg C on rare occasion. The measurement for each sample was done with a double conductivity ratio and defined as the median of 31 readings of the salinometer. Data collection was started 5 seconds after filling the cell with the sample and it took about 10 seconds to collect 31 readings by a personal computer. Data were taken for the sixth and seventh filling of the cell. In the case of the difference between the double conductivity ratio of these two fillings being smaller than 0.00002, the average value of the double conductivity ratio was used to calculate the bottle salinity with the algorithm for the practical salinity scale, 1978 (UNESCO, 1981). If the difference was greater than or equal to 0.00003, an eighth filling of the cell was done. In the case of the difference between the double conductivity ratio of these two fillings being smaller than 0.00002, the average value of the double conductivity ratio was used to calculate the bottle salinity. The measurement was conducted in about 4 hours per day and the cell was cleaned with soap after the measurement of the day.

(4) Results

a. Standard Seawater

Standardization control of the salinometer was set to 688 and all measurements were done at this setting. The value of STANDBY was 24+5196~5197 and that of ZERO was 0.0-0001~0000. The conductivity ratio of IAPSO Standard Seawater batch P154 was 0.99990 (double conductivity ratio was 1.99980) and was used as the standard for salinity. 19 bottles of P154 were measured.

Fig.5.11-1 shows the history of the double conductivity ratio of the Standard Seawater batch P154. The average of the double conductivity ratio was 1.99982 and the standard deviation was 0.00003 which is equivalent to 0.0007 in salinity.

Fig.5.11-2 shows the history of the double conductivity ratio of the Standard Seawater batch P154 after correction. The average of the double conductivity ratio after correction was 1.99980 and the standard deviation was 0.00002, which is equivalent to 0.0004 in salinity.

The specifications of SSW used in this cruise are shown as follows ;

batch	:	P154
conductivity ratio	:	0.99990
salinity	:	34.996
use by	:	20 th October 2014

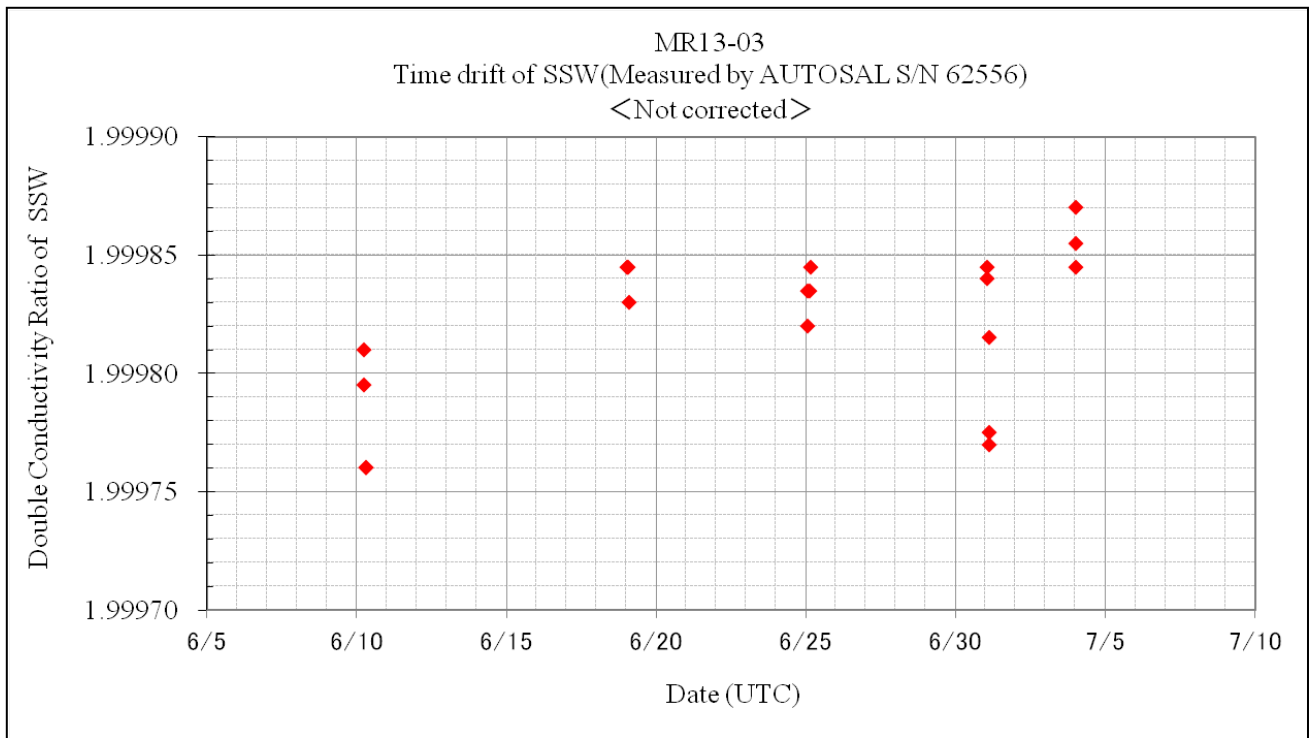


Fig. 5.11-1: History of double conductivity ratio for the Standard Seawater batch P154 (before correction)

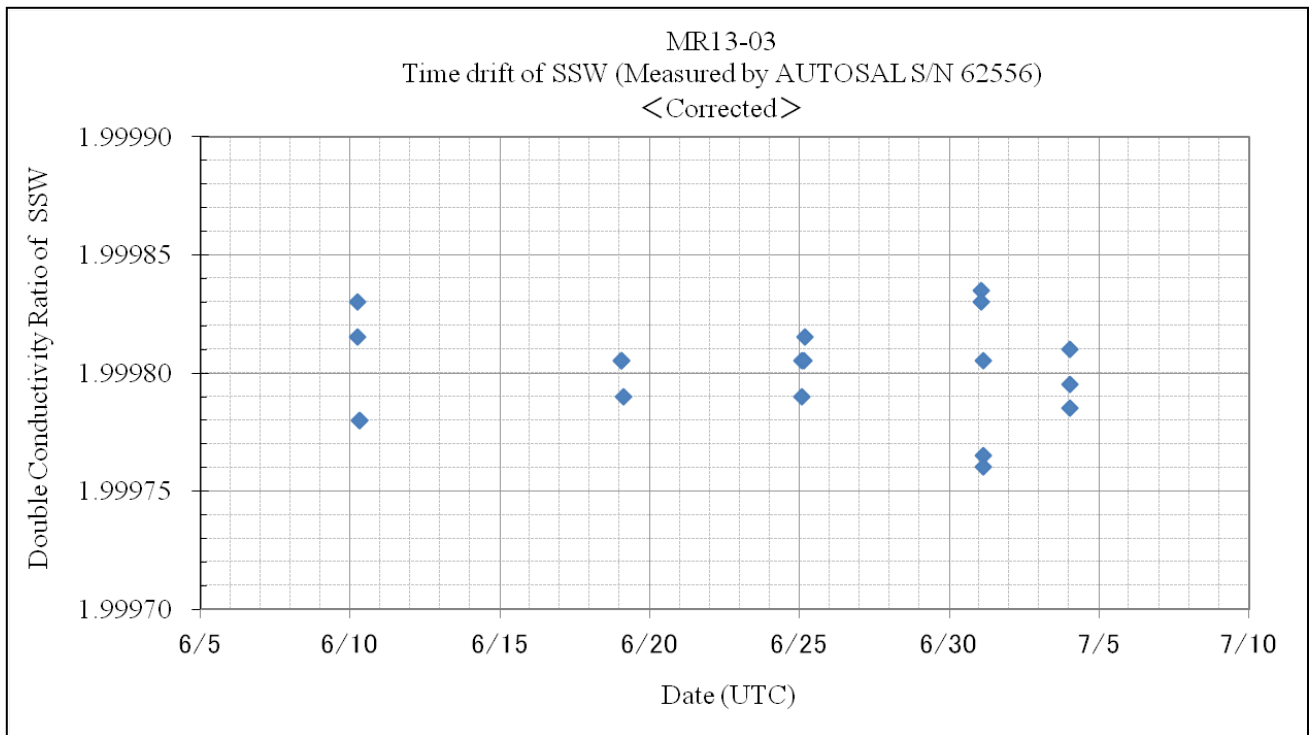


Fig. 5.11-2: History of double conductivity ratio for the Standard Seawater batch P154 (after correction)

b. Sub-Standard Seawater

Sub-standard seawater was made from Surface-sea water filtered by a pore size of 0.22 micrometer and stored in a 20 liter container made of polyethylene and stirred for at least 24 hours before measuring. It was measured about every 6 samples in order to check for the possible sudden drifts of the salinometer.

c. Replicate Samples

We estimated the precision of this method using 20 pairs of replicate samples taken from the same Niskin bottle. The average and the standard deviation of absolute difference among 20 pairs of replicate samples were 0.0002 and 0.0001 in salinity, respectively.

(5) Data archive

These raw datasets will be submitted to JAMSTEC Data Management Group (DMG).

(6) Reference

- Aoyama, M., T. Joyce, T. Kawano and Y. Takatsuki : Standard seawater comparison up to P129. Deep-Sea Research, I, Vol. 49, 1103~1114, 2002
- UNESCO : Tenth report of the Joint Panel on Oceanographic Tables and Standards. UNESCO Tech. Papers in Mar. Sci., 36, 25 pp., 1981

5.12 Dissolved oxygen of sampled water

(1) Personnel (*: Leg-1, **: Leg-2, ***: Leg-1+2)

Masaki Katsumata*** (JAMSTEC) - Principal Investigator (Leg-1+2)
Hideki Yamamoto** (MWJ)
Misato Kuwahara*** (MWJ) - Operation Leader (Leg-1+2)

(2) Objectives

Determination of dissolved oxygen in seawater by Winkler titration.

(3) Instruments and Methods

Following procedure is based on an analytical method, entitled by “Determination of dissolved oxygen in sea water by Winkler titration”, in the WHP Operations and Methods (Dickson, 1996).

a. Instruments

Burette for sodium thiosulfate and potassium iodate:

APB-620 manufactured by Kyoto Electronic Co. Ltd. / 10 cm³ of titration vessel.

Detector:

Automatic photometric titrator (DOT-01X) manufactured by Kimoto Electronic Co. Ltd.

Software:

DOT Terminal version 1.2.0

b. Reagents

Pickling Reagent I: Manganese chloride solution (3 mol dm⁻³)

Pickling Reagent II: Sodium hydroxide (8 mol dm⁻³) / sodium iodide solution (4 mol dm⁻³)

Sulfuric acid solution (5 mol dm⁻³)

Sodium thiosulfate (0.025 mol dm⁻³)

Potassium iodide (0.001667 mol dm⁻³)

CSK standard of potassium iodide:

Lot DCE2131, Wako Pure Chemical Industries Ltd., 0.0100N

c. Sampling

Seawater samples were collected with Niskin bottle attached to the CTD-system. Seawater for oxygen measurement was transferred from sampler to a volume calibrated flask (ca. 100 cm³). Three times volume of the flask of seawater was overflowed. Temperature was measured by digital thermometer during the overflowing. Then two reagent solutions (Reagent I and II) of 0.5 cm³ each were added immediately into the sample flask and the stopper was inserted carefully into the flask. The sample flask was then shaken vigorously to mix the contents and to disperse the precipitate finely throughout. After the precipitate has settled at least halfway down the flask, the flask was shaken again vigorously to disperse the precipitate. The sample flasks containing pickled samples were stored in a laboratory until they were titrated.

d. Sample measurement

At least two hours after the re-shaking, the pickled samples were measured on board. 1 cm³ sulfuric acid solution and a magnetic stirrer bar were added into the sample flask and stirring began. Samples were titrated by sodium thiosulfate solution whose morality was determined by potassium iodate solution. Temperature of sodium thiosulfate during titration was recorded by a digital thermometer. During this cruise, we measured dissolved oxygen concentration using 2 sets of the

titration apparatus. Dissolved oxygen concentration ($\mu\text{mol kg}^{-1}$) was calculated by sample temperature during seawater sampling, CTD salinity, flask volume, and titrated volume of sodium thiosulfate solution without the blank.

e. Standardization and determination of the blank

Concentration of sodium thiosulfate titrant was determined by potassium iodate solution. Pure potassium iodate was dried in an oven at 130 °C. 1.7835 g potassium iodate weighed out accurately was dissolved in deionized water and diluted to final volume of 5 dm³ in a calibrated volumetric flask (0.001667 mol dm⁻³). 10 cm³ of the standard potassium iodate solution was added to a flask using a volume-calibrated dispenser. Then 90 cm³ of deionized water, 1 cm³ of sulfuric acid solution, and 0.5 cm³ of pickling reagent solution II and I were added into the flask in order. Amount of titrated volume of sodium thiosulfate (usually 5 times measurements average) gave the molarity of sodium thiosulfate titrant.

The oxygen in the pickling reagents I (0.5 cm³) and II (0.5 cm³) was assumed to be 3.8×10^{-8} mol (Murray *et al.*, 1968). The blank due to other than oxygen was determined as follows. 1 and 2 cm³ of the standard potassium iodate solution were added to two flasks respectively using a calibrated dispenser. Then 100 cm³ of deionized water, 1 cm³ of sulfuric acid solution, and 0.5 cm³ of pickling reagent solution II and I each were added into the flask in order. The blank was determined by difference between the first (1 cm³ of KIO₃) titrated volume of the sodium thiosulfate and the second (2 cm³ of KIO₃) one. The results of 3 times blank determinations were averaged.

(4) Preliminary Results

Table 5.12-1 shows results of the standardization and the blank determination during this cruise.

Table 5.12-1: Results of the standardization and the blank determinations.

Data	KIO ₃ ID	Na ₂ S ₂ O ₃	DOT-01X(No.7)		DOT-01X(No.8)	
			Vstd	Vblk	Vstd	Vblk
2013/06/04	20120420-11-11	20120615-05	3.960	-0.002	-	-
2013/06/04	CSK DCE2131	20120615-05	3.961	-0.002	-	-
2013/06/13	20120420-11-10	20120615-05	3.960	-0.003	3.962	-0.003
2013/06/20	20120420-11-08	20120615-05	3.961	-0.002	3.963	-0.003
2013/06/27	20120420-11-07	20120615-05	3.962	-0.002	3.962	-0.003
2013/07/03	20120420-11-09	20120615-05	3.963	0.000	3.962	-0.002

f. Repeatability of sample measurement

Replicate samples were taken at every CTD casts. Total amount of the replicate sample pairs of good measurement was 34. The standard deviation of the replicate measurement was 0.07 $\mu\text{mol kg}^{-1}$ that was calculated by a procedure in Guide to best practices for ocean CO₂ measurements Chapter4 SOP23 Ver.3.0 (2007).

(5) Data archive

All raw datasets will be submitted to JAMSTEC Data Management Group (DMG).

(6) References

Dickson, A.G., Determination of dissolved oxygen in sea water by Winkler titration. (1996)

Dickson, A.G., Sabine, C.L. and Christian, J.R. (Eds.), Guide to best practices for ocean CO₂ measurements. (2007)

Culberson, C.H., WHP Operations and Methods July-1991 "Dissolved Oxygen", (1991)

Japan Meteorological Agency, Oceanographic research guidelines (Part 1). (1999)

KIMOTO electric CO. LTD., Automatic photometric titrator DOT-01X Instruction manual

5.13 Thermistor chain to profile the water temperature near surface

(1) Personnel

Masaki KATSUMATA	(JAMSTEC)	- Principal Investigator
Hiroshi MATSUNAGA	(MWJ)	- Operation Leader
Hiroki USHIROMURA	(MWJ)	
Shinsuke TOYODA	(MWJ)	
Satoshi OZAWA	(MWJ)	(not on board)
Toru IDAI	(MWJ)	(not on board)

(2) Objectives

To investigate air-sea interaction in detail, it is desired to measure the detailed vertical profile of the temperature and other parameters in the ocean near surface nearby the vessel where bunch of instruments onboard are operated to obtain various parameters simultaneously. However the ship body and maneuver disturb the water around the vessel and therefore the natural status are difficult to measure. To measure the undisturbed vertical profile of the water temperature in surface 10 meters, we deployed the “thermistor chain” (T-chain) at the bow of the vessel.

(3) Methods

The T-chain in this study equips four SBE39 sensor units (to measure temperature and pressure) and ten SBE56 sensor units (to measure temperature). These sensor units (see specifications for Table 5.13-1) are attached to wire as in Table 5.13-2 to consist the “chain”. The wire is hung down from the boom (“albedo boom”) projected from the bow, as in Fig. 5.13-1. The high-frequency sampling (more than 1 Hz) and the pitching of the vessel (roughly 10 seconds for a period) enable the T-chain to measure the vertical profile of the water temperature in detailed temporal and vertical resolutions.

The periods of the deployment are summarized in Table 5.13-3. During the deployment, we cruises the vessel at or slower than 2 knots in speed, to keep the T-chain as vertical as possible and to keep the T-Chain away from the ship body.

The data are stored in the memory inside the each sensor unit. After the recovery of the T-chain, dataset in each sensor is recovered.

Table 5.13-1: Specifications of sensors used in the T-chain.

Name	SBE39	SBE56	
Manufacturer	Sea-Bird Electronics, Inc.		
Sampling interval	About 0.75 seconds (estimated from recorded data)	0.5 seconds	
Data memory	> 30 days (0.75-sec interval)	> 90 days (0.5-sec interval)	
Power endurance	> 50 days (0.75-sec interval) (with external battery pack (*1))	> 30 days (0.5-sec interval)	
Parameter	Pressure	Temperature	Temperature
Initial accuracy	0.1% of full scale range	0.002 deg.C	0.002 deg.C
Typical stability	0.05% of full scale range / year	0.0002 deg.C / month	0.0002 deg.C / month
Resolution	0.002% of full range scale	0.0001 deg.C	0.0001 deg.C

*1: External battery pack BPA-50A (WET Labs, Inc.)

Table 5.13-2: Configuration of the T-chain in the present experiment.

Sensor No.	Position on wire [m]	Sensor unit	S/N	Parameter
1	0.0	SBE56	02343	T
2	0.6	SBE56	02344	T
3	1.3	SBE56	02345	T
4	2.0	SBE39	0240	T, P
5	3.0	SBE56	02346	T
6	3.6	SBE56	02347	T
7	4.3	SBE56	02348	T
8	5.0	SBE39	0104	T, P
9	6.0	SBE56	02349	T
10	7.0	SBE56	02350	T
11	8.0	SBE39	0105	T, P
12	9.0	SBE56	02351	T
13	10.0	SBE56	02352	T
14	11.0	SBE39	0241	T, P

Note: “Position on wire” indicates the relative distance (downward) of each sensor unit (position of probe) from the No.1 sensor along the wire.

Table 5.13-3: Periods that the T-chain was deployed during the cruise.

	Deployed	Recovered
Period 1	0726UTC 13 Jun. 2013	0107UTC 14 Jun. 2013
Period 2	0715UTC 14 Jun. 2013	0630UTC 15 Jun. 2013
Period 3	0704UTC 15 Jun. 2013	0345UTC 21 Jun. 2013
Period 4	0418UTC 21 Jun. 2013	0054UTC 30 Jun. 2013

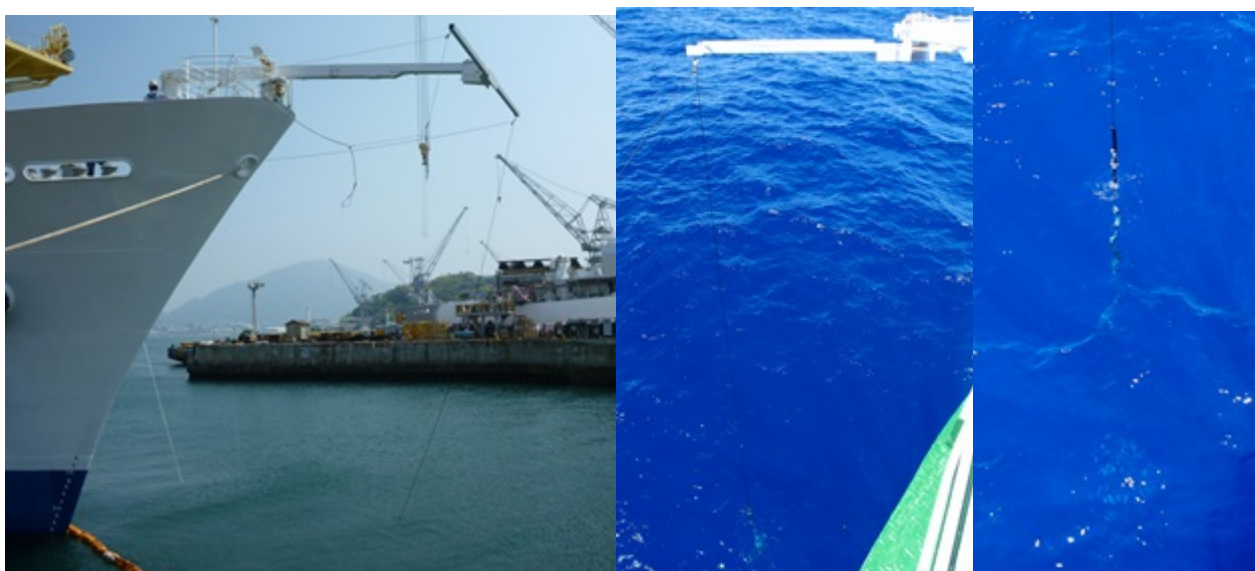


Fig. 5.13-1: Photos of the T-chain deployed from the bow of R/V Mirai. (Left) The “albedo boom” at the bow with the hung wire of the T-chain (when tested at the dockyard). (Center) The view from the vessel (at sea) for the wire of the T-chain hung down onto the sea surface. (Right) The top of the T-chain when the top sensor was on the surface (at sea).

(4) Preliminary Results

All the sensors successfully provide the data for the whole periods shown in Table 5.13-3. The data will be processed after the end of the cruise.

(5) Data Archive

All data obtained during this cruise will be submitted to the JAMSTEC Data Management Group (DMG).

(6) Acknowledgement

The SBE39 sensor units are kindly provided by the Arctic Ocean Climate System Research Team in JAMSTEC/RIGC.

5.14 LADCP

(1) Personnel

Masaki KATSUMATA	(JAMSTEC)	- Principal Investigator
Ayako SEIKI	(JAMSTEC)	(not on board)
Hiroshi MATSUNAGA	(MWJ)	- Operation Leader
Hiroki USHIROMURA	(MWJ)	
Shinsuke TOYODA	(MWJ)	
Rei ITO	(MWJ)	
Masahiro ORUI	(MWJ)	
Sonoka WAKATSUKI	(MWJ)	
Hideki YAMAMOTO	(MWJ)	

(2) Objectives

To obtain horizontal current velocity in high vertical resolution

(3) Methods

To measure velocity structure at small vertical scales we used a high frequency ADCP in lowered mode (LADCP). The instrument, a Teledyne RDI Workhorse Sentinel 600kHz ADCP rated for 1000m depth, was attached to the CTD frame using a wide metal collar made of two halves joined by six retaining bolts (three on each side, as shown in Fig. 5.21-1). A rubber sleeve was wrapped around the instrument to prevent direct contact between the instrument and the metal collar and to prevent vertical slippage. A rope was tied to the top of the instrument and attached to the CTD frame to further reduce vertical slippage and for added safety. The instrument was deployed on all CTD stations during the cruise. The instrument is self-contained with an internal battery pack. The health of the battery is monitored by the recorded voltage count.

(4) Preliminary results

During the cruise, 141 profiles were obtained in total, including 138 profiles with CTD at station (12N, 135E) and 3 profiles at stations where ARGO-type float was deployed. All the data has to be converted and quality-controlled before the analyses. The further analyses will be in near future.

(5) Data archive

All data obtained during this cruise will be submitted to the JAMSTEC Data Management Group (DMG).



Fig. 5.14-1: Teledyne RDI Workhorse Sentinel 600kHz ADCP attached to the CTD frame

5.15. Shipboard ADCP

(1) Personnel

Masaki KATSUMATA (JAMSTEC): Principal Investigator

Kazuho YOSHIDA (Global Ocean Development Inc., GODI)

Koichi INAGAKI (GODI)

Wataru TOKUNAGA (GODI)

Souichiro SUEYOSHI (GODI)

Ryo KIMURA (MIRAI Crew)

(2) Objective

To obtain continuous measurement of the current profile along the ship's track.

(3) Methods

Upper ocean current measurements were made in MR13-03 cruise, using the hull-mounted Acoustic Doppler Current Profiler (ADCP) system, which consists of following components;

- 1) R/V MIRAI has installed vessel-mount ADCP (75 kHz "Ocean Surveyor", Teledyne RD Instruments). It has a phased-array transducer with single assembly and creates 4 acoustic beams electronically.
- 2) For heading source, we use ship's gyro compass (Tokimec, Japan), continuously providing heading to the ADCP system directly. Also, we have Inertial Navigation System (Phins, IXBLUE) which provide high-precision heading and attitude information, are stored in ".N2R" data files with a time stamp.
- 3) DGPS system (Trimble SPS751 & StarFixXP) providing position fixes.
- 4) We used VmDas version 1.4.6 (TRD Instruments) for data acquisition.
- 5) To synchronize time stamp of pinging with GPS time, the clock of the logging computer is adjusted to GPS time every 2 minutes.
- 6) The sound speed at the transducer does affect the vertical bin mapping and vertical velocity measurement, is calculated from temperature, salinity (constant value; 35.0 psu) and depth (6.5 m; transducer depth) by equation in Medwin (1975).

Data was configured for 16 m intervals and 8 m blanking distance starting 31 m below the surface, or 8 m intervals and 8 m blanking distance starting 23 m below the surface. The vertical interval was changed at 07:47 UTC on 05 Jun. 2013. Every ping was recorded as raw ensemble data (.ENR). Also, 60 seconds and 300 seconds averaged data were recorded as short term average (.STA) and long term average (.LTA) data, respectively. Major parameters for the measurement (Direct Command) are shown in Table 5.15-1.

(4) Preliminary results

Fig.5.15-1 shows time series of U and V components of current during stationary observation period. Fig.5.15-2 - Fig.5.15-4 show vertical sections U and V components of current.

P (0), R (0): Manual EP, ER (0 degree)

S (0): Manual ES

T (1): Internal transducer sensor

U (0): Manual EU

Timing Commands

TE = 00:00:02.00 Time per Ensemble (hrs:min:sec.sec/100)

TP = 00:02.00 Time per Ping (min:sec.sec/100)

Water-Track Commands

WA = 255 False Target Threshold (Max) (0-255 count)

WB = 1 Mode 1 Bandwidth Control (0=Wid, 1=Med, 2=Nar)

WC = 120 Low Correlation Threshold (0-255)

WD = 111 100 000 Data Out (V; C; A; PG; St; Vsum; Vsum^2;#G;P0)

WE = 1000 Error Velocity Threshold (0-5000 mm/s)

WF = 0800 Blank After Transmit (cm)

WG = 001 Percent Good Minimum (0-100%)

WI = 0 Clip Data Past Bottom (0 = OFF, 1 = ON)

WJ = 1 Rcvr Gain Select (0 = Low, 1 = High)

WM = 1 Profiling Mode (1-8)

WP = 00001 Pings per Ensemble (0-16384)

WT = 000 Transmit Length (cm) [0 = Bin Length]

WV = 0390 Mode 1 Ambiguity Velocity (cm/s radial)

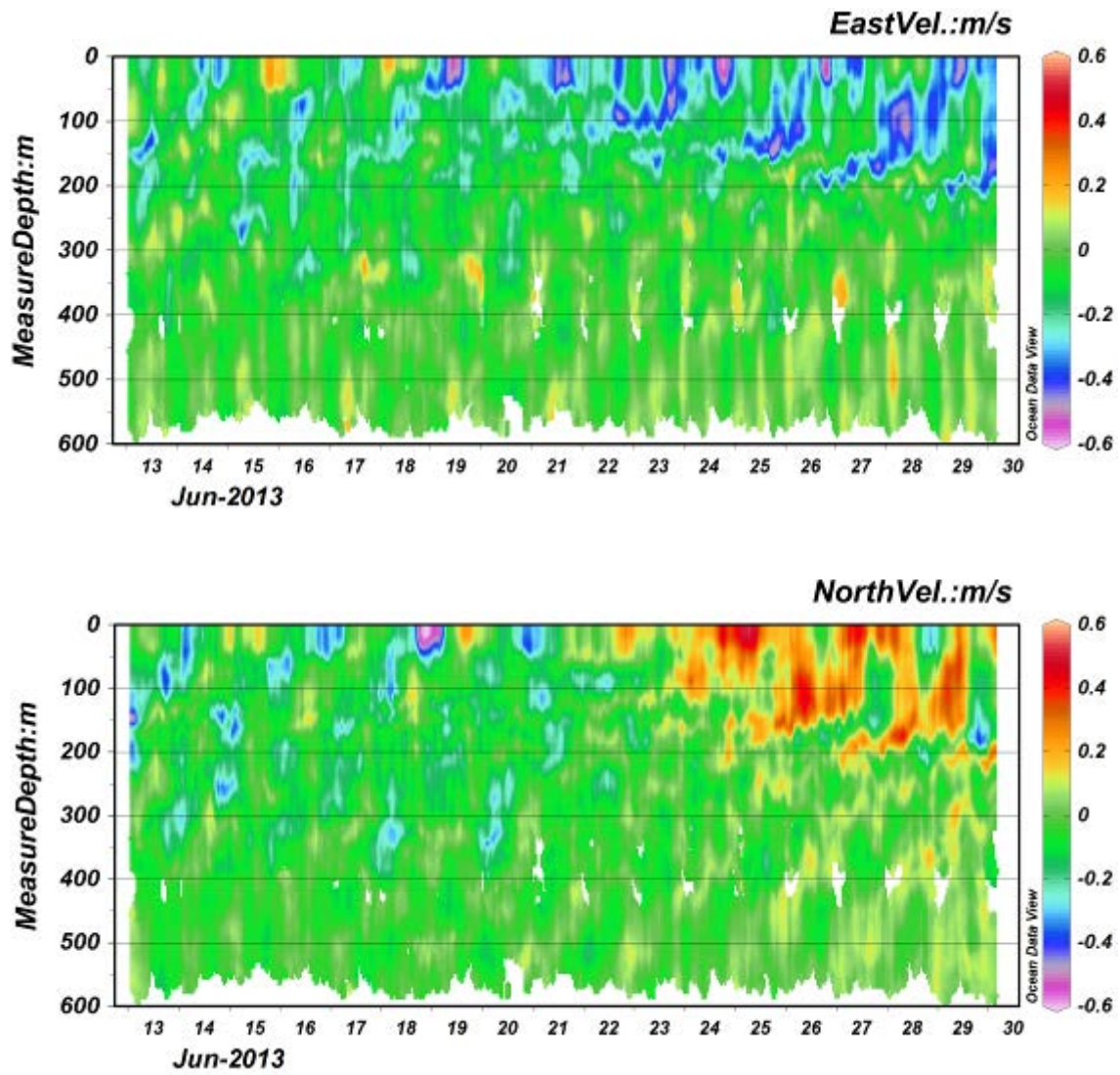


Fig 5.15-1. Time depth cross section of zonal (upper) and meridional (lower) components of current during stationary observation period.

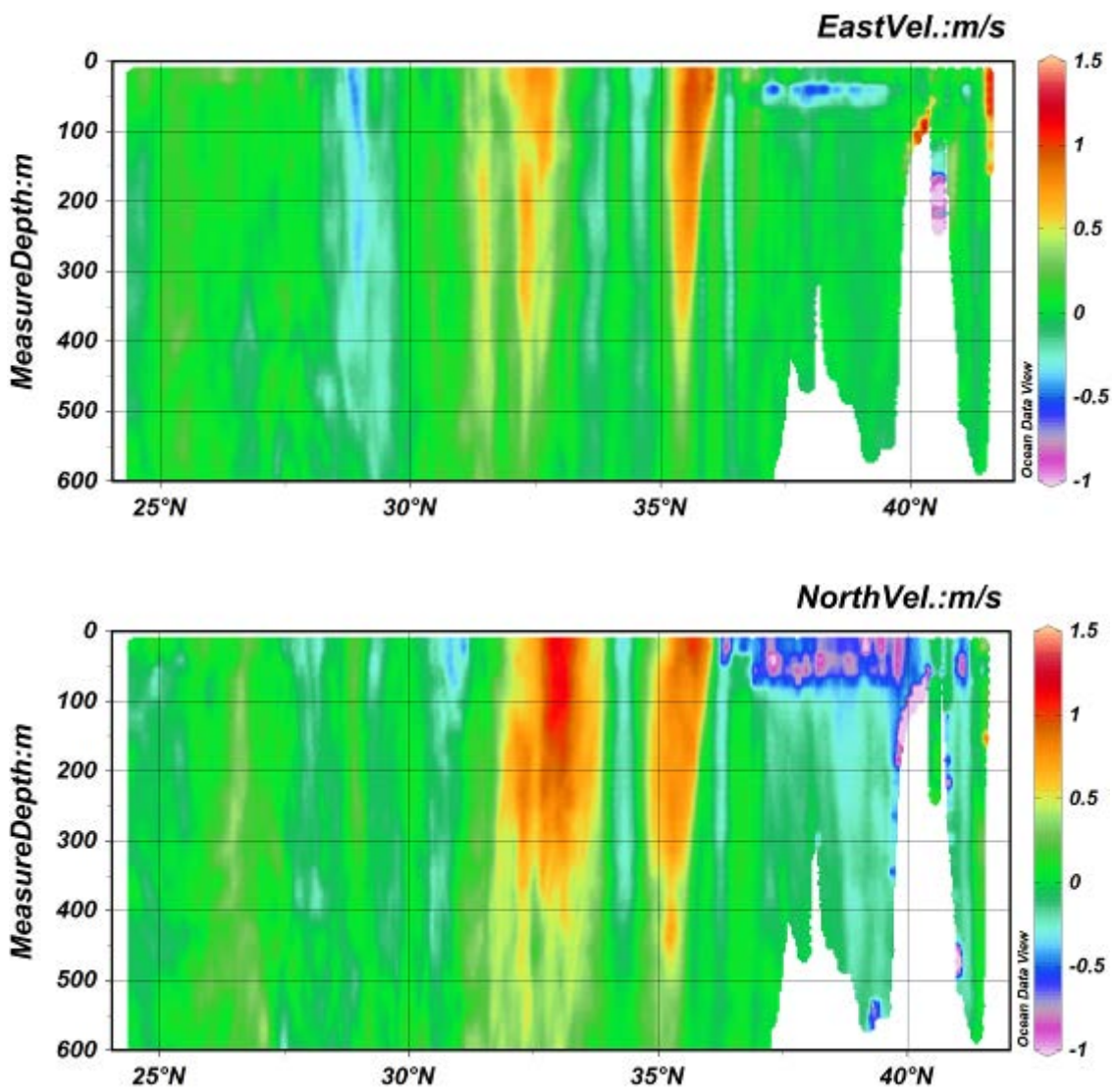


Fig 5.15-2. Latitude-depth cross section of zonal (upper) and meridional (lower) components of current obtained during Leg-1 (with 16m of depth bin size (as setting-1)).

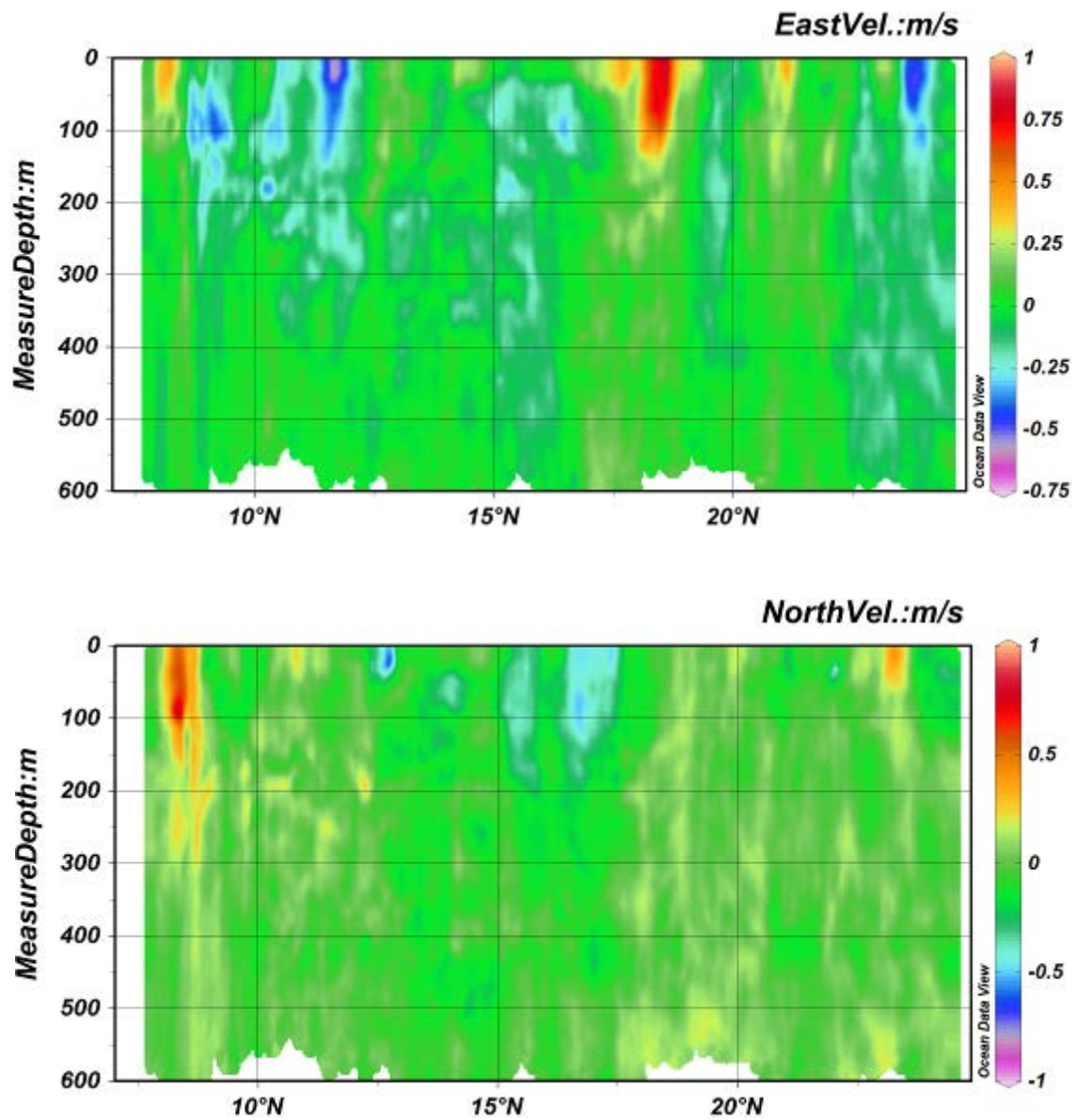


Fig 5.15-3. Latitude-depth cross section of zonal (upper) and meridional (lower) components of current obtained during Leg-1 (with 8 m of depth bin size (as setting-2)).

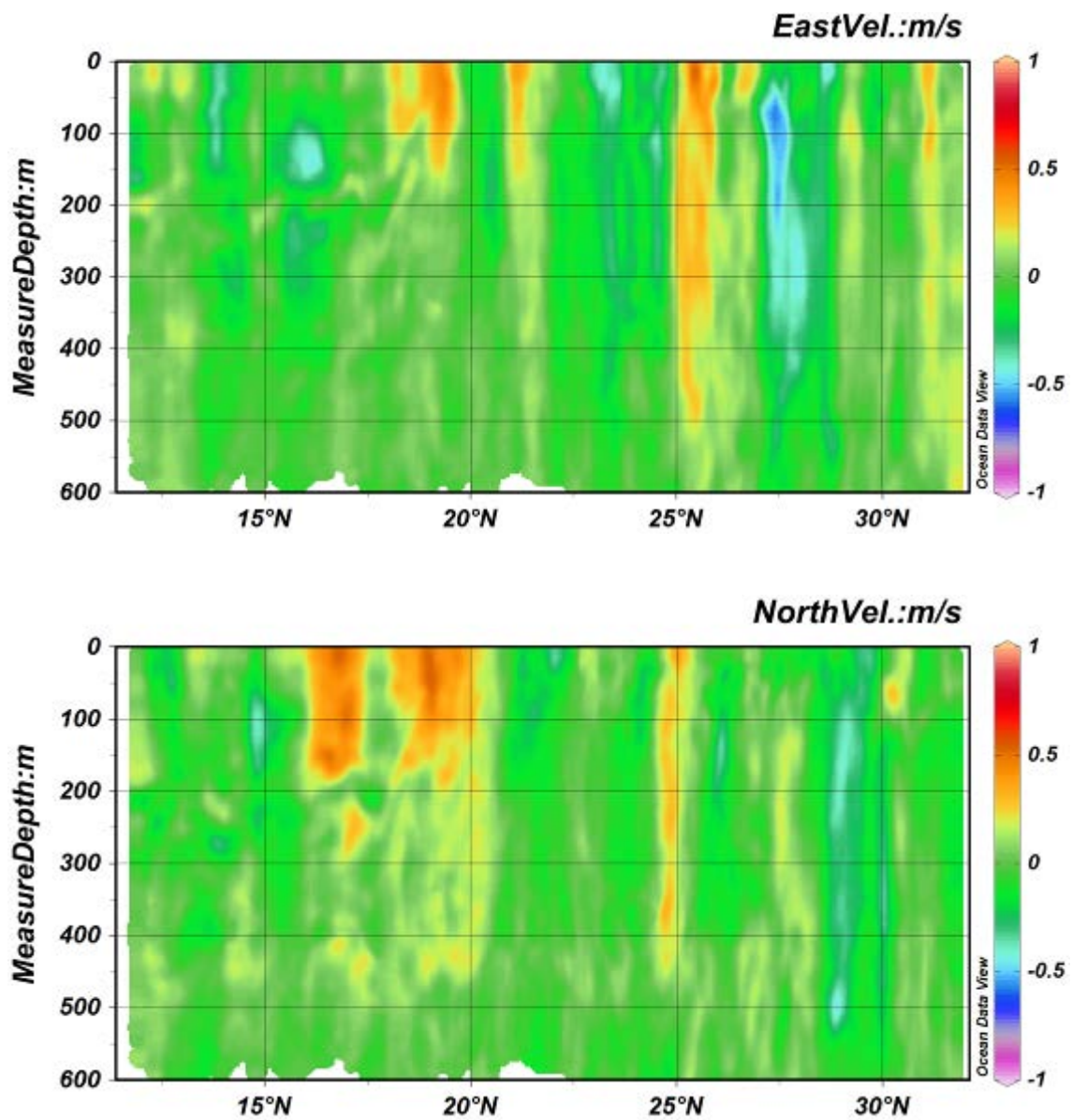


Fig 5.15-4. Latitude-depth cross section of zonal (upper) and meridional (lower) components of current obtained during Leg-2 (with 8 m of depth bin size (as setting-2)).

5.16 Underway CTD

(1) Personal

Takuya HASEGAWA	(JAMSTEC)	- Principal Investigator
Satoru YOKOI	(JAMSTEC)	
Masaki KATSUMATA	(JAMSTEC)	
Qoosaku MOTEKI	(JAMSTEC)	
Ayumi MASUDA	(JAMSTEC)	
Hiroaki YOSHIOKA	(JAMSTEC)	
Satoki TSUJINO	(Nagoya Univ.)	
Hiroshi MATSUNAGA	(MWJ)	- Operation Leader
Hiroki USHIROMURA	(MWJ)	
Shinsuke TOYODA	(MWJ)	
Rei ITO	(MWJ)	
Masahiro ORUI	(MWJ)	

(2) Objective

The “Underway CTD” (UCTD) system measures vertical profiles of temperature, conductivity and pressure like traditional CTD system. The strongest point of the UCTD system is to obtain good-quality CTD profiles from moving vessels with repeatable operation. In addition, the UCTD data are much accurate than those from XCTD because the sensor of the UCTD is basically same as that used in the traditional CTD system.

This is the first time to operate the UCTD system on R/V Mirai. The observation in this cruise is dedicated to confirm procedures to operate UCTD system on R/V Mirai, to check the data quality, and to examine some possible patterns of the observation in near future.

(3) Methods

The UCTD system, manufactured by Oceanscience Group, is utilized in this cruise.

The system consists of the probe unit and on-deck unit with the winch and the rewinder, as in Fig. 1. After spooling the line for certain length onto the probe unit (in “tail spool” part), the probe unit is released from the vessels into the ocean, and then measure temperature, conductivity and pressure during its free-fall with speed of roughly 4 m/s in the ocean. The probe unit is physically connected to the winch on the vessel by line. Releasing the line from the tail spool ensure the probe unit to be fall without physical forcing by the movement of the vessel. After the probe unit reaches the deepest layer for observation, it is recovered by using the winch on the vessel. The observed data are stored in the memory within the probe unit. The dataset can be downloaded into PCs via Bluetooth communication on the deck.

The specifications of the sensors are in Table 5.16-1. The UCTD system used in this cruise can observe temperature, conductivity and pressure from surface to 1000 m depth with 16 Hz sampling rate.

During the profiling, the vessel can be cruised (straight line recommended). The manufacturer recommends the maximum speed of the vessel during the profiling as in Table 5.16-2. In this cruise, we examine various cruising speed up to 12 knot and confirm there are no apparent problem for the examined speeds.

Table 5.16-1: Specification of the sensors of the UCTD system in this cruise.

Parameter	Accuracy	Resolution	Range
Temperature (deg.C)	0.004	0.002	-5 to 43
Conductivity (S/m)	0.0003	0.0005	0 to 9
Pressure (dbar)	1.0	0.5	0 to 2000

Table 5.16-2: Maximum speed of the vessel during profile, recommended by the manufacturer.

Max. depth to profile	Max Speed (knot)
0 to 350 m	13
350 to 400 m	12
400 to 450 m	11
450 to 500 m	10
500 to 550 m	8
550 to 600 m	6
600 to 650 m	4
650 to 1000 m	2

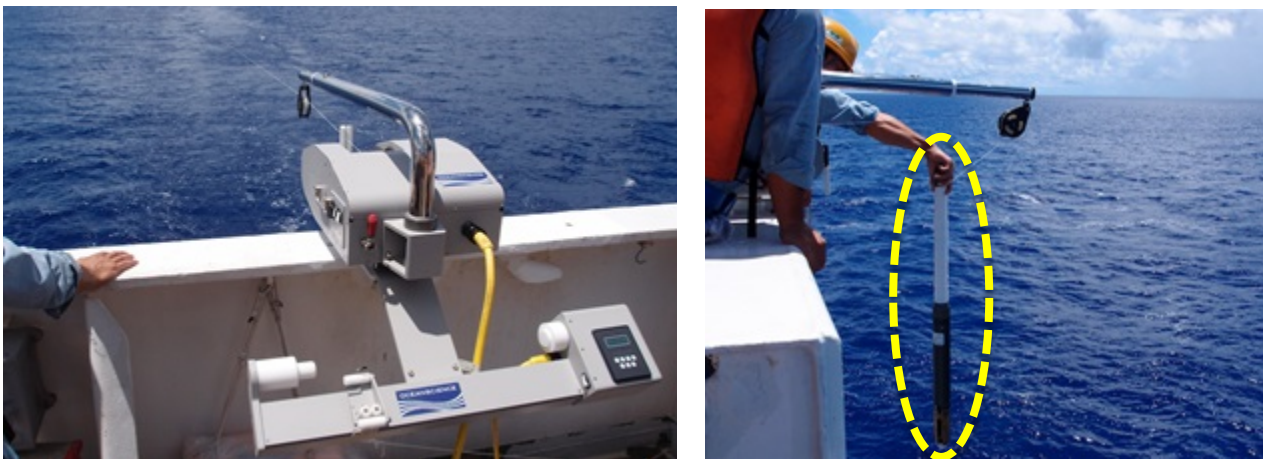


Fig. 1: UCTD system installed and operated on R/V Mirai. (left) On-deck unit, consists of the winch and the rewinder. (right) Probe unit, consists of sensor probe (bottom half) and tail spool (top half). The right figure is just before towing from the upper deck.

(4) Preliminary Results

During the cruise, the UCTD was deployed onto the sea for 42 times. All the deployments are listed in Table 5.16-3. Most of the deployments utilize full UCTD system, except followings: The dummy probe without sensor was utilized for the test of the system for three times at station P001, P002 and P003. The probe was attached to the metal frame for CTD / Carousel system to compare the results directly to the CTD system (see Section 5.10) for three times at station 009, 012 and 013.

As an example, the profile obtained at Station 002 Cast 1 is shown in Fig. 2. Mixed layer is clearly seen above 40 m depth with uniform density value, in which values of temperature and salinity is

roughly 22.5 deg.C and 34.58 PSU, respectively. It can be speculated that spike-noise in salinity appears due to the difference in response time between temperature and conductivity sensors especially when strong change of the descent rate of the probe occurs. Figure 2 shows that descending rate ranges from 3.5 m/s to 4.5 m/s which is around the expected free-fall speed of the probe (i.e., 4.0 m/s). Though there are several peaks in the descent rate, it seems that the spike-like noise of salinity do not correspond to such peaks of the descent rate.

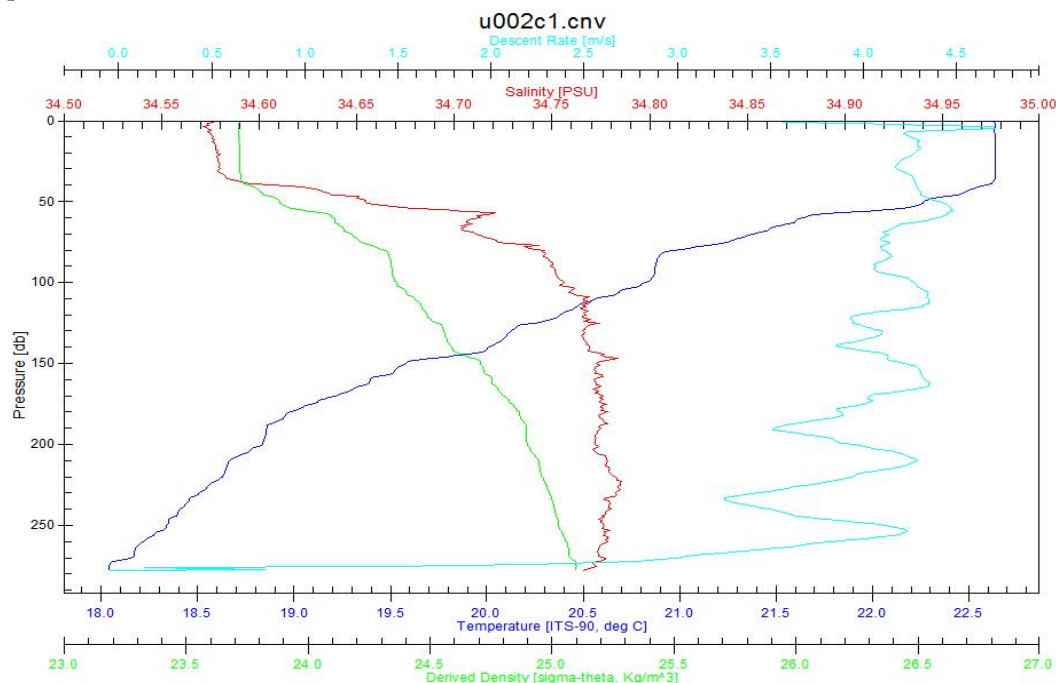


Figure 2: Profile of temperature (blue line), salinity (red line), density (green line), and descent rate (light blue line) at 002C1. 1db vertical averaged

The accuracy of UCTD-derived parameters is ensured by comparing the results to these from CTD measurements. First, the UCTD probed was attached to the metal frame for CTD system when CTD was deployed onto 500 m depth. The result (Fig. 3) indicates the values from two systems match excellently (lines are almost identical and hard to distinguish).

On the other hand, we towed UCTD several times just after the CTD casting to compare each other. Figure 4 is an example of the comparison. In all such sequential deployment, the profile seems to shift vertically, not only between CTD profile and UCTD profile but also UCTD profiles. Regarding the result from Fig. 4, it is reasonable to say that such vertical shift is by the natural phenomenon, not by the bias between instruments or other artificial issue.

As mentioned above, UCTD observation can be conducted without stopping the vessel. In future observation, spatially high-resolution UCTD observation for wide area can be done during a short period as compared to CTD observation, which can explore detailed spatial and/or temporal change of upper ocean structure related to barrier layer and other oceanic and atmospheric phenomena. The observation in MR13-03 indicates that the UCTD provide good quality oceanic data and also will contribute to reveal unknown aspect of the oceanic variation.

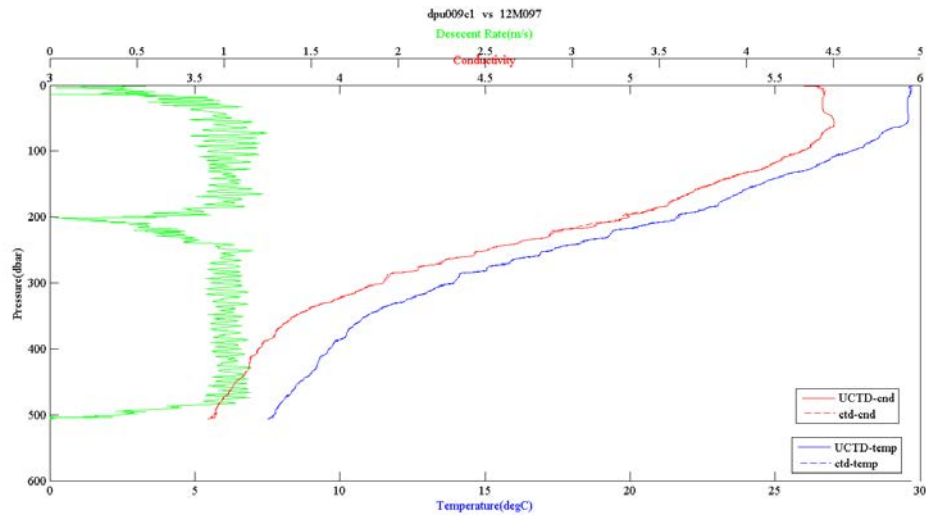


Fig. 3: Vertical profiles of temperature, salinity and descending rate from CTD and UCTD at 06UTC on Jun. 25, when CTD system was deployed with UCTD probe attached at the frame of CTD system and descending rate from CTD and UCTD at 06UTC on Jun. 25, when CTD system was deployed with UCTD probe attached at the frame of CTD system

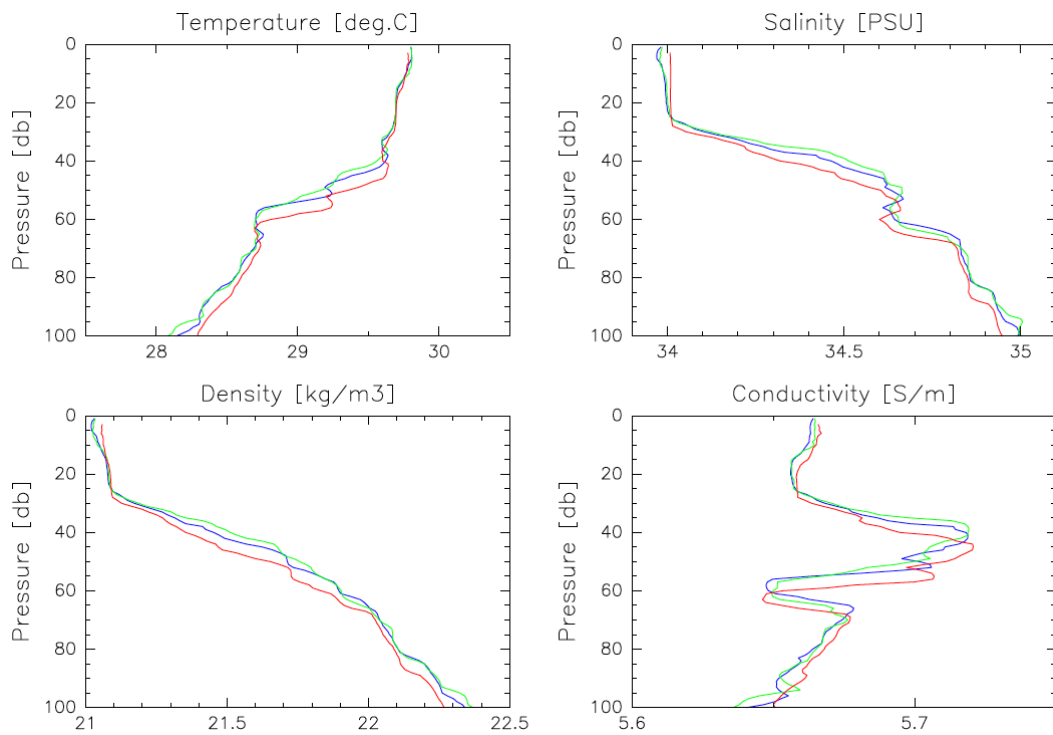


Fig. 4: Vertical profiles of temperature, salinity, density and conductivity from CTD and UCTD around 06UTC on Jun.28. Red lines are from CTD (start profiling at 0540UTC), while blue and green lines are from UCTD (start profiling from 0609UTC and 0627UTC, respectively).

(5) Data Archive

All data obtained during this cruise will be submitted to the JAMSTEC Data Management Group (DMG).

(6) Acknowledgments

The UCTD system is kindly provided by EMS Co. Ltd.

Table 5.16-3: List of the deployment of the UCTD onto the sea.

Station	Cast	Time Towed (UTC)		Position Towed		Depth to go	Ship speed		Notes
				Lat.	Lon.		Tow	Rcvry	
Leg-1									
P001	C1	Jun.03	23:45	31-01.18N	140-47.67E	200	6.9	2.0	w/ dummy probe
001	C1	Jun.04	01:09	30-48.55N	140-45.61E	200	7.1	2.0	
002	C1	Jun.04	01:40	30-43.33N	140-44.68E	200	10.0	5.0	
	C2	Jun.04	02:08	30-39.22N	140-43.81E	200	10.0	6.0	
	C3	Jun.04	02:37	30-31.80N	140-41.77E	200	10.0	7.0	
003	C1	Jun.05	00:02	25-58.87N	138-58.54E	200	11.7	8.0	
	C2	Jun.05	00:38	25-53.90N	138-56.31E	200	11.5	9.0	
	C3	Jun.05	01:09	25-48.30N	138-54.27E	200	11.7	9.8	
004	C1	Jun.05	01:39	25-42.90N	138-52.24E	500	9.9	10.1	
005	C1	Jun.06	00:29	21-27.42N	137-08.10E	500	9.8	9.8	
	C2	Jun.06	01:14	21-19.84N	137-05.26E	500	9.5	10.1	
	C3	Jun.06	01:59	21-12.58N	137-02.51E	500	9.7	9.8	
P002	C1	Jun.07	12:00	15-06.23N	135-12.00E	200	11.5	11.5	w/ dummy probe
006	C1	Jun.07	12:22	15-01.70N	135-00.50E	200	11.6	11.5	
007	C1	Jun.08	00:30	12-58.57N	135-00.27E	1000	1.9	1.9	after CTD N02M01
Leg-2									
008	C1	Jun.24	06:12	12-00.38N	134-59.99E	500	2.0	2.0	
009	C1	Jun.25	05:41	11-59.88N	135-00.02E	500	-	-	attached on CTD frame at CTD d12M097
010	C1	Jun.26	06:10	12-00.12N	134-59.95E	500	1.1	0.9	after CTD d12M105
	C2	Jun.26	06:29	12-00.04N	134-59.97E	500	1.1	1.1	
011	C1	Jun.26	12:12	11-59.90N	134-59.51E	500	1.0	0.9	after CTD d12M107
	C2	Jun.26	12:33	11-59.79N	134-59.64E	500	1.0	1.1	
012	C1	Jun.27	05:40	11-59.97N	134-59.96E	500	-	-	attached on CTD frame at CTD d12M113
013	C1	Jun.27	08:42	11-59.99N	134-59.79E	500	-	-	attached on CTD frame at CTD d12M114
	C1	Jun.28	06:09	12-00.25N	135-00.00E	500	1.1	1.1	after CTD d12M121
014	C2	Jun.28	06:27	12-00.05N	135-00.03E	500	1.2	1.1	
P003	C1	Jun.28	12:10	12-00.27N	134-59.69E	500	1.0	1.1	w/ dummy probe
015	C1	Jun.28	12:28	12-00.05N	134-59.89E	500	1.1	1.0	after CTD d12M123
	C2	Jun.28	12:46	11-59.82N	135-00.09E	500	1.2	0.9	
101	C1	Jun.30	03:55	12-05.96N	134-59.94E	250	10.1	10.0	forming triangle (#1)
	C2	Jun.30	04:28	12-01.40N	135-57.23E	250	10.0	10.0	
	C3	Jun.30	05:16	11-57.03N	134-54.59E	250	9.2	9.2	
	C4	Jun.30	05:49	11-56.98N	135-00.08E	250	10.2	10.1	
	C5	Jun.30	06:32	11-57.06N	135-05.49E	250	8.8	9.5	
	C6	Jun.30	07:14	12-01.56N	135-02.72E	250	9.9	9.9	
	C7	Jun.30	07:44	12-06.00N	135-00.00E	250	10.2	10.1	
102	C1	Jun.30	09:44	12-06.00N	134-59.93E	250	7.9	10.0	forming triangle (#2)
	C2	Jun.30	10:19	12-01.46N	134-57.20E	250	10.1	9.9	
	C3	Jun.30	11:00	11-57.09N	134-54.54E	250	9.6	9.7	
	C4	Jun.30	11:34	11-56.98N	135-00.02E	250	10.1	10.0	
	C5	Jun.30	12:22	11-57.00N	135-05.42E	250	9.9	10.2	
	C6	Jun.30	12:50	12-01.51N	135-02.74E	250	10.2	10.3	
	C7	Jun.30	13:35	12-05.99N	134-59.98E	250	10.0	10.1	

5.17 XCTD

(1) Personnel

Masaki KATSUMATA (JAMSTEC) - Principal Investigator
Takuya HASEGAWA (JAMSTEC)
Kazuho YOSHIDA (Global Ocean Development Inc., GODI) - Operation Leader
Wataru TOKUNAGA (GODI)
Kouichi INAGAKI (GODI)
Ryo KIMURA (Mirai Crew)

(2) Objective

The objective of XCTD (eXpendable Conductivity, Temperature & Depth profiler) observation in this cruise is to obtain the vertical profiles off Palau Islands.

(3) Methods

We observed the vertical profiles of the sea water temperature and salinity measured by XCTD-1 (manufactured by Tsurumi-Seiki Co.). The signal was converted by MK-150N (Tsurumi-Seiki Co.) and was recorded by AL-12B software (Ver.1.1.4; Tsurumi-Seiki Co). The specifications of the measured parameters are as in Table 5.17-1. We launched 1 probe by using automatic launcher during Leg-1 as listed in Table 5.17-2.

Table 5.17-1: The range and accuracy of parameters measured by XCTD-1.

<u>Parameter</u>	<u>Range</u>	<u>Accuracy</u>
Conductivity	0 ~ 60 [mS/cm]	+/- 0.03 [mS/cm]
Temperature	-2 ~ 35 [deg-C]	+/- 0.02 [deg-C]
Depth	0 ~ 1000 [m]	5 [m] or 2 [%] (either of them is major)

(4) Preliminary results

The obtained vertical profile of temperature and salinity is displayed in Fig. 5.17-1.

(5) Data archive

This data obtained in this cruise will be submitted to the Data Management Group (DMG) of JAMSTEC.

Table 5.17-2: List of XCTD observations. SST (sea surface temperature) and SSS (sea surface salinity) at each launch are obtained by TSG (Section 5.8).

No.	Date	Time	Latitude [dd-mm.mmmm]	Longitude [ddd-mm.mmmm]	SST [deg-C]	SSS [PSU]	Probe S/N
01	2013/6/9	08:44	07-46.4862N	134-17.6736E	30.016	33.575	12099316

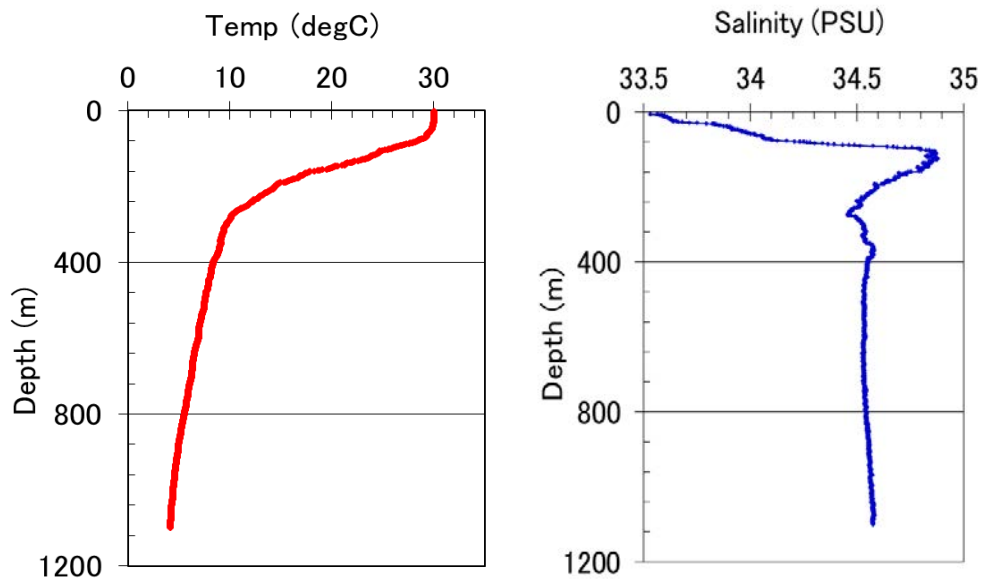


Fig.5.17-1: Vertical profile of the temperature (left) and the salinity (right) by XCTD observation.

5.18 Argo-type float

(1) Personnel

Satoru YOKOI (JAMSTEC) - Principal Investigator
Ayako SEIKI (JAMSTEC) - not on board
Takuya HASEGAWA (JAMSTEC)
Hiroki USHIROMURA (MWJ)

(2) Objective

To measure vertical profiles of sea-water temperature and salinity for investigating oceanic mixed layer structure and tropical air-sea interaction.

(3) Method

Three NEMO-type Argo floats (manufactured by Optimare Systems GmbH) were deployed in the middle of Leg-1. Serial numbers and deployment date and location are listed in Table 5.18-1. These floats measure vertical profile of seawater temperature and salinity above 500db at about 03LT (18UTC) every day. They use the Iridium transmitter to send observational data via satellite.

(4) Results

All of the three floats were deployed successfully. Figure 5.18-1 shows their positions and time-depth cross sections of observed seawater temperature and salinity until 25 June 2013. The data observed by the floats are transmitted successfully as of 5 July 2013.

(5) Data archive

The real-time data are provided officially via the Web site of Global Data Assembly Center (GDAC: <http://www.usgodae.org/argo/argo.html>, <http://www.coriolis.eu.org/>) in netCDF format. The Argo group in JAMSTEC (<http://www.jamstec.go.jp/ARGO/J-ARGO/>) also provides the real-time quality-controlled data in ASCII format.

Table 5.18-1. Deployments of the floats

Type	Serial number	WMO number	Date and time (UTC)	Latitude	Longitude	Type
NEMO	267	5904869	June 7, 2013, 07:25	15-5976N	135-00.10E	Iridium
NEMO	268	5904870	June 8, 2013, 00:20	12-59.88N	135-00.22E	Iridium
NEMO	269	5904871	June 8, 2013, 16:39	09-58.88N	134-58.98E	Iridium

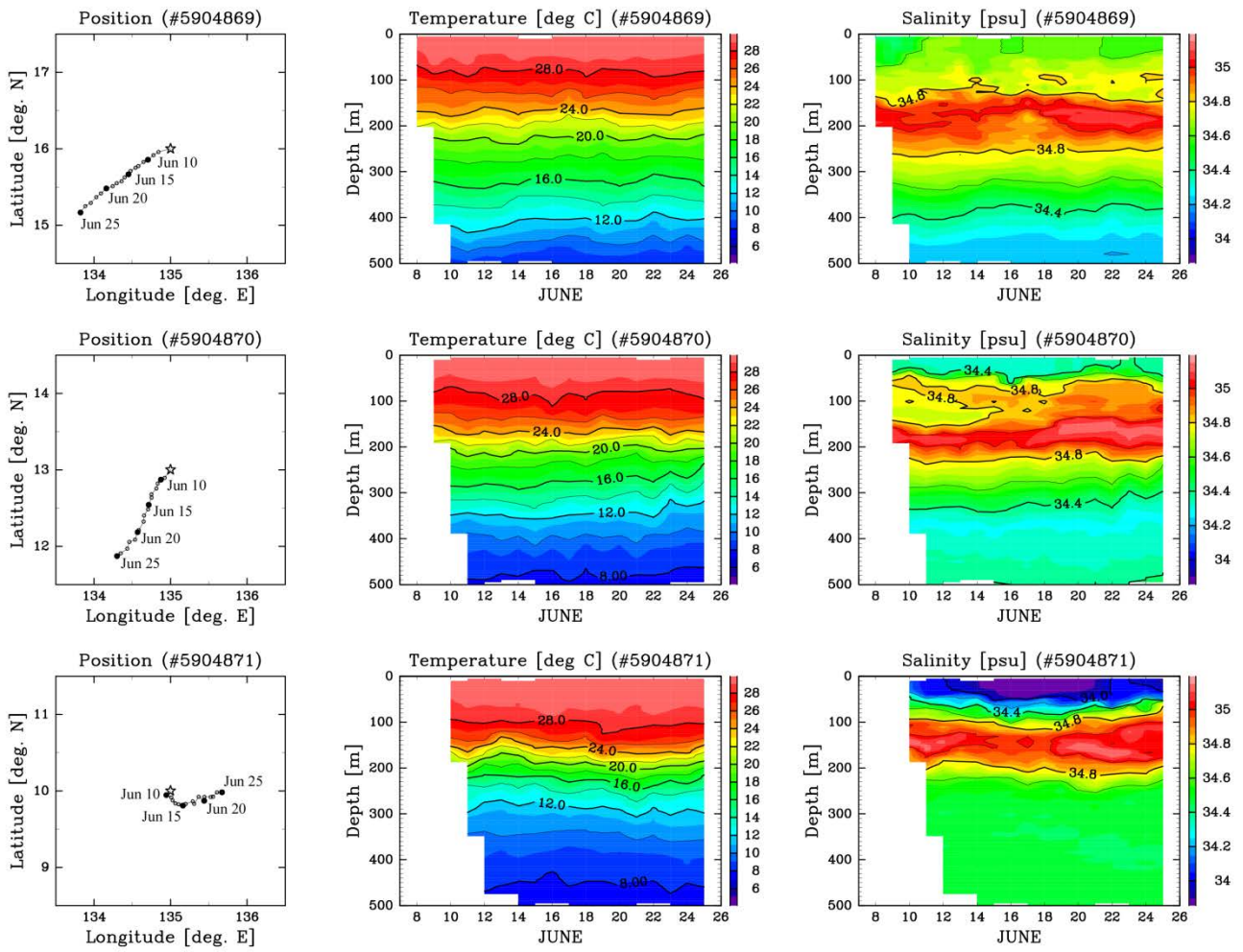


Fig. 5.18-1: (Left) The track of three floats until 25 June 2013. Stars indicate deployment points. (Center and right) Time-depth cross sections of seawater temperature and salinity observed by the floats until 25 June 2013.

5.19 Distribution and ecology of oceanic *Halobates* and their response to environmental factors

(1) Personnel

Tetsuo HARADA (Kochi Univ.) - Principal Investigator
Takero SEKIMOTO (Kochi Univ.)

(2) Introduction and Objectives

Many great voyages were launched to explore the oceans and what lies beyond, because they have always held a great fascination to us. A great variety of marine organisms were collected and describe during these voyages, but insects appear to have received little attention (Andersen and Chen, 2004). Although they are the most abundant animals on land, insects are relatively rare in marine environments (Cheng, 1985). However, a few thousand insect species belonging to more than 20 orders are considered to be marine (Cheng and Frank, 1993; Cheng, 2003). The majority of marine insects belong to the Coleoptera, Hemiptera, and Diptera, and they can be found in various marine habitats. However, the only insects to live in the open ocean are members of the genus *Halobates*, commonly known as sea-skaters. They belong to the family Gerridae (Heteroptera), which comprises the common pond-skaters or water-striders. Unlike most of its freshwater relatives, the genus *Halobates* is almost exclusively marine. Adults are small, measuring only about 0.5 cm in body length, but they have rather long legs and may have a leg span of 1.5 cm or more except for a new species, *Halobates megamoomario*. This new species which has very long body length of 0.9 cm and large mid-leg span of 3.2 cm has been newly and recently collected in the tropical Pacific Ocean during the cruise, MR-06-05-Leg 3, and described (Harada et al., submitted). They are totally wingless at all stages of their life cycle and are confined to the air-sea interface, being an integral member of the pleuston community (Cheng, 1985). One may wonder how much tiny insects have managed to live in the open sea, battling waves and storms. In life, sea-skaters appear silvery. On calm days ocean-going scientists have probably seen them as shiny spiders skating over the sea surface. It is not known whether ancient mariners ever saw them, and no mention of their presence has been found in the logs of Christopher Columbus's (1451-1506) ships or other ships that sailed to and from the New World (Andersen and Cheng, 2004).

Forty-seven species of *Halobates* are now known (Andersen and Cheng, 2004; Harada *et al.*, submitted). Six are oceanic and are widely distributed in the Pacific, Atlantic and the Indian Oceans. The remaining species occur in near-shore areas of the tropical seas associated with mangrove or other marine plants. Many are endemic to islands or island groups (Cheng, 1989).

The only insects that inhabit the open sea area are seven species of sea skaters: *Halobates micans*, *H. sericeus*, *H. germanus*, *H. splendens*, *H. sobrinus* (Cheng, 1985) and new two species of *H. megamoomario* and *H. moomario* under description (Harada *et al.*, submitted). Three species, *Halobates sericeus*, *H. micans* and *H. germanus* inhabit tropical and temperate areas of the Pacific Ocean in the northern hemisphere, including The Kuroshio Current and the East China Sea (Andersen and Polhemus, 1976, Cheng, 1985). *Halobates sericeus*, *H. micans* and *H. germanus* are reported from latitudes of 13°N-40°N, 0°N-35°N and 0°N-37°N, respectively, in the Pacific Ocean (Miyamoto and Senta, 1960; Andersen and Polhemus, 1976; Ikawa et al., 2002). However, this information was collected on different cruises and in different times of the years. There have been several ecological studies based on samples collected in a specific area in a particular season during the six cruises of R/V HAKUHO-MARU: KH-02-01, KH-06-02, TANSEI-MARU: KT-07-19, KT-08-23 and R/V MIRAI: MR-06-05-Leg 3, MR-08-02.

During one cruise, KH-02-01, one sea skater species, *Halobates sericeus*, was collected at 18 locations in the East China Sea area (27°10' N- 33°24' N, 124°57' E - 129°30' E) (Harada, 2005), and *H. micans* and/or *H. germanus* at only 8 locations in the area south of 29° 47'N, where water temperatures were more than 25°C. At three locations, where the water temperature was less than 23°C, neither *H. micans* nor *H. germanus* were

caught.

During another cruise, KH-06-02, in the latitude area of 12°N to 14°30'N, *Halobates micans* were caught at 6 of 7 locations, while *H. germanus* and *H. sericeus* were caught at only 3 and 1 location(s), respectively (Harada et al, 2006). However, at 15°00'N or northern area, *H. germanus* were caught at 14 of 19 locations, whereas *H. micans* and *H. sericeus* were caught at only 8 and 6 locations, respectively (Harada et al, 2006).

In the cruise, MR-06-05-Leg 3, larvae of both *H. micans* and *H. germanus* were very abundant at 6° N, whereas adults of *H. germanus* alone were completely dominant at 2° N on the longitudinal line of 130°E. On the longitudinal line of 138°E, larvae and adults of *H. micans* alone were dominant at points of 5 ° and 8°N, while adults of *H. germanus* were abundant between 0° and 2°N. At the two stations of St. 37 (6° N, 130° E) and St. 52 (5° N, 138° E), relatively great number of larvae of *H. sericeus* were collected. This species has been known to be distributed in the northern area of the Pacific Ocean. At St. 52 (6° N, 138° E), it was heavily raining around the ship while trailed.

In the cruise, KT-07-19 on the northern edge of Kuroshio Current, *H. sericeus* was mainly collected in the northern-eastern area of 135°-140°E, 34°-35°N whereas *H. germanus* and *H. micans* were mainly collected in the relatively southern-western area of 131°-133°E., 31°-33°N. Only *H. sericeus* can be transferred by the Kuroshio Current onto the relatively northern-eastern area and to do reproduce at least in the summer season. In the cruise of KT-08-23, Most of “domestic” specimen collected in the area northern to Kuroshio current and near to Kyushu and Shikoku islands in September were *H. germanus* (Harada *et al.*, submitted).

All samplings of *Halobates* have been performed at different geographical positions in any cruise in the Pacific Ocean so far. However, there has been no information on the dynamics in species and individual compositions in relatively eastern area of 145-160°E, 0-10°N of tropical Pacific Ocean. This study aims, first, to perform samplings in this area of the Western Pacific Ocean and examine dynamics of the species composition and reproductive and growth activity and compare these data to the data in the past which were got in more western area of 130-137°E, 0-10°N in the cruise, MR-06-05- Leg 3 (Harada et al., 2007; Harada et al., 2011a).

During the cruise, MR-08-02, on the longitudinal line of 130°E, larvae of both *H. micans* and *H. germanus* were very abundant at 5-12° N, whereas adults of *H. sericeus* alone were dominant at 17° N. In the lower latitude area of 5-8 ° N, all the three described species, *H. micans*, *H. germanus* and *H. sericeus* and un-described species, *Halobates moomario* (Harada *et al.*, unpublished) were collected. At a fixed point located at 12°N, 135°E, *H. micans* was dominant through the sampling period of 20 days, whereas *H. sericeus* was collected mainly in the latter half of the period. Higher number of *Halobates* (593) was collected in the first half of the sampling period (8th – 17th June, 2008) when the weather was very fine than that (427) in the second half (18th – 27th June, 2008) when the typhoon No 6 was born and developed near the fixed sampling point.

In this cruise of MR-09-04, on the longitudinal line of 155-156°E *H. germanus* was very dominant, whereas three adults of *H. micans*, *H. germanus* and *H. sericeus* were dominant at 5° N on the longitudinal line of 147 °E during this cruise held in Nov 4-Dec 12, 2009 (Harada et al., 2009; Harada et al., 2010a). Among several latitudes of 0-10 ° N, peak of number of individuals collected was located at 8 ° N, 5 ° N and 0-2 ° N for *H.m.*, *H.g.* and *H.s.*, respectively, on the longitudinal line of 155-156 ° E. From latitudinal point of view, *H. micans* and *H.germanus*. were abundant in 5-8 ° N, whereas *H. sericeus* and *H. moomario* were in 0-5 ° N. Except for St. 6 at 3 ° N, 147 ° E, more than half of specimen collected were larvae at the remaining St. 1-5 and St.7,8.. Un-described new species, *Halobates moomario* was mostly on the longitudinal line of 147°E. On the longitudinal line of 147 ° E, more newly hatched larvae were collected than those on the line of 155-156E. *Halobates micans* was dominantly inhabiting at a fixed point of 3N, 139E in the tropical Pacific Ocean during a science cruise of MR-10-03 administered in May and June of 2010.

In the cruise, KH-10-04-Leg. 1 (Harada et al., 2010b), the samplings of *Halobates* inhabiting temperate and

subtropical Pacific Ocean along the cruise track from Tokyo to Honolulu for the 2 weeks showed that four species of *Halobates micans*, *H. germanus*, *H. sericeus*, *H. moomario* inhabited in the relatively northern and western area of 30°N-34°N and 140°E-144°E, although *H. sericeus* was dominant species. In the relatively southern and eastern area of 19°N-29°N and 147°E-163°W, only *H. sericeus* was exclusively inhabiting. Many larvae of this species were collected through all the stations and the reproductive activity of *H. sericeus* seems to be active in this area. Significantly more female-adults were collected rather than male-adults in total (χ^2 -test, $P < 0.01$). The extent of positive phototaxis by females may be higher than that of males, or avoiding behavior from the opening of the Neuston Net might be more active by males than females.

In the cruise, KH-10-04-Leg 2 (Harada et al., 2010c), the samplings of *Halobates* in Central or Eastern Tropical Pacific Ocean showed that *Halobates sericeus* was dominant at 13°59'N, 162°06'W, while *Halobates megamoomario* and *Halobates moomario* were dominant in the areas of 2°35'N-2°45'N, 164°W-166°W and 14°N-17°N, 172°W-176°W, respectively. In the sampling area of the Central or Eastern Tropical Pacific ocean, the population density of *Halobates* is relatively low of 3626.4/km².

In the cruise, KH-10-05-Leg 1 (Harada et al., 2010d), the samplings of *Halobates* in Tropical Indian Ocean showed that *Halobates micans* was dominant with estimated population density of about 58000 individuals/km² along the cruise track from 04°09'S, 094°26'E to 08°40'S, 084°04'E, while *H. micans* was also dominant but estimated population density was relatively low of 0-21523 /km² on the line of cruise track from 10°12'S, 080°24'E to 15°23'S, 067°48'E. Positive and negative correlations were shown between chlorophyll conc. and the number of *Halobates* (mostly *H. micans*) individuals collected and between oxygen and the number of sea skaters inhabiting in Tropical Indian Ocean, respectively.

In the cruise, MR-11-07-Leg 1, the samplings of *Halobates* inhabiting two locations at 01°55'S, 083°24'E (Station 1) and 08°00'S, 080°30'E (Stations 2-17) in subtropical Indian Ocean showed that two species of *Halobates micans* and *H. germanus* inhabited in the tropical Indian Ocean, although most of individuals collected are *H. micans* and it was completely dominant species. This result coincides with results of the past study (Andersen and Cheng, 2004; Harada et al., 2010a; Harada et al., 2011b). At the fixed location of 08°00'S, 080°30'E, one third of the density of *H. micans* can be estimated, compared with the density in relatively wide area of 8°N-6°S, 76°E-86°E (KH-10-05) in the Indian Ocean. Probably the low activity of photosynthesis and relatively high oxygen consumption which can be suggested by low amount of chlorophyll in surface sea water in this fixed location may be related to relatively low density of *Halobates*, because low photosynthesis activity and high dissolved oxygen show extremely low amount of animals like as zooplankton and nekton which mean low amount of foods for sea skaters. Samplings at the fixed location at 08°00'S, 080°30'E showed that higher population density (20491.4 individuals/km²) of *Halobates micans* was estimated at the stations where air temperature was 27.5°C than that (12070.9 individuals/km²) in the stations at which air temp. was less than 27.5 °C (Mann-Whitney U-test: $z = -2.614$, $p = 0.009$). Similar result in the population density of larvae (481 larvae of *H. micans* and 70 ones of *H. germanus* were collected in total at Stations 1-17) implies higher reproductive activity when the air temperature become higher than 27.5 °C ($z = -2.935$, $p = 0.003$).

In the cruise, KH-12-01-Leg 2, the samplings of *Halobates* inhabiting temperate and subtropical Pacific Ocean along the cruise track from Honolulu to Tokyo for the 2 weeks showed that 68-198 individuals of only one species of *H. sericeus*, were exclusively collected at the three stations around the cruise track from 24°30'N, 177°32'W to 26°27'N, 174°15' E. At another station of 27°42'N 169°24' E, the number of individuals of *H. sericeus* were small of 42. At the two stations located in northern area (30°15'N, 159°04' E; 31°27'N, 154°07' E), no individuals were collected any more in this season. Northern limit of the distribution of *H. sericeus* would be located between 27°42'N and 30°15'N in the season of late Feb and the beginning of Mar in the central Pacific Ocean. Andersen and Cheng (2004) mentioned about the lower limit for surface water temperature which can be located around 25°C. This study shows that *Halobates sericeus* which distributed also to the northern area of 40 degree north can be survived even in the sea surface temperature of

22°C.

This study aims, first, to examine the relationship between the individual number and species components of the oceanic sea skaters of *Halobates* and oceanic dynamism on several factors like as precipitation, waves, air temperature, chlorophyll conc. and dissolved oxygen conc. in surface water during samplings in the area of 14°N-24°N, 135°E-138°E of the subtropical and tropical Pacific Ocean.

Fresh water species in Gerridae seem to have temperature tolerance from -3°C to 42°C (Harada, 2003), because water temperature in fresh water in ponds and river highly changes daily and seasonally. However, water temperatures in the ocean are relatively stable and only range from 24°C to 30 °C in the center of Kuroshio current in southern front of western Japan (Harada, 2005). Adults of *Halobates germanus* showed semi-heat-paralysis (SHP: static posture with no or low frequency to skate on water surface), when they were exposed to temp. higher than 32°C (Harada unpublished, data in the TANSEIMARU cruise: KT-05-27).

In contrast to the temperate ocean, water temperature in the tropical ocean area, is more stable around 30°C. Therefore, the tropical species of *H. micans* is hypothesized to have lower tolerances to temperature changes than the tropical-temperate species, *H. cericeus*. This hypothesis was true in the laboratory experiment during the cruise of KH-06-02-Leg 5 (Harada *et al.*, submitted). When the water temperature increased stepwise 1°C every 1 hour, heat-paralysis (ventral surface of thorax attached to water surface and unable to skate) occurred at 29°C to >35 °C (increase by 1 to >7 °C). Three of four specimens in *Halobates sericeus* were not paralyzed even at 35 °C and highly resistant to temperature change, while only one of nine in *H. micans*. and only four of twelve in *H. germanus* were not paralyzed at 35 °C. On average, *H. sericeus*, *H. germanus* and *H. micans* were paralyzed at >35.6 °C (SD: 0.89), >32.9 °C(SD: 2.17) and >31.6 °C (SD: 2.60) on average, respectively (Harada *et al.*, submitted).

As an index of cold hardiness, super cooling points (SCPs) have been used in many insects (Bale, 1987, 1993; Worland, 2005). The absence of ice-nucleating agents and/or the lack of an accumulation of cryo-protective elements can often promote higher super cooling points (Milonas and Savopoulou-Soultani, 1999). SCPs, however, might be estimated as only the lower limits of supercooling capacity and only a theoretical lower threshold for the survival of insects as freeze-non-tolerant organisms. Many insects show considerable non-freezing mortality at temperatures well above the SCPs, a “chill-injury” species (Carrillo *et al.*, 2005; Liu *et al.*, 2007). Liu *et al.* (2009) recently showed that SCPs change in accordance with the process of winter diapauses, decreasing in Dec-Feb and increasing rapidly in Feb-Apr (diapauses completing season) due to making glycogen from trehalose as a “blood suger” leading to lower osmotic pressure in haemolymph due to low “trehalose” level. This relation supports the possibility of SCPs available as an indirect indicator of cold hardiness of insects.

The 0-10°N latitude-area in the Pacific Ocean has very complicated dynamic systems of ocean and atmosphere. Because of such complicated system, water/air temperatures and water conductivity (salinity) can be in dynamic change temporally and spatially. Sea skaters inhabiting this area of the Pacific Ocean show relatively high tolerance to temperature changes (heat tolerance) (Harada *et al.*, 2011a), and *H. sericeus* which is inhabiting wide latitude area of 40°N-40°S in the Pacific Ocean is more hardy to temperature increase than other two oceanic sea skaters, *H. germanus* and *H. micans* inhabiting narrower latitude range of 25°S-25°N and 20°S-20°N in the Indian and Pacific Ocean (Harada *et al.*, 2011a). Adult specimens of *Halobates micans* living at 6°S, 89°E where currents from south and north directions hit and get together than those living at other places of 8°N, 89°E in the tropical Indian Ocean (Harada *et al.*, 2011c). Due to 3 or 4°C of temperature decrease when rain falls, tolerance to high temperature by *H. micans* becomes weaker in the tropical Pacific Ocean (Harada *et al.*, 2011c). Recently, a cross-tolerance to high and low severe temperature has been reported by fresh water species of semi-aquatic bug, *Aquarius paludum* (Harada *et al.*, 2010e). Also oceanic sea skaters (all four species of *H. micans*, *H. germanus*, *H. sericeus* and *H.sp.*) inhabiting tropical ocean showed a negative correlation between heat coma temperature and SCP (Harada *et al.*, 2009: the cruise report of

MR-09-04). Similar correlation was also observed only for males of *H. sericeus* collected on the cruise track between Tokyo and Honolulu, Hawaii (Harada et al., 2010b: the cruise report of KH-10-04-Leg 1).

This study aims, second, to examine whether sea skaters, living in the area of 14°N-24°N, 135°E-138°E of the subtropical and tropical Pacific Ocean show a high cross tolerance of higher cool tolerance and lower super cooling points (SCP) (whether SCP can be or not an index of cold hardiness) and also to examine some relationship between the cold hardiness plus SCP and oceanic dynamism on several factors like as precipitation, waves, air temperature, chlorophyll conc. and dissolved oxygen conc. in surface water.

(3) Materials and Methods

Samplings

Samplings were performed on 5th, 13th, 15th, 17th, 19th, 21st, 23rd, 25th, 27th, and 29th June, 2012 with a Neuston NET (6 m long and with diameter of 1.3 m.) (Photos 1,2). The Neuston NET was trailed for 15 mm x 3 times on the sea surface at 1 station located at 24°00'N 138°10'E and the other 10 stations around a fixed point of 12°00'N 135°00'E of the subtropical and tropical Pacific Ocean on the starboard side of R/V MIRAI (8687t) which is owned by JAMSTEC (Japan Agency for Marine-earth Science and TEChnology). The trailing was performed for 15min exclusively at night with the ship speed of 2.0 knot to the sea water (Photo 1). It was repeated 2 times in each station. Surface area which was swept by Neuston NET was evaluated as an expression of [flow-meter value x 1.3m of width of the Neuston NET (Photo 1).

Samples were transferred from the sample bottle at the end of the Neuston net to transparent aquarium (Photo 3).

All the sea skaters were picked up with tweezers for planktons from the transparent aquarium on the white paper in a tray (Photo 4). The samples as sea skaters were examined very carefully and the species and stage of all the specimens were identified (after Andersen and Cheng, 2004) and the number of them was counted and recorded (Tables 1, 2, 3).

Laboratory experiment

Sea skaters trapped in the pants (grey plastic bottle) (Photo 2) located and fixed at the end of Neuston NET (Photo 2) were paralyzed with the physical shock due to the trailing of the NET. Such paralyzed sea skaters were transferred on the surface of paper towel to respire. Then, the paralysis of some ones was discontinued within 20min. When sea skaters were trapped in the jelly of jelly fishes, the jelly was removed from the body of sea skaters very carefully and quickly by hand for the recovering out of the paralysis.

Adults which recovered out of the paralysis were moved on the sea water in the aquaria set in the laboratory for the Cool Coma Experiments (Photo 5) and measuring Super Cooling Points (Photo 6). Many white cube aquaria (30cm × 30cm × 40cm) were used in the laboratory of the ship for rearing of the adults which were recovered out of the paralysis due to the trailing. Each aquarium contained ten to forty adults of *Halobates*. Both the room temperature and sea water temperature in the aquaria were kept at 29±2°C. For 11-12 hours after the collection, sea skaters were kept in the aquaria before the Cool Coma Experiment. All the individuals of *Halobates* kept in the aquaria were fed on larvae of fishes (eg. Sardine and relatives) which were caught by the Neuston net trailings and/or adult flies, *Lucillia illustris*. Foods were given only for 8 hours of 10:00-18:00 and sea water in the aquaria were replaced by the new one two times at 8:00 and at 18:00 because of avoidance from water pollution due to the foods.

No foods were given more than 12 hours before measuring SCP, because the contents of alimentary canal would be possible to become ice-nuclei substances. The transparent round-shaped aquarium as the experimental arena has sea water with the same temperature (mostly 28 or 30°C) as that of the aquarium where

sea skaters had been kept. Ten or eleven adult specimens were moved to the Low Temperature Thermostatic Water Bath (Thomas: T22LA) (55cm × 40cm × 35cm). Temperature was gradually decreased (1 °C per 5 min) by 1°C every 15 min by the automatic cooling system of the water bath till the cool temperature coma occurring in all the experimental specimens.

Temperature was very precisely controlled by automatic thermo-stat system of the water bath. Temperature at which Semi Cool Coma (Semi Cool Coma Temperature [SCCT]: little or no movement on the water surface more than 3 seconds) occurs and Temperature at which Cool Coma (Cool Coma Temperature [CCT]: ventral surface of the body was caught by sea water film and no ability to skate any more) occurs were recorded (Table 4).

Determination of super cooling point (SCP)

Measurements of super cooling points and increasing temperature value at the moment of an exothermic event occurred in the body of the specimen (ITSCP: increased temperature at SCP) were performed for the adult specimen paralyzed by low temperature of the three species of oceanic *Halobates* (*H. micans*, *H. germanus*, *H. sericeus*) just after the cool coma experiment during this cruise (Table 4)

Surface of each adult was dried with filter paper, and thermocouples which consist of nickel and bronze were attached to the abdominal surface of the thorax and connected to automatic temperature digital recorders (Digital Thermometer, Yokogawa Co, LTD, Model 10, Made in Japan). The thermocouple was completely fixed to be attached to the ventral surface of abdomen by a kind of Scotch tape. The specimen attached to thermocouples was placed into a compressed-Styrofoam box (5×5×3 cm³) which was again set inside another insulating larger compressed Styrofoam to ensure that the cooling rate was about 1°C/min for recording the SCP in the freezer in which temperature was -35°C. The lowest temperature which reached before an exothermic event occurred due to release of latent heat was regarded as the SCP (Zhao and Kang, 2000). All tested specimen were killed by the body-freezing when SCP was determined.

(4) Results and Discussion

Population density and other Meteorological factors

The samplings at 24°01'N 138°10'E (Station 1) and 12°00'N 135°00'E as a fixed place (Stations 2-10) in subtropical and tropical Pacific Ocean showed that two species of *Halobates micans* and *H. sericeus* inhabited at Station 1 and *H. micans* and *H. germanus* inhabited at the fixed place (Stations 2-10).

These results coincides with results of the past study (Andersen, 1982; Andersen and Cheng, 2004; Harada et al., 2009; Harada et al., 2010a). However, this study shows that *Halobates sericeus* inhabits More higher latitude area than the other two species at the same season.

High density near to 100,000 individuals per 1 km² of *H. sericeus* could be estimated at the Station 1 in this study.

Laboratory experiment

Semi-cool-coma temperature (SCCT), cool-coma temperature (CCT), gap temperature for cool coma (GTCC) super cooling point (SCP) and increased temperature at super cooling point (ITSCP) were ranged 14 °C to 28 °C, 14 °C to 23°C, 6°C to 15°C, -20.9°C to -8.6°C and 0.8°C to 10.1°C, respectively (Table 4).

No significant negative correlation between CCT and SCP was shown in the combined data from the three species at the individual level (Pearson's correlation test: $r=-0.093$, $p=0.363$, $n=98$). However, the comparison of CCT and SCP between *H. micans* and *H. germanus* from the same sampling sites showed some correlative relationship, lower cool-coma temperature and lower SCP shown by *H. germanus* than *H. micans*.

(Table 5-A).

This relationship implies that SCP could be possible to be used as an index showing the ‘cold hardiness’ of oceanic sea skaters. However, more experiments which measure CCT and SCP of the same individuals showing higher variables among individuals are needed for the decision of whether the SCP can or cannot be used as the index of cold hardiness. In this study, *Halobates sericeus* and *H. germanus* showed significantly higher cold hardiness than *H. micans*. The wider latitude range of the both species than *H. micans* would be related to the higher cold hardiness.

As shown by Table 5-B, the exposure to lower temperature during the cool coma experiments would be possible to depress the super cooling points. This depression would be explained as a kind of “cold acclimation effect”.

(5) Additional Analyses

It will be analyzed how the data on field samplings in this study are related to environmental data as the oceanography data at the three sampling stations: 24°01'N 138°10'E (Station 1) and 12°00'N 135°00'E as a fixed place (Stations 2-10) in the Pacific Ocean at the cruise, MR-13-03. This relationship can be compared to other similar analyses on the data collected in the area of 4°S to 13°S and 8°N to 6°S in the Indian Ocean at two cruises, KH-10-05-Leg 1 (Harada et al., 2010d) and KH-07-04-Leg1 (Harada et al., 2008), respectively and also in the area of 30°-35°N along the Kuroshio Current at the cruises, KT-07-19, KT-08-23, KT-09-20 and the other R/V TANSEIMARU cruises held in the past. The relationship between the sampling data and oceanographic data (for example, surface sea temperature and air temperature, chlorophyll contents and dissolved oxygen level) will be analyzed.

The comparative studies will be done on the relationship between cold tolerance and SCP data, and other oceanographic data. Dissection data (for example reproductive maturation), chemical contents data (example lipids) and gene data of MtDNA from *Halobates* samples should be analyzed in the future.

(6) Data Archive

All data during this cruise will be submitted to the JAMSTEC Data Management Group (DMG).

(7) Acknowledgements

We would like to thank Dr. Katsuro KATSUMATA (Head Scientist of the cruise: MR-13-03) for the permission to do this study during the R/V MIRAI cruise, for his warm suggestion on ocean and atmosphere dynamics, and encouragement and help throughout this cruise. The samplings and the experimental study were also possible due to supports from all of the crew (Captain: Mr. Yoshiharu TSUTSUMI) and all the scientists and the engineers from GODI and MWJ in this cruise. We would like to give special thanks to them.

(8) References

Andersen NM, Chen L 2004: The marine insect *Halobates* (Heteroptera: Gerridae): Biology, adaptations distribution, and phylogeny. *Oceanography and Marine Biology: An Annual Review* 42, 119-180.

- Andersen NM, Polhemus JT 1976: Water-striders (Hemiptera: Gerridae, Vellidae, etc). In L. Cheng L. (ed): *Marine Insects*. North-Holland Publishing Company, Amsterdam, pp 187-224.
- Bale JS 1987: Insect cold hardiness: freezing and supercooling- an ecophysiological perspective. *J. Insect Physiol.*, 33: 899-908.
- Bale JS 1993: Classes of Insect Cold Hardiness. *Functional Ecol.* 7: 751-753.
- Carrillo MA, Heimpel GE, Moon RD, Cannon CA, Hutchison WD 2005: Cold hardiness of *Habrobracon hebetor* (Say) (Hymenoptera: Braconidae), a parasitoid of pyralid moths. *J. Insect Physiol.* 51: 759-768.
- Cheng L 1985: Biology of Halobates (Heteroptera: Gerridae) *Ann. Rev. Entomol.* 30, 111-135.
- Cheng L 1989: Factors limiting the distribution of Halobates species. In *Reproduction, Genetics and Distribution of Marine Organisms*, J.S. Ryland & P.A. Tyler (eds), Fredensbor, Denmark: Olsen & Olsen, 23rd European Marine Biology Symposium, pp. 357-362.
- Cheng L 2003: Marine insects. In Resh VH & Carde RT (eds), *Encyclopedia of Insects*, pp. 679-682, Academic Press, San Diego.
- Cheng L, Frank JH 1993: Marine insects and their reproduction. *Oceanography and Marine Biology: An Annual Review* 31, 479-506.
- Harada T 2003: Hardiness to low temperature and drought in a water strider, *Aquarius paludum* in comparison with other insect groups *Trends in Entomology(Research Trends, Trivandrum, India)*, 3, 29-41.
- Harada T 2005: Geographical distribution of three oceanic Halobates spp. and an account of the behaviour of *H. sericeus* (Heteroptera: Gerridae). *Eur. J. Entomol.* 102, 299-302.
- Harada T, Ishibashi T, Inoue T 2006: Geographical distribution and heat-tolerance in three oceanic *Halobates* species (Heteroptera: Gerridae). *The Cruise Report of KH-06-02-Leg 5*.
- Harada T, Nakajyo M, Inoue T 2007: Geographical distribution in the western tropical Pacific Ocean and heat-tolerance in the oceanic sea skaters of *Halobates*. (Heteroptera: Gerridae) and oceanic dynamics. *The Cruise Report of MR-06-05-Leg3*.
- Harada T, Iyota K, Shiraki T, Katagiri C 2009: Distribution, heat-tolerance and super cooling point of the oceanic sea skaters of *Halobates*. (Heteroptera: Gerridae) inhabiting tropical area of western Pacific Ocean and oceanic dynamics. *The Cruise Report of MR-09-04*
- Harada T, Sekimoto T, Iyota K, Shiraki T, Takenaka S, Nakajyo M, Osumi O and Katagiri C 2010a: Comparison of the population density of oceanic sea skater of *Halobates* (Heteroptera: Gerridae) among several areas in the tropical pacific ocean and the tropical Indian Ocean. *Formosan Entomol.*, 30, 307-316.
- Harada T, Iyota K, Osumi Y, Shiraki T, Sekimloto T, Yokogawa S, Oguma K 2010b: Distribution, heat-tolerance and supercooling point of the oceanic sea skaters of *Halobates* (Heteroptera: Gerridae) inhabiting temperate and Subtropical Pacific Ocean along the cruise track from Tokyo to Honolulu. *The Cruise Report of KH-10-04-Leg 1*.
- Harada T, Iyota K, Osumi Y, Shiraki T, Sekimoto T 2010c: Distribution and tolerance to brackish and fresh water bodies as a habitat in oceanic sea skater of *Halobates* (Heteroptera: Gerridae) inhabiting Eastern & Central Tropical Pacific Ocean. *The Cruise Report of KH-10-04-Leg 2*.
- Harada T, Iyota K, Sekimoto T 2010d: Distribution and tolerance to brackish water bodies as habitat in oceanic sea Skater of *Halobates* (Heteroptera: Gerridae) inhabiting Tropical Indian Ocean. *The Cruise Report of KH-10-05-Leg 1*.
- Harada T, Ikeda S, Ishibashi T 2010e: Cross tolerance between heat and cold stress by warm temperate *Aquarius paludum paludum* and subtropical *Aquarius paludum amamiensis*, semi-aquatic bugs (Gerridae, Heteroptera). *Formosan Entomol.*, 30:87-101.

- Harada T, Takenaka S, Sekimoto T, Nakajyo M, Inoue T, Ishibashi T, Katagiri C 2011a: Heat coma as an indicator of resistance to environmental stress and its relationship to ocean dynamics in the sea skaters, *Halobates* (Heteroptera: Gerridae). *Insect Sci.*, 18, 73-711.
- Harada T, Sekimoto T, Osumi Y, Kobayashi A, Shiraki T 2011b: Distribution and ecology of oceanic *Halobates* inhabiting tropical area of Indian Ocean and their responding system to several environmental factors. The Cruise Report of MR-11-07 (23rd September, 2011 ~ 2nd December, 2011)
- Harada T, Takenaka S, Sekimoto T, Osumi Y, Nakajyo M, Katagiri C 2011c: Heat coma and its relationship to ocean dynamics in the oceanic sea skaters of *Halobates* (Heteroptera: Gerridae) inhabiting Indian and Pacific Oceans. *J. Thermal Biol.*, 36: 299–305.
- Ikawa T, Okabe H, Hoshizaki S, Suzuki Y, Fuchi T, Cheng L 2002: Species composition and distribution of ocean skaters *Halobates* (Hemiptera: Gerridae) in the western pacific ocean. *Entomol. Sci.* 5, 1-6.
- Liu ZD, Gong PY, Wu KJ, Wei W, Sun JH, Li DM 2007: Effects of larval host plants on over-wintering preparedness and survival of the cotton bollworm, *Helicoverpa armigera* (Hübner) (Lepidoptera: Noctuidae). *J. Insect Physiol.* 53: 1016-1026.
- Liu ZD, Gong PY, Heckel DG, Wei W, Sun JH, Li DM 2009: Effects of larval host plants on over-wintering physiological dynamics and survival of the cotton bollworm, *Helicoverpa armigera* (Hübner)(Lepidoptera: Noctuidae). *J. Insect Physiol.* 55: 1-9.
- Milonas P, Savopoulou-Soultani M 1999: Cold hardiness in diapause and non-diapause larvae of the summer fruit tortorix, *Adoxophes orana* (Lepidoptera: Tortricidae). *Eur. J. Entomol.* 96: 183-187.
- Miyamoto S, Senta T 1960: Distribution, marine condition and other biological notes of marine water-striders, *Halobates* spp., in the south-western sea area of Kyushu and western area of Japan Sea. *Sieboldia* (In Japanese with English summary). 2, 171-186.
- Worland M. R. 2005: Factors that influence freezing in the sub-antarctic springtail *Tullbergia antarctica*. *J. Insect Physiol.* 51: 881-894.

Table 1-A. Number of *Halobates* collected at locations in the subtropical and tropical Pacific Ocean on 5th, 13th, 15th, 17th, 19th, 21st, 23rd, 25th, 27th, 29th June and 1st July 2012 (N: Total number of individuals collected; *H.m.*: *Halobates micans*; *H.g.*: *Halobates germanus*; *H.s.*: *Halobates sericeus*; Stat: Station number; WT: Water temperature (°C); AT: Air temp.; L: N of larvae; A: N of adults, E: N of exuviae; Date: sampling date; Sampling was performed for 45min. EG: eggs on some substrates like as polystyrene form thousands of eggs laid on the substrate. S: Surface area which was swept by Neuston NET was expressed as value of flow-meter x 1.3m of width of Neuston NET; WS: wind speed (m/s); W: weather; TD: Time of day; WS: Wind speed, CS: Current speed(m/s)CD: Current direction; F: female; M: male; DO: dissolved oxygen (μmol/kg); Chl: Chlorophyll-A conc.(relative fluorescent value); SL: salinity(‰)

Latitude	Longitude	N	L	A	<i>H.m.</i>	<i>H.g.</i>	<i>H.s.</i>	EG	E	Stat	WT	AT	WS	W	CS	CD	TD	Date	S(x1.3 m ²)	DO	Chl	SL	
		F		M																			
24°01'N	138°10'E	142	89	32	21	5	0	137	0	4	St.1-1	27.6	27.9	5.1	C	0.8	239°	19:04~19	Jun 5	768.2	244.49	-	34.8
23°59'N	138°10'E	146	82	32	32	0	0	146	0	6	St.1-2	27.6	27.9	9.0	R	0.8	233°	19:33~48	Jun 5	875.5	243.43	-	34.8
23°59'N	138°10'E	17	8	5	4	1	0	16	0	0	St.1-3	27.6	27.9	4.5	C	0.9	248°	19:55~20:10	Jun 5	786.6	243.91	-	34.6
12°00'N	135°00'E	9	6	2	1	7	2	0	0	0	St.2-1	29.5	29.5	9.8	F/R	0.3	290°	21:17~32	Jun 13	642.0	-	-	32
11°59'N	135°00'E	22	19	2	1	11	11	0	0	0	St.2-2	29.5	29.5	7.1	F/R	0.2	267°	21:38~53	Jun 13	642.3	-	-	32
11°59'N	135°00'E	89	74	9	6	33	56	0	0	0	St.2-3	29.5	29.5	9.4	F/R	0.4	279°	22:00~15	Jun 13	821.0	-	-	32
12°00'N	135°00'E	25	21	4	0	8	17	0	0	0	St.3-1	29.0	29.4	10.6	F/R	0.1	343°	21:10~58	Jun 15	741.0	-	-	33
12°00'N	135°00'E	39	30	2	7	16	23	0	0	0	St.3-2	29.0	29.4	8.3	F/R	0.3	311°	21:32~47	Jun 15	683.5	-	-	33
12°00'N	135°00'E	33	25	4	4	14	19	0	0	0	St.3-3	29.0	29.4	9.8	F/R	0.3	304°	21:53~22:08	Jun 15	-	-	-	33
12°01'N	135°00'E	17	11	3	3	5	12	0	0	0	St.4-1	28.4	29.3	11.1	F/R	0.7	267°	21:12~27	Jun 17	689.5	-	-	33
12°00'N	135°00'E	14	7	3	4	7	7	0	0	0	St.4-2	28.4	29.3	12.5	F/R	0.6	281°	20:32~47	Jun 17	519.1	-	-	33
12°00'N	134°59'E	11	7	2	2	4	7	0	0	0	St.4-3	28.4	29.3	10.2	F/R	0.6	265°	21:53~22:08	Jul 17	680.0	-	-	33
12°01'N	135°00'E	42	39	2	1	32	10	0	0	0	St.5-1	28.4	29.3	5.0	F	1.1	274°	21:13~28	Jun 19	893.0	-	-	34
12°00'N	134°59'E	38	37	1	0	15	23	0	0	0	St.5-2	28.4	29.3	3.8	F	1.1	290°	21:35~50	Jun 19	718.8	-	-	34
12°00'N	134°59'E	23	21	1	1	13	10	0	0	0	St.5-3	28.4	29.3	5.0	F	1.1	287°	21:55~22:10	Jun 19	691.0	-	-	34
12°01'N	135°00'E	38	36	2	0	22	16	0	0	0	St.6-1	29.4	29.4	8.7	F	10.0	257°	21:11~26	Jun 21	980.8	-	-	33
12°00'N	135°00'E	55	47	7	1	29	26	0	0	0	St.6-2	29.4	29.4	8.9	F	0.8	257°	21:32~47	Jun 21	980.0	-	-	33
11°59'N	135°00'E	21	19	0	2	11	10	0	0	0	St.6-3	29.4	29.4	8.6	F	1.0	265°	21:53~22:08	Jun 21	856.0	-	-	33
12°01'N	134°59'E	18	11	3	4	5	13	0	0	0	St.7-1	29.7	29.6	8.2	F	0.5	297°	21:15~30	Jun 23	857.0	-	-	33
12°00'N	135°00'E	19	17	2	0	7	12	0	0	1	St.7-2	29.7	29.6	7.6	F	0.5	288°	20:36~51	Jun 23	930.2	-	-	33
12°00'N	135°00'E	16	14	1	1	8	8	0	0	0	St.7-3	29.7	29.6	9.2	F	0.5	290°	21:57~22:12	Jul 23	854.3	-	-	33
12°01'N	135°00'E	11	4	4	3	4	7	0	0	0	St.8-1	29.6	29.5	6.2	F	0.7	352°	21:11~26	Jun 25	708.0	-	-	33
12°01'N	135°00'E	9	5	1	3	2	7	0	0	0	St.8-2	29.6	29.5	6.0	F	0.7	346°	21:32~47	Jun 25	701.0	-	-	33
12°00'N	135°00'E	10	4	4	2	5	5	0	0	0	St.8-3	29.6	29.5	6.0	F	0.7	340°	21:53~22:08	Jun 25	823.8	-	-	33
12°01'N	134°59'E	4	3	0	1	0	4	0	0	0	St.9-1	29.4	29.6	8.6	F	1.2	310°	21:10~25	Jun 27	817.0	-	-	34
12°01'N	134°59'E	11	9	2	0	7	4	0	0	0	St.9-2	29.4	29.6	10.6	F	1.1	318°	21:31~46	Jun 27	692.0	-	-	34

Table 2: A comparison of population density of oceanic sea skaters, *Halobates* among four areas of open Indian and Pacific Oceans. Samplings were performed during the four cruises including this cruise. *H.m.*: *Halobates micans*; *H.g.*: *H. germanus*; *H.s.*: *H. sericeus*; *H.p.*: *H. princeps*; sp.: *H. sp.*: Density: individual number/km²

1. MR-10-03: Western Tropical Pacific Ocean, 5°N, 139°30'E (Harada et al., 2010f)

	Total		<i>H.m</i>	<i>H.g</i>	<i>H. s .</i>	<i>H. p or sp</i>	AS [#]
	Nymphs	Adults					
Number	3772	383	4059	66	1	28	0.105310
Density	35834.0	3638.5	38560.5	627.0	9.5	266.0	-

2.KH-07-04-Leg 1: Eastern Tropical Indian Ocean, 8°N-6°35'S, 86°E- 76°36'E) (Harada et al., 2008)

	Total		<i>H.m</i>	<i>H.g</i>	<i>H. s .</i>	<i>H. p or sp</i>	AS [#]
	Nymphs	Adults					
Number	1291	706	1886	111	0	0	0.044292
Density	29147.5	15939.7	42581.1	2506.1	0	0	-

3. MR-11-07-Leg 1 (this cruise, Stations 1-17): Eastern Tropical Indian Ocean, 01°55'S, 083°24E; 8°S, 80°30'E)

(Harada et al., 2011b)

	Total		<i>H.m</i>	<i>H.g</i>	<i>H. s .</i>	<i>H. p or sp</i>	AS [#]
	Nymphs	Adults					
Number	551	255	697	109	0	0	0.0438607
Density	12562.5	5813.9	15891.2	2485.1	0	0	-

4.MR-12-05-Leg 1 (this cruise, Stations 1-3): Western Subtropical and Tropical Pacific Ocean

	Total		<i>H.m</i>	<i>H.g</i>	<i>H. s .</i>	<i>H. p or sp</i>	AS [#]
	Nymphs	Adults					
A. 13°59'N 149°16'E							
Number	44	73	43	0	74	0	0.0061659
Density	7136.0	11839.3	6973.8	0	12001.5	0	-

	<u>Total</u>	<u>H.m</u>	<u>H.g</u>	<u>H. s .</u>	<u>H. p or sp</u>	<u>AS[#]</u>	
	<u>Nymphs</u>	<u>Adults</u>					
<i>B. 01°55'N 150°31'E</i>							
Number	66	379	8	437	0	0	0.0043914
Density	15029.4	86305.1	1821.7	99512.7	0	0	-
<i>C. 26°55'S 165°34'E</i>							
Number	71	183	0	0	254	0	0.0066742
Density	10638.0	27419.0	0	0	38057.0	0	-

5. MR-13-03 (this cruise, Stations 10): Western Subtropical and Tropical Pacific Ocean

	<u>Total</u>	<u>H.m</u>	<u>H.g</u>	<u>H. s .</u>	<u>H. p or sp</u>	<u>AS[#]</u>	
	<u>Nymphs</u>	<u>Adults</u>					
<i>A. 24°00'N 138°10'E (Station 1)</i>							
Number	179	126	6	0	299	0	0.0031594
Density	56656.5	39881.1	1899.1	0	94638.5	0	-

	<u>Total</u>	<u>H.m</u>	<u>H.g</u>	<u>H. s .</u>	<u>H. p or sp</u>	<u>AS[#]</u>	
	<u>Nymphs</u>	<u>Adults</u>					
<i>B. 12°00'N 135°00'E (Stations 2-10)</i>							
Number	484	119	276	327	0	0	0.02802519
Density	17270.2	4246.2	9848.3	11688.1	0	0	-

[#] AS : Area of surface where the Neuston net has swept (km²)

Table 3-A. Components of instars of larvae and adults of oceanic sea skaters, *Halobates micans*, *H. germanus* and *H. sericeus* sampled mostly sampled at 8000N, 8030E in the tropical Indian Ocean.

	<i>Halobates micans</i>							<i>H. germanus</i>							<i>H. sericeus</i>						
	Adults							Adults							Adults						
	1 st	2 nd	3 rd	4 th	5 th	F	M	1 st	2 nd	3 rd	4 th	5 th	F	M	1 st	2 nd	3 rd	4 th	5 th	F	M
St1-1	0	0	0	0	0	3	2	0	0	0	0	0	0	0	9	18	22	15	25	29	19
St1-2	0	0	0	0	0	0	0	0	0	0	0	0	0	0	11	11	18	17	25	32	32
St1-3	0	0	0	0	0	1	0	0	0	0	0	0	0	0	3	0	1	0	4	4	4
St2-1	0	1	1	2	2	0	1	0	0	0	0	0	2	0	0	0	0	0	0	0	0
St2-2	0	3	4	2	2	0	0	0	3	2	0	3	2	1	0	0	0	0	0	0	0
St2-3	1	9	9	6	6	1	1	1	15	12	6	9	8	5	0	0	0	0	0	0	0
St3-1	0	0	3	0	5	0	0	1	2	2	1	7	4	0	0	0	0	0	0	0	0
St3-2	0	2	3	3	5	0	3	1	5	2	6	3	2	4	0	0	0	0	0	0	0
St3-3	0	1	6	2	2	1	2	1	0	6	3	4	3	2	0	0	0	0	0	0	0
St4-1	0	0	1	1	1	1	1	0	2	3	1	2	2	2	0	0	0	0	0	0	0
St4-2	0	0	2	2	0	1	2	0	1	1	0	1	2	2	0	0	0	0	0	0	0
St4-3	0	1	0	2	0	1	0	1	2	1	0	0	1	2	0	0	0	0	0	0	0
St5-1	0	6	11	7	6	2	0	0	4	3	2	0	0	1	0	0	0	0	0	0	0
St5-2	0	4	5	3	3	0	0	4	3	12	2	1	1	0	0	0	0	0	0	0	0
St5-3	0	1	6	5	1	0	0	0	4	1	2	1	1	1	0	0	0	0	0	0	0
St6-1	0	1	8	8	5	0	0	0	3	5	2	4	2	0	0	0	0	0	0	0	0
St6-2	0	3	8	8	5	4	1	0	2	10	8	3	3	0	0	0	0	0	0	0	0
St6-3	0	1	5	2	2	0	1	0	3	3	2	1	0	1	0	0	0	0	0	0	0
St7-1	0	1	0	0	3	1	0	0	4	2	0	1	2	4	0	0	0	0	0	0	0
St7-2	0	0	1	2	4	0	0	1	1	2	3	3	2	0	0	0	0	0	0	0	0
St7-3	0	1	5	1	0	1	0	0	2	3	0	2	0	1	0	0	0	0	0	0	0
St8-1	0	0	2	1	1	0	0	0	0	0	0	0	4	3	0	0	0	0	0	0	0
St8-2	0	0	0	0	1	0	1	1	0	2	1	0	1	2	0	0	0	0	0	0	0
St8-3	0	0	1	1	0	3	0	0	0	2	0	0	1	2	0	0	0	0	0	0	0
St9-1	0	0	0	0	0	0	0	1	1	0	0	1	0	1	0	0	0	0	0	0	0
St9-2	0	3	2	1	0	1	0	0	1	2	0	0	1	0	0	0	0	0	0	0	0
St9-3	0	0	1	2	3	1	4	1	0	1	2	1	2	1	0	0	0	0	0	0	0
St10-1	0	0	0	0	0	0	0	1	0	1	0	0	0	0	0	0	0	0	0	0	0
St10-2	0	0	0	0	0	0	0	1	0	0	0	0	0	0	0	0	0	0	0	0	0
St10-3	0	0	0	0	0	0	0	0	0	2	1	1	1	2	0	0	0	0	0	0	0

Table 4-Sheet 1. Results of “Cool-coma” experiments and SCP (Super Cooling Point) measurement performed on adults of *Halobates micans* (H.m.) and *H. sericeus* (H.s.); TA: temp. at which specimen adapted, SHCT: temp. at which semi-cool coma occurred; CCT: temp. at which cool coma occurred ; GTCC: gap temp. for cool coma (from base temp.); “Date and Time of Day” when experiments were performed. (MR-13-03: May 31-July 6, 2013), ITSCP: Increased temperature at SCP was detected; TD: Time of day when cool coma experiment was performed

St.No.	Latitude	Longitude	Exp.No.	TA	SCCT	CCT	GTCC	SCP	ITSCP	Species	Stage (sex)	Date	TD
St. 1	24°00'N	138°10'E	1	28	23	20	8	-15.1	6.8	H.m.	Adult (female)	June 6	08:55~
St. 1	24°00'N	138°10'E	1	28	20	20	8	-13.9	6.8	H.s.	Adult(male)	June 6	08:55~
St. 1	24°00'N	138°10'E	1	28	19	19	9	-9.7	3.8	H.s.	Adult(female)	June 6	08:55~
St. 1	24°00'N	138°10'E	1	28	19	19	9	-14.7	6.1	H.s.	Adult (male)	June 6	08:55~
St. 1	24°00'N	138°10'E	1	28	19	19	9	-18.2	1.8	H.s.	Adult (male)	June 6	08:55~
St. 1	24°00'N	138°10'E	1	28	18	18	10	-9.9	4.5	H.s.	Adult (female)	June 6	08:55~
St. 1	24°00'N	138°10'E	1	28	17	17	11	-8.6	4.1	H.s.	Adult(female)	June 6	08:55~
St. 1	24°00'N	138°10'E	1	28	17	17	11	-17.3	4.4	H.s.	Adult (female)	June 6	08:55~
St. 1	24°00'N	138°10'E	1	28	18	17	11	-12.8	3.6	H.s.	Adult (male)	June 6	08:55~
St. 1	24°00'N	138°10'E	1	28	16	16	12	-11.3	5.8	H.m.	Adult (female)	June 6	08:55~
St. 1	24°00'N	138°10'E	1	28	16	15	13	-14.5	6.4	H.s.	Adult(female)	June 6	08:55~
St. 1	24°00'N	138°10'E	2	29	23	17	12	-17.1	5.9	H.s.	Adult (female)	June 7	08:30~
St. 1	24°00'N	138°10'E	2	29	19	17	12	-18.3	6.7	H.s.	Adult(male)	June 7	08:30~
St. 1	24°00'N	138°10'E	2	29	17	17	12	-17.8	4.2	H.s.	Adult(female)	June 7	08:30~
St. 1	24°00'N	138°10'E	2	29	17	17	12	-13.7	6.4	H.s.	Adult (male)	June 7	08:30~
St. 1	24°00'N	138°10'E	2	29	17	17	12	-12.0	3.1	H.s.	Adult (male)	June 7	08:30~
St. 1	24°00'N	138°10'E	2	29	17	17	12	-15.1	4.7	H.s.	Adult (male)	June 7	08:30~
St. 1	24°00'N	138°10'E	2	29	16	16	13	-15.0	3.5	H.s.	Adult(female)	June 7	08:30~
St. 1	24°00'N	138°10'E	2	29	16	15	14	-11.4	5.2	H.s.	Adult (male)	June 7	08:30~
St. 1	24°00'N	138°10'E	2	29	15	15	14	-14.8	3.2	H.s.	Adult (female)	June 7	08:30~
St. 1	24°00'N	138°10'E	2	29	15	15	14	-11.4	4.3	H.s.	Adult (female)	June 7	08:30~
St. 1	24°00'N	138°10'E	3	29	28	19	10	-18.0	3.3	H.s.	Adult (male)	June 8	08:30~
St. 1	24°00'N	138°10'E	3	29	18	17	12	-18.1	7.8	H.s.	Adult(male)	June 8	08:30~
St. 1	24°00'N	138°10'E	3	29	26	16	13	-15.6	5.5	H.s.	Adult(female)	June 8	08:30~
St. 1	24°00'N	138°10'E	3	29	17	16	13	-17.3	2.9	H.s.	Adult (male)	June 8	08:30~
St. 1	24°00'N	138°10'E	3	29	15	15	14	-20.7	2.0	H.s.	Adult (male)	June 8	08:30~
St. 1	24°00'N	138°10'E	3	29	18	15	14	-16.8	6.3	H.s.	Adult (female)	June 8	08:30~
St. 1	24°00'N	138°10'E	3	29	16	15	14	-16.6	6.6	H.s.	Adult(female)	June 8	08:30~
St. 1	24°00'N	138°10'E	3	29	15	15	14	-17.8	4.6	H.s.	Adult (female)	June 8	08:30~
St. 1	24°00'N	138°10'E	3	29	15	15	14	-14.5	5.9	H.s.	Adult (female)	June 8	08:30~

Table 4-Sheet 2. Results of “Cool-coma” experiments and SCP (Super Cooling Point) measurement performed on adults of *Halobates micans* (H.m.) and *H. sericeus* (H.s.); TA: temp. at which specimen adapted, SHCT: temp. at which semi- cool coma occurred; CCT: temp. at which cool coma occurred ; GTCC: gap temp. for cool coma (from base temp.); “Date and Time of Day” when experiments were performed. (MR-13-03: May 31-July 6, 2013), ITSCP: Increased temperature at SCP was detected; TD: Time of day when cool coma experiment was performed; * : Moist on the Thermocouple was wiped up by the paper before the measurement.

St.No.	Latitude	Longitude	Exp.No.	TA	SCCT	CCT	GTCC	SCP	ITSCP	Species	Stage (sex)	Date	TD
St. 1	24°00'N	138°10'E	3	29	14	14	15	-17.1	4.8	H.s.	Adult (female)	June 8	08:30~
St. 1	24°00'N	138°10'E	4	28	27	21	7	-12.5	3.8	H.s..	Adult (male)	June 9	08:30~
St. 1	24°00'N	138°10'E	4	28	20	20	8	-18.9	8.4	H.s.	Adult(female)	June 9	08:30~
St. 1	24°00'N	138°10'E	4	28	19	19	9	-13.5	7.9	H.s.	Adult(female)	June 9	08:30~
St. 1	24°00'N	138°10'E	4	28	20	19	9	-12.3	6.1	H.s.	Adult (male)	June 9	08:30~
St. 1	24°00'N	138°10'E	4	28	20	19	9	-15.5	4.8	H.s.	Adult (male)	June 9	08:30~
St. 1	24°00'N	138°10'E	4	28	19	19	9	-16.5	1.0	H.s.	Adult (male)	June 9	08:30~
St. 1	24°00'N	138°10'E	4	28	18	18	10	-12.7	3.5	H.s.	Adult (male)	June 9	08:30~
St. 1	24°00'N	138°10'E	4	28	18	17	11	-16.0	0.8	H.s.	Adult (female)	June 9	08:30~
St. 1	24°00'N	138°10'E	4	28	17	17	11	-11.8	4.2	H.s.	Adult (female)	June 9	08:30~
St. 1	24°00'N	138°10'E	4	28	17	17	11	-12.2	1.8	H.s.	Adult (female)	June 9	08:30~
St. 1	24°00'N	138°10'E	5	28	25	22	6	-18.5	2.5	H.s..	Adult (male)	June 10	08:15~
St. 1	24°00'N	138°10'E	5	28	21	21	7	-18.3	5.9	H.s.	Adult (male)	June 10	08:15~
St. 1	24°00'N	138°10'E	5	28	23	20	8	-16.7	7.0	H.s.	Adult (female)	June 10	08:15~
St. 1	24°00'N	138°10'E	5	28	19	19	9	-13.6	1.6	H.s.	Adult (male)	June 10	08:15~
St. 1	24°00'N	138°10'E	5	28	19	19	9	-13.4	6.4	H.s.	Adult (female)	June 10	08:15~
St. 1	24°00'N	138°10'E	5	28	19	19	9	-14.0	3.5	H.s.	Adult (male)	June 10	08:15~
St. 1	24°00'N	138°10'E	5	28	19	18	10	-12.6	6.5	H.s.	Adult (female)	June 10	08:15~
St. 1	24°00'N	138°10'E	5	28	19	18	10	-13.4	6.3	H.s.	Adult (female)	June 10	08:15~
St. 1	24°00'N	138°10'E	5	28	19	18	10	-12.5	8.0	H.s.	Adult (female)	June 10	08:15~
St. 1	24°00'N	138°10'E	5	28	19	18	10	-11.5	3.2	H.s.	Adult (male)	June 10	08:15~
St. 1	24°00'N	138°10'E	6	29	-#	-#	-#	-18.6*	5.3*	H.s.	Adult (female)	June 11	08:30~
St. 1	24°00'N	138°10'E	6	29	-#	-#	-#	-17.4*	8.9*	H.s.	Adult(female)	June 11	08:30~
St. 1	24°00'N	138°10'E	6	29	-#	-#	-#	-13.4	4.9	H.s.	Adult(female)	June 11	08:30~
St. 1	24°00'N	138°10'E	6	29	-#	-#	-#	-10.9	5.4	H.s.	Adult (female)	June 11	08:30~
St. 1	24°00'N	138°10'E	6	29	-#	-#	-#	-12.3	7.5	H.s.	Adult (female)	June 11	08:30~
St. 1	24°00'N	138°10'E	6	29	-#	-#	-#	-11.4	8.1	H.s.	Adult (female)	June 11	08:30~
St. 1	24°00'N	138°10'E	6	29	-#	-#	-#	-11.9	4.5	H.s.	Adult(female)	June 11	08:30~
St. 1	24°00'N	138°10'E	6	29	-#	-#	-#	-16.6*	8.1*	H.s.	Adult (male)	June 11	08:30~

Table 4-Sheet 3. Results of “Cool-coma” experiments and SCP (Super Cooling Point) measurement performed on adults of *Halobates micans* (H.m.) and *H. sericeus* (H.s.); TA: temp. at which specimen adapted, SHCT: temp. at which semi-cool coma occurred; CCT: temp. at which cool coma occurred ; GTCC: gap temp. for cool coma (from base temp.); “Date and Time of Day” when experiments were performed. (MR-13-03: May 31-July 6, 2013), ITSCP: Increased temperature at SCP was detected; TD: Time of day when cool coma experiment was performed; * : Moist on the Thermocouple was wiped up by the paper before the measurement.

St.No.	Latitude	Longitude	Exp.No.	TA	SCCT	CCT	GTCC	SCP	ITSCP	Species	Stage (sex)	Date	TD
St. 1	24°00'N	138°10'E	6	29	-#	-#	-#	-12.2	6.8	H.s.	Adult (male)	June 11	08:30~
St. 1	24°00'N	138°10'E	6	29	-#	-#	-#	-13.2*	6.3*	H.s.	Adult (male)	June 11	08:30~
St. 1	24°00'N	138°10'E	6	29	-#	-#	-#	-14.5	4.0	H.s.	Adult(male)	June 11	08:30~
St. 1	24°00'N	138°10'E	6	29	-#	-#	-#	-19.5*	7.1*	H.s.	Adult (male)	June 11	08:30~
St. 1	24°00'N	138°10'E	6	29	-#	-#	-#	-14.1	6.8	H.s.	Adult(male)	June 11	08:30~
St. 1	24°00'N	138°10'E	6	29	-#	-#	-#	-16.6*	6.2*	H.s.	Adult(male)	June 11	08:30~
St. 1	24°00'N	138°10'E	6	29	-#	-#	-#	-14.8	7.4	H.s.	Adult (male)	June 11	08:30~
St. 1	24°00'N	138°10'E	6	29	-#	-#	-#	-18.8*	2.3*	H.s.	Adult (female)	June 12	08:30~
St. 1	24°00'N	138°10'E	6	29	-#	-#	-#	-17.5*	7.3*	H.s.	Adult (female)	June 12	08:30~
St. 1	24°00'N	138°10'E	6	29	-#	-#	-#	-17.7*	6.5*	H.s.	Adult(female)	June 12	08:30~
St. 1	24°00'N	138°10'E	6	29	-#	-#	-#	-18.2*	7.3*	H.s.	Adult (female)	June 12	08:30~
St. 1	24°00'N	138°10'E	6	29	-#	-#	-#	-14.7*	9.6*	H.s.	Adult (female)	June 12	08:30~
St. 1	24°00'N	138°10'E	6	29	-#	-#	-#	-17.0*	5.9*	H.s.	Adult (female)	June 12	08:30~
St. 1	24°00'N	138°10'E	6	29	-#	-#	-#	-17.6*	7.1*	H.s..	Adult (female)	June 12	08:30~
St. 1	24°00'N	138°10'E	6	29	-#	-#	-#	-17.5*	3.0*	H.s.	Adult(female)	June 12	08:30~
St. 1	24°00'N	138°10'E	6	29	-#	-#	-#	-18.0*	5.9*	H.s.	Adult(female)	June 12	08:30~
St. 1	24°00'N	138°10'E	6	29	-#	-#	-#	-17.0*	8.2*	H.s.	Adult (male)	June 12	08:30~
St. 1	24°00'N	138°10'E	6	29	-#	-#	-#	-19.7*	5.5*	H.s.	Adult (male)	June 12	08:30~
St. 1	24°00'N	138°10'E	6	29	-#	-#	-#	-18.5*	6.4*	H.s.	Adult (male)	June 12	08:30~
St. 1	24°00'N	138°10'E	6	29	-#	-#	-#	-15.5*	7.7*	H.s.	Adult(male)	June 12	08:30~
St. 2	11°59'N	135°00'E	7	29	20	20	9	-17.5*	5.4*	H.g.	Adult (female)	June 14	08:15~
St.2	11°59'N	135°00'E	7	29	19	19	10	-18.5*	8.0*	H.g.	Adult (female)	June 14	08:15~
St. 2	11°59'N	135°00'E	7	29	18	18	11	-20.7*	8.6*	H.g.	Adult (female)	June 14	08:15~
St. 2	11°59'N	135°00'E	7	29	19	18	11	-16.9*	7.0*	H.g.	Adult (male)	June 14	08:15~
St. 2	11°59'N	135°00'E	7	29	17	17	12	-20.3*	6.3*	H.g.	Adult(female)	June 14	08:15~
St. 2	11°59'N	135°00'E	7	29	17	17	12	-20.9*	6.1*	H.g.	Adult(male)	June 14	08:15~
St. 3	12°00'N	135°00'E	8	29	19	19	10	-16.4*	10.1*	H.m.	Adult (female)	June 16	08:45~
St. 3	12°00'N	135°00'E	8	29	19	19	10	-18.0*	6.6*	H.m.	Adult (male)	June 16	08:45~
St. 3	12°00'N	135°00'E	8	29	18	18	11	-13.6*	5.0*	H.m.	Adult (male)	June 16	08:45~

Table 4-Sheet 4. Results of “Cool-coma” experiments and SCP (Super Cooling Point) measurement performed on adults of *Halobates micans* (H.m.) and *H. sericeus* (H.s.); TA: temp. at which specimen adapted, SHCT: temp. at which semi-cool coma occurred; CCT: temp. at which cool coma occurred ; GTCC: gap temp. for cool coma (from base temp.); “Date and Time of Day” when experiments were performed. (MR-13-03: May 31-July 6, 2013), ITSCP: Increased temperature at SCP was detected; TD: Time of day when cool coma experiment was performed; * : Moist on the Thermocouple was wiped up by the paper before the measurement.

<u>St.No.</u>	<u>Latitude</u>	<u>Longitude</u>	<u>Exp.No.</u>	<u>TA</u>	<u>SCCT</u>	<u>CCT</u>	<u>GTCC</u>	<u>SCP</u>	<u>ITSCP</u>	<u>Species</u>	<u>Stage (sex)</u>	<u>Date</u>	<u>TD</u>
St. 3	12°00'N	135°00'E	8	29	17	16	13	-20.8*	7.9*	H.g.	Adult (male)	June 16	08:45~
St. 4	12°00'N	135°00'E	9	29	23	23	6	-17.5*	9.1*	H.m.	Adult (male)	June 18	08:30~
St. 4	12°00'N	135°00'E	9	29	22	22	7	-14.5*	7.6*	H.m.	Adult (female)	June 18	08:30~
St. 4	12°00'N	135°00'E	9	29	21	21	8	-15.7*	8.6*	H.m.	Adult (female)	June 18	08:30~
St. 4	12°00'N	135°00'E	9	29	21	21	8	-18.8*	5.4*	H.g.	Adult (male)	June 18	08:30~
St. 4	12°00'N	135°00'E	9	29	21	21	8	-18.2*	8.9*	H.g.	Adult (male)	June 18	08:30~
St. 4	12°00'N	135°00'E	9	29	20	20	9	-16.0*	6.8*	H.g.	Adult (male)	June 18	08:30~
St. 4	12°00'N	135°00'E	9	29	19	19	10	-19.3*	6.2*	H.g.	Adult (female)	June 18	08:30~
St. 5	12°01'N	135°00'E	10	29	21	21	8	-19.3*	6.2*	H.m.	Adult (female)	June 20	08:15~
St. 5	12°01'N	135°00'E	10	29	19	19	10	-17.1*	8.3*	H.m.	5 th instar	June 20	08:15~
St. 5	12°01'N	135°00'E	10	29	18	18	11	-15.7*	9.9*	H.m.	Adult (female)	June 20	08:15~
St. 5	12°01'N	135°00'E	10	29	18	18	11	-	-	H.m.	Adult (female)	June 20	08:15~
St. 5	12°01'N	135°00'E	10	29	17	17	12	-17.6*	7.0*	H.g.	Adult (female)	June 10	08:15~
St. 5	12°01'N	135°00'E	10	29	16	16	13	-16.1*	7.7*	H.g.	Adult (female)	June 20	08:15~
St. 6	12°00'N	135°00'E	11	29	23	20	9	-	-	H.m.	Adult(female)	June 22	08:45~
St. 6	12°00'N	135°00'E	11	29	20	20	9	-14.6*	7.1*	H.m.	Adult(female)	June 22	08:45~
St. 6	12°00'N	135°00'E	11	29	20	20	9	-17.2*	9.6*	H.m.	Adult(female)	June 22	08:45~
St. 6	12°00'N	135°00'E	11	29	20	20	9	-	-	H.m.	Adult(female)	June 22	08:45~
St. 6	12°00'N	135°00'E	11	29	19	17	12	-	-	H.g.	Adult(male)	June 22	08:45~
St. 6	12°00'N	135°00'E	11	29	16	16	13	-17.8*	8.1*	H.g.	Adult (female)	June 22	08:45~
St. 6	12°00'N	135°00'E	11	29	16	16	13	-14.0*	7.9*	H.g.	Adult (female)	June 22	08:45~
St. 6	12°00'N	135°00'E	11	29	15	15	14	-19.4*	7.0*	H.g.	Adult (female)	June 22	08:45~
St. 7	12°01'N	134°59'E	12	28	22	22	6	-20.0*	7.4*	H.g.	Adult (male)	June 24	08:30~
St. 7	12°01'N	134°59'E	12	28	21	21	7	-19.0*	1.5*	H.m.	Adult (female)	June 24	08:30~
St. 7	12°01'N	134°59'E	12	28	21	21	7	-16.9*	9.1*	H.g.	Adult(male)	June 24	08:30~
St. 7	12°01'N	134°59'E	12	28	18	18	10	-18.0*	7.1*	H.g.	Adult(female)	June 24	08:30~
St. 7	12°01'N	134°59'E	12	28	18	18	10	-18.3*	5.3*	H.g.	Adult(female)	June 24	08:30~
St. 7	12°01'N	134°59'E	12	28	17	17	11	-16.6*	7.0*	H.g.	Adult(female)	June 24	08:30~
St. 7	12°01'N	134°59'E	12	28	17	17	11	-15.9*	6.5*	H.g.	Adult(female)	June 24	08:30~

Table 4-Sheet 5. Results of “Cool-coma” experiments and SCP (Super Cooling Point) measurement performed on adults of *Halobates micans* (H.m.) and *H. sericeus* (H.s.); TA: temp. at which specimen adapted, SHCT: temp. at which semi-cool coma occurred; CCT: temp. at which cool coma occurred ; GTCC: gap temp. for cool coma (from base temp.); “Date and Time of Day” when experiments were performed. (MR-13-03: May 31-July 6, 2013), ITSCP: Increased temperature at SCP was detected; TD: Time of day when cool coma experiment was performed; * : Moist on the Thermocouple was wiped up by the paper before the measurement.; *: At which A kind of leg lame began to be observed

<u>No.</u>	<u>Latitude</u>	<u>Longitude</u>	<u>Exp.No.</u>	<u>TA</u>	<u>SCCT</u>	<u>CCT</u>	<u>GTCC</u>	<u>SCP</u>	<u>ITSCP</u>	<u>Species</u>	<u>Stage (sex)</u>	<u>Date</u>	<u>TD</u>
St. 8	12°01'N	135°00'E	13	29	18 (22*)	18	11	-16.7*	2.9*	H.g.	Adult(male)	June 26	08:30~
St. 8	12°01'N	135°00'E	13	29	17 (21*)	17	12	-20.0*	2.4*	H.g.	Adult(male)	June 26	08:30~
St. 8	12°01'N	135°00'E	13	29	17 (21*)	17	12	-16.5*	4.0*	H.g.	Adult(male)	June 26	08:30~
St. 8	12°01'N	135°00'E	13	29	17 (23*)	17	12	-16.7*	6.9*	H.g.	Adult(female)	June 26	08:30~
St. 8	12°01'N	135°00'E	13	29	17 (23*)	17	12	-15.2*	5.6*	H.g.	Adult(female)	June 26	08:30~
St. 8	12°01'N	135°00'E	13	29	16 (21*)	16	13	-19.6*	5.7*	H.g.	Adult (female)	June 26	08:30~
St. 8	12°01'N	135°00'E	13	29	16(21*)	16	13	-17.4*	8.0*	H.g.	Adult(male)	June 26	08:30~
St. 9	12°00'N	134°59'E	13	29	22(23*)	22	7	-16.9*	6.4*	H.m.	Adult(male)	June 28	08:45~
St. 9	12°00'N	134°59'E	13	29	21(22*)	21	8	-13.9*	6.0*	H.g.	Adult (male)	June 28	08:45~
St. 9	12°00'N	134°59'E	13	29	20(24*)	20	9	-17.4*	9.5*	H.m.	Adult (female)	June 28	08:45~
St. 9	12°00'N	134°59'E	13	29	16(22*)	16	13	-16.7*	6.8*	H.g.	Adult (female)	June 28	08:45~
St. 10	12°00'N	135°00'E	14	29	19(23*)	19	10	-18.2*	2.0*	H.g.	Adult (male)	June 30	09:15~
St. 10	12°00'N	135°00'E	14	29	18(22*)	18	11	-18.8*	6.5*	H.g.	Adult (male)	June 30	09:15~
St. 10	12°00'N	135°00'E	14	29	18(22*)	18	11	-15.0*	7.3*	H.g.	Adult(female)	June 30	09:15~

Table 5-A. Comparison of Semi-Cool-Coma Temperature (SCCT), Cool Coma Temperature (CCT), Gap Temperature for Cool Coma (GTHC), Super-Cooling Point (Temperature) (SCP) and Increased Temperature at Super Coolig Point (ITSCP) among *Halobates micans*, *H. germanus* and *H. sericeus*. Experiments were performed in the period of 6th Jun to 30th Jun, 2013 in the wet-lab. 2 of R/V Mirai during the cruise of MR-13-03 [Mean±SD(n)]

1. Combined data of specimens collected in the Tropical Pacific Region at 12°00'N, 135°00'E (Stations 2-10) during MR-13-03-Leg 2

	SCCT	CCT	GTCC	SCP	ITSCP
<i>H. micans</i>	20.2±2.0(19)	19.8±1.7(19)	9.0±1.6(19)	-16.2±2.1(16)	7.4±2.2(16)
<i>H. germanus</i>	18.0±1.8(35)	17.9±1.8(35)	10.9±1.9(35)	-17.7±1.9(34)	6.5±1.7(34)
Total	18.8±2.1(54)	18.6±2.0(54)	10.3±2.0(54)	-17.3±2.1(50)	6.8±1.9(50)
Mann-Whitney U-test between <i>H. micans</i> and <i>H. germanus</i>					
Z	-3.550	-3.481	-3.458	-2.289	-1.581
P	<0.001	<0.001	0.001	0.022	0.114

C. Data of specimens collected in the Temperate Pacific Region at 24°00'N 138°10'E (Station 1)

	SCCT	CCT	GTCC	SCP	ITSCP
<i>H. sericeus</i>	18.7±3.1(48)	17.5±1.9(48)	10.9±2.3(48)	-15.2±2.8(76)	5.4±2.0(76)
Kruskal-Wallis-test among the three species, <i>H. sericeus</i>, <i>H. germanus</i> and <i>H. micans</i>					
χ^2 -value	12.427	17.794	12.298	18.953	15.965
df	2	2	2	2	2
P	0.002	<0.001	0.002	<0.001	<0.001

Table 5-B. Evaluation of the effects of exposure to low temperature during Cool Coma Experiments (CCE) on super cooling points (SCPs) and increased temperature at SCP in *Halobates sericeus*.

1. Data of specimens collected in the Temperate Pacific Region at 24°00'N 138°10'E (Station 1)

	SCP	ITSCP
Just after CCE	-14.8±2.8(48)	4.7±1.9(48)
Without CCE	-12.8±1.4(9)	6.2±1.5(9)
Total	-14.5±2.7(57)	5.0±1.9(57)
Mann-Whitney U-test between specimens after CCE and those without CCE exposure		
Z	-2.134	-2.179
P	0.033	0.029

5.20 Underway Geophysics

Personnel

Takeshi MATSUMOTO (University of the Ryukyus) : Principal Investigator (Not on-board)
Kazuho YOSHIDA (Global Ocean Development Inc., GODI)
Koichi INAGAKI (GODI)
Wataru TOKUNAGA (GODI)
Souichiro SUEYOSHI (GODI)
Ryo KIMURA (MIRAI Crew)

5.20.1 Sea surface gravity

(1) Introduction

The local gravity is an important parameter in geophysics and geodesy. We collected gravity data at the sea surface.

(2) Parameters

Relative Gravity [CU: Counter Unit]
[mGal] = (coef1: 0.9946) * [CU]

(3) Data Acquisition

We measured relative gravity using LaCoste and Romberg air-sea gravity meter S-116 (Micro-g LaCoste, LLC) during the MR13-03 cruise.

To convert the relative gravity to absolute one, we measured gravity, using portable gravity meter CG-5 (Scintrex), at Sekinehama and Yokohama as the reference point.

(4) Preliminary Results

Absolute gravity table was shown in Table 5.20.1-1.

(5) Data Archives

Surface gravity data obtained during this cruise will be submitted to the Data Management Group (DMG) in JAMSTEC, and will be archived there.

(6) Remarks

- 1) The following period, data acquisition was suspended in the territorial waters.
21:30UTC 9 Jun. 2013 to 5:50UTC 12 Jun. 2013 (Republic of Palau)

Table 5.20.1-1 Absolute gravity table

No	Date	UTC	Port	Absolute Gravity [mGal]	Sea Level [cm]	Draft [cm]	Gravity at Sensor * ¹ [mGal]	L&R* ² Gravity [mGal]
#1	May/29	06:26	Sekinehama	980,371.93	234	636	980,372.89	12,732.14
#2	Jul/9		Yokohama					

*¹: Gravity at Sensor = Absolute Gravity + Sea Level*0.3086/100 + (Draft-530)/100*0.2222

*²: LaCoste and Romberg air-sea gravity meter S-116

5.20.2 Sea surface three-component magnetometer

(1) Introduction

Measurement of magnetic force on the sea is required for the geophysical investigations of marine magnetic anomaly caused by magnetization in upper crustal structure. We measured geomagnetic field using a three-component magnetometer during the MR13-03 cruise.

(2) Principle of ship-board geomagnetic vector measurement

The relation between a magnetic-field vector observed on-board, H_{ob} , (in the ship's fixed coordinate system) and the geomagnetic field vector, F , (in the Earth's fixed coordinate system) is expressed as:

$$H_{ob} = \tilde{\mathbf{A}} \tilde{\mathbf{R}} \tilde{\mathbf{P}} \tilde{\mathbf{Y}} F + H_p \quad (a)$$

where $\tilde{\mathbf{R}}$, $\tilde{\mathbf{P}}$ and $\tilde{\mathbf{Y}}$ are the matrices of rotation due to roll, pitch and heading of a ship, respectively. $\tilde{\mathbf{A}}$ is a 3 x 3 matrix which represents magnetic susceptibility of the ship, and H_p is a magnetic field vector produced by a permanent magnetic moment of the ship's body. Rearrangement of Eq. (a) makes

$$\tilde{\mathbf{R}} H_{ob} + H_{bp} = \tilde{\mathbf{R}} \tilde{\mathbf{P}} \tilde{\mathbf{Y}} F \quad (b)$$

where $\tilde{\mathbf{R}} = \tilde{\mathbf{A}}^{-1}$, and $H_{bp} = -\tilde{\mathbf{R}} H_p$. The magnetic field, F , can be obtained by measuring $\tilde{\mathbf{R}}$, $\tilde{\mathbf{P}}$, $\tilde{\mathbf{Y}}$ and H_{ob} , if $\tilde{\mathbf{R}}$ and H_{bp} are known. Twelve constants in $\tilde{\mathbf{R}}$ and H_{bp} can be determined by measuring variation of H_{ob} with $\tilde{\mathbf{R}}$, $\tilde{\mathbf{P}}$ and $\tilde{\mathbf{Y}}$ at a place where the geomagnetic field, F , is known.

(3) Instruments on R/V MIRAI

A shipboard three-component magnetometer system (Tierra Tecnica SFG1214) is equipped on-board R/V MIRAI. Three-axes flux-gate sensors with ring-cored coils are fixed on the fore mast. Outputs from the sensors are digitized by a 20-bit A/D converter (1 nT/LSB), and sampled at 8 times per second. Ship's heading, pitch, and roll are measured by the Inertial Navigation System (INS) for controlling attitude of a Doppler radar. Ship's position (GPS) and speed data are taken from LAN every second.

(4) Data Archives

These data obtained in this cruise will be submitted to the Data Management Group (DMG) of JAMSTEC.

(5) Remarks

- 1) The following period, data acquisition was suspended in the territorial waters.
21:30UTC 9 Jun. 2013 to 5:50UTC 12 Jun. 2013 (Republic of Palau)
- 2) For calibration of the ship's magnetic effect, we made a "figure-eight" turn (a pair of clockwise and anti-clockwise rotation). This calibration was carried out as below.
6:23UTC to 6:44UTC 9 Jun. 2013 (8-05N, 134-18E)
4:01UTC to 4:25UTC 5 Jul. 2013 (32-25N, 139-20E)

5.20.3 Swath Bathymetry

(1) Introduction

R/V MIRAI is equipped with a Multi narrow Beam Echo Sounding system (MBES), SEABEAM 3012 Upgrade Model (L3 Communications ELAC Nautik). The objective of MBES is collecting continuous bathymetric data along ship's track to make a contribution to geological and geophysical investigations and global datasets.

(2) Data Acquisition

The "SEABEAM 3012 Upgrade Model" on R/V MIRAI was used for bathymetry mapping during the MR13-03 cruise.

To get accurate sound velocity of water column for ray-path correction of acoustic multibeam, we used Surface Sound Velocimeter (SSV) data to get the sea surface (6.62m) sound velocity, and the deeper depth sound velocity profiles were calculated by temperature and salinity profiles from CTD, XCTD and Argo float data by the equation in Del Grosso (1974) during the cruise. Table 5.20.3-1 shows system configuration and performance of SEABEAM 3012 system.

Table 5.20.3-1 SEABEAM 3012 System configuration and performance

Frequency:	12 kHz
Transmit beam width:	1.6 degree
Transmit power:	20 kW
Transmit pulse length:	2 to 20 msec.
Receive beam width:	1.8 degree
Depth range:	100 to 11,000 m
Beam spacing:	0.5 degree athwart ship
Swath width:	150 degree (max) 120 degree to 4,500 m 100 degree to 6,000 m 90 degree to 11,000 m
Depth accuracy:	Within < 0.5% of depth or ±1m, Whichever is greater, over the entire swath. (Nadir beam has greater accuracy; typically within < 0.2% of depth or ±1m, whichever is greater)

(3) Preliminary Results

The results will be published after primary processing.

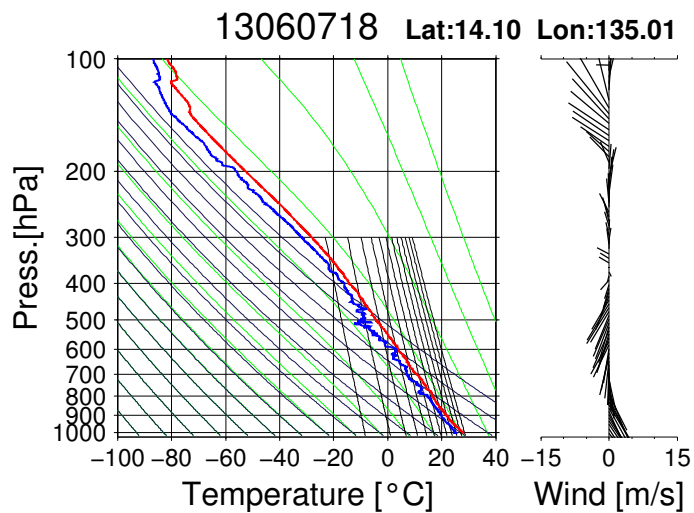
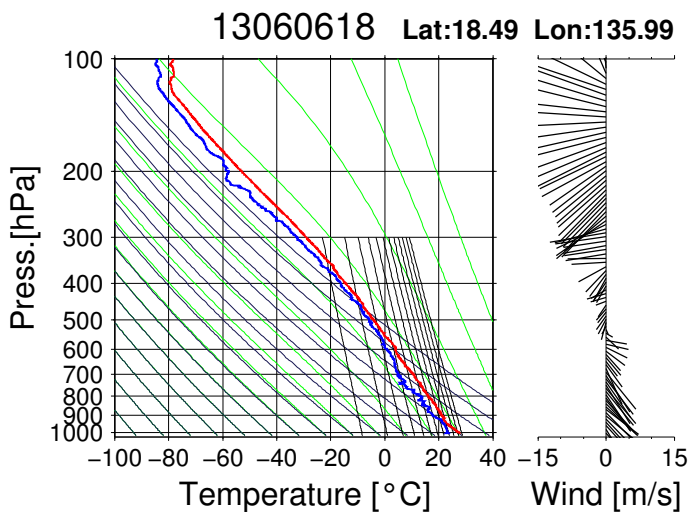
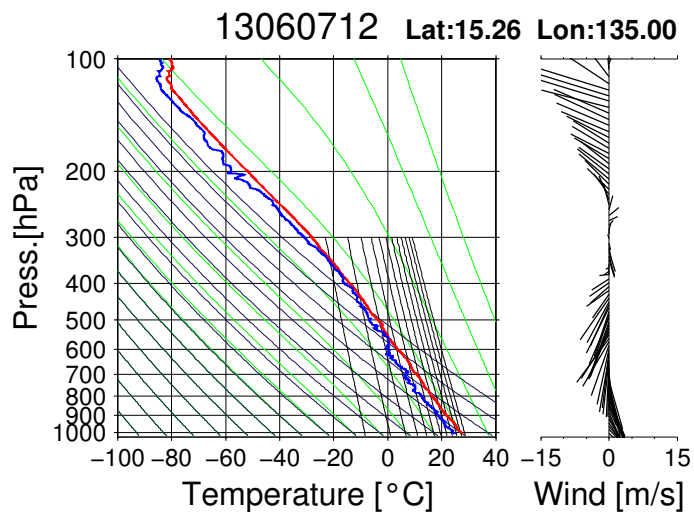
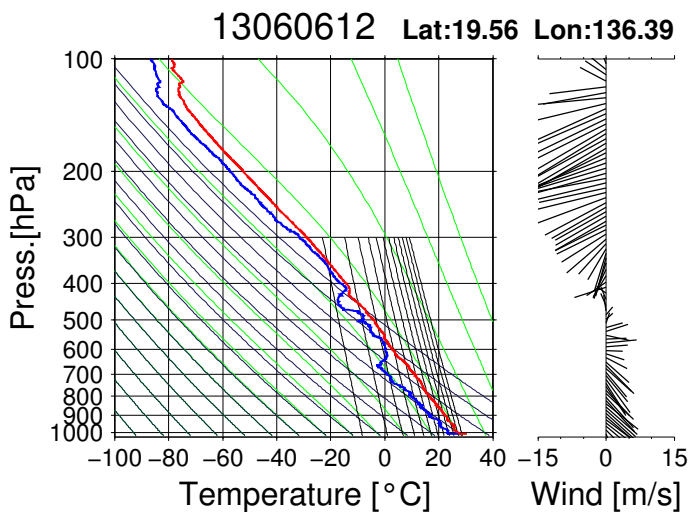
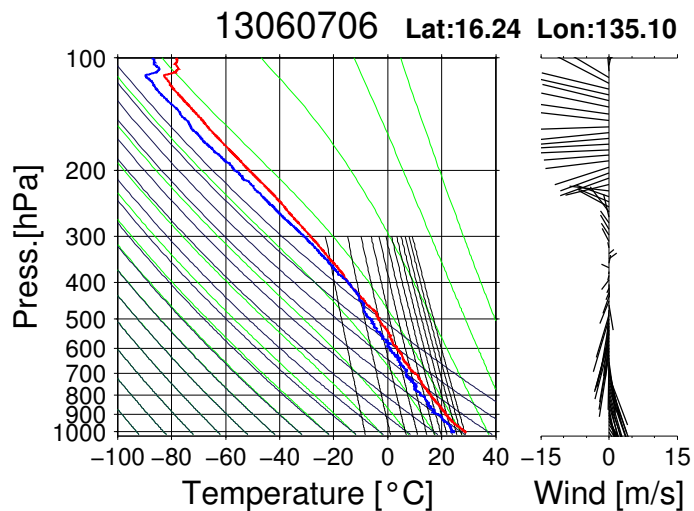
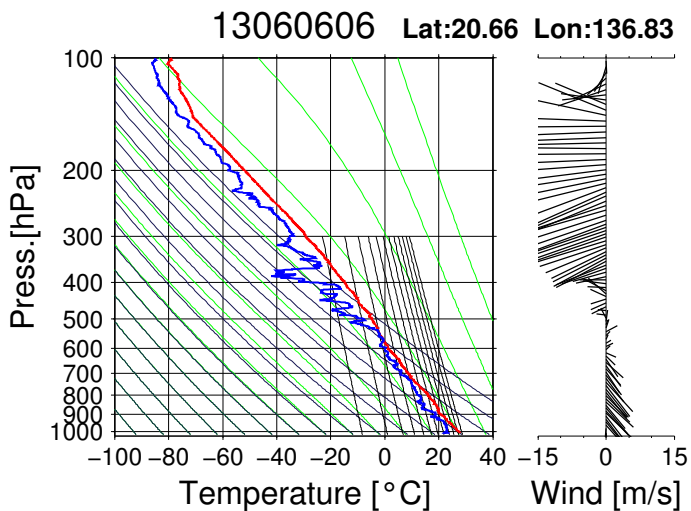
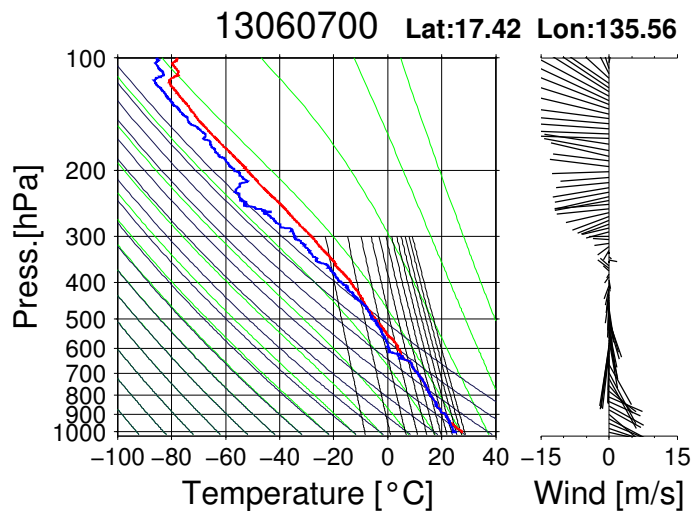
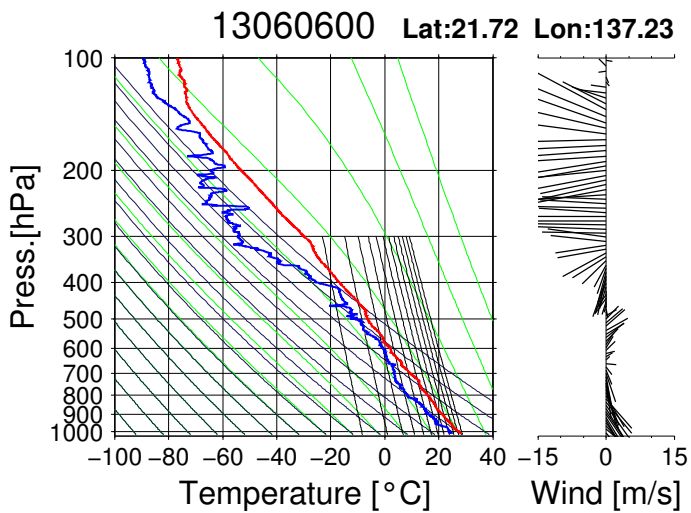
(4) Data Archives

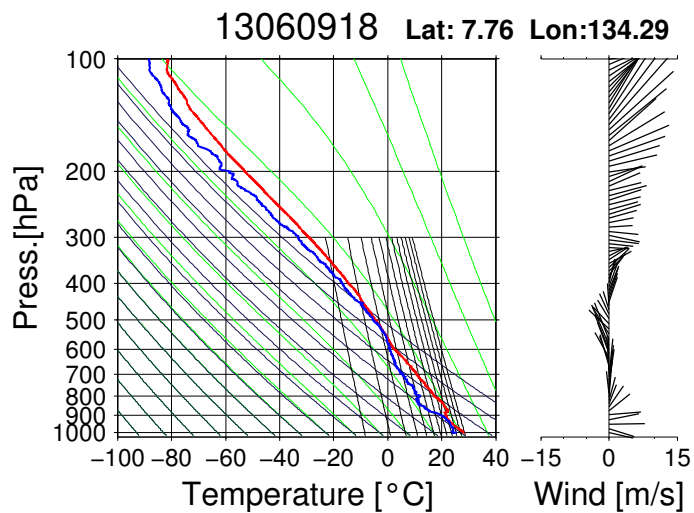
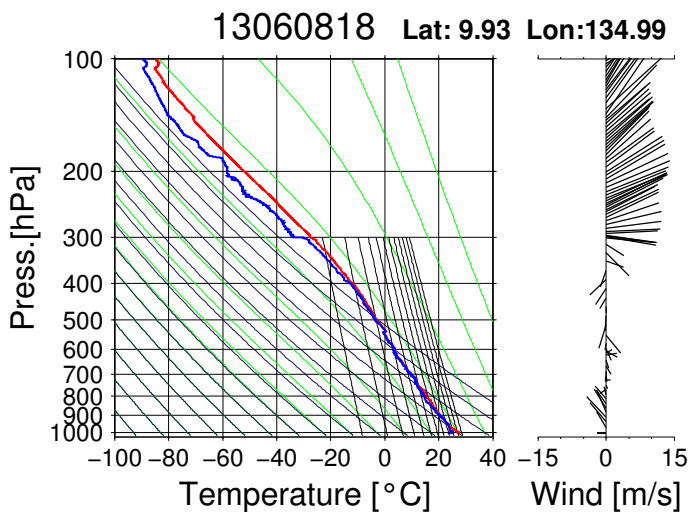
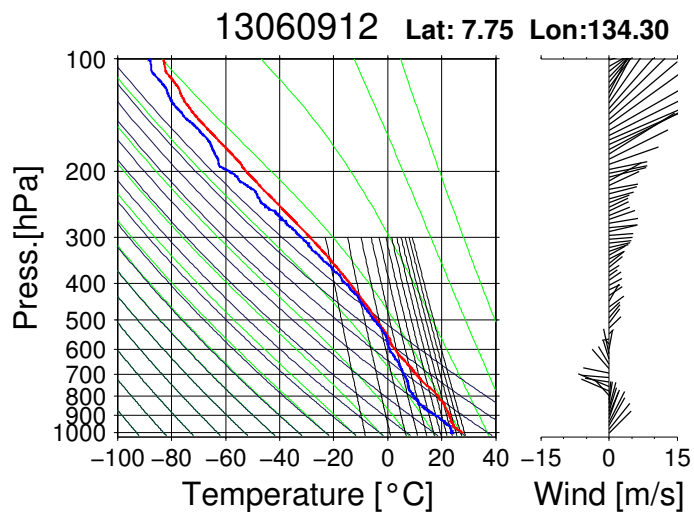
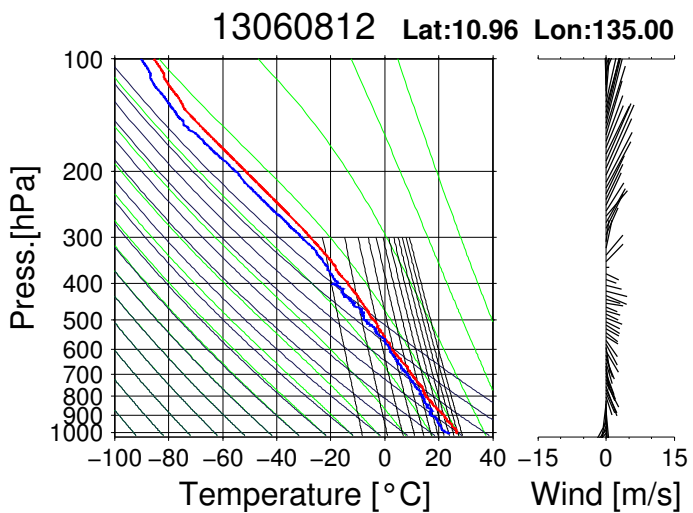
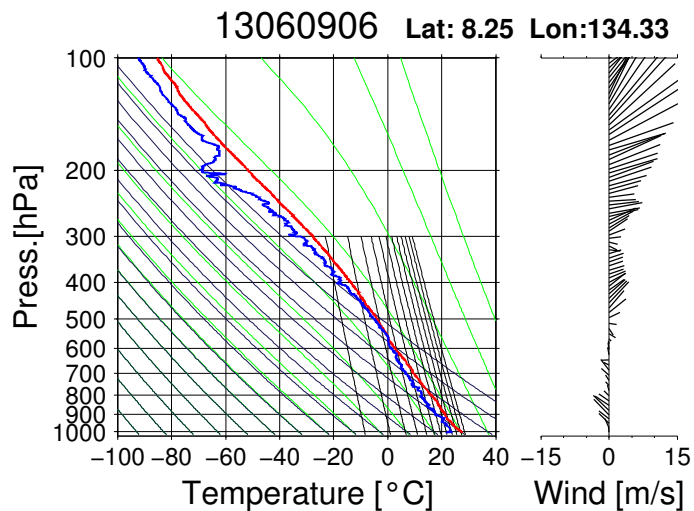
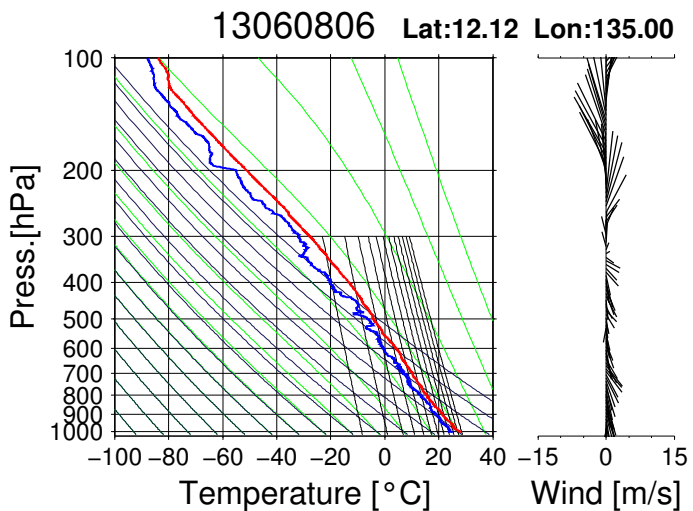
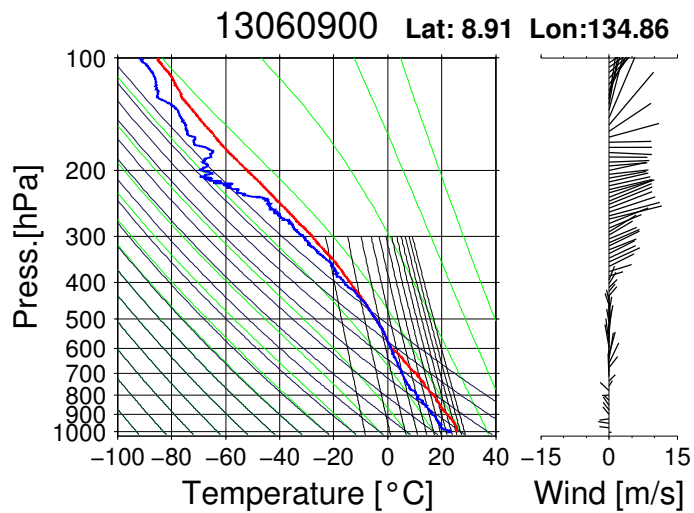
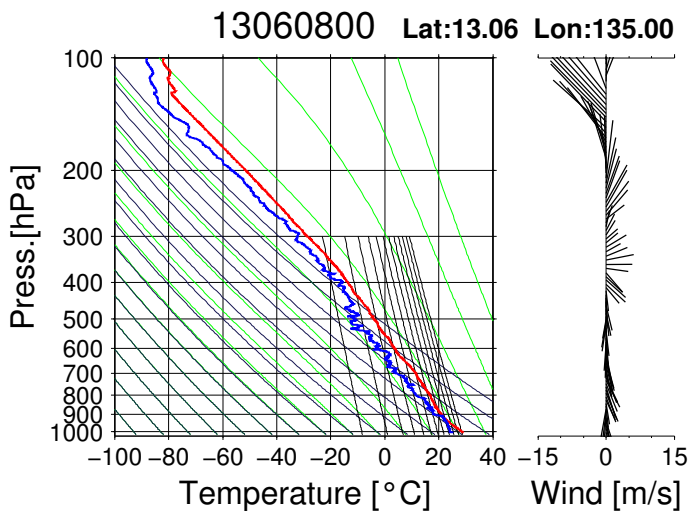
Bathymetric data obtained during this cruise will be submitted to the Data Management Group (DMG) in JAMSTEC, and will be archived there.

(5) Remarks

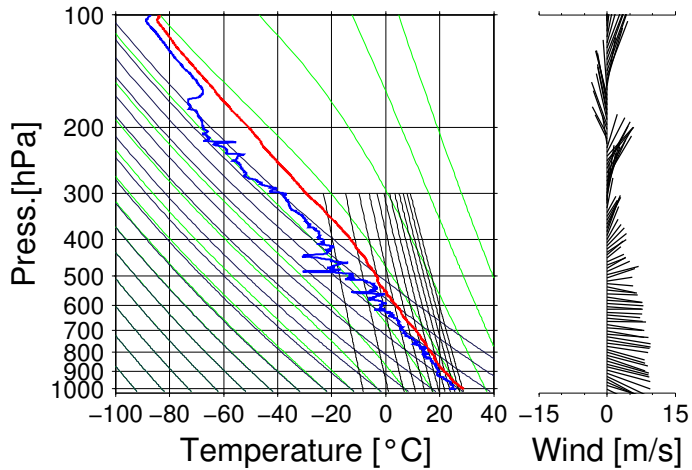
- 1) The following period, data acquisition was suspended in the territorial waters.
21:11UTC 9 Jun. 2013 to 6:12UTC 12 Jun. 2013 (Republic of Palau)

Appendix-A: Atmospheric profiles by the radiosonde observations

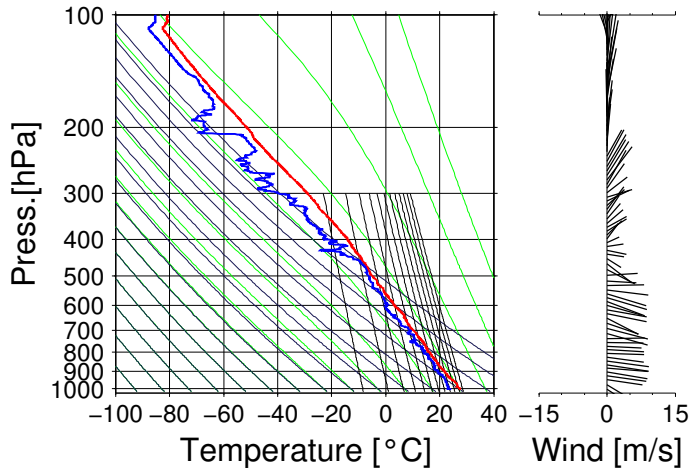




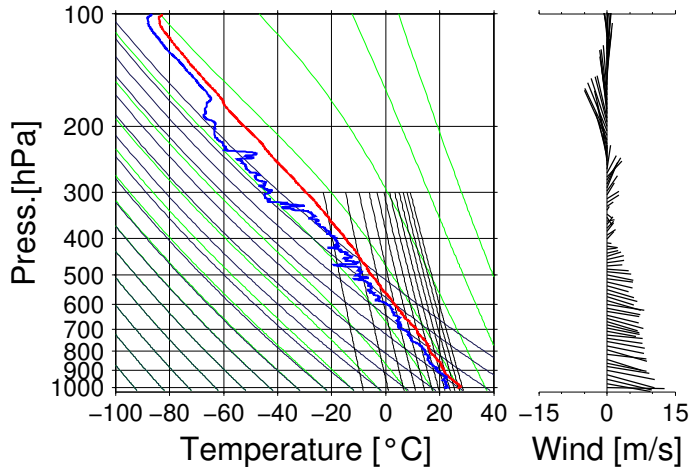
13061212 Lat: 9.38 Lon:134.56



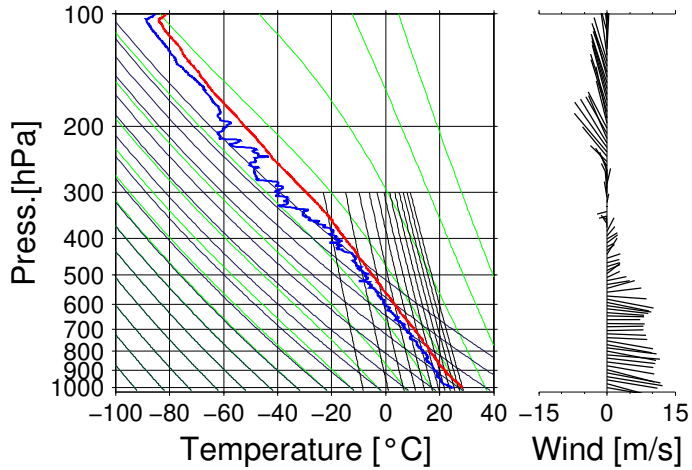
13061215 Lat: 9.89 Lon:134.65

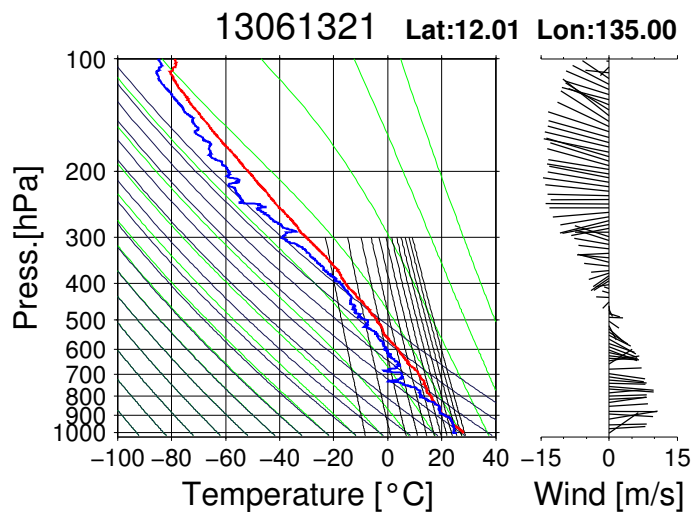
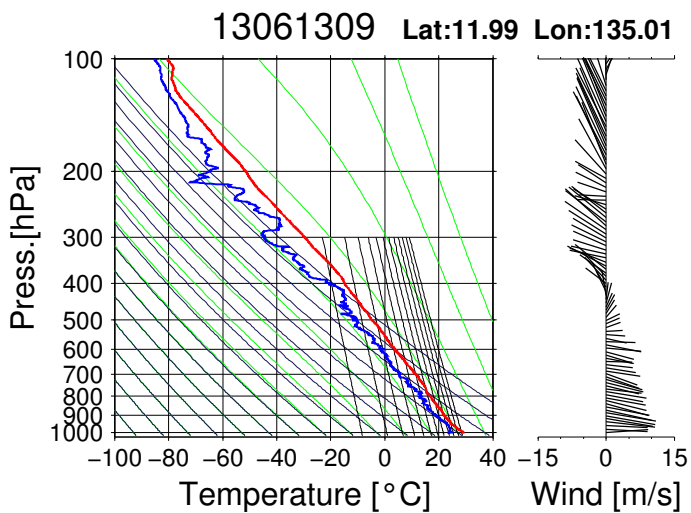
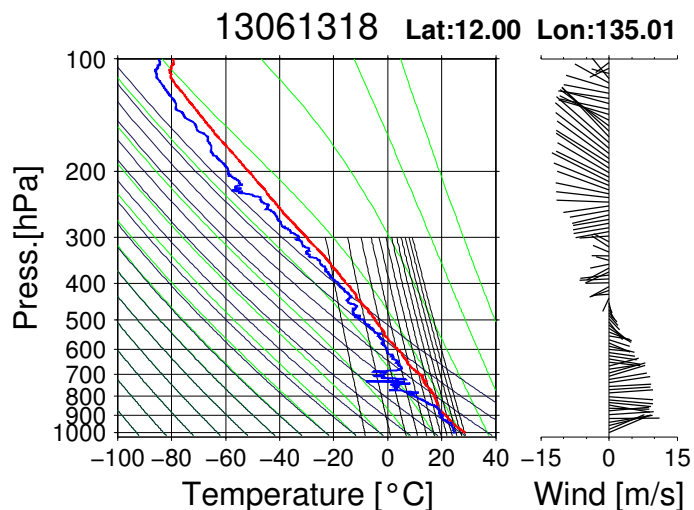
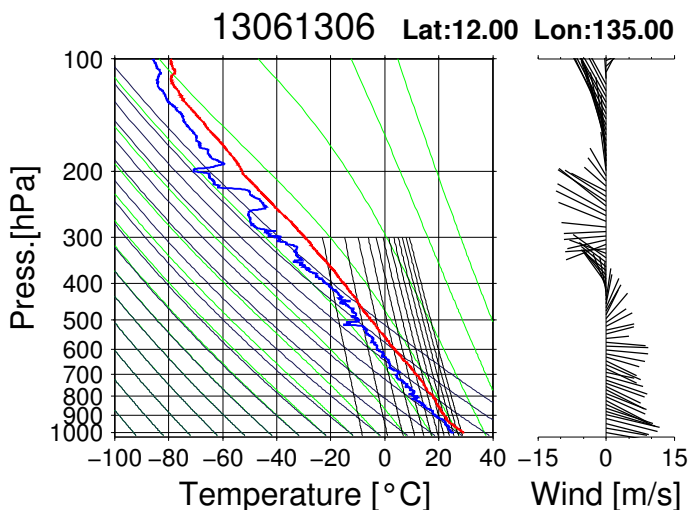
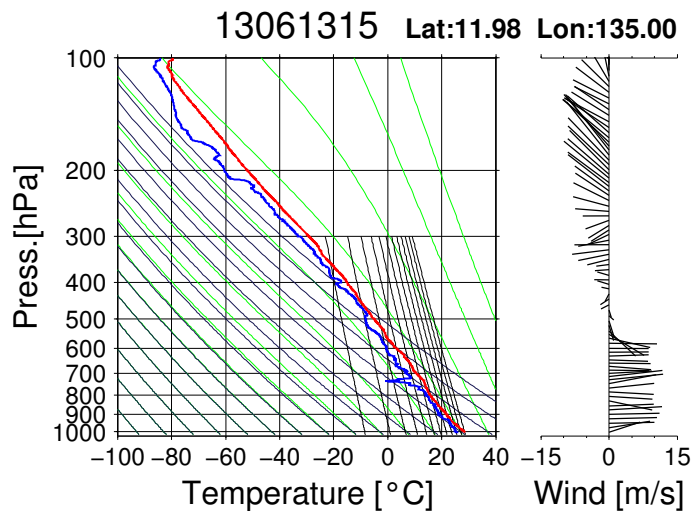
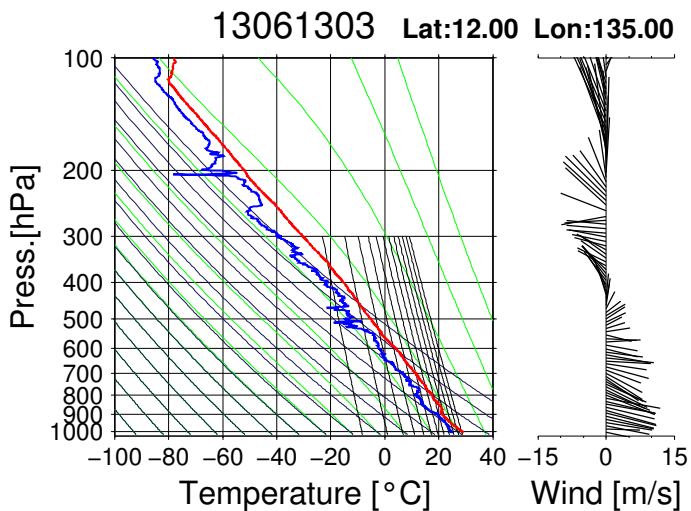
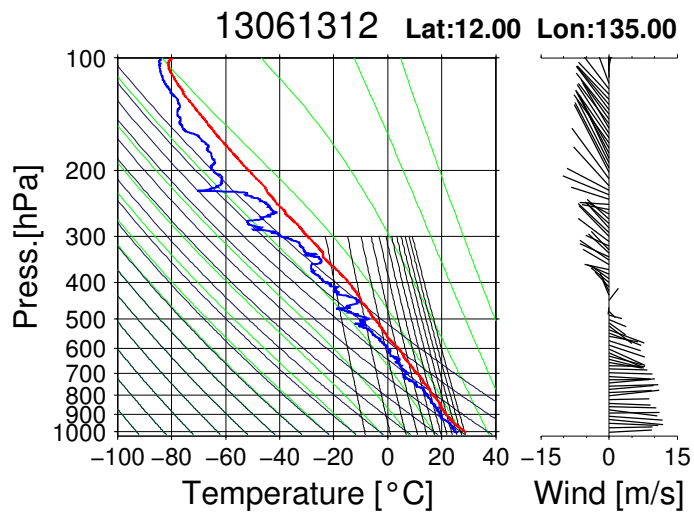
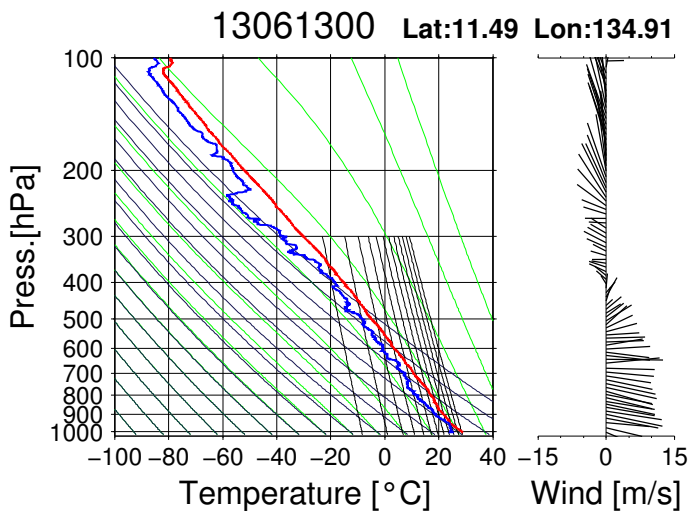


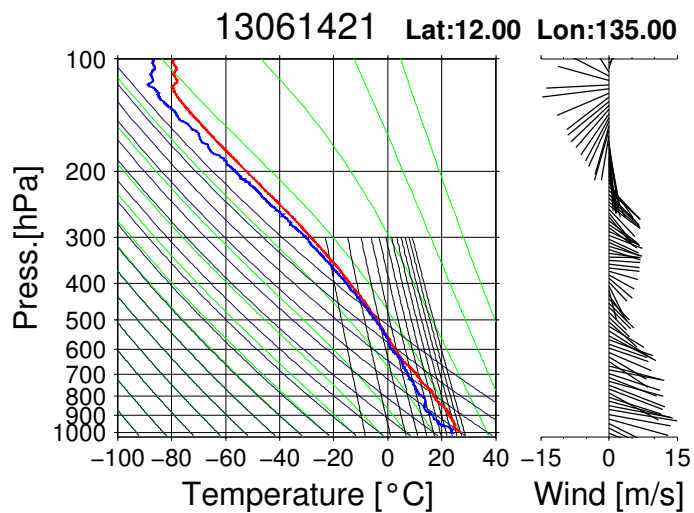
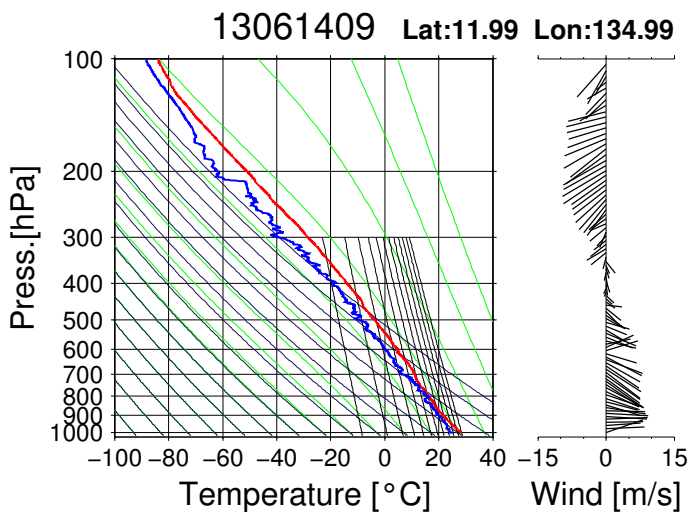
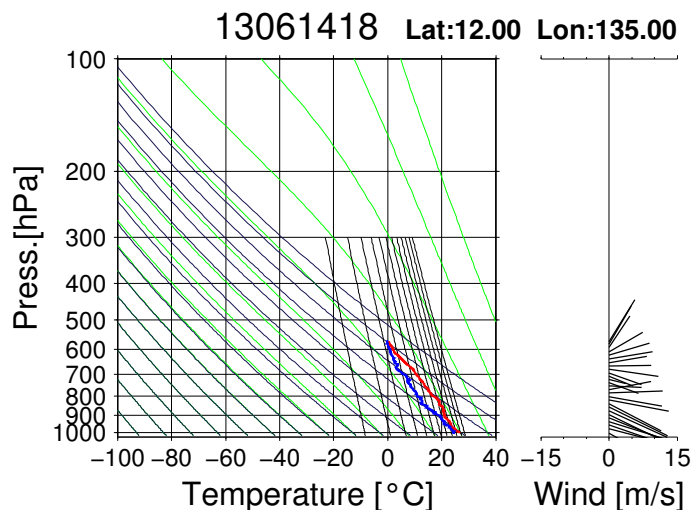
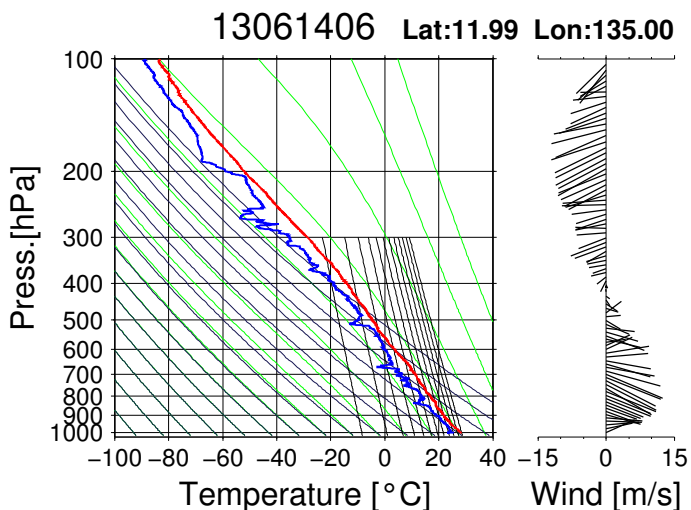
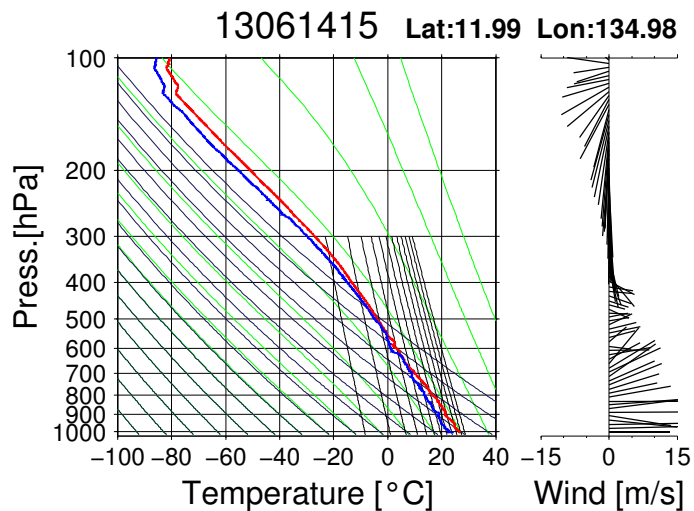
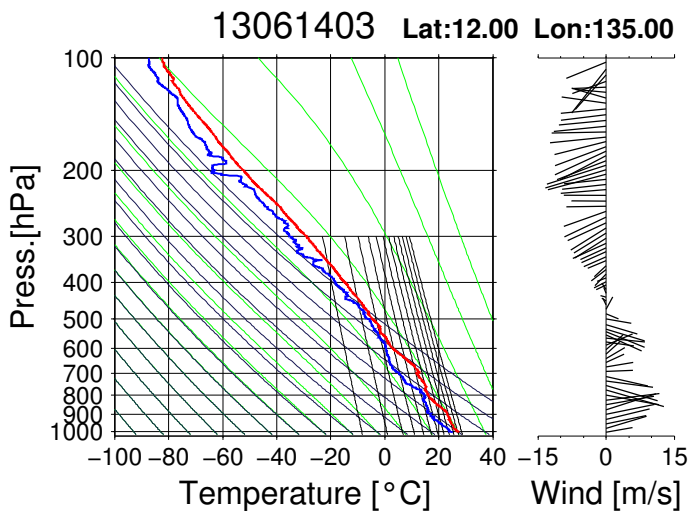
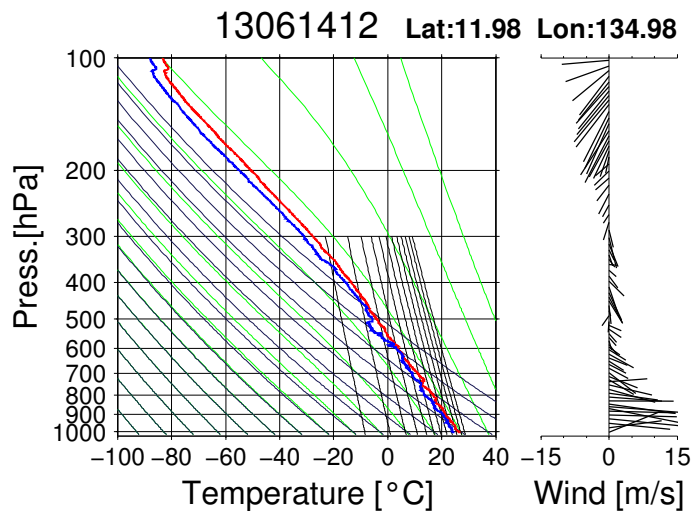
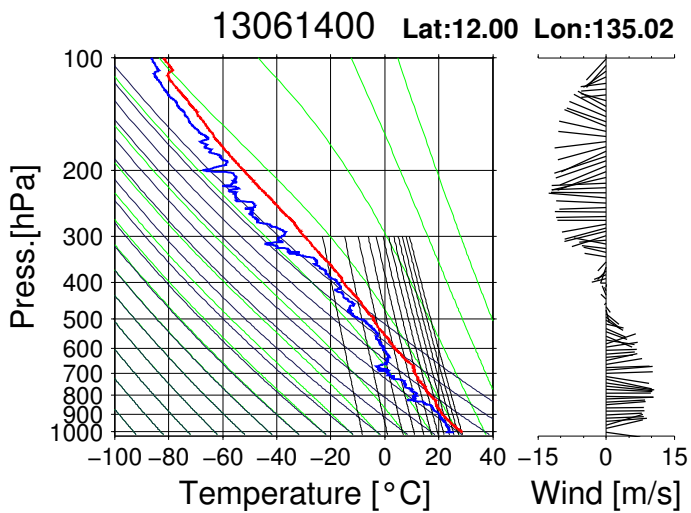
13061218 Lat:10.43 Lon:134.73

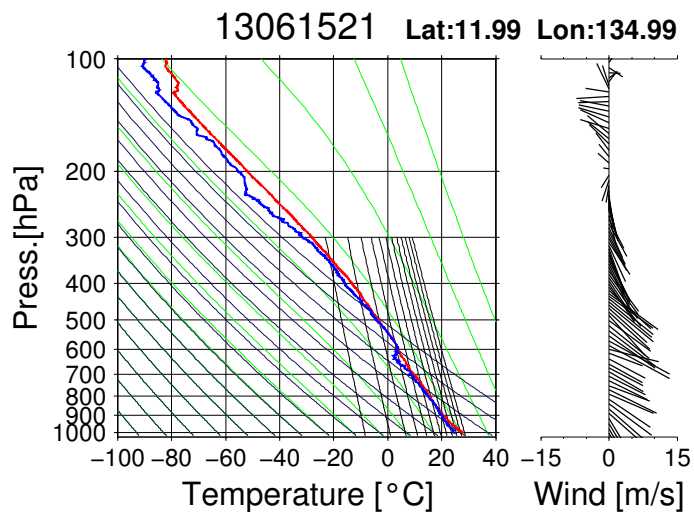
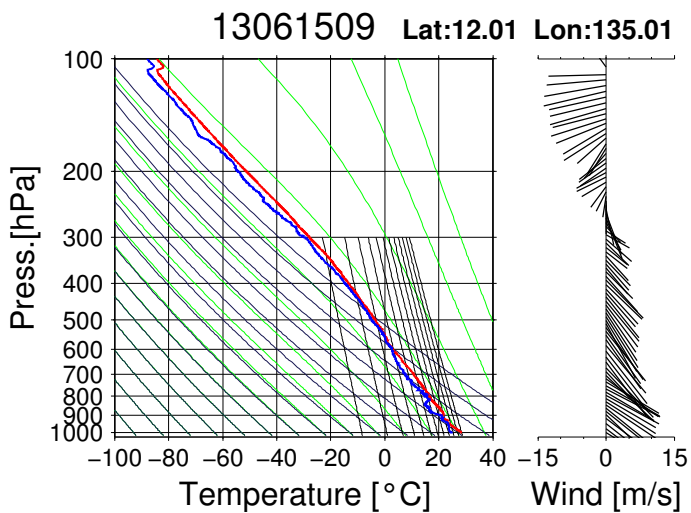
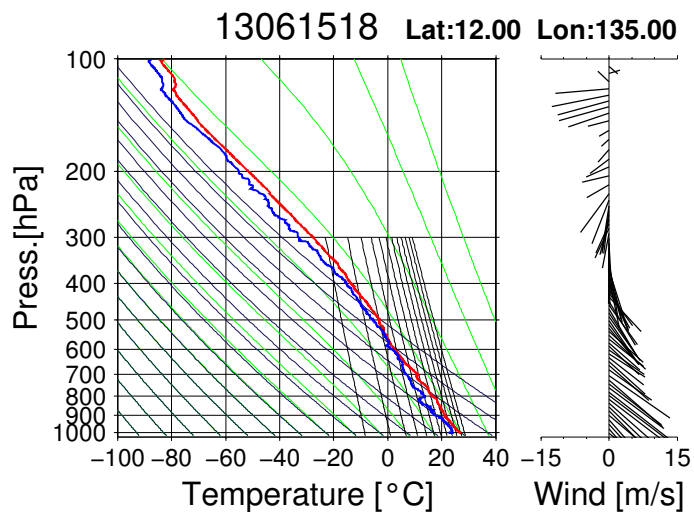
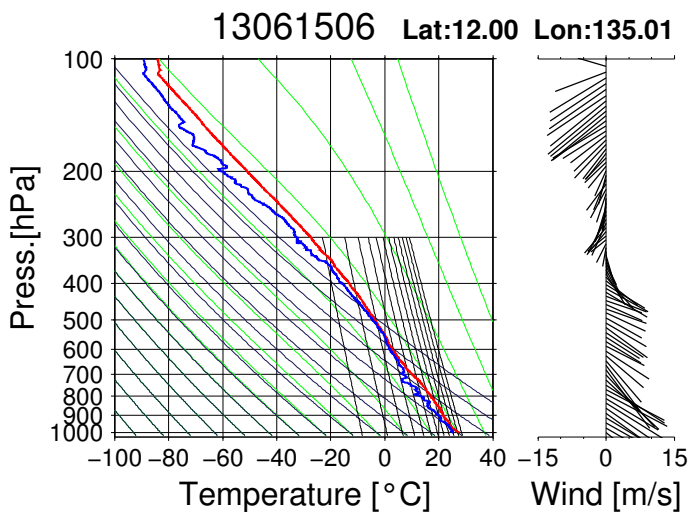
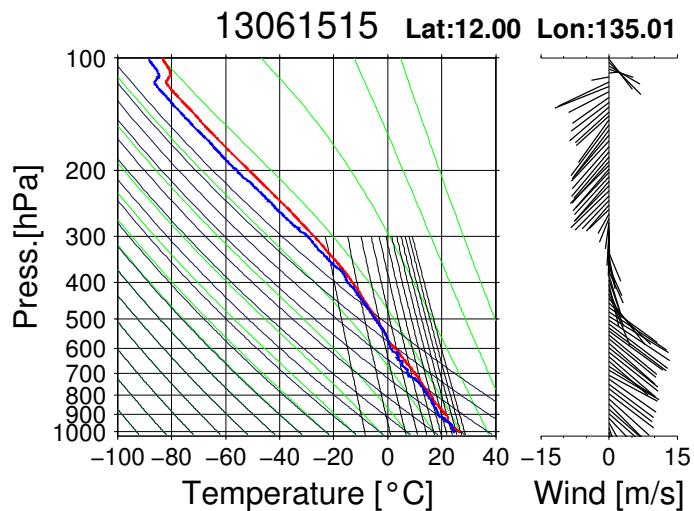
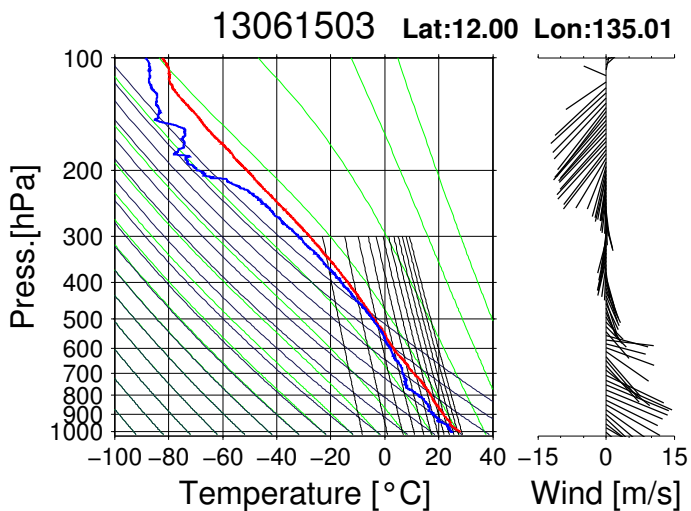
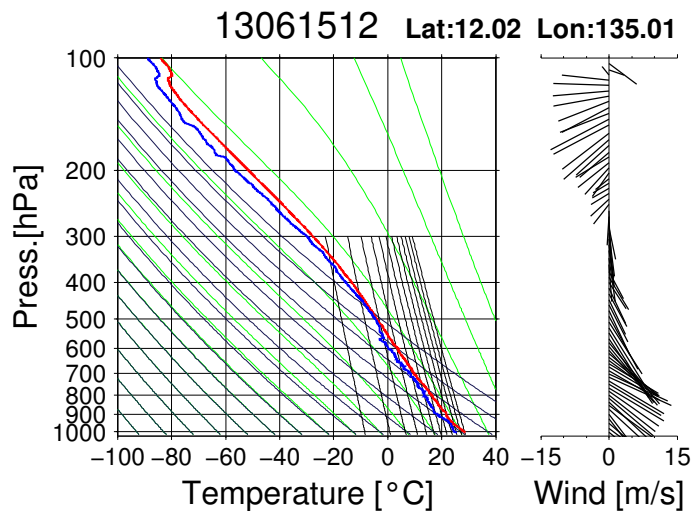
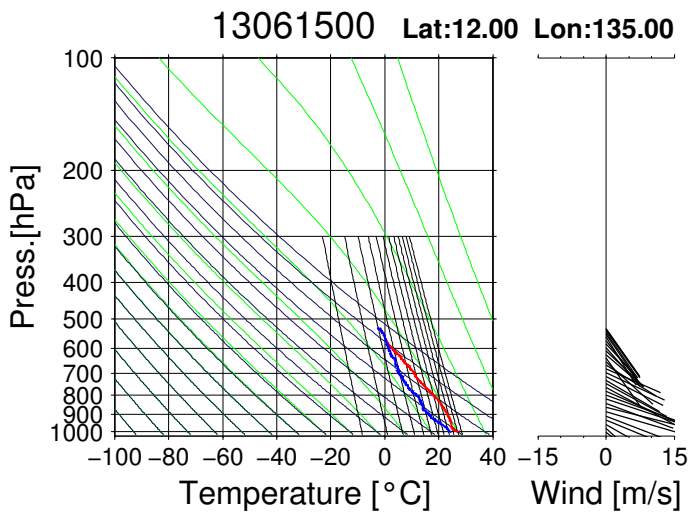


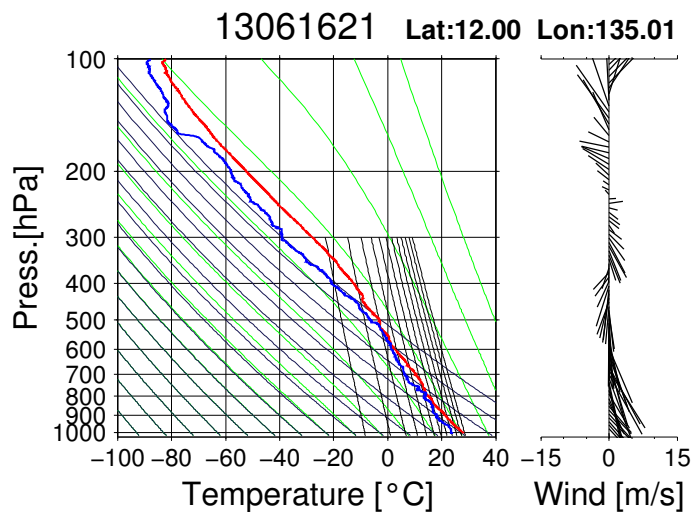
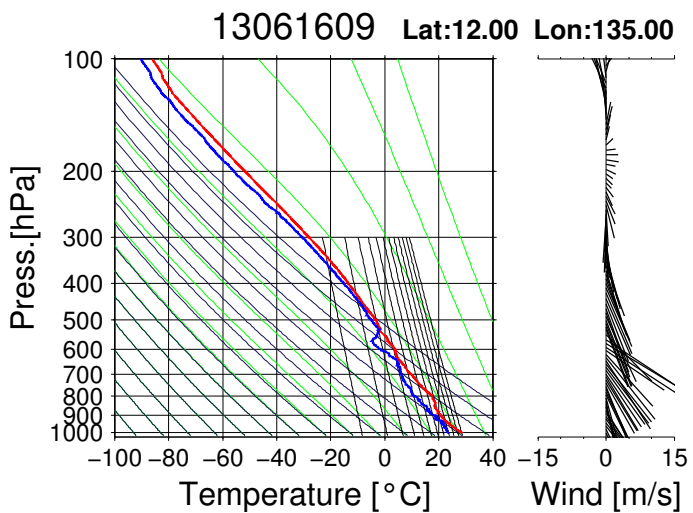
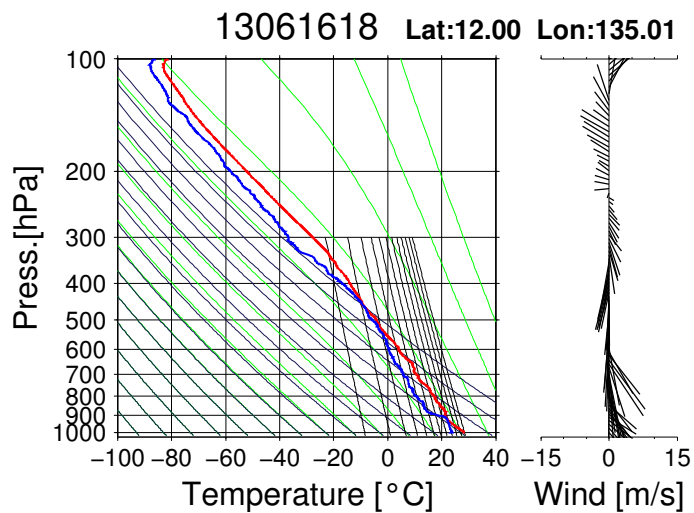
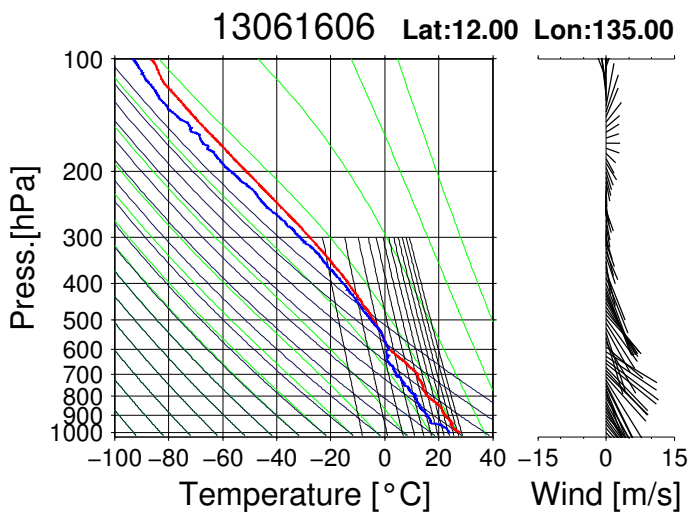
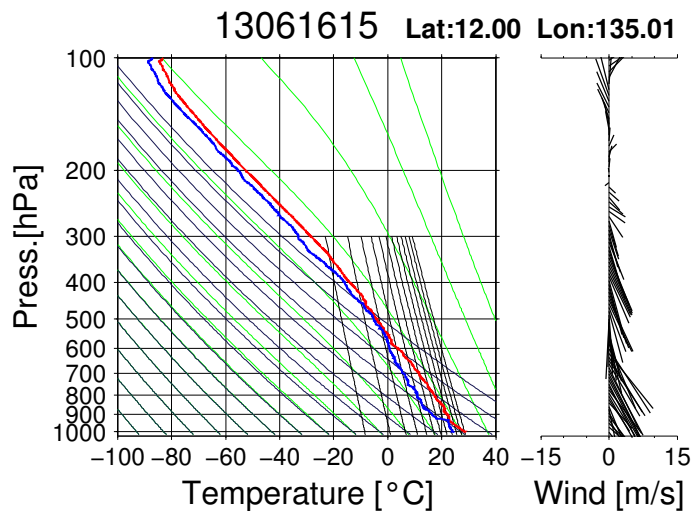
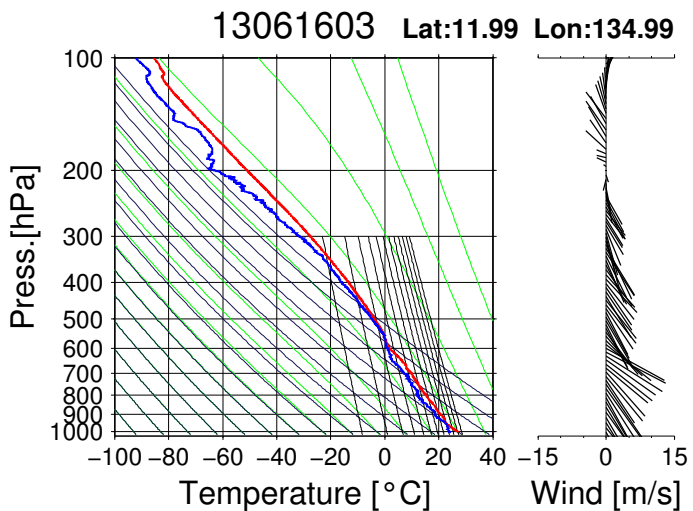
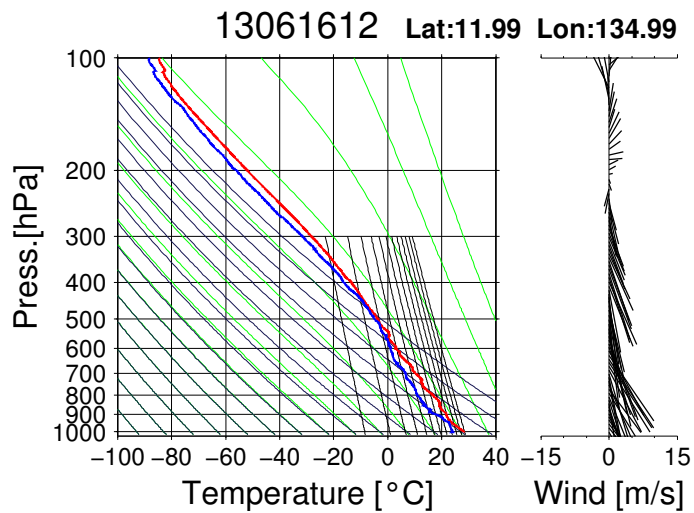
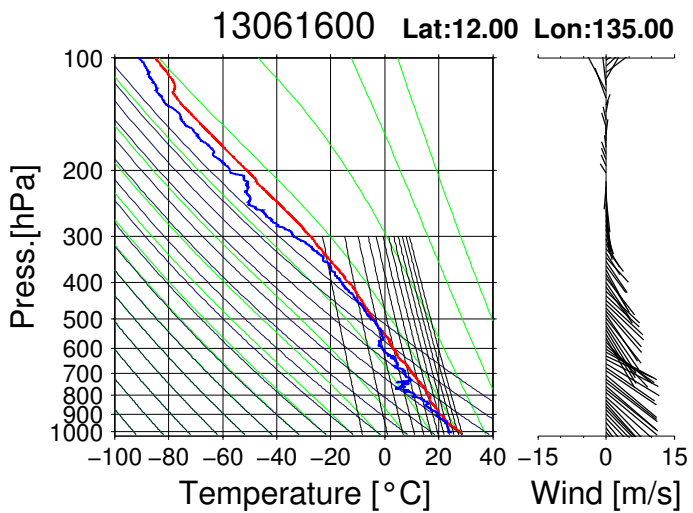
13061221 Lat:10.98 Lon:134.83

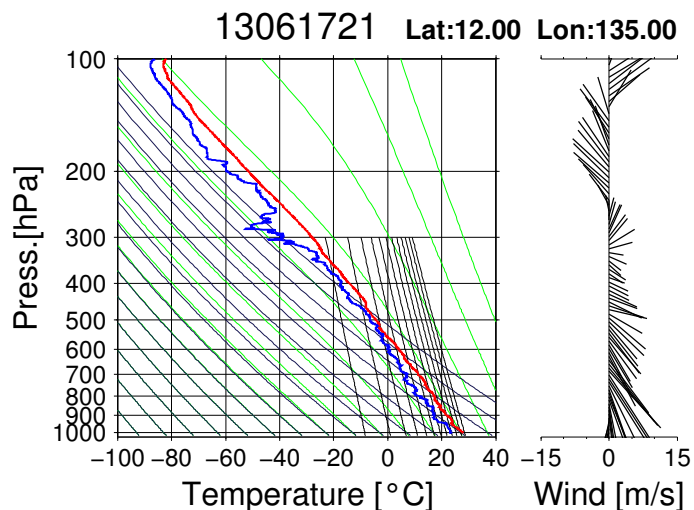
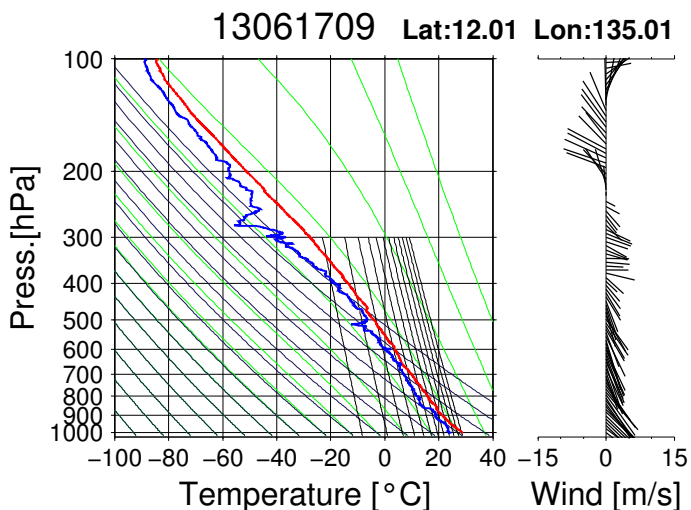
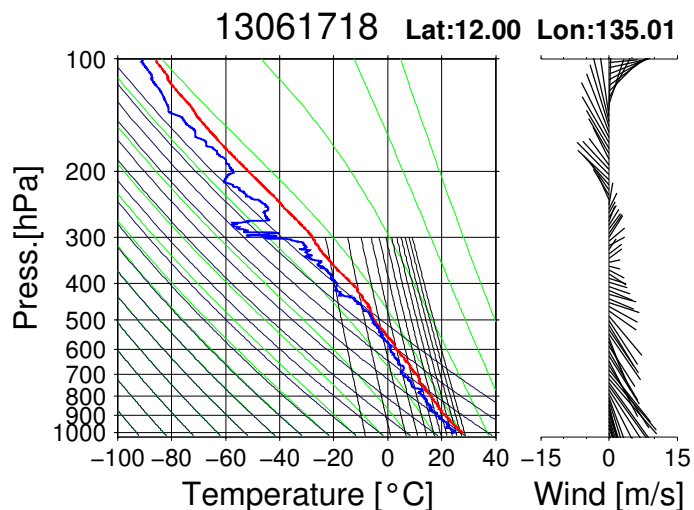
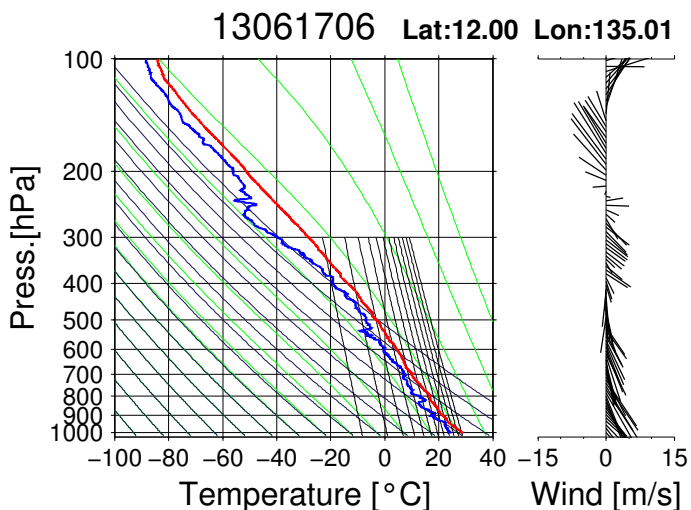
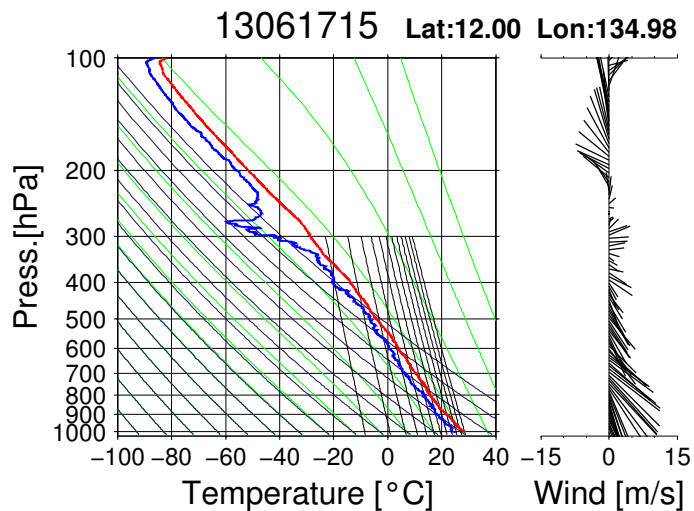
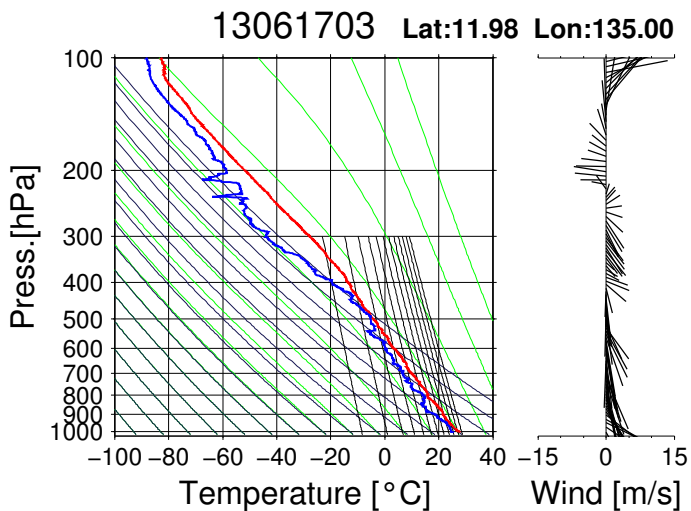
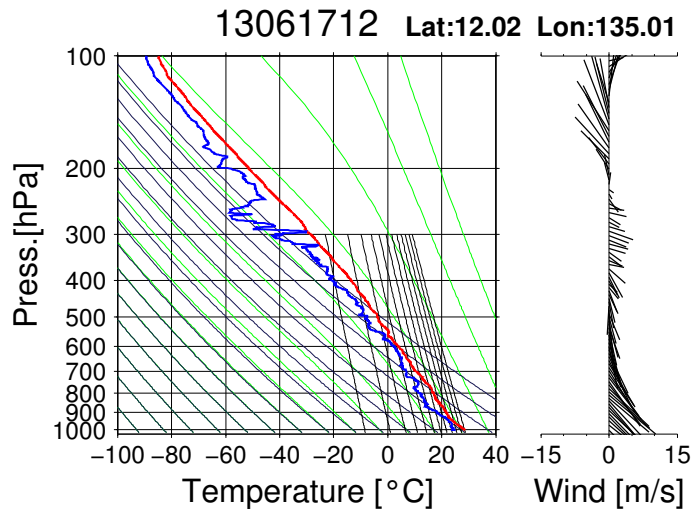
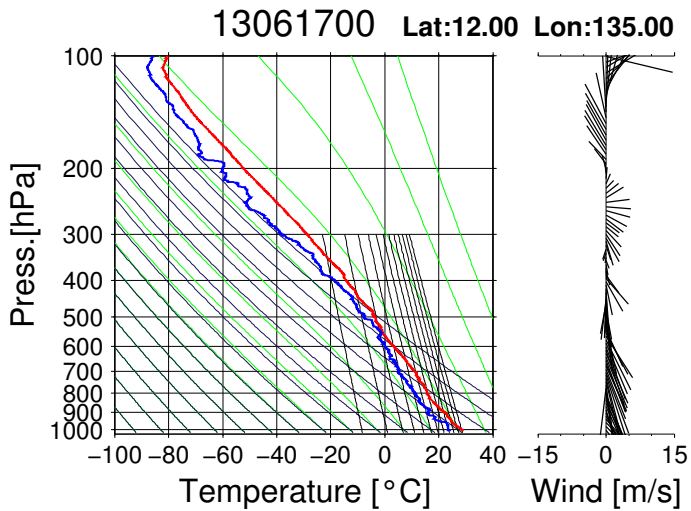


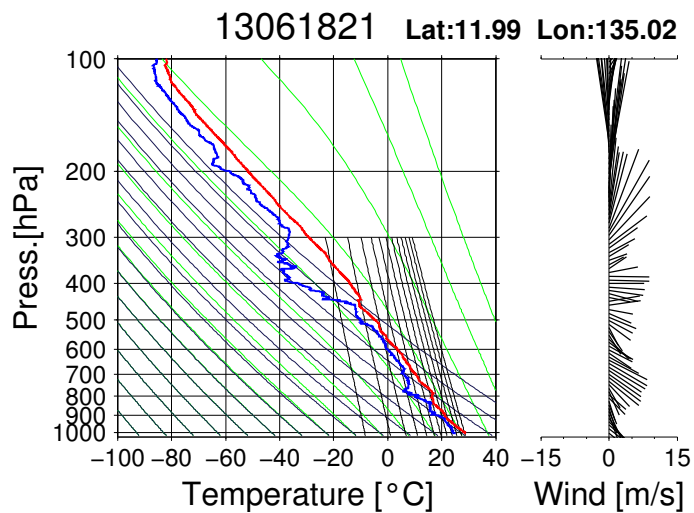
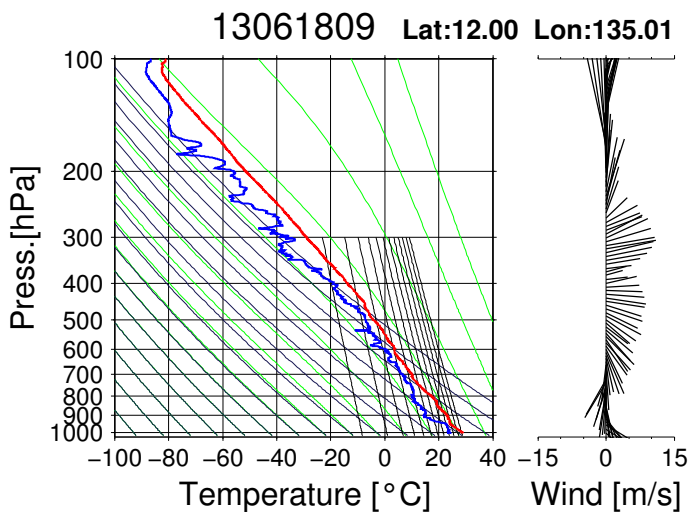
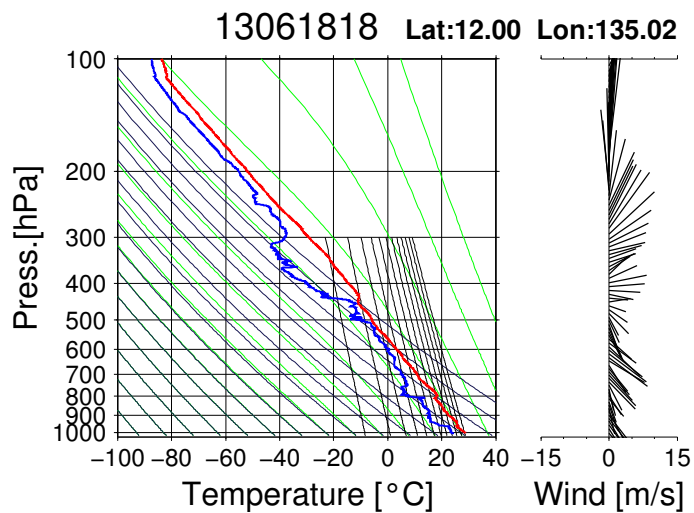
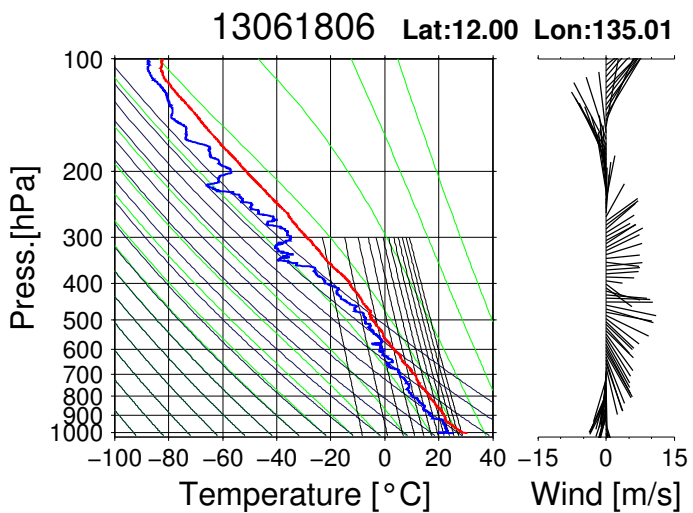
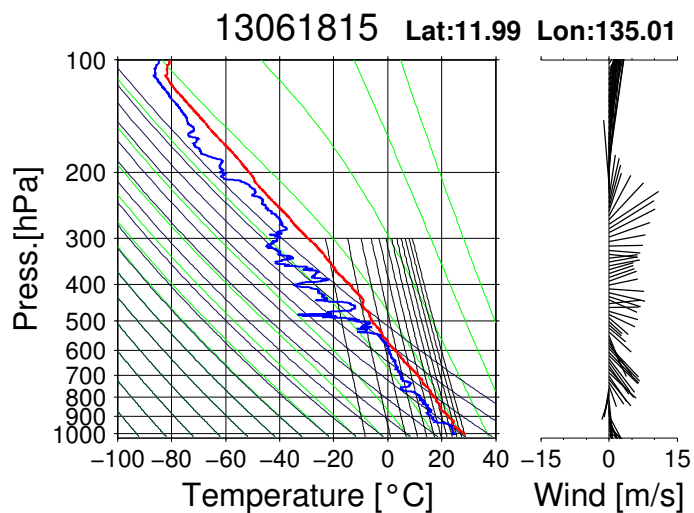
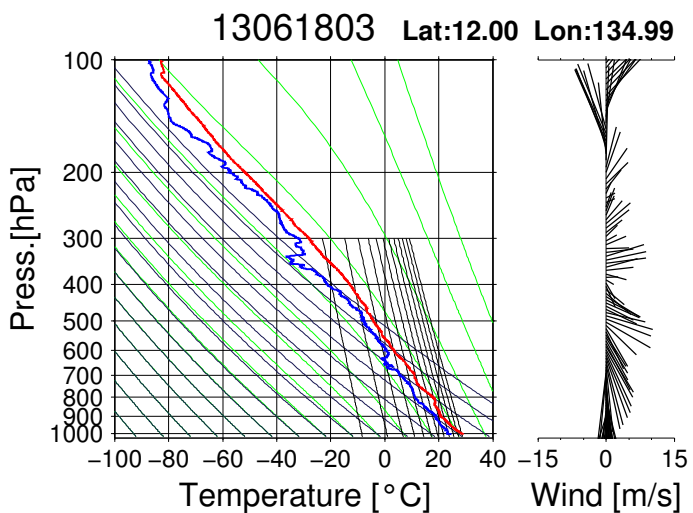
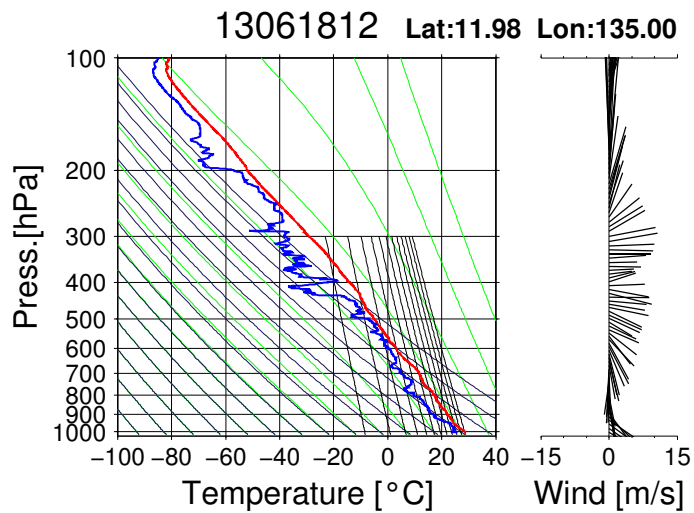
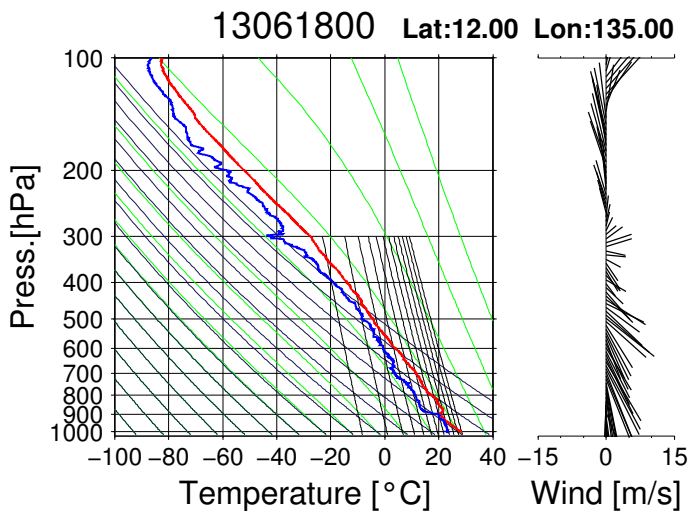


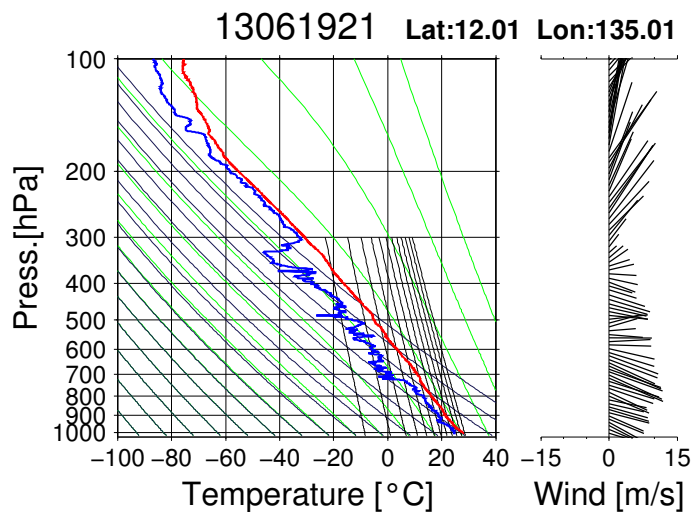
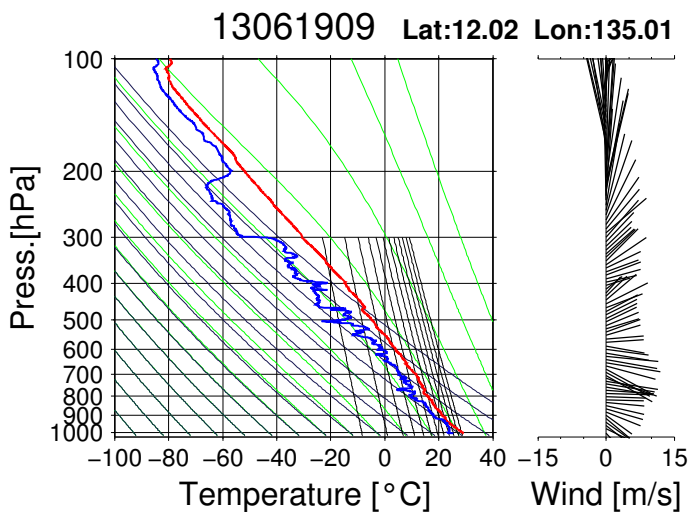
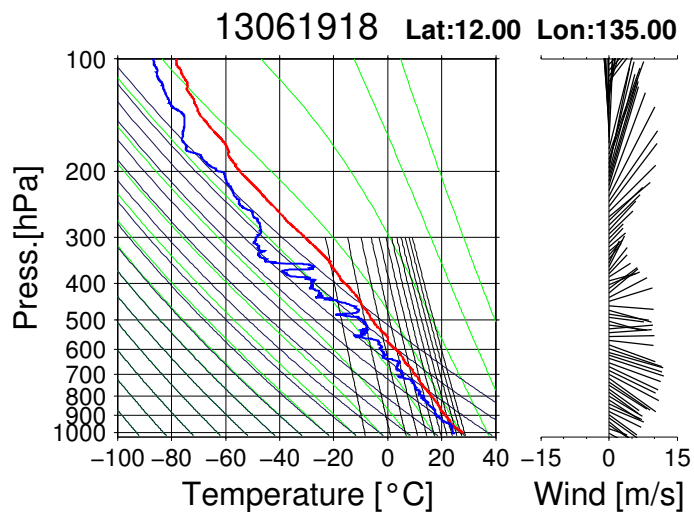
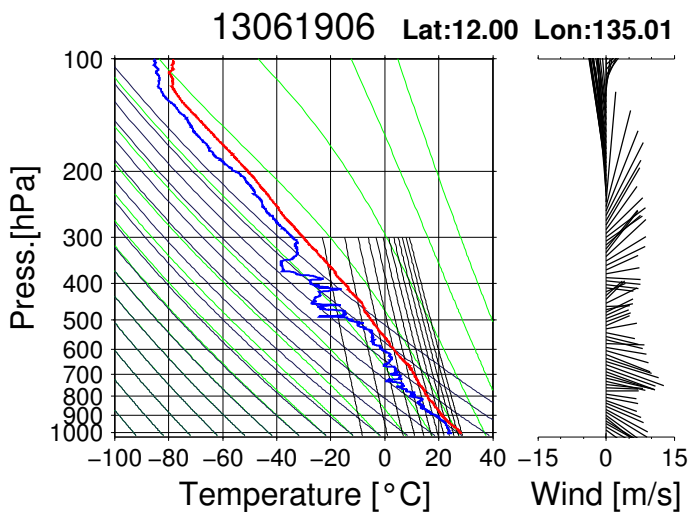
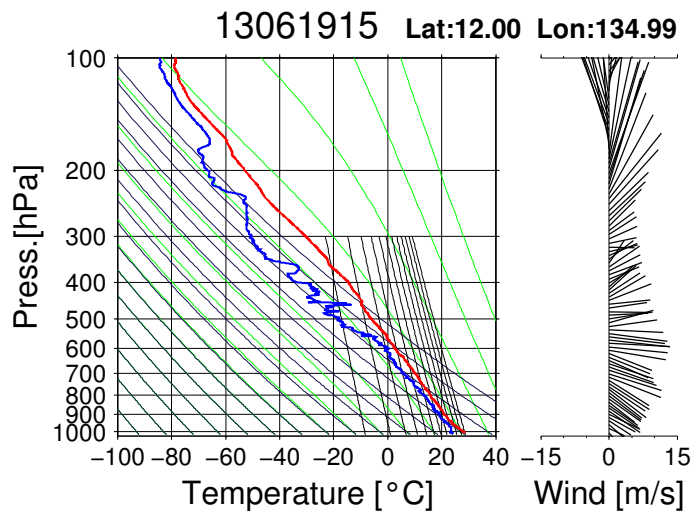
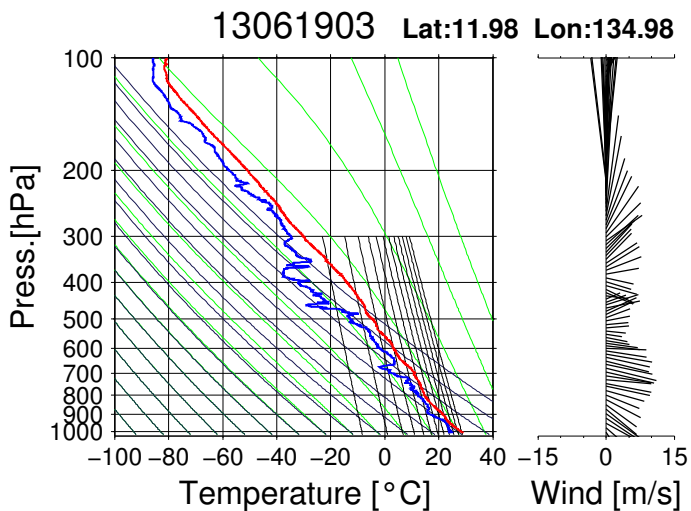
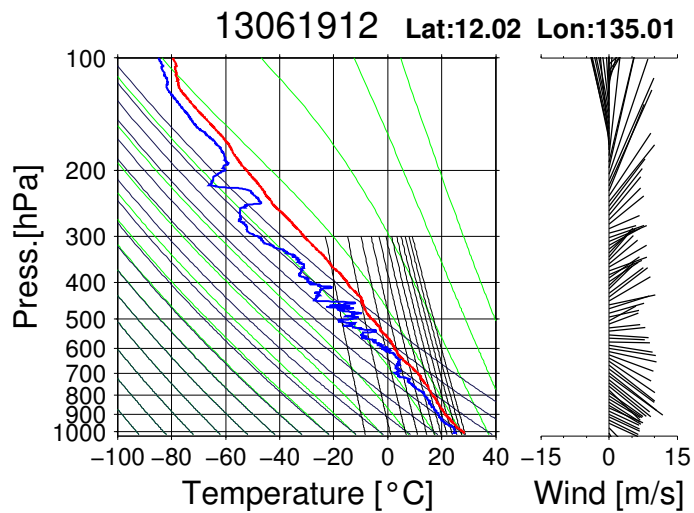
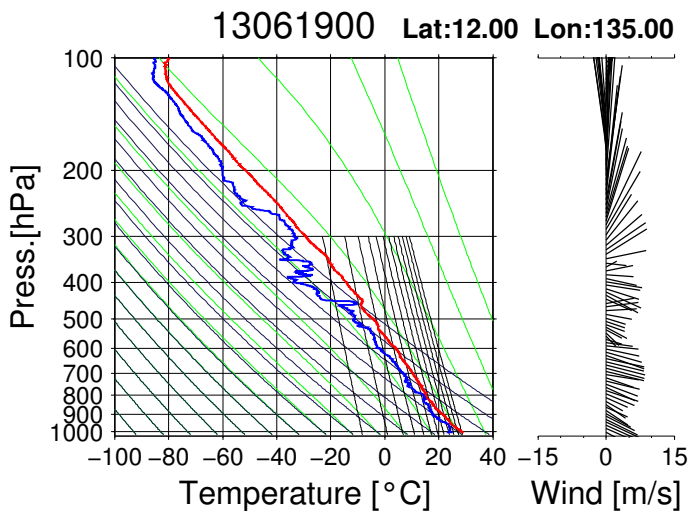


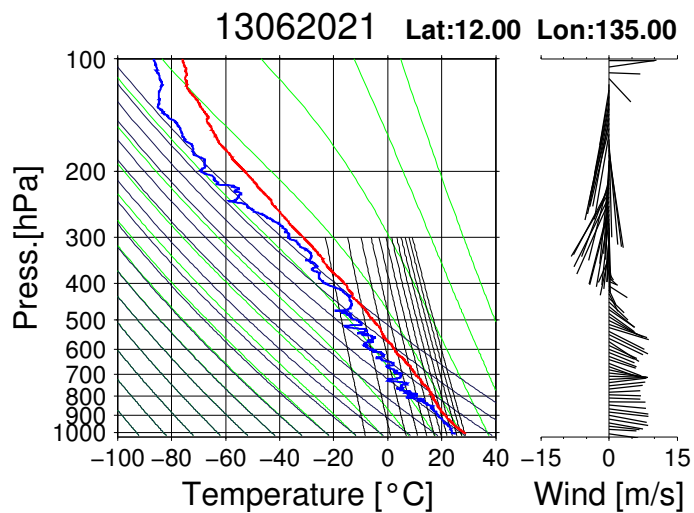
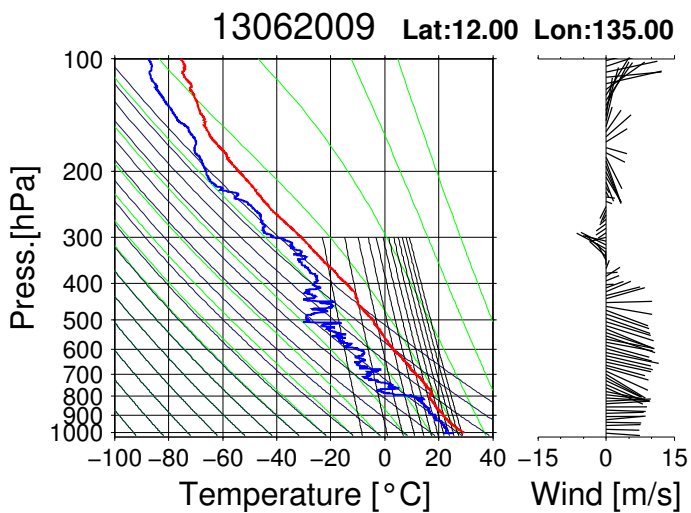
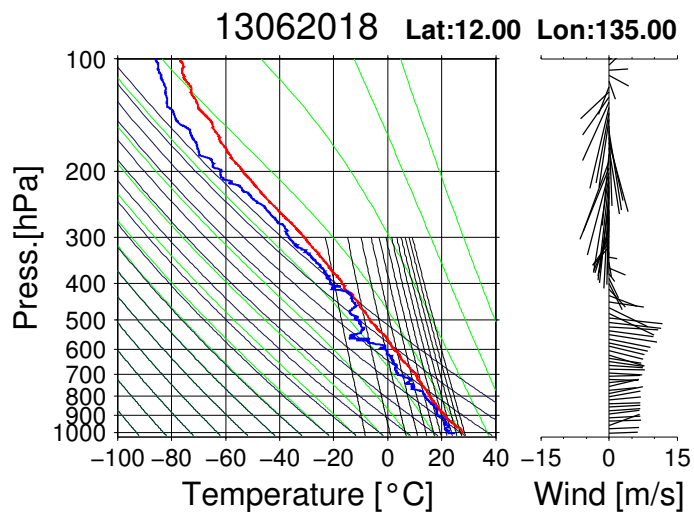
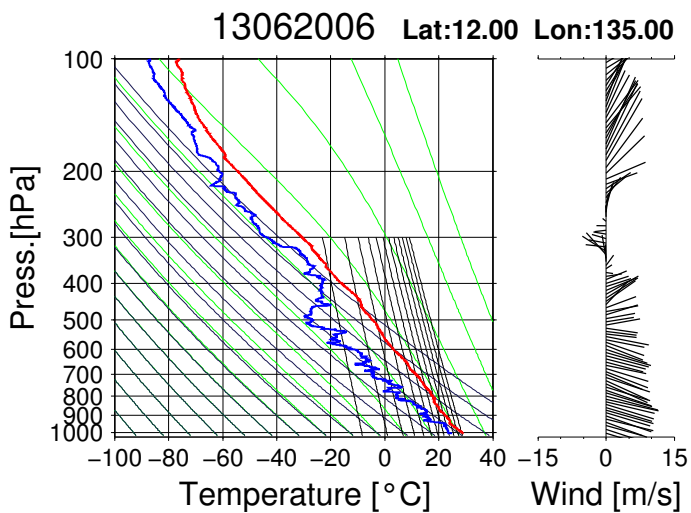
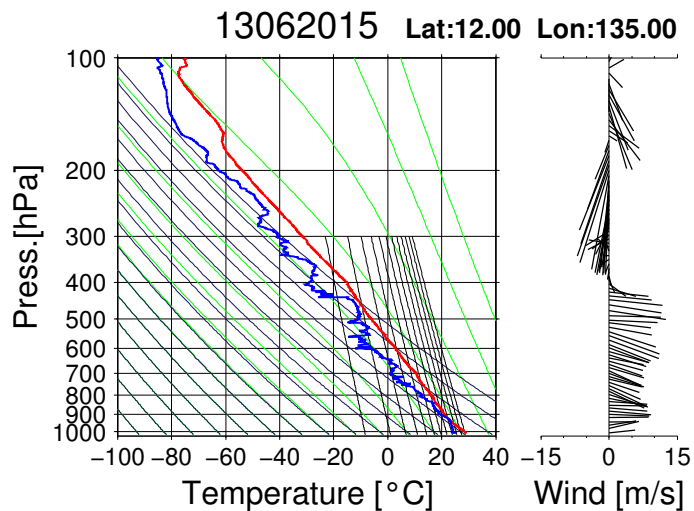
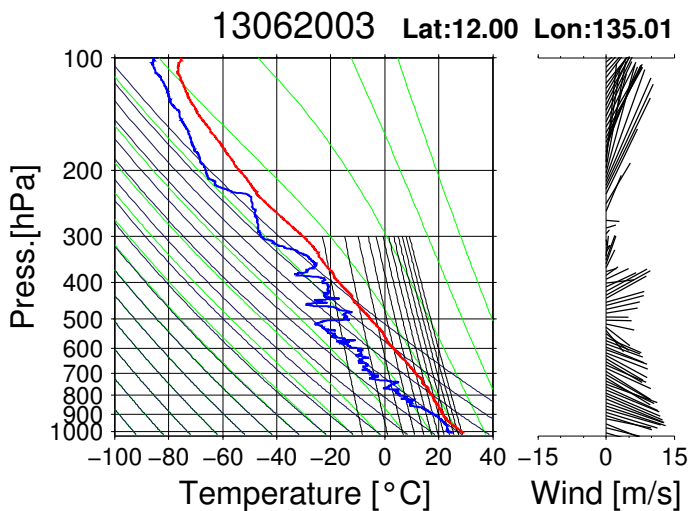
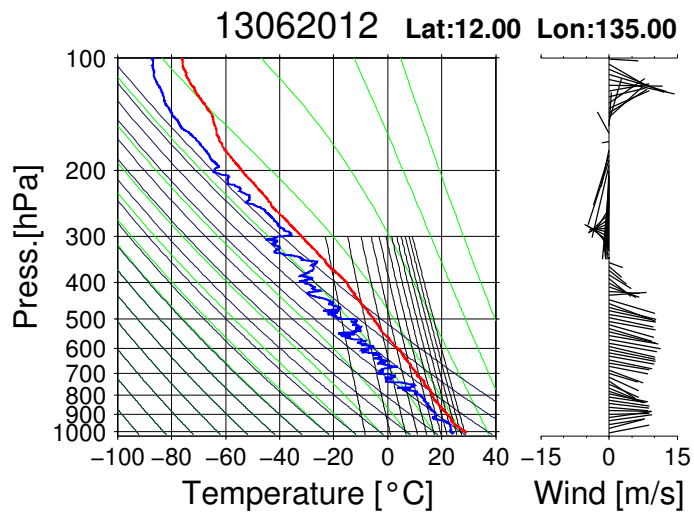
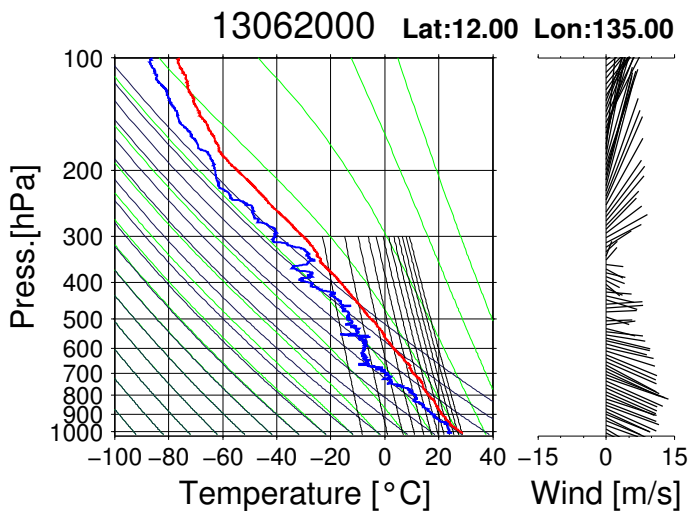


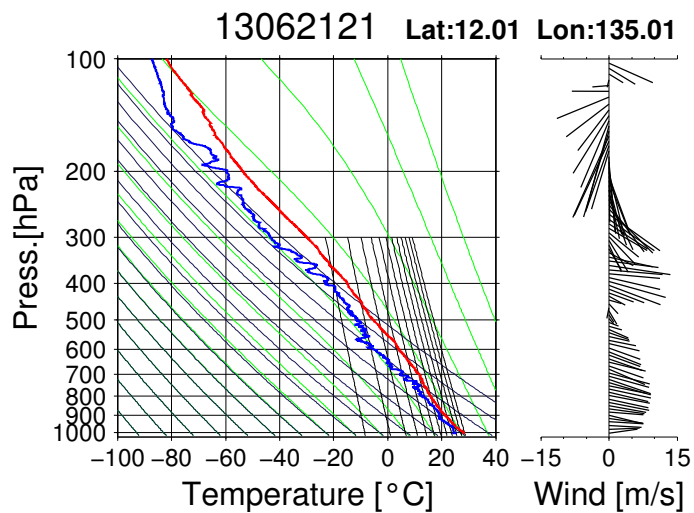
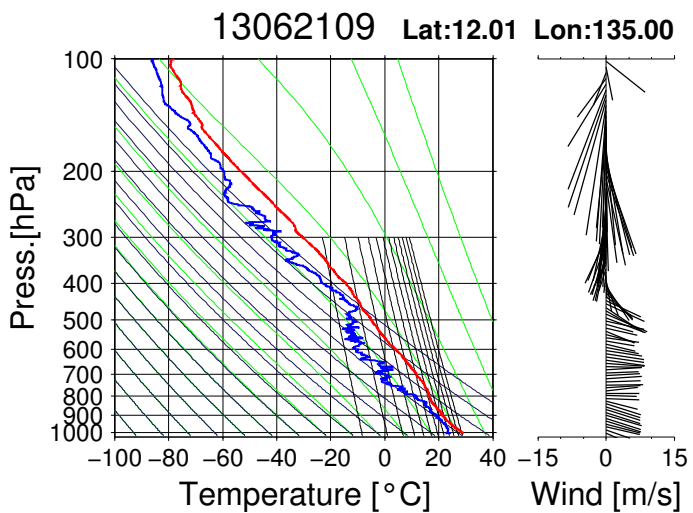
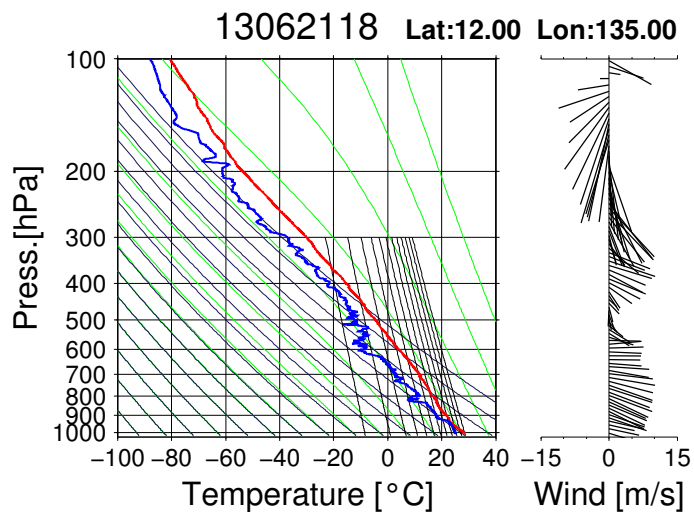
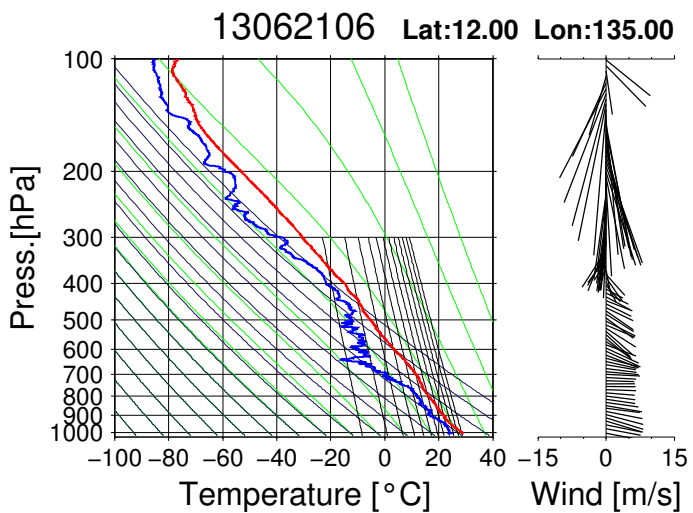
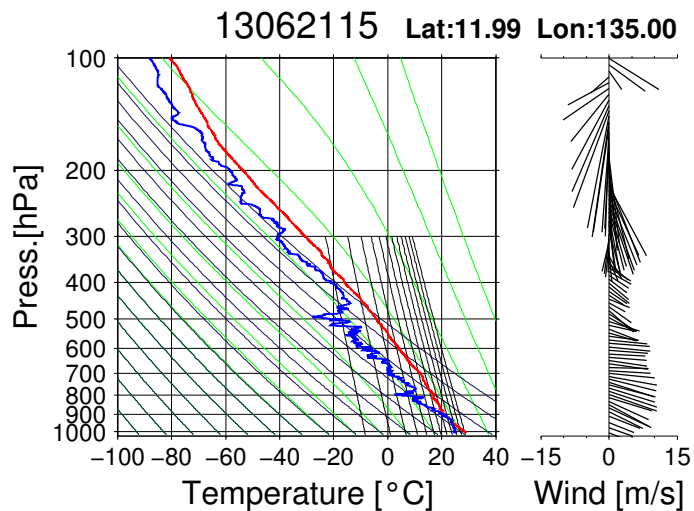
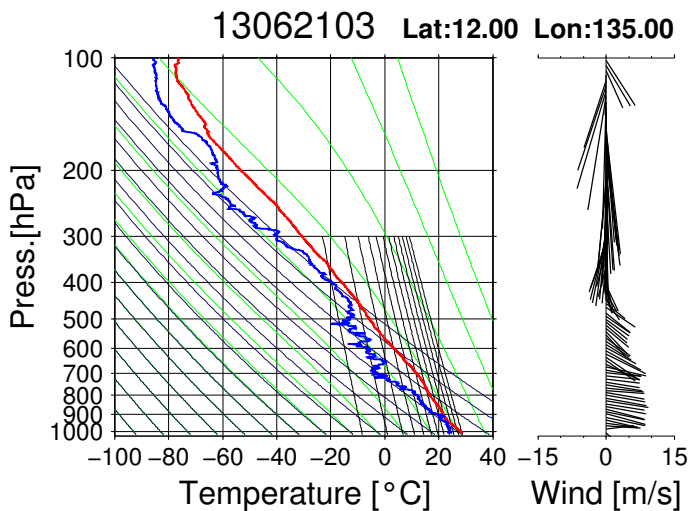
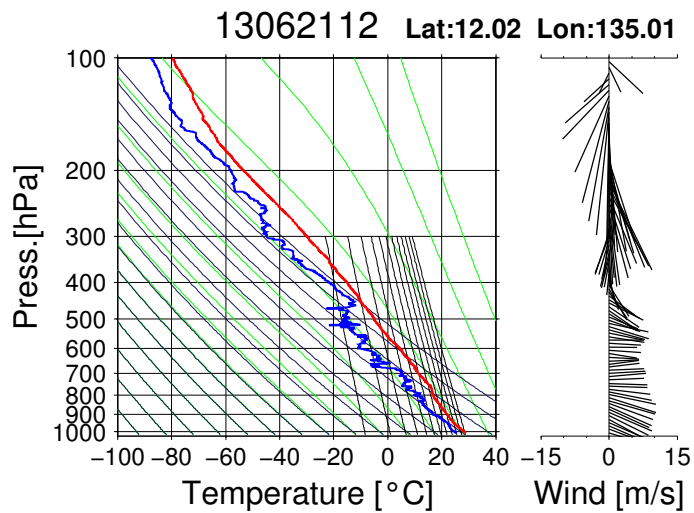
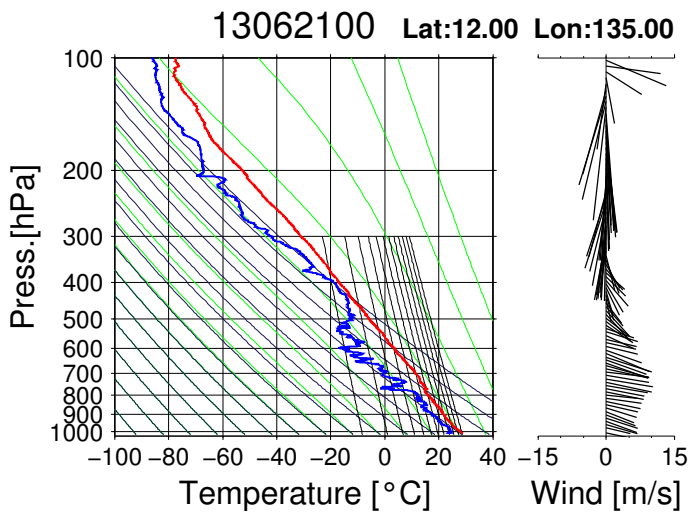


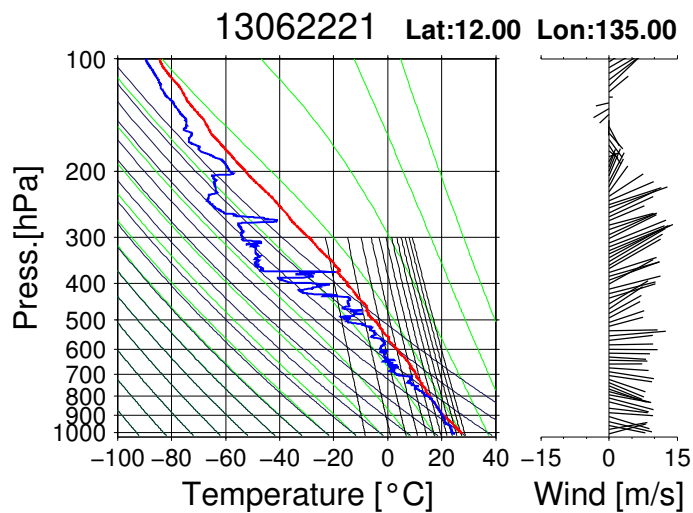
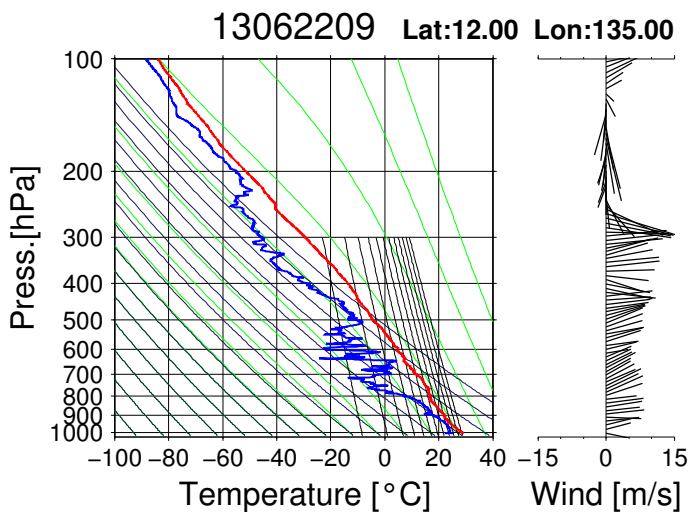
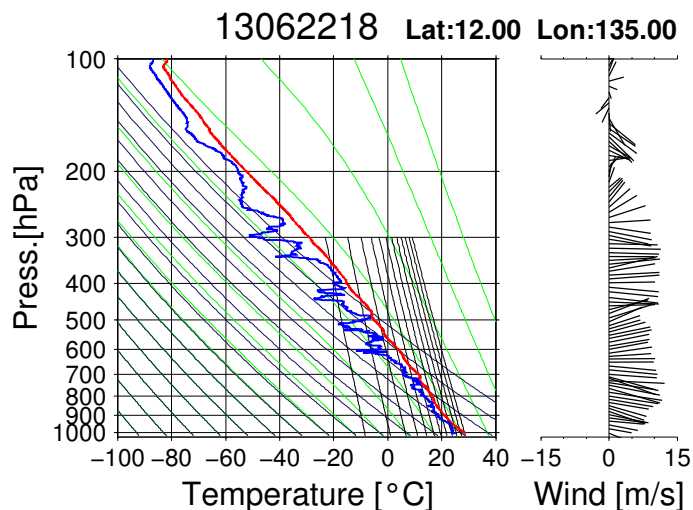
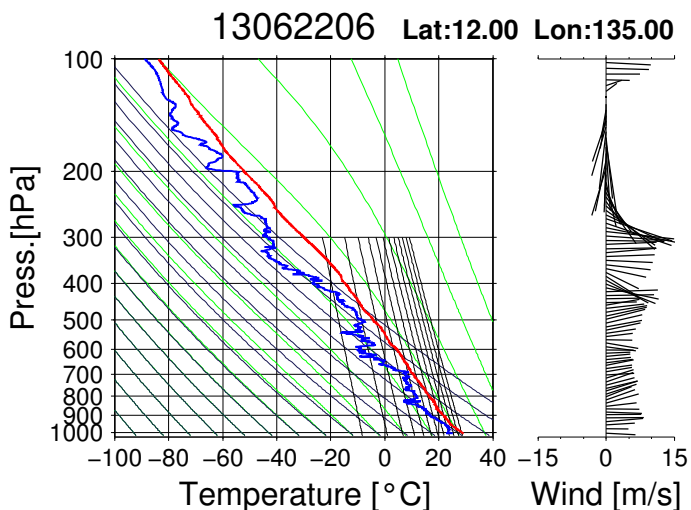
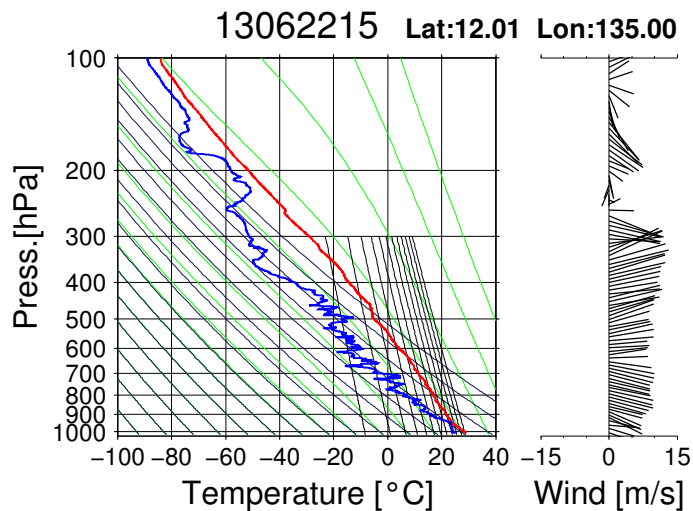
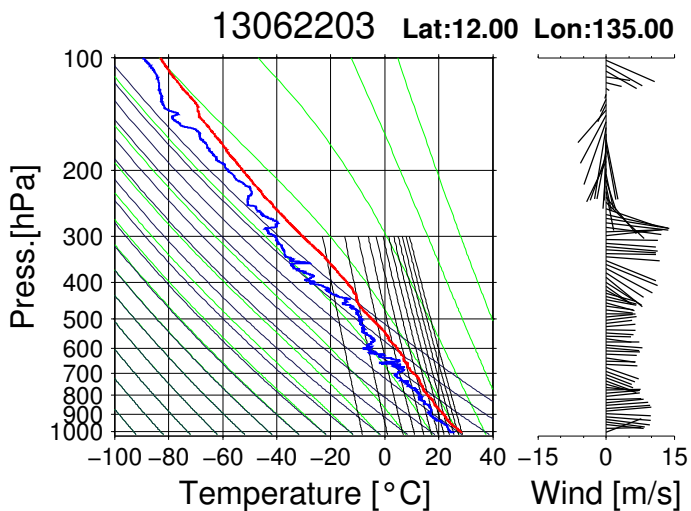
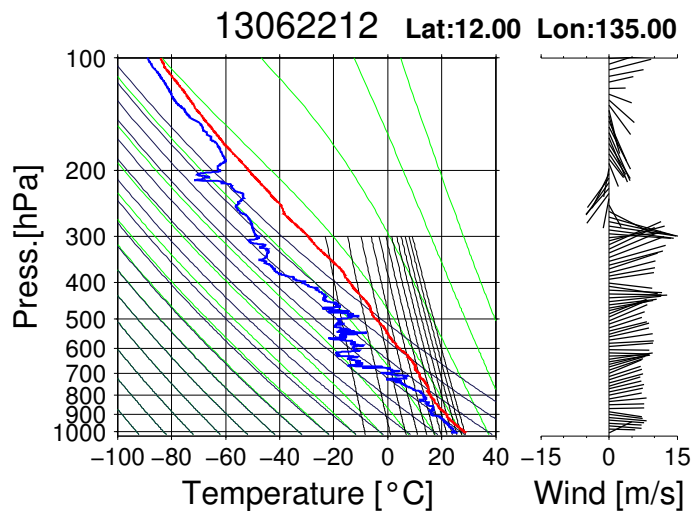
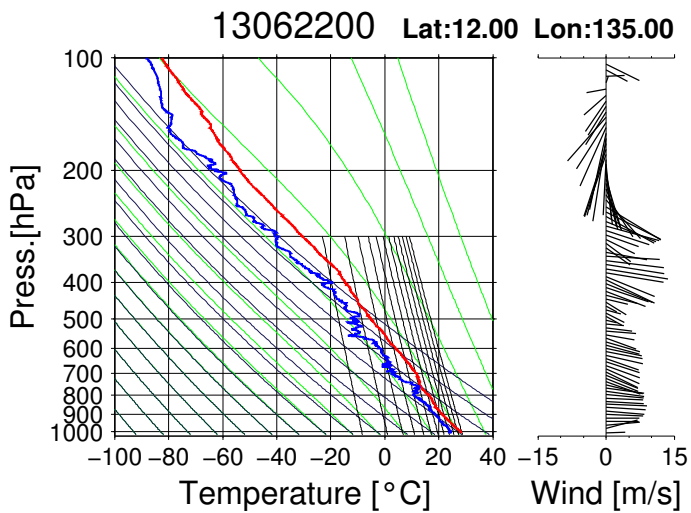


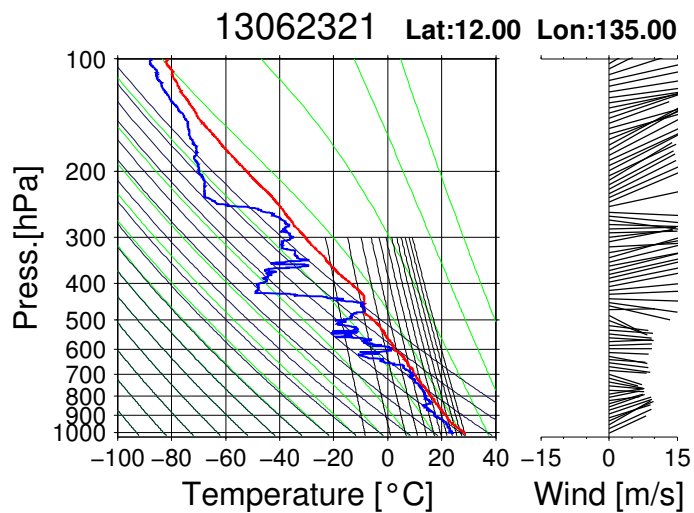
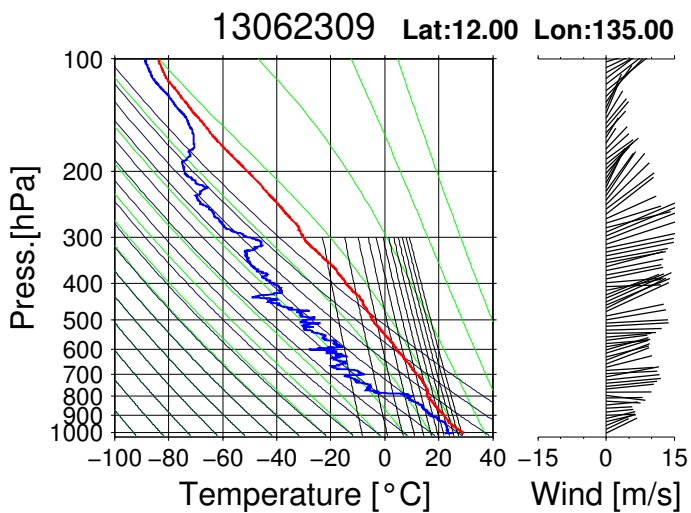
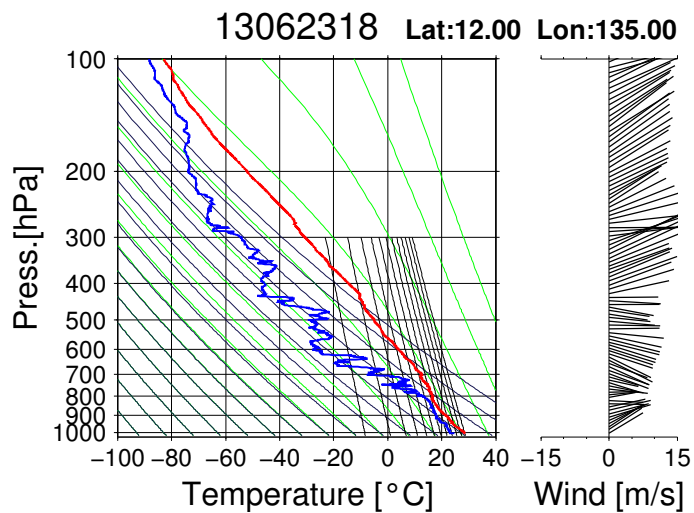
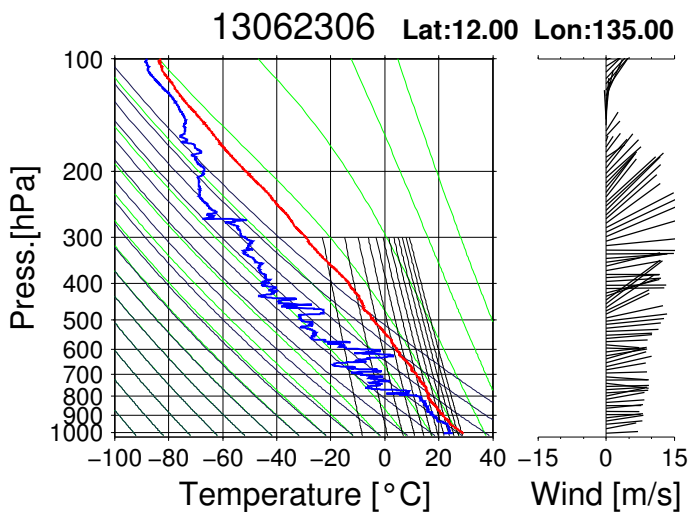
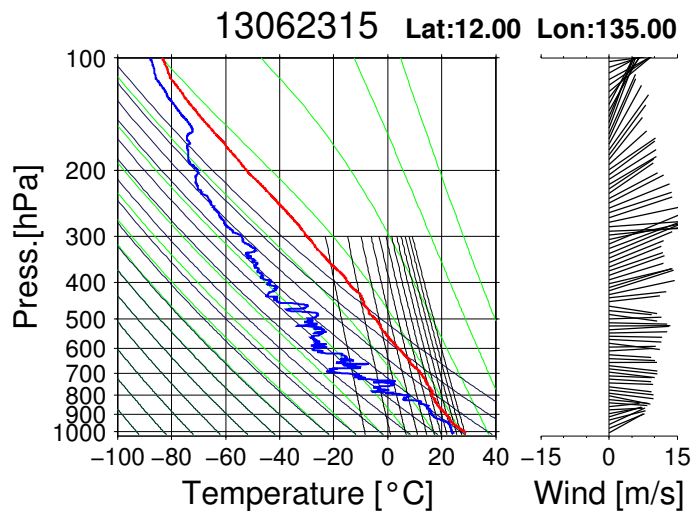
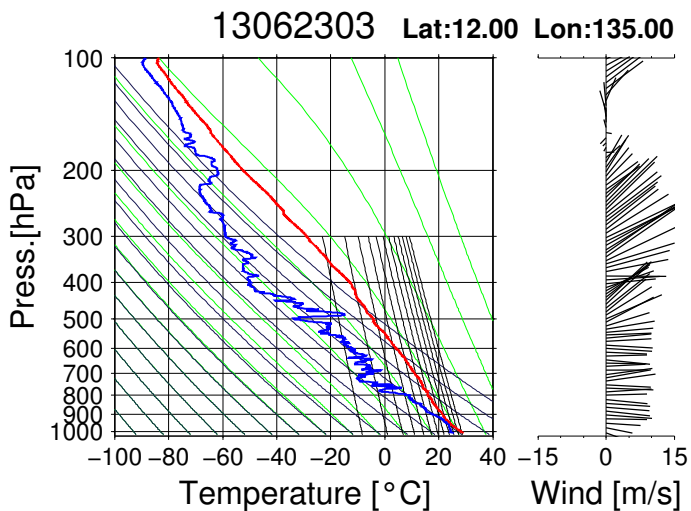
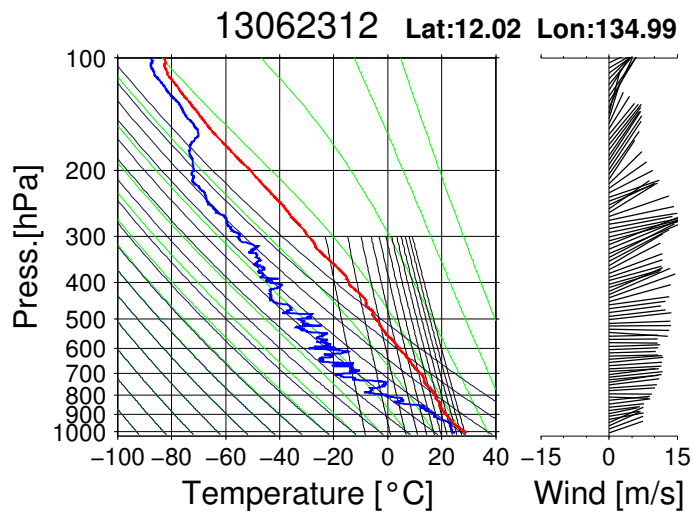
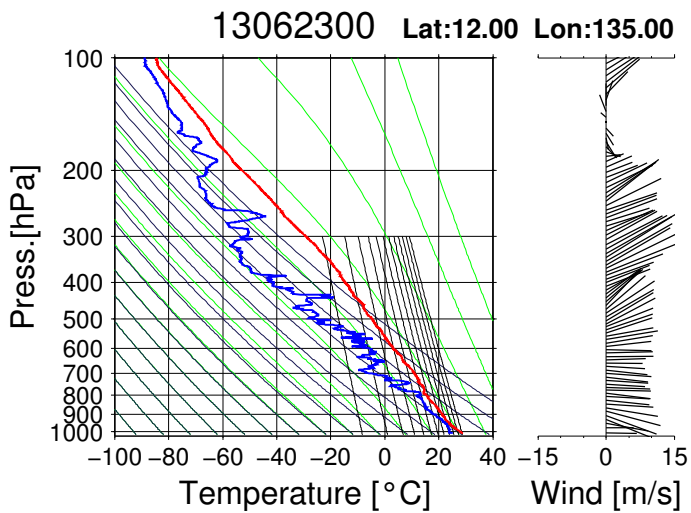


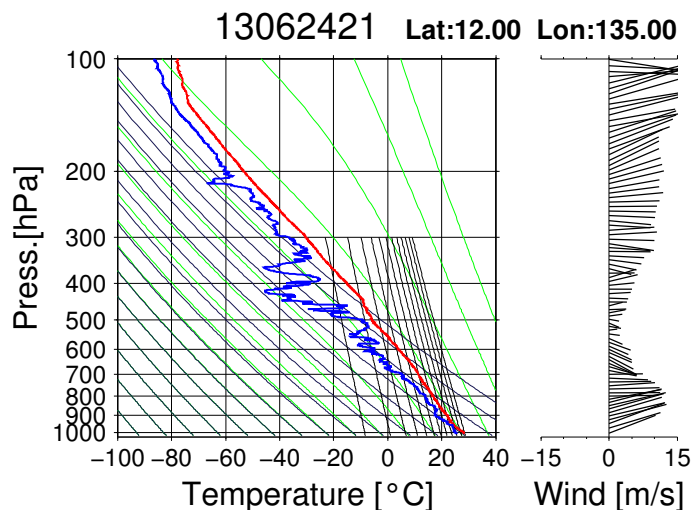
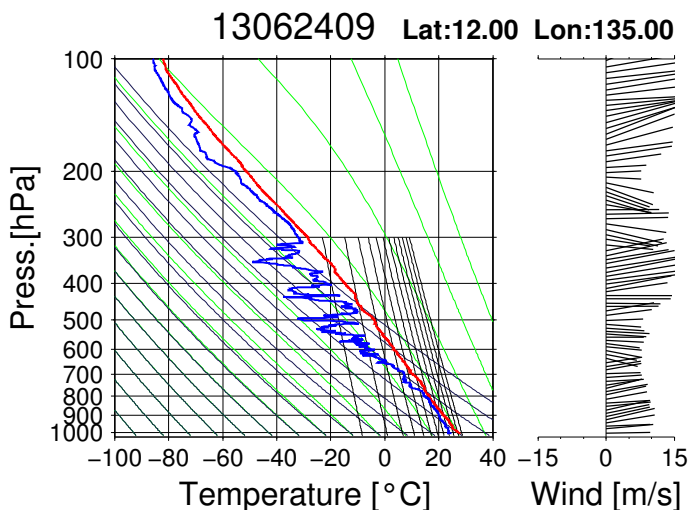
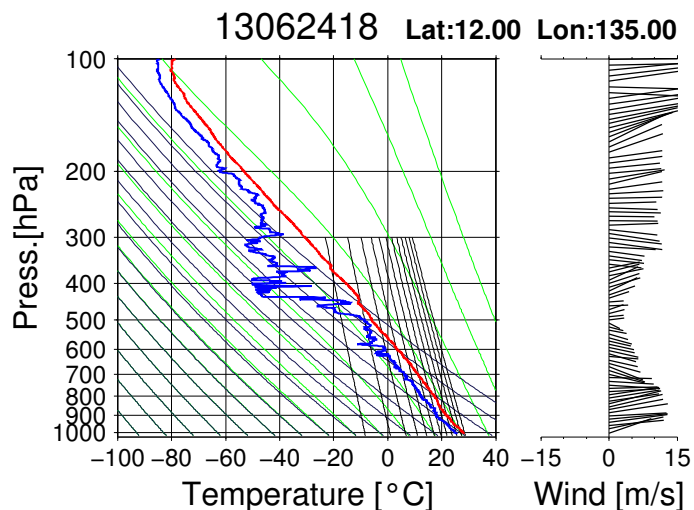
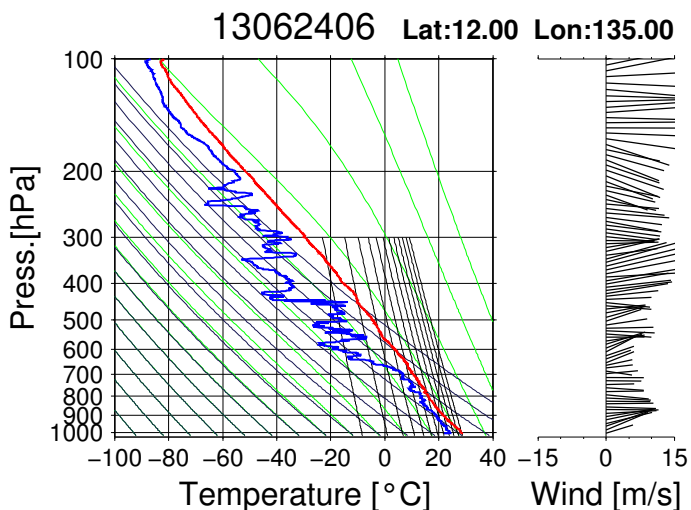
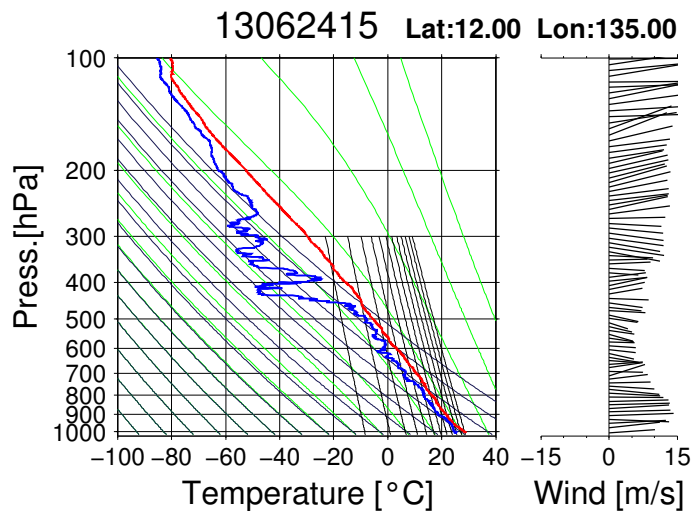
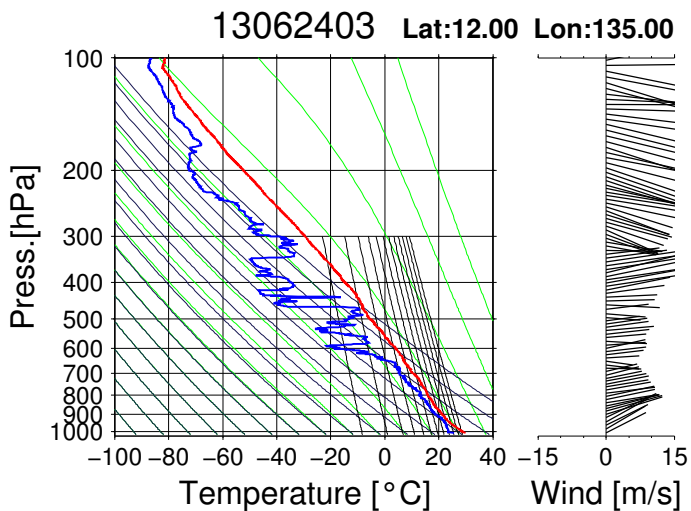
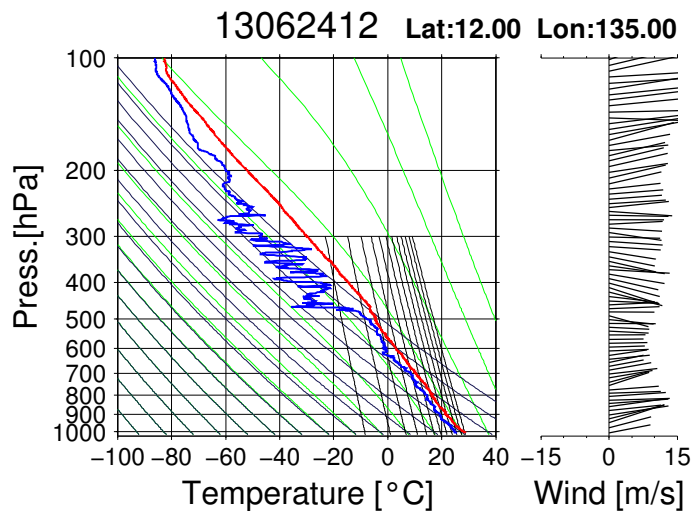
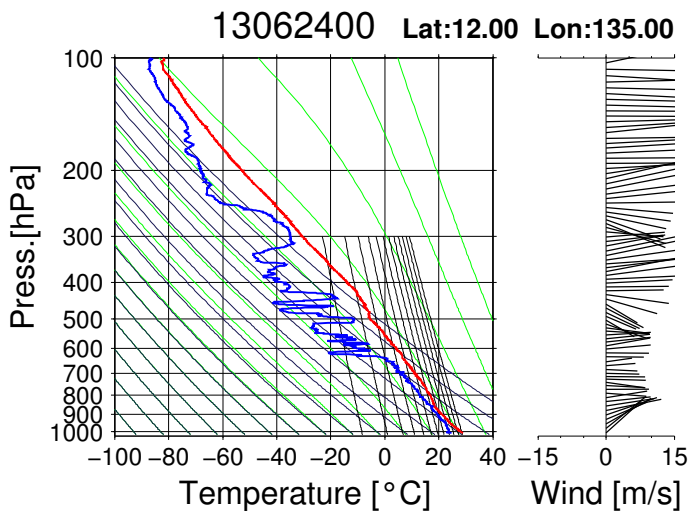


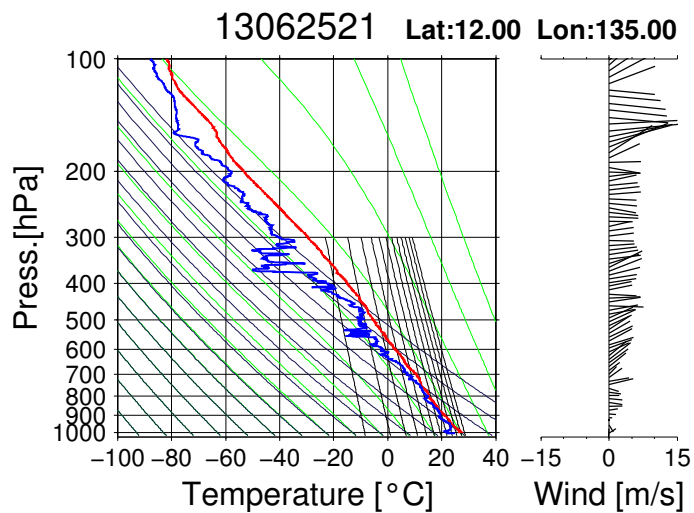
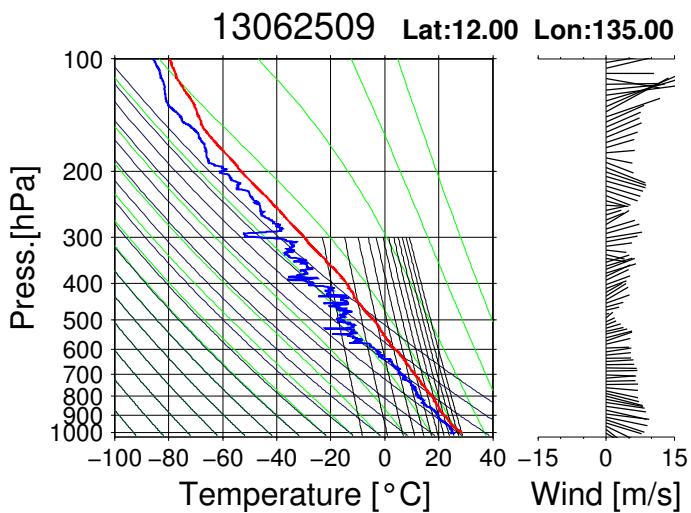
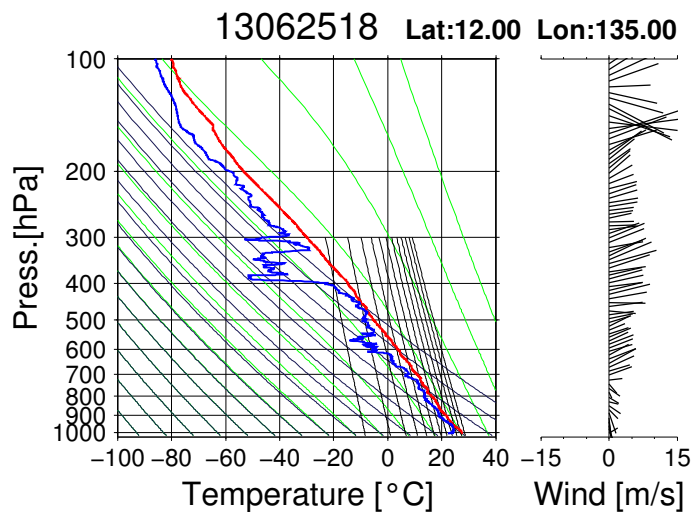
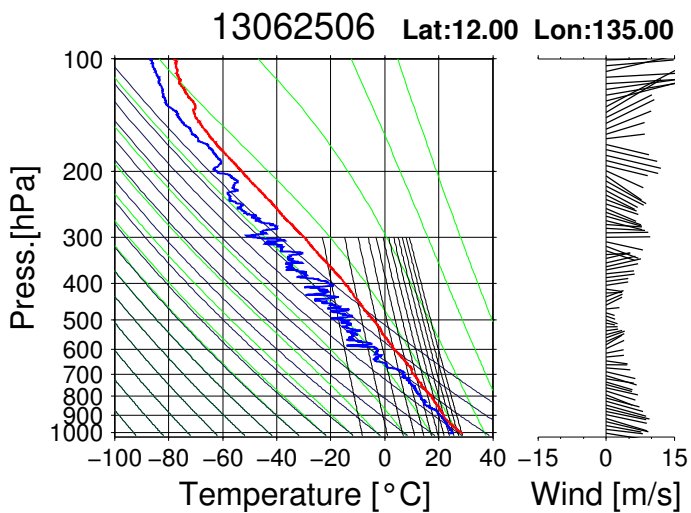
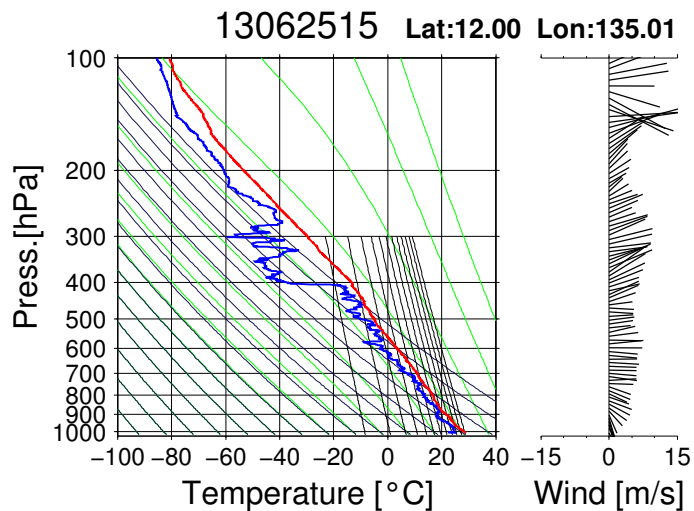
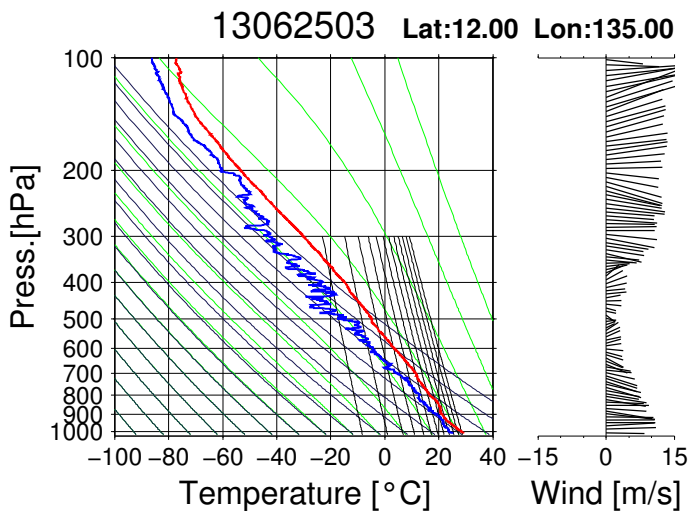
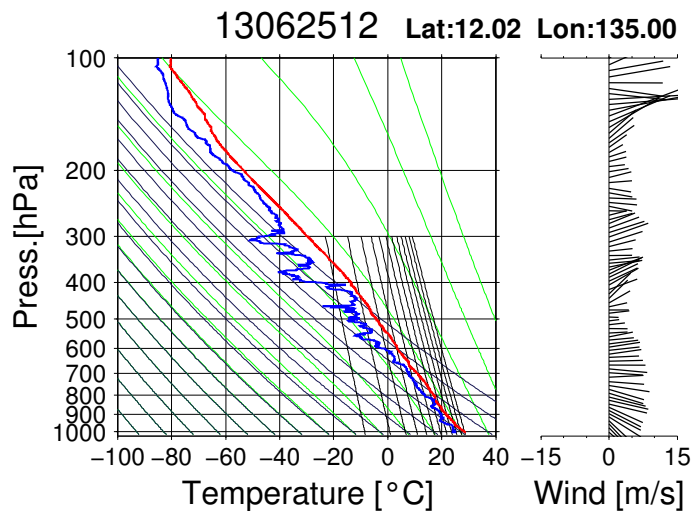
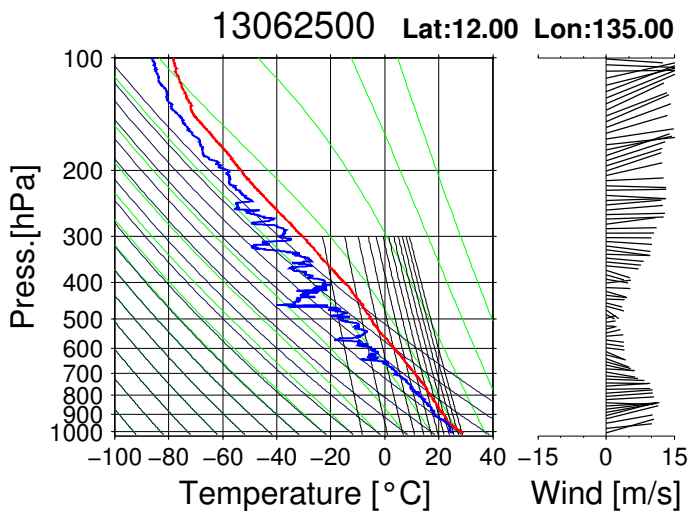


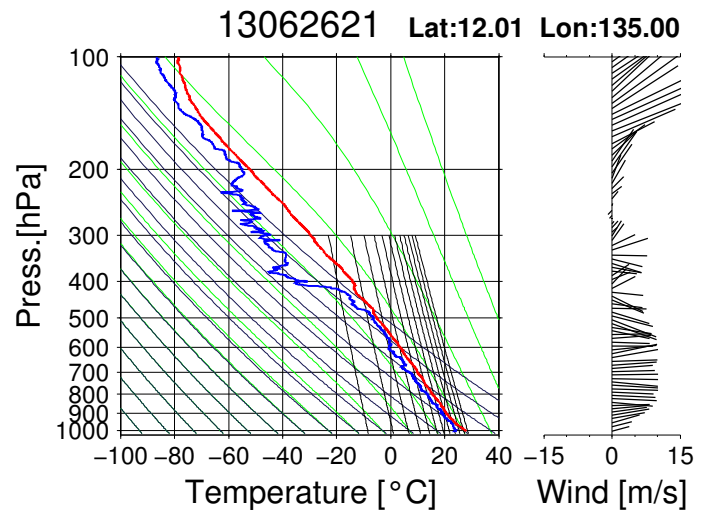
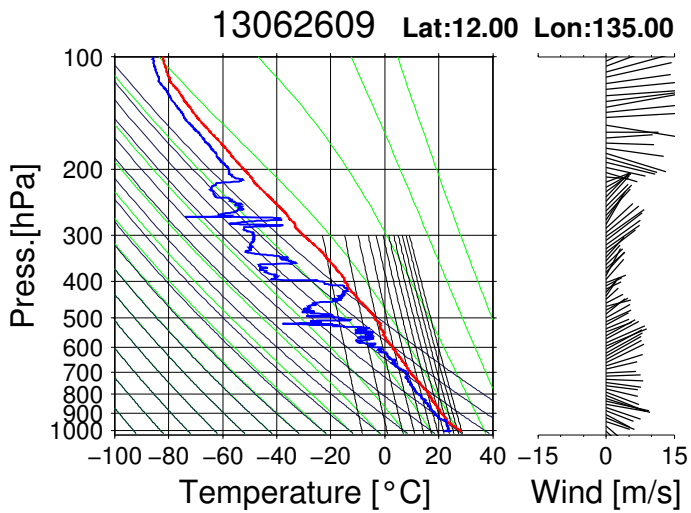
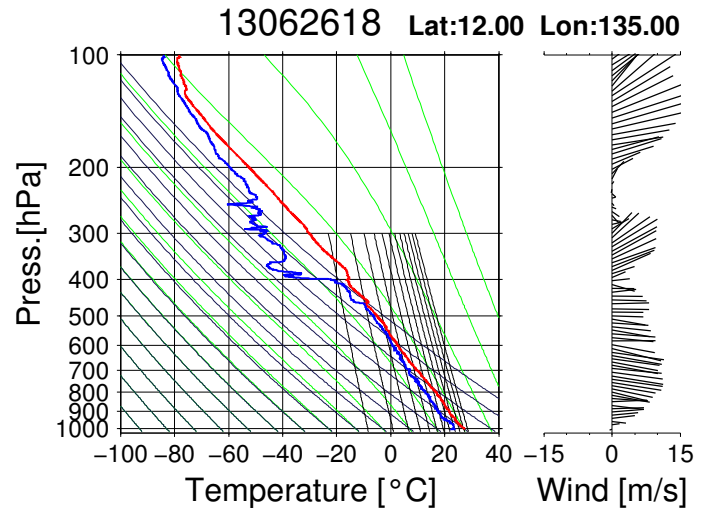
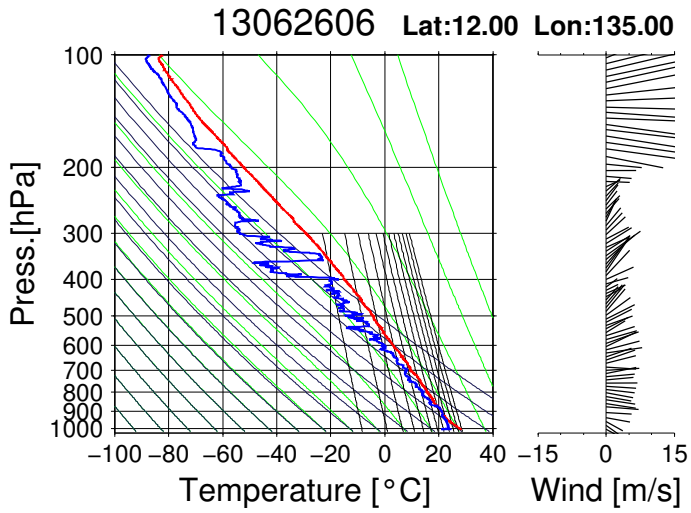
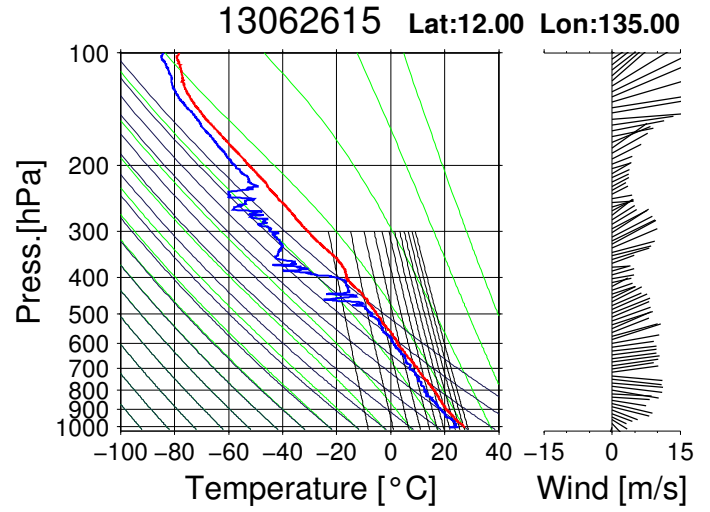
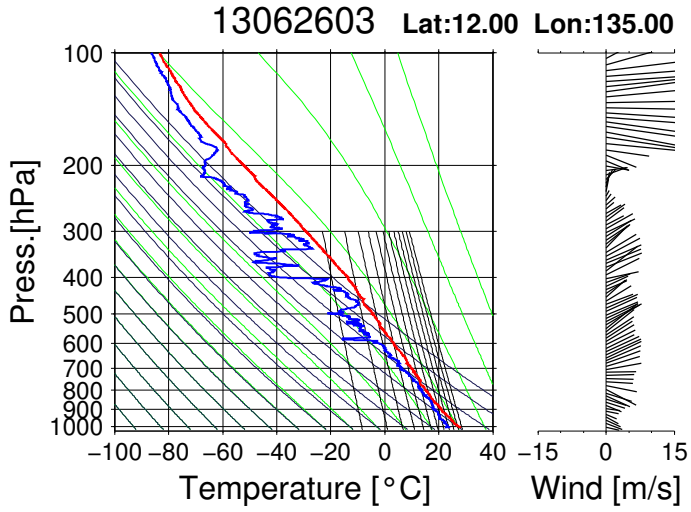
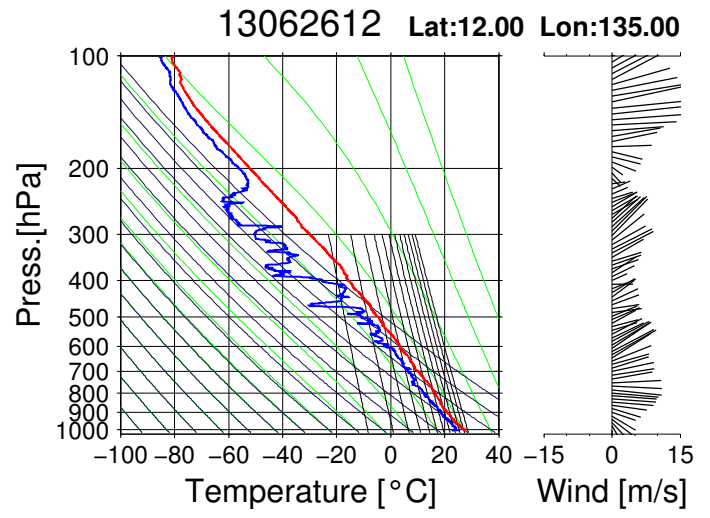
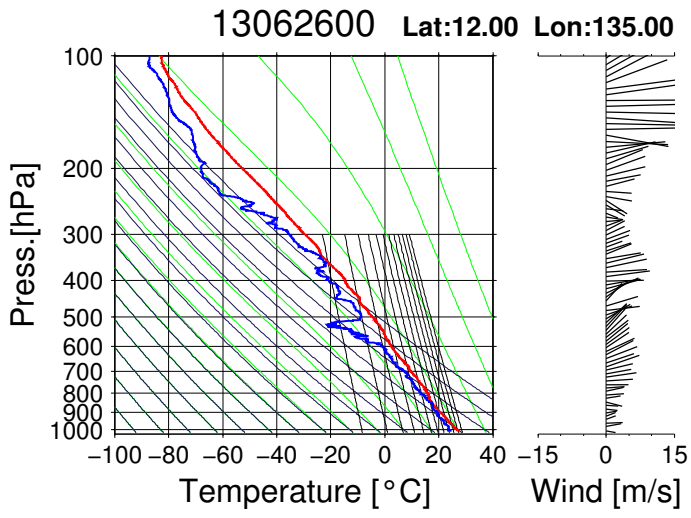


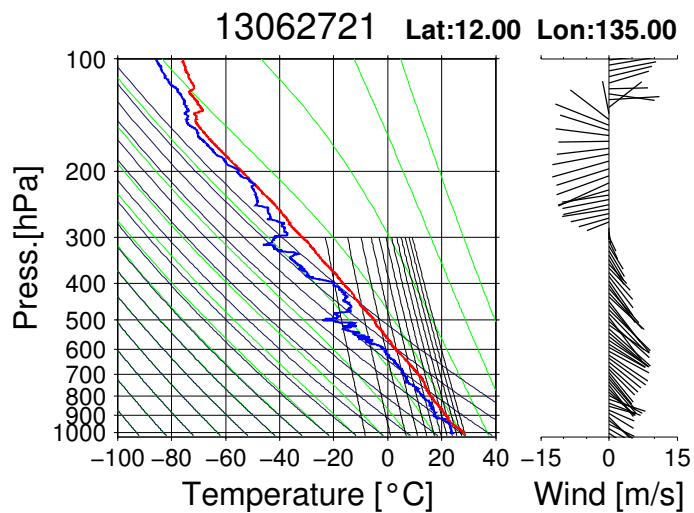
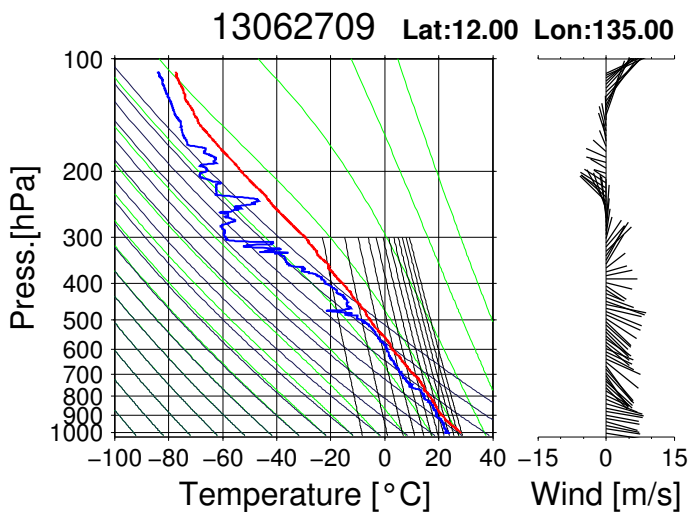
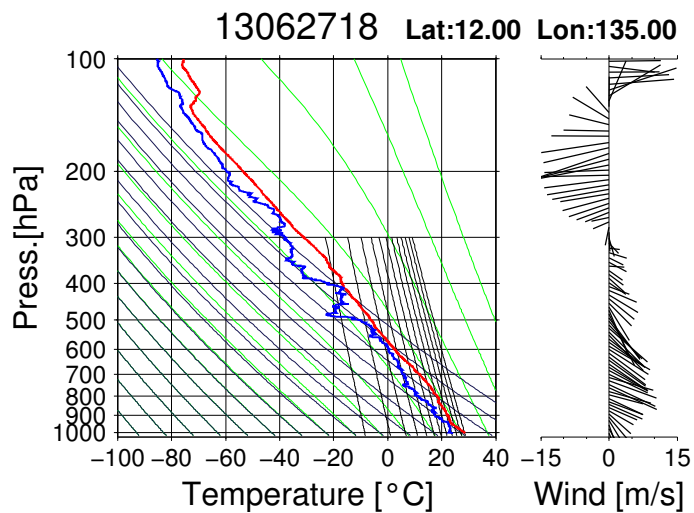
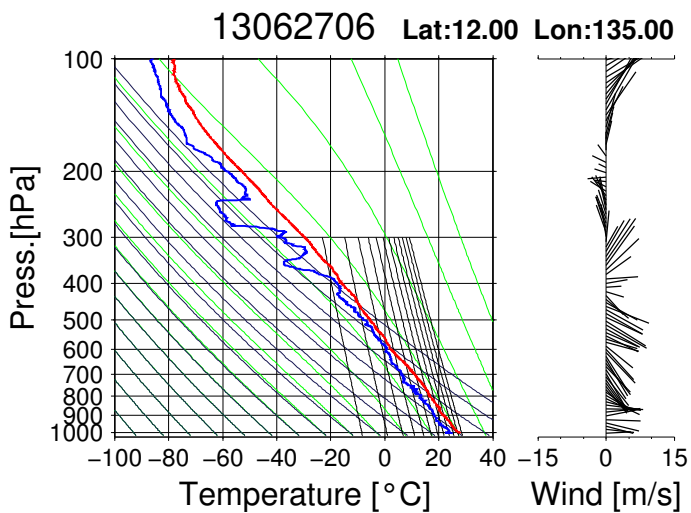
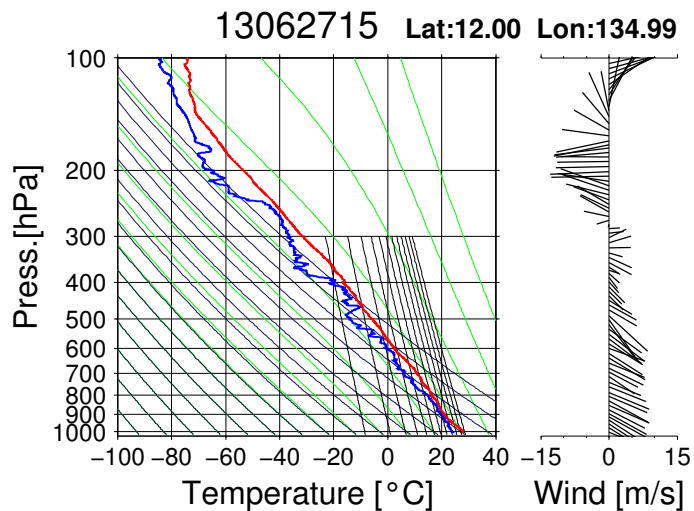
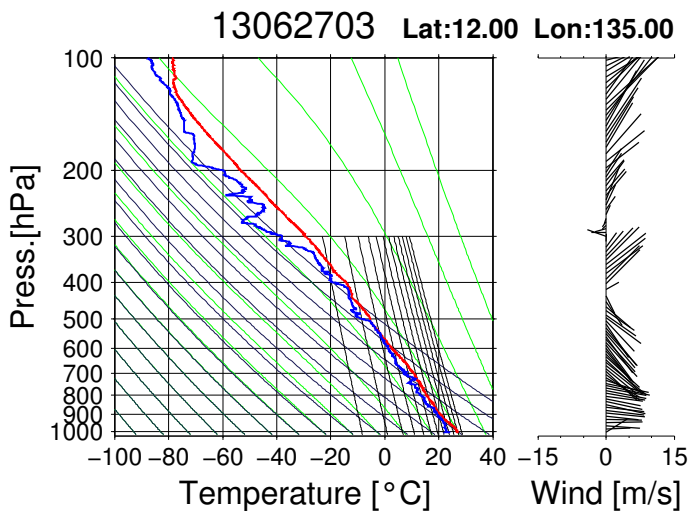
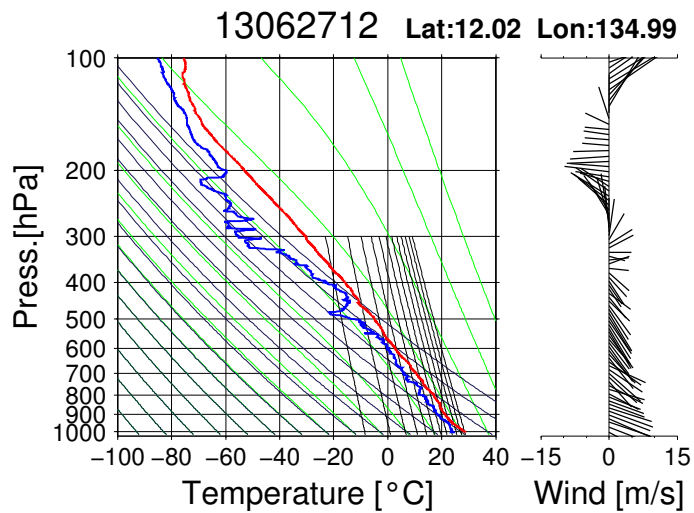
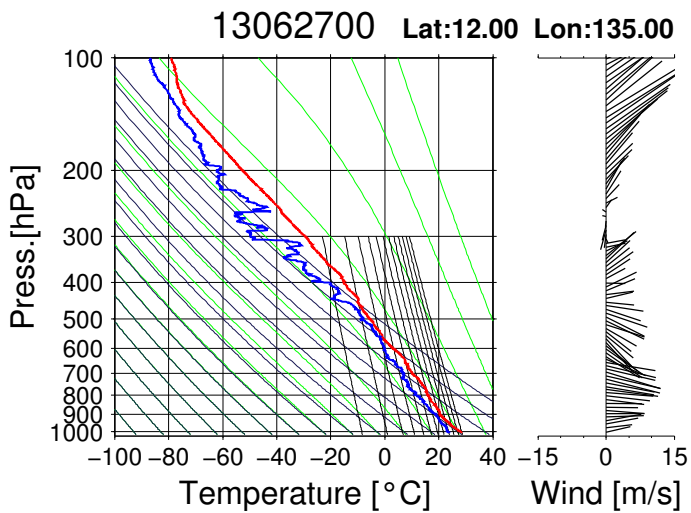


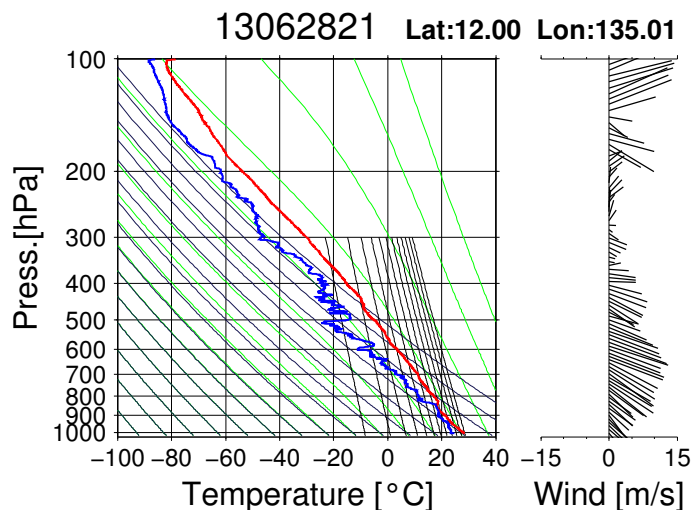
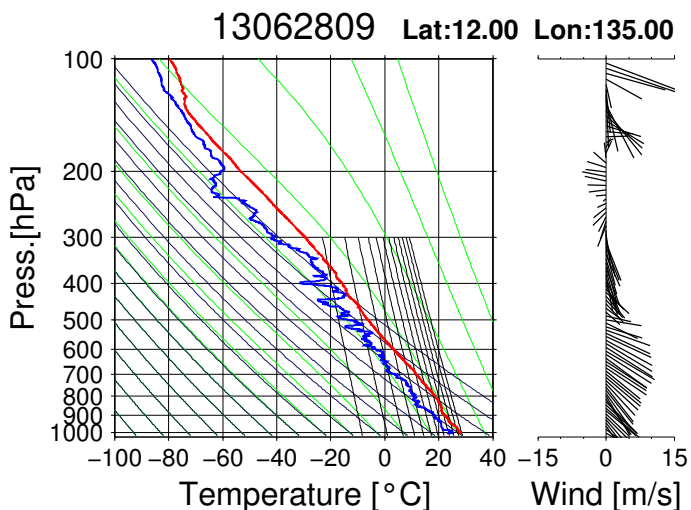
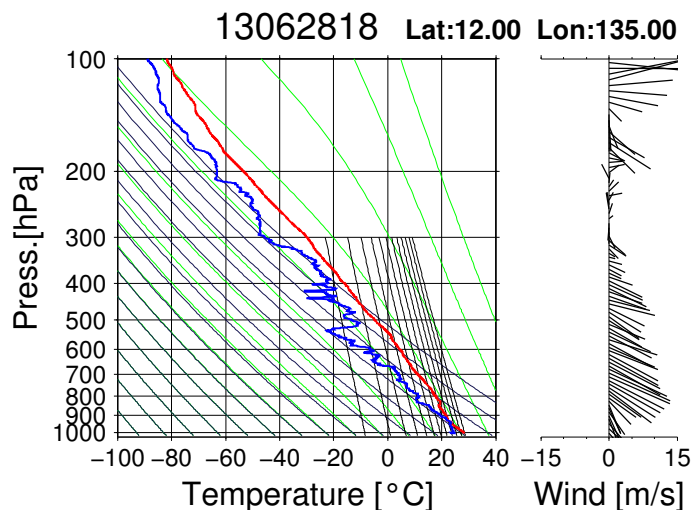
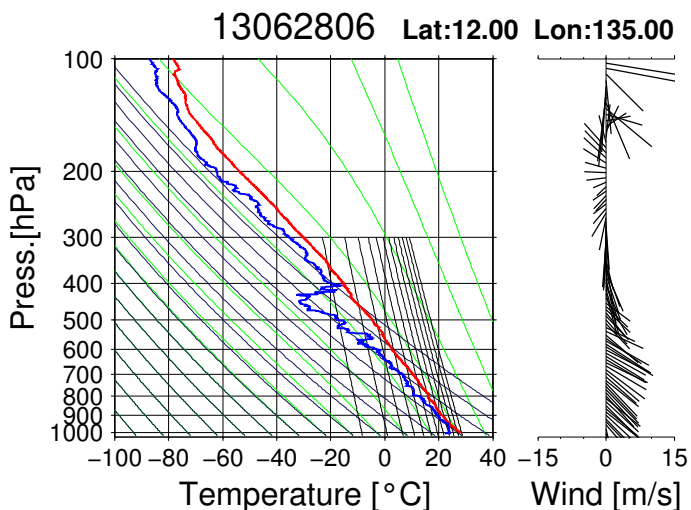
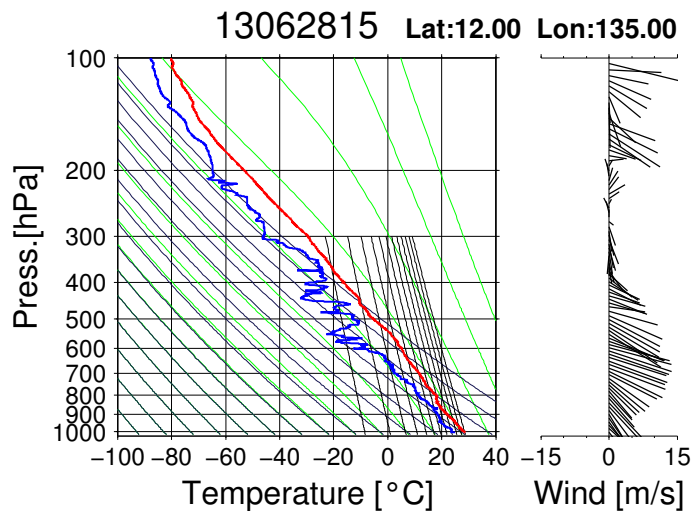
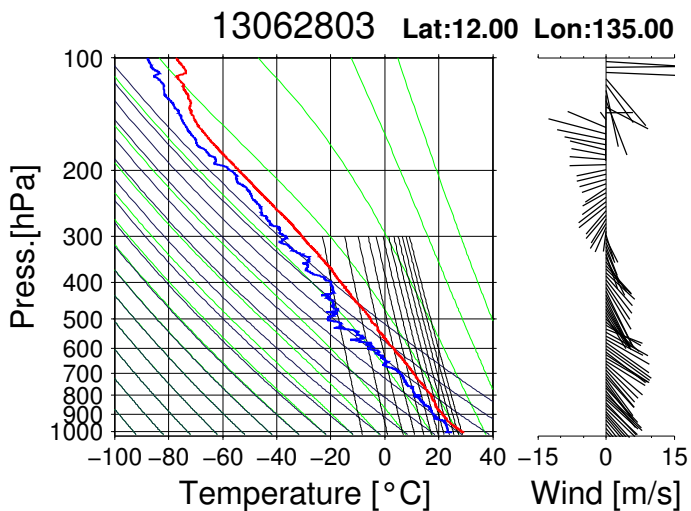
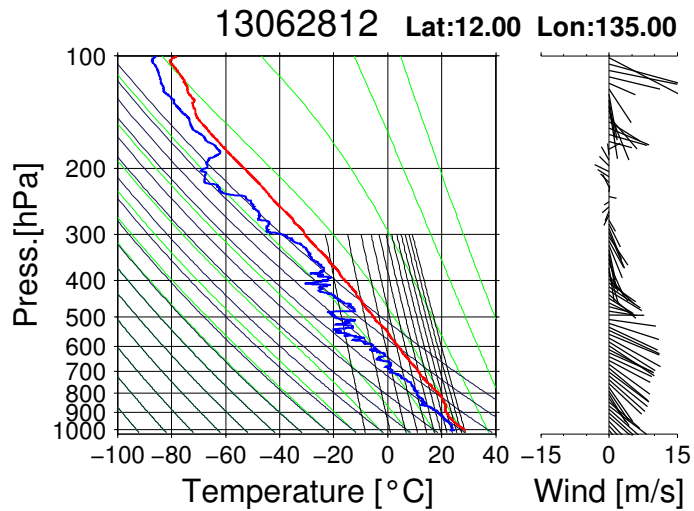
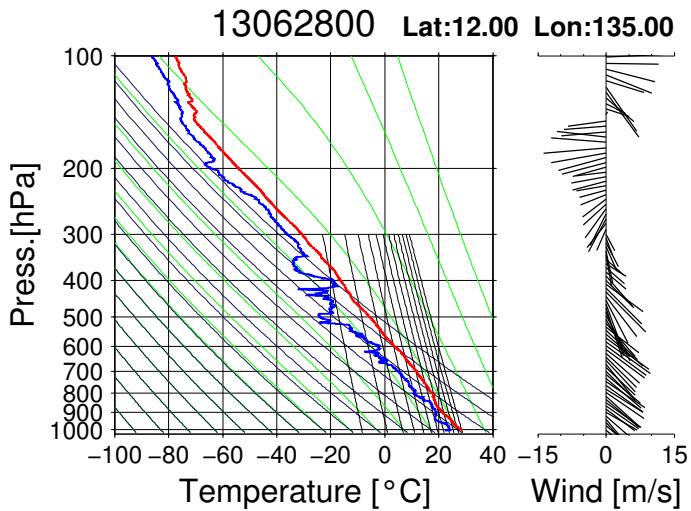


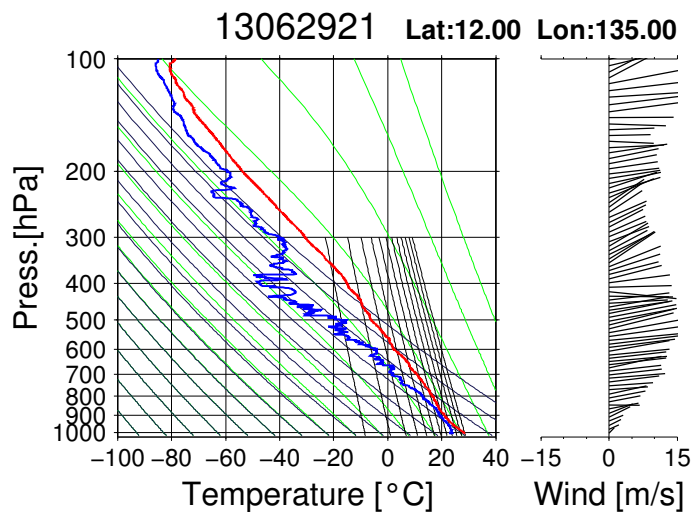
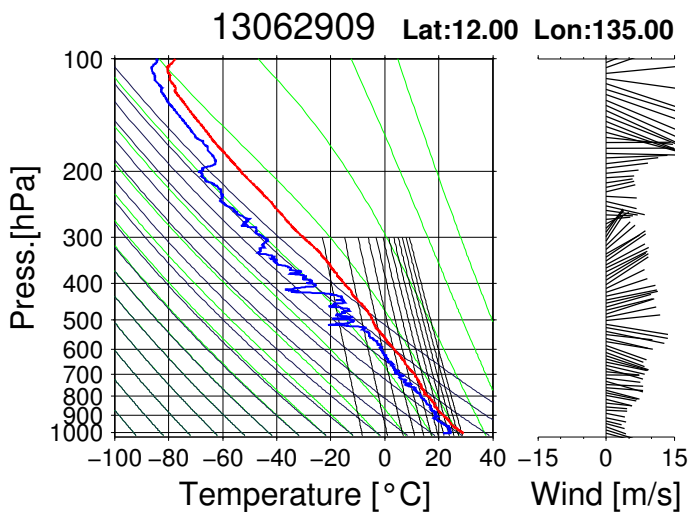
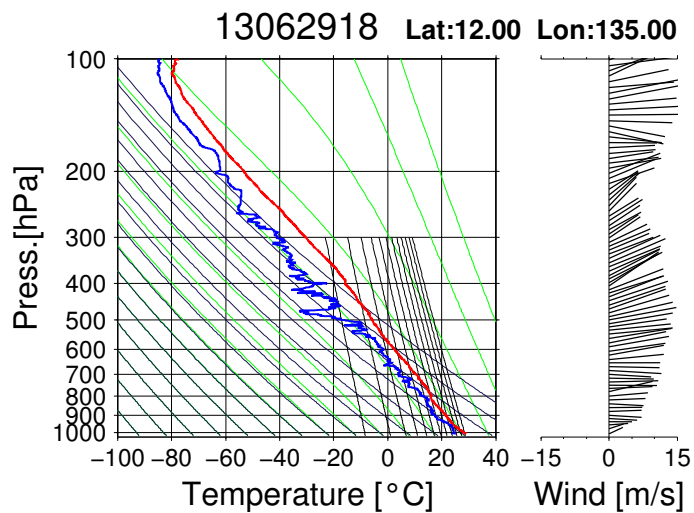
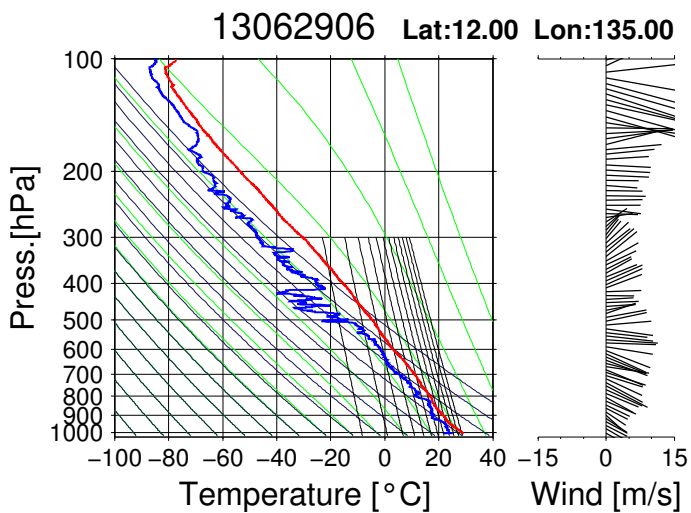
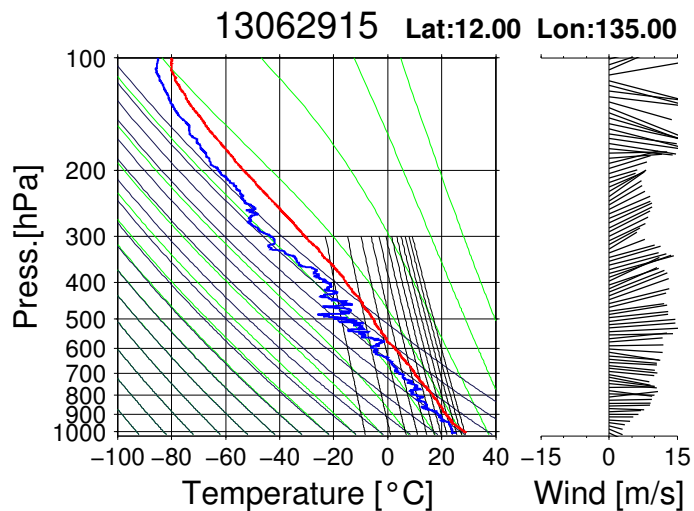
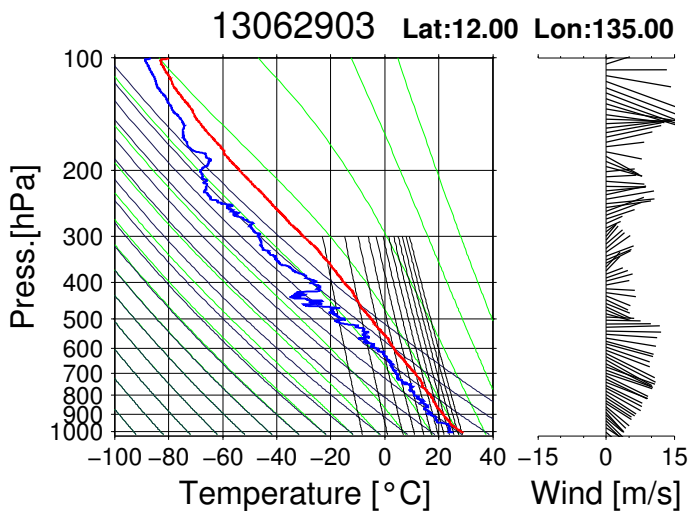
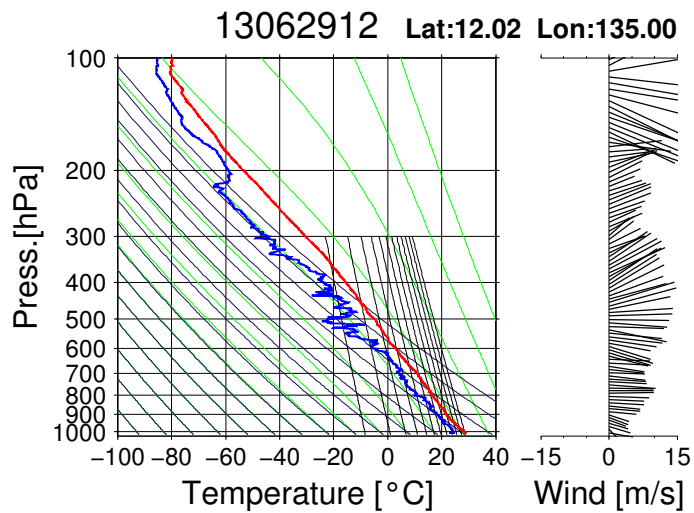
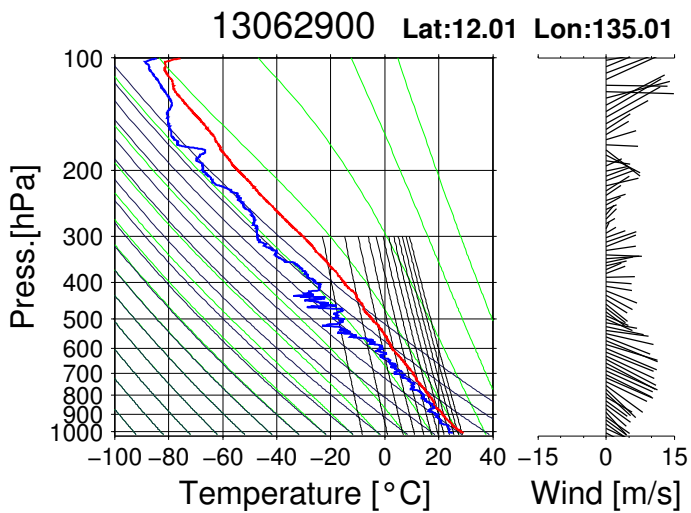


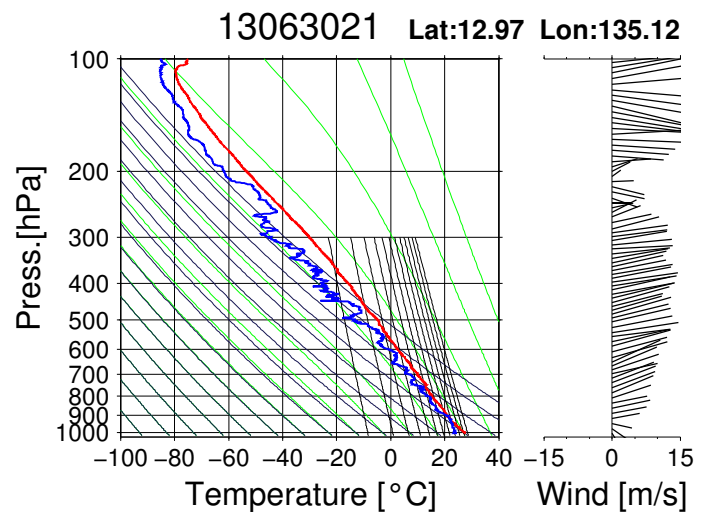
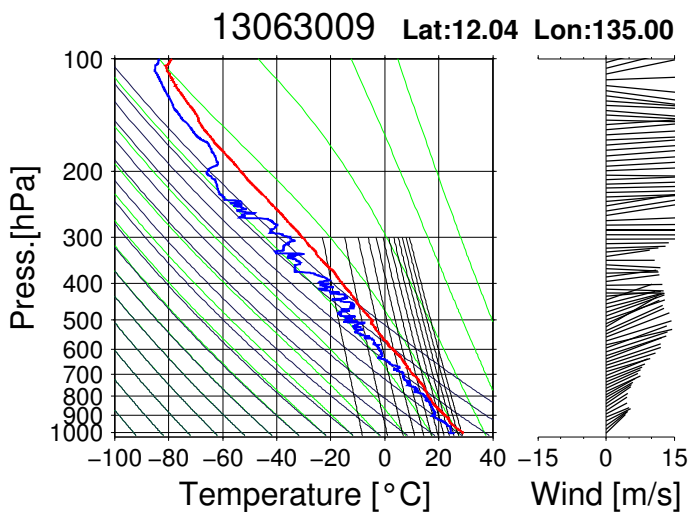
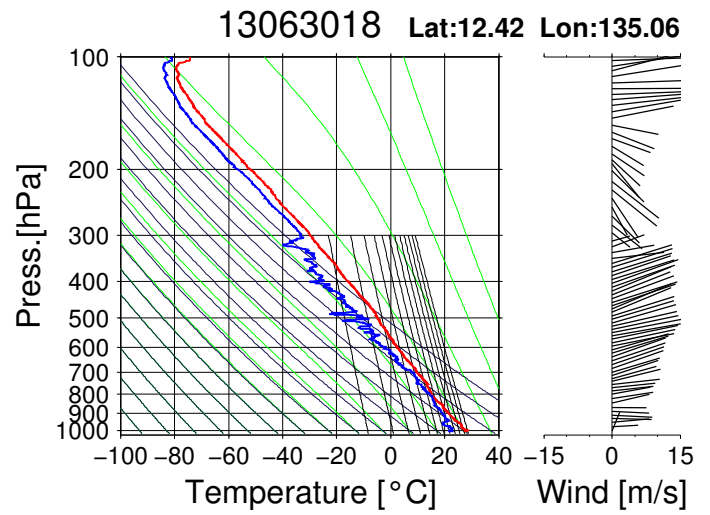
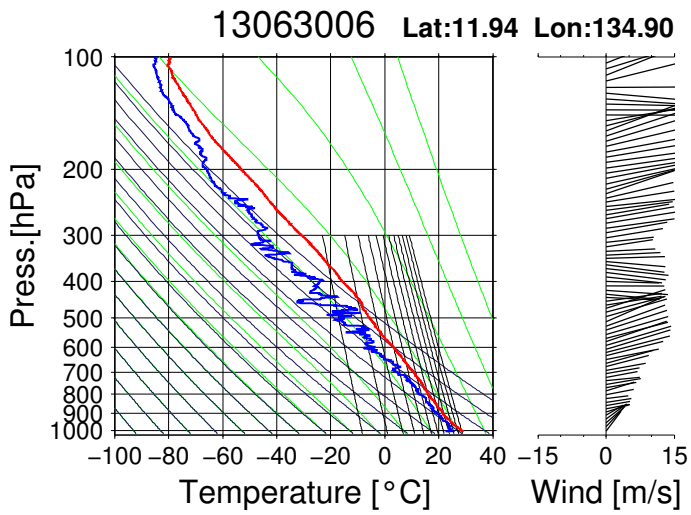
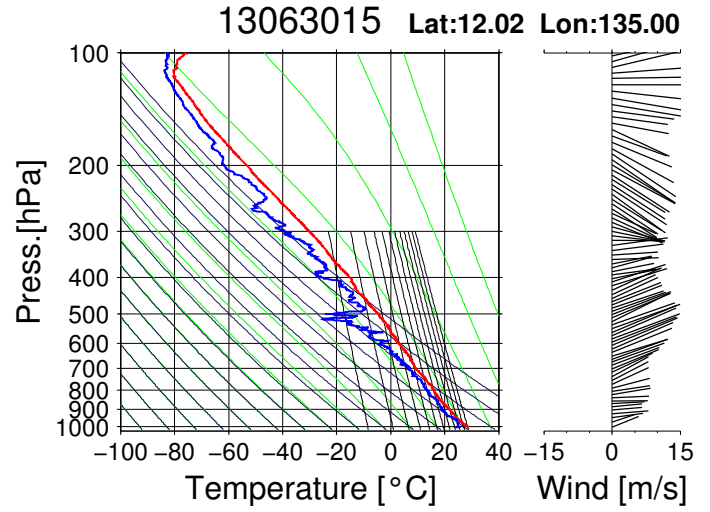
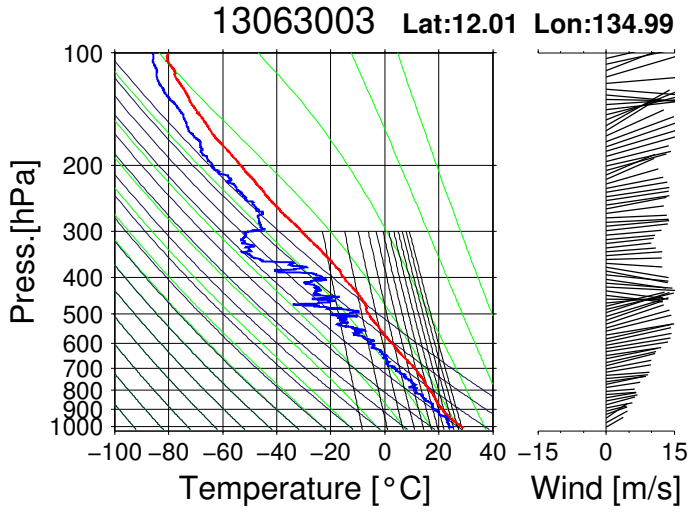
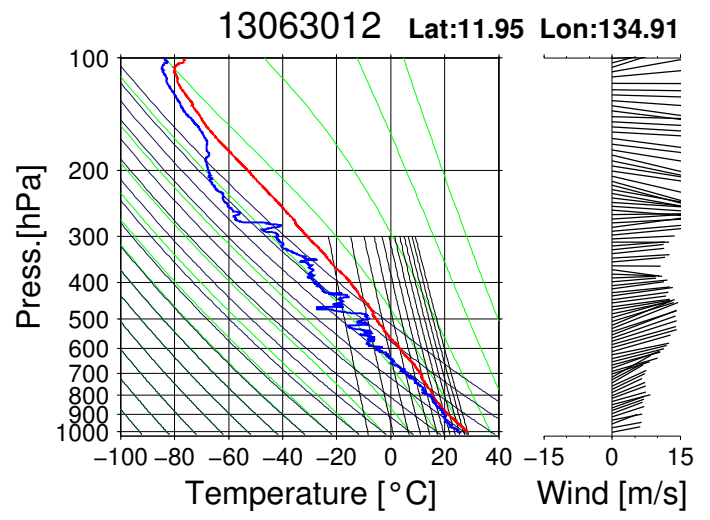
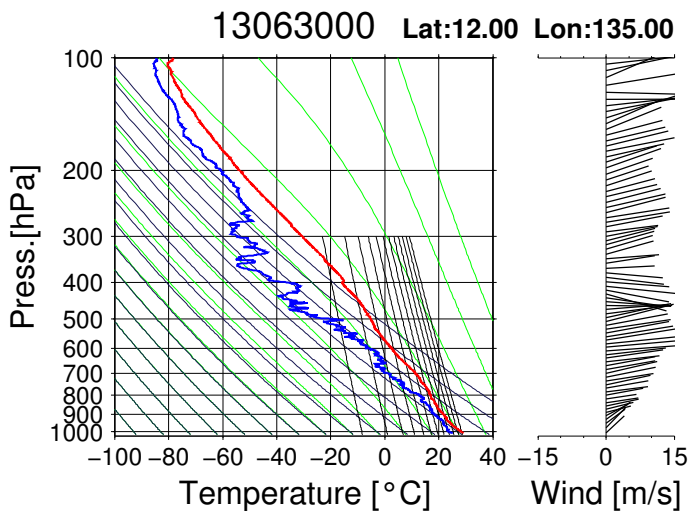


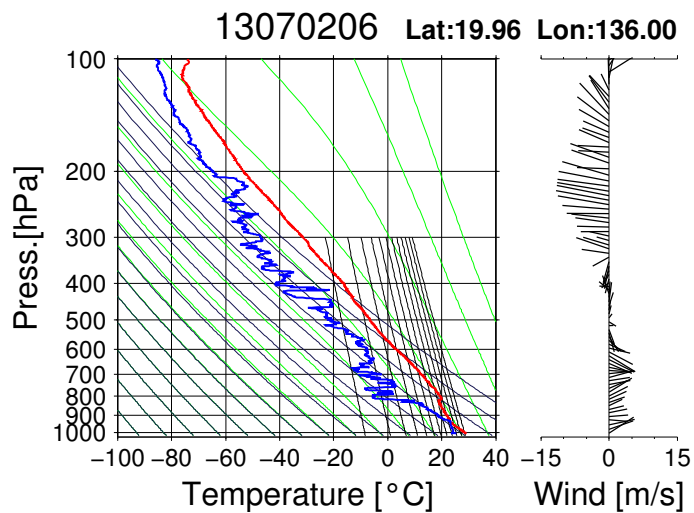
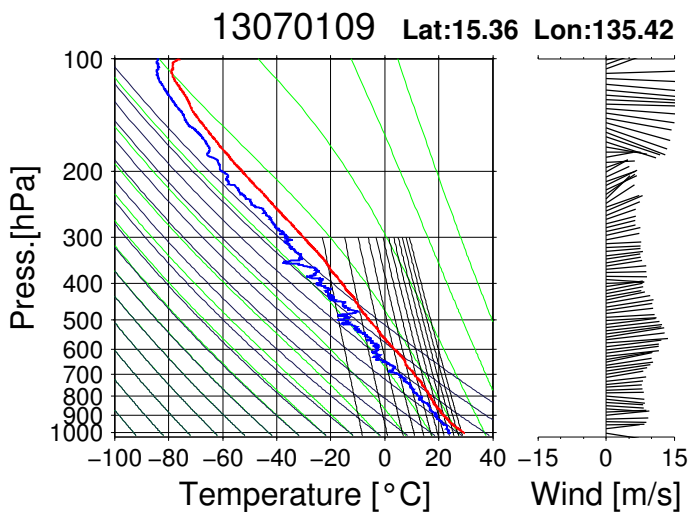
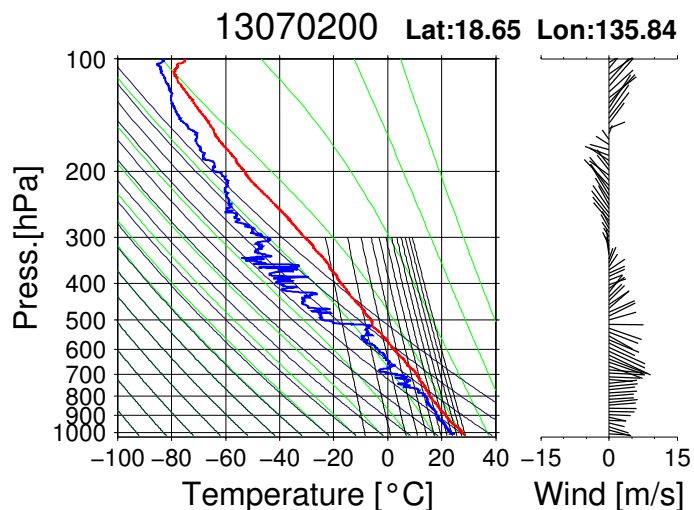
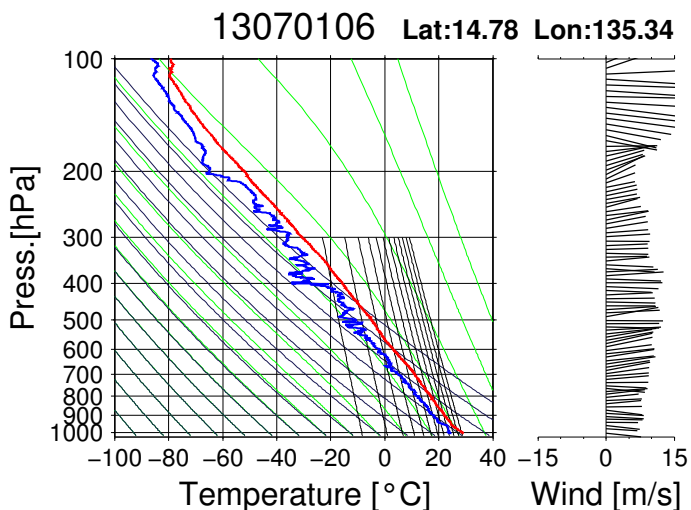
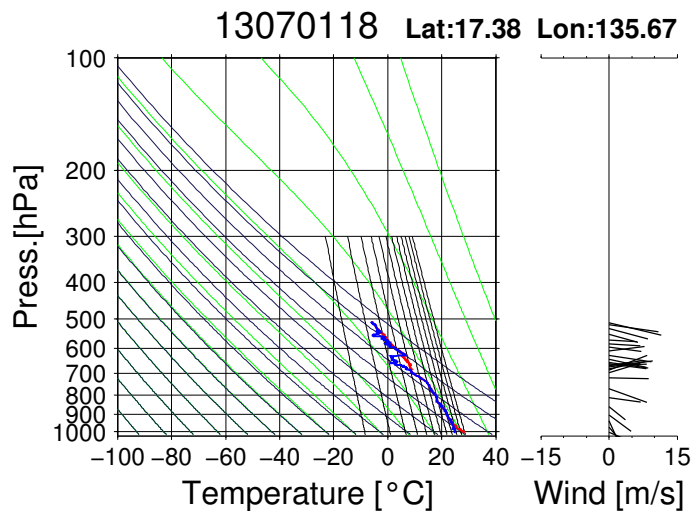
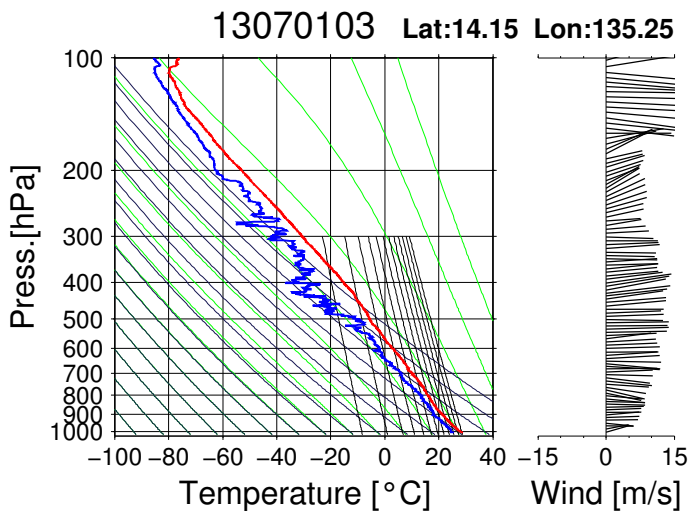
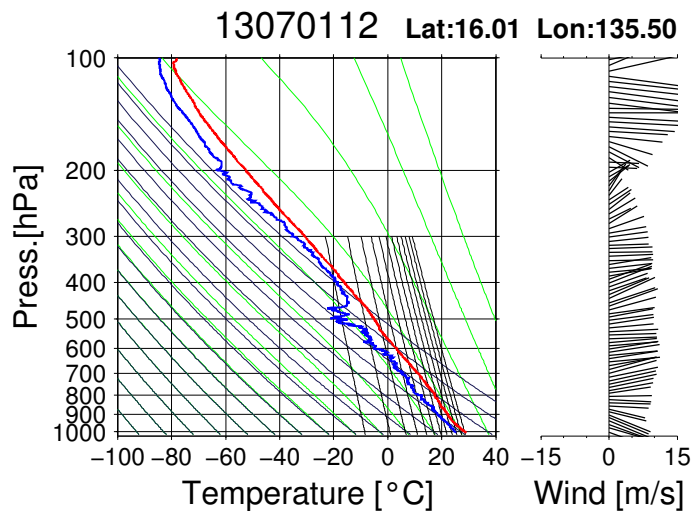
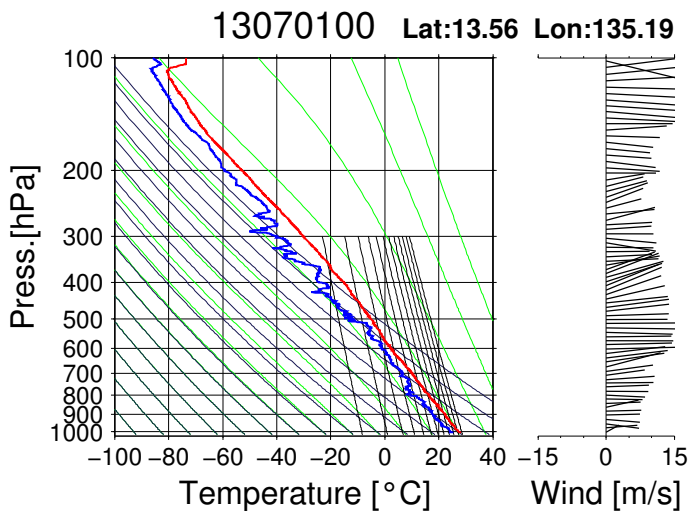




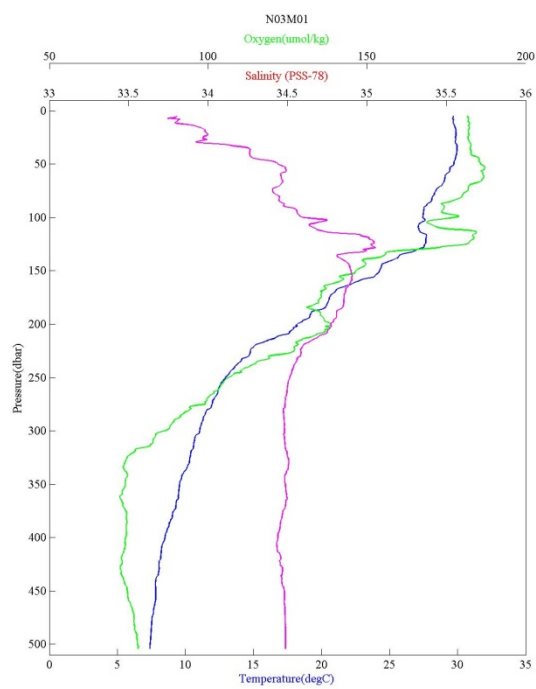
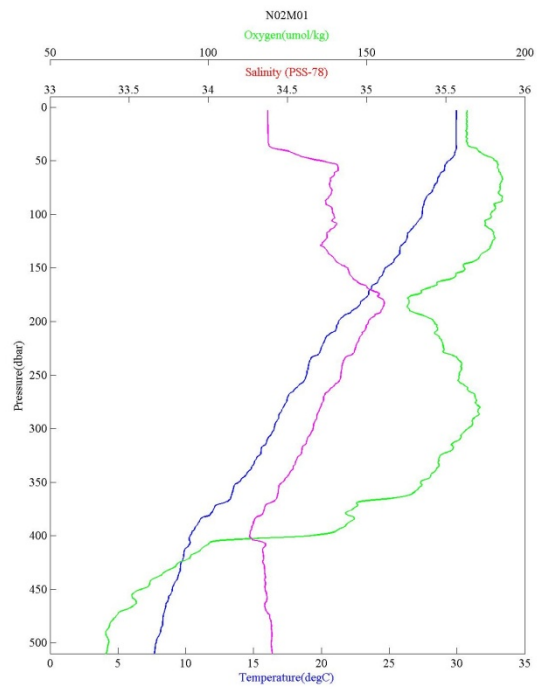
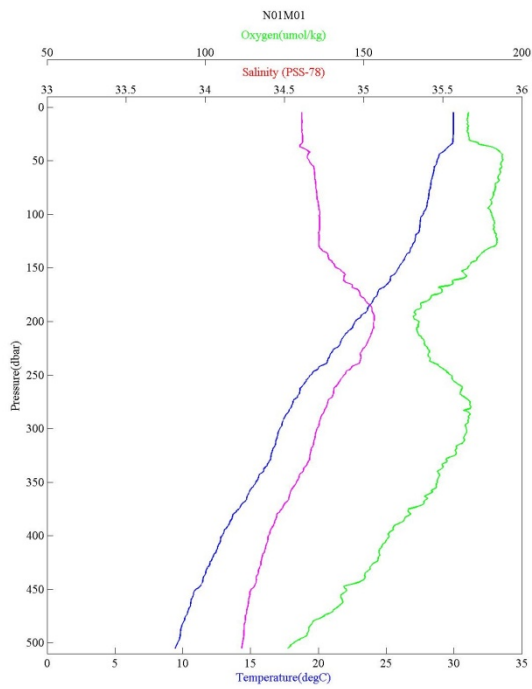




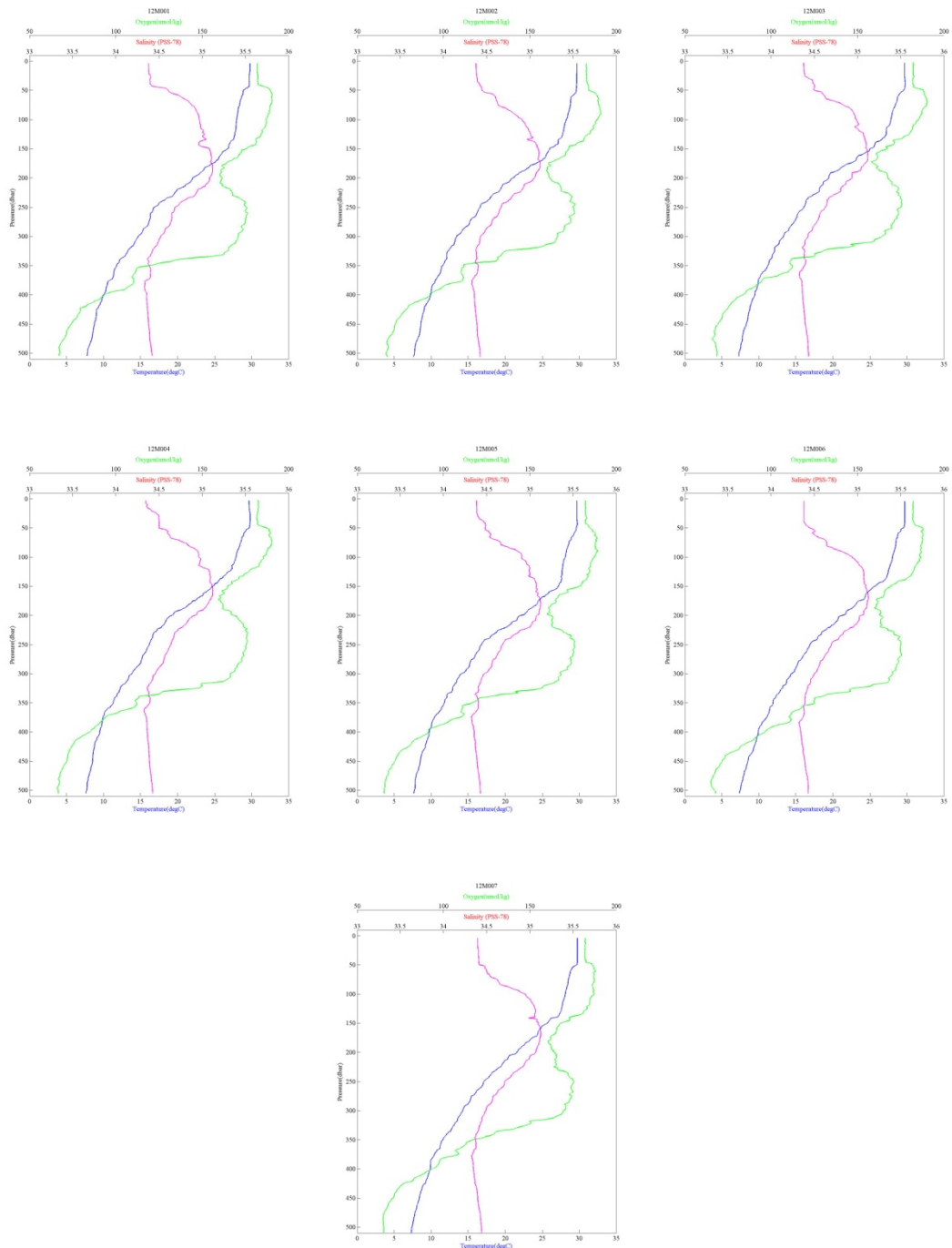




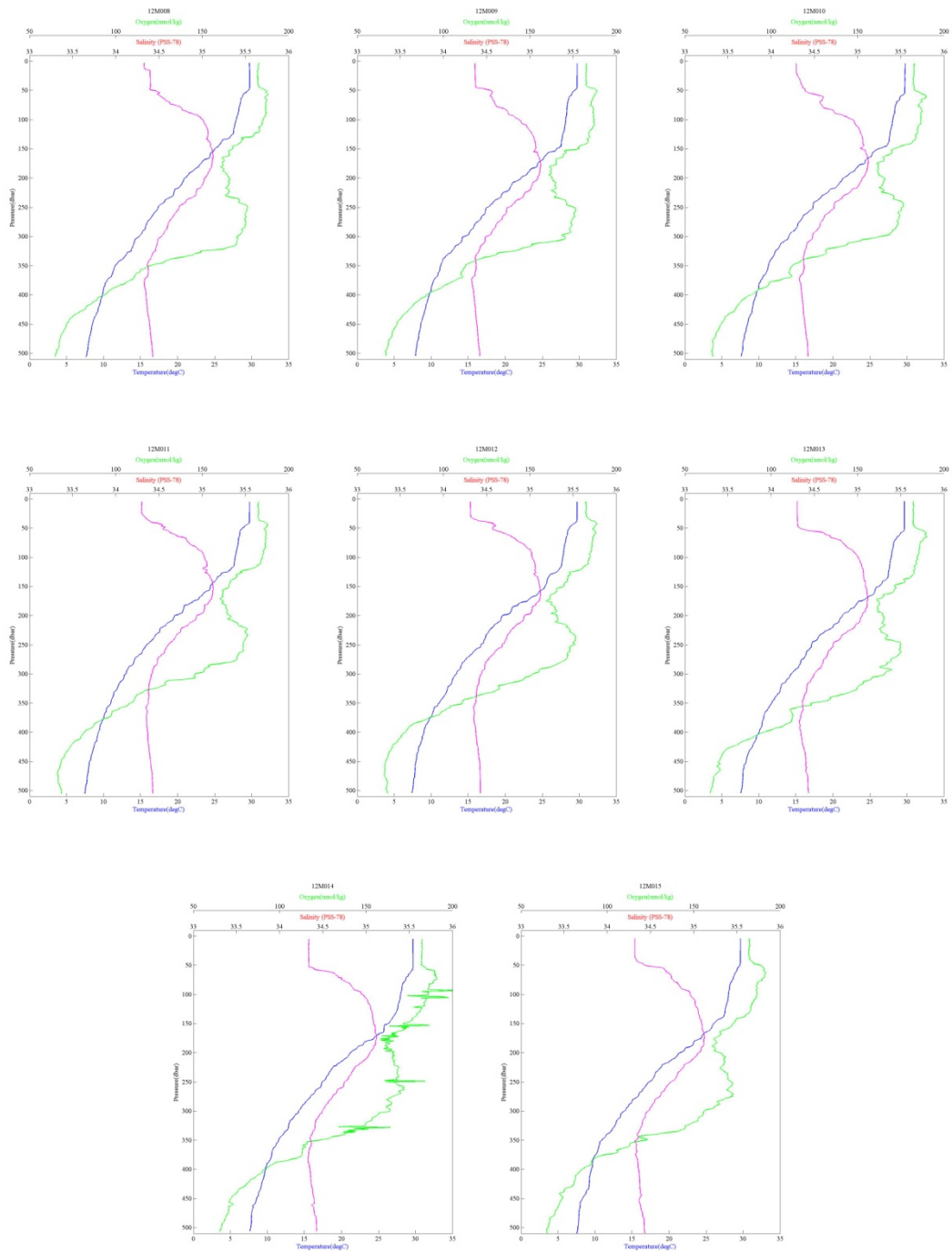
Appendix-B: Oceanic profiles by the CTDO observations



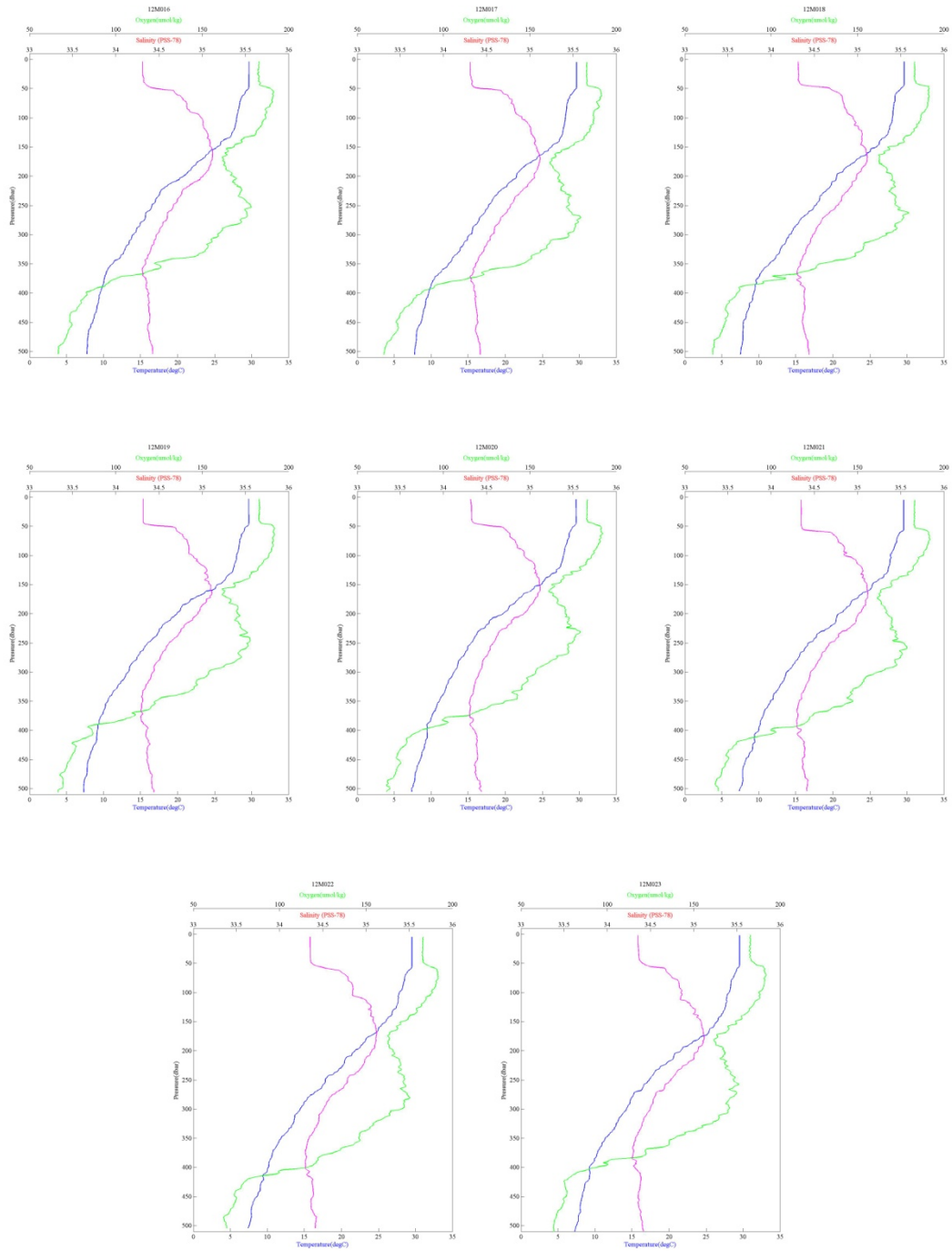
CTD profile (N01M01, N02M01 and N03M01)



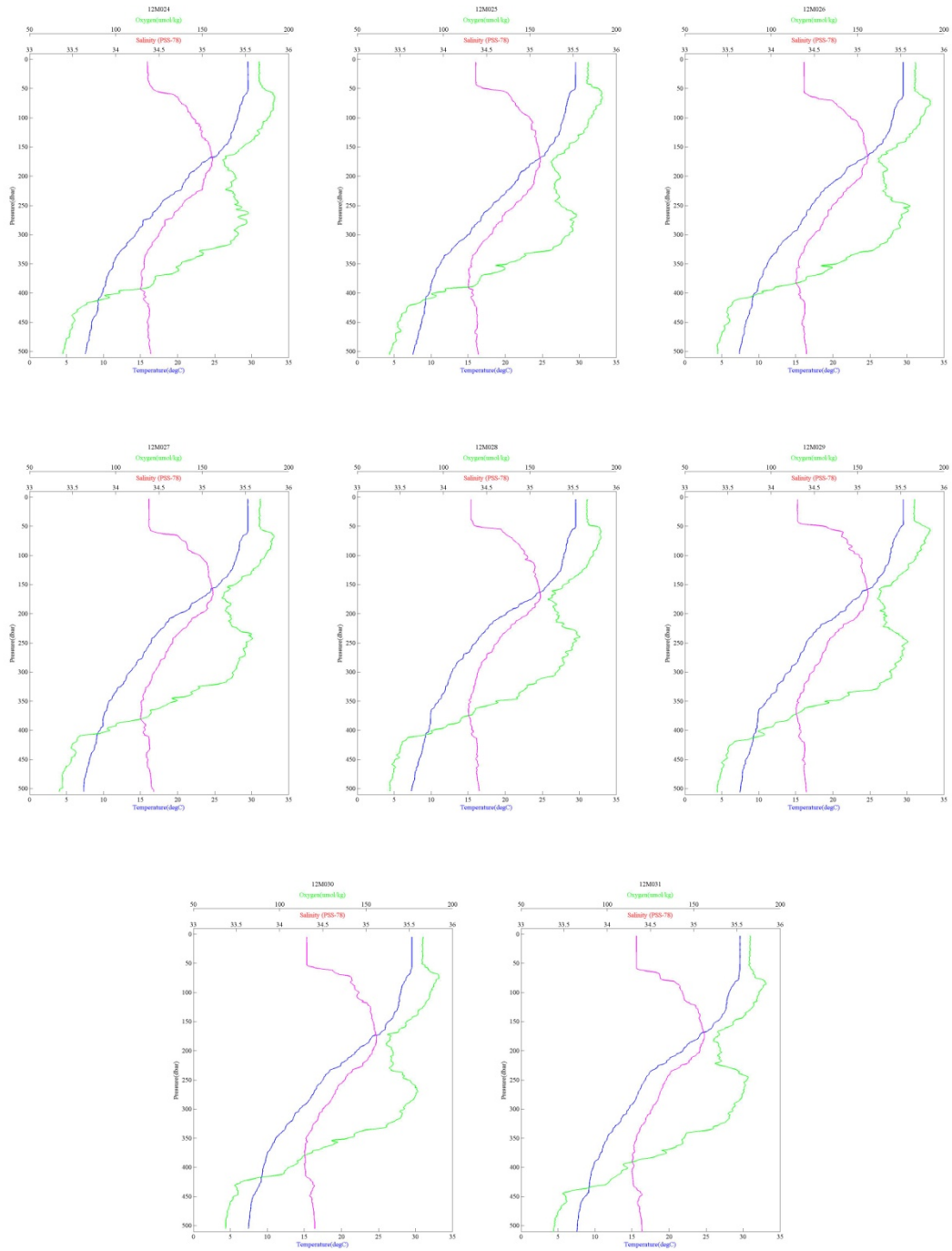
CTD profile (13 Jun 2013 casts)



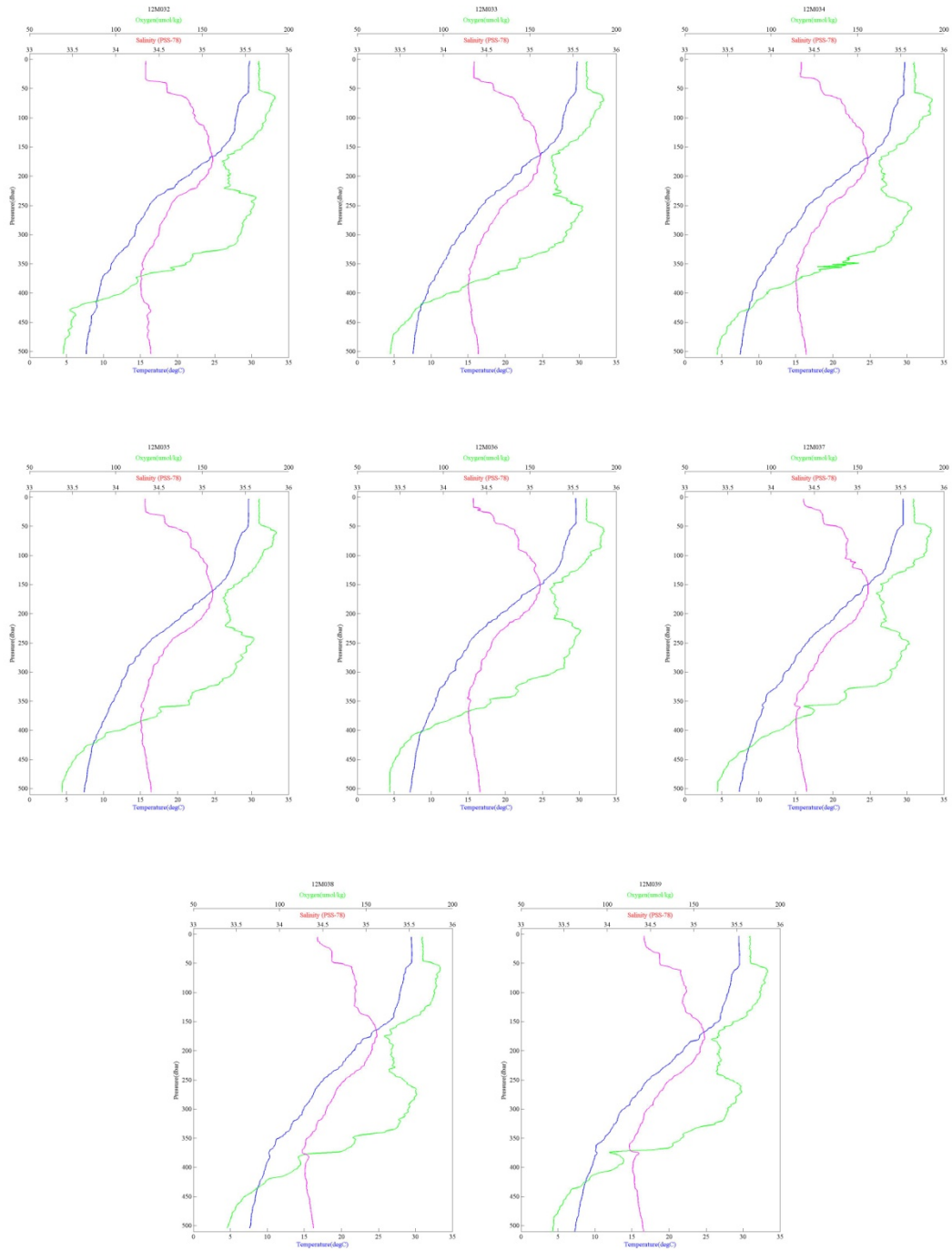
CTD profile (14 Jun 2013 casts)



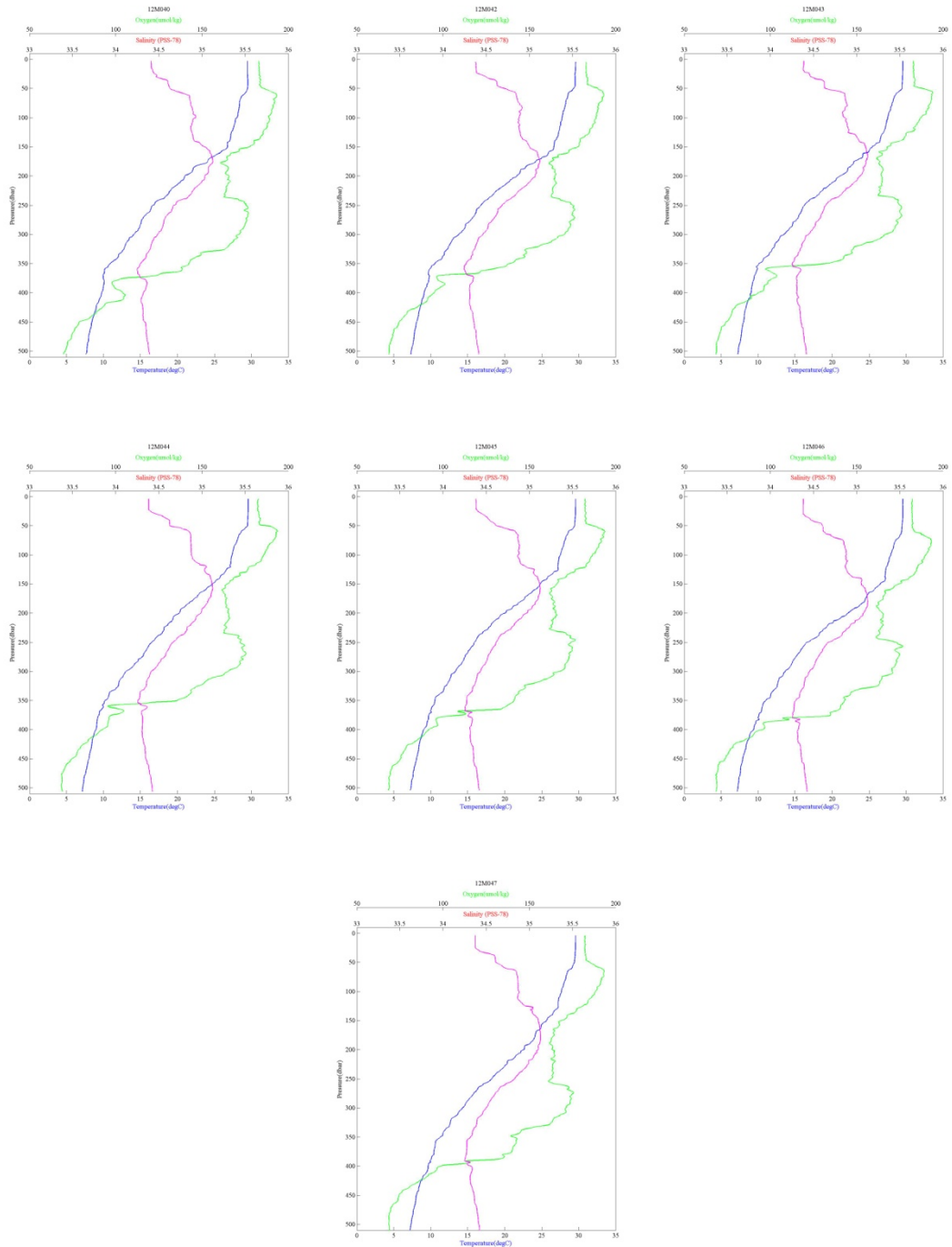
CTD profile (15 Jun 2013 casts)



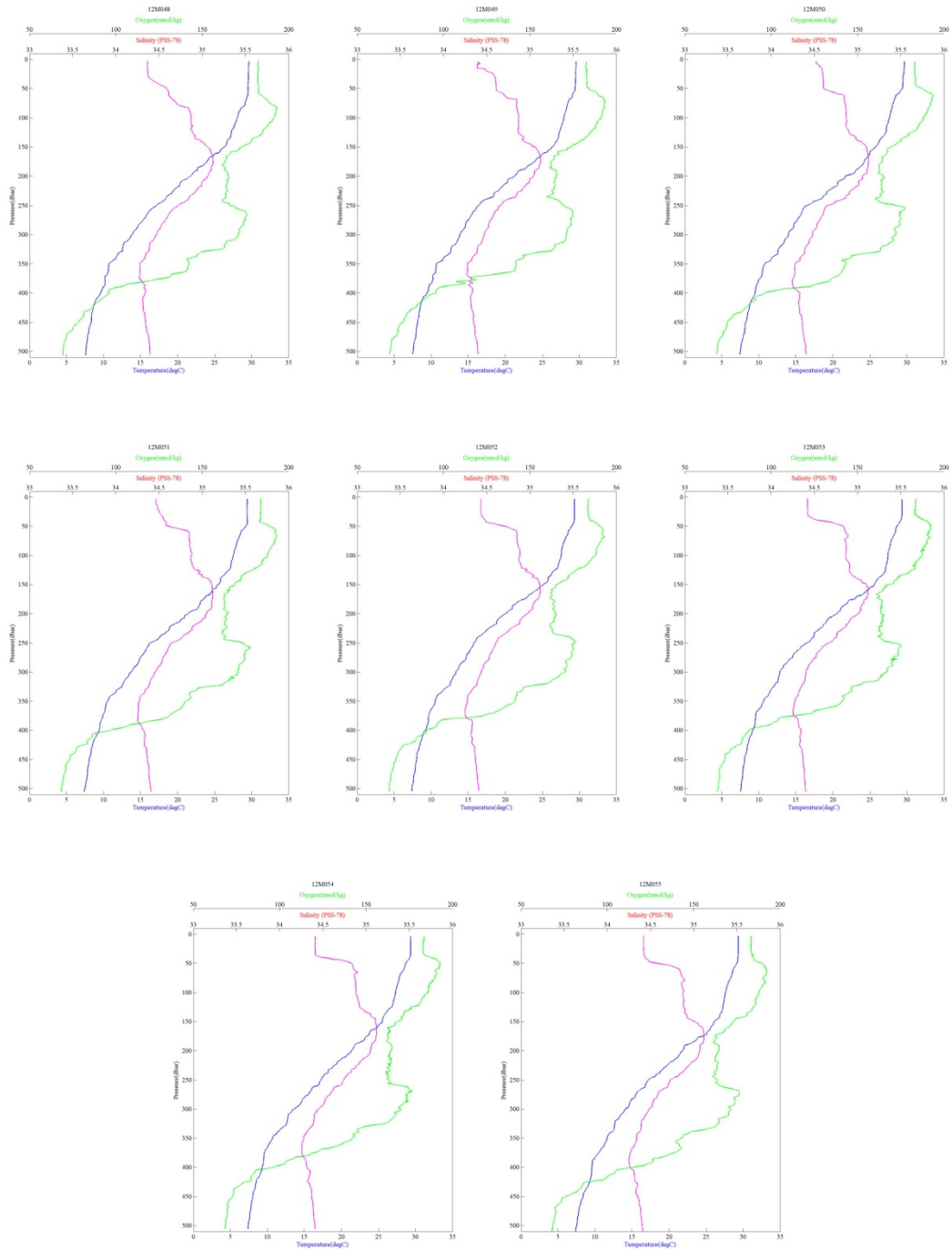
CTD profile (16 Jun 2013 casts)



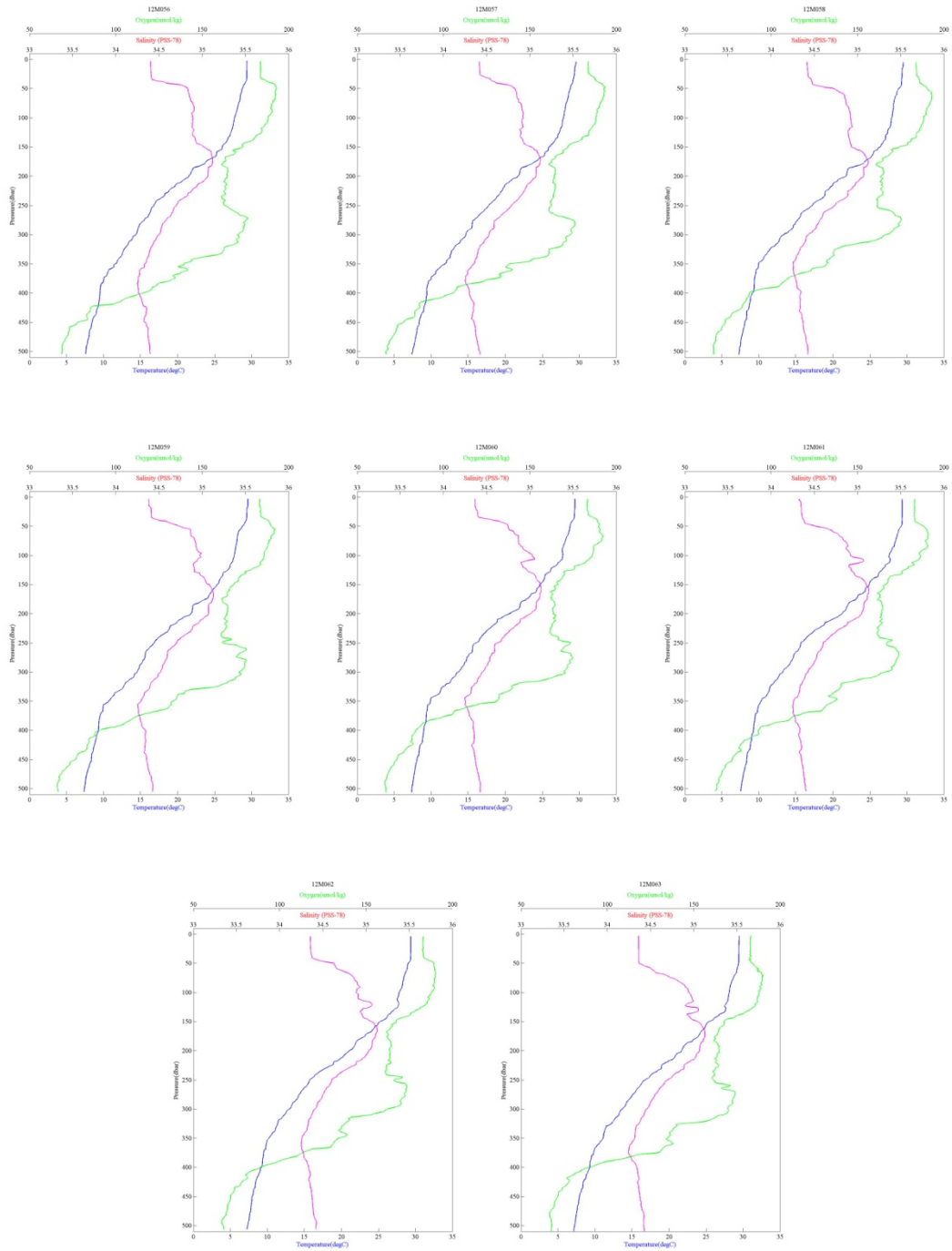
CTD profile (17 Jun 2013 casts)



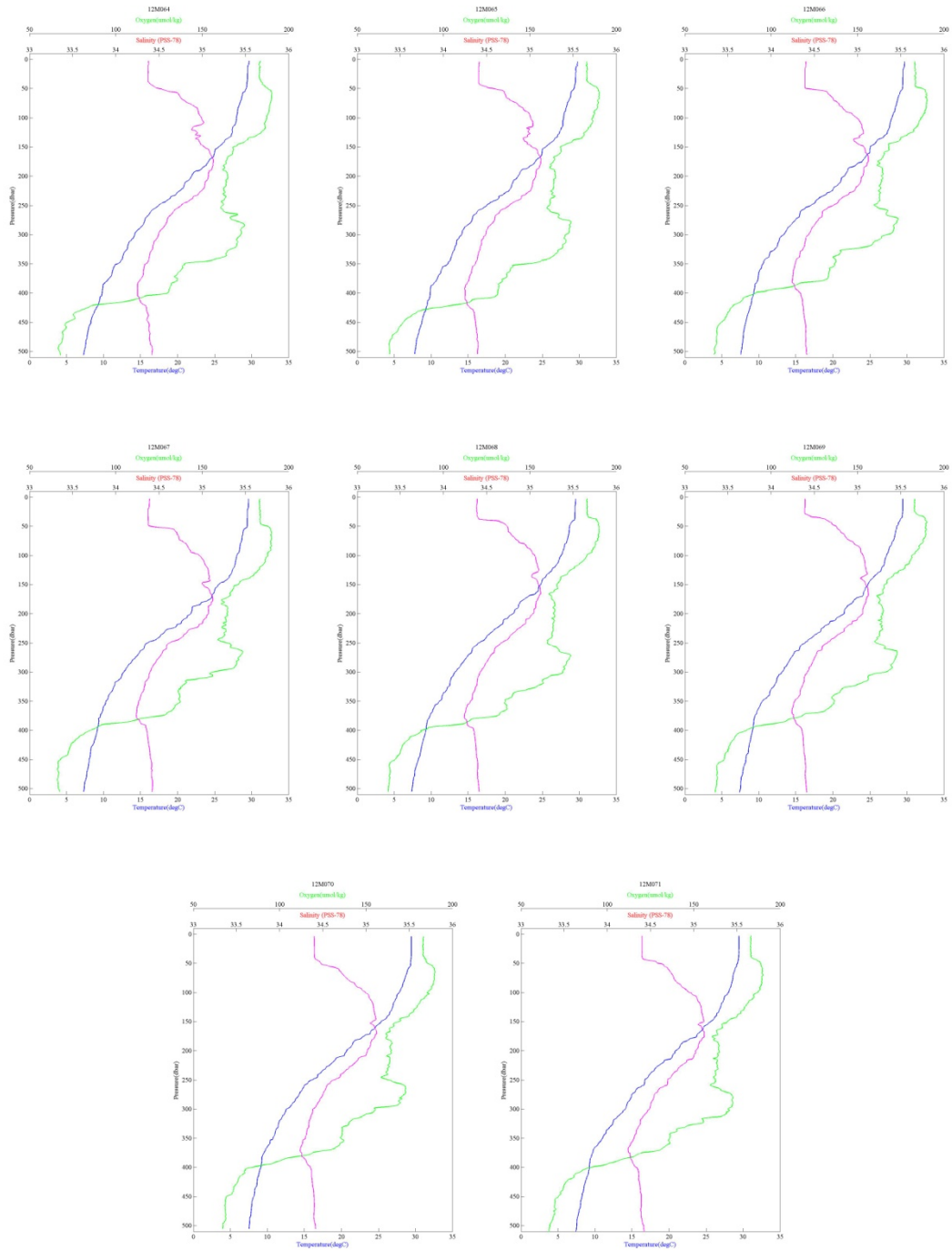
CTD profile (18 Jun 2013 casts)



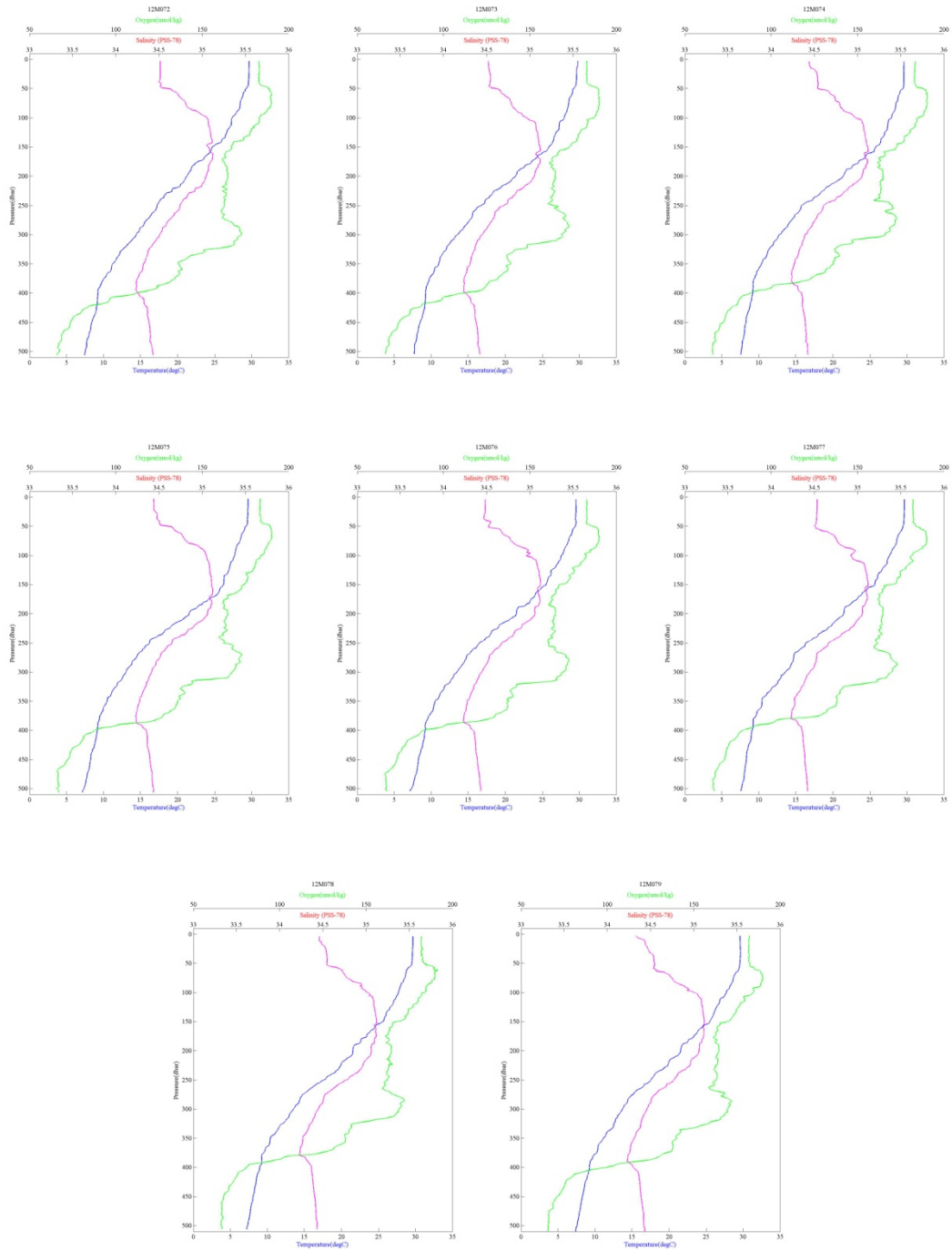
CTD profile (19 Jun 2013 casts)



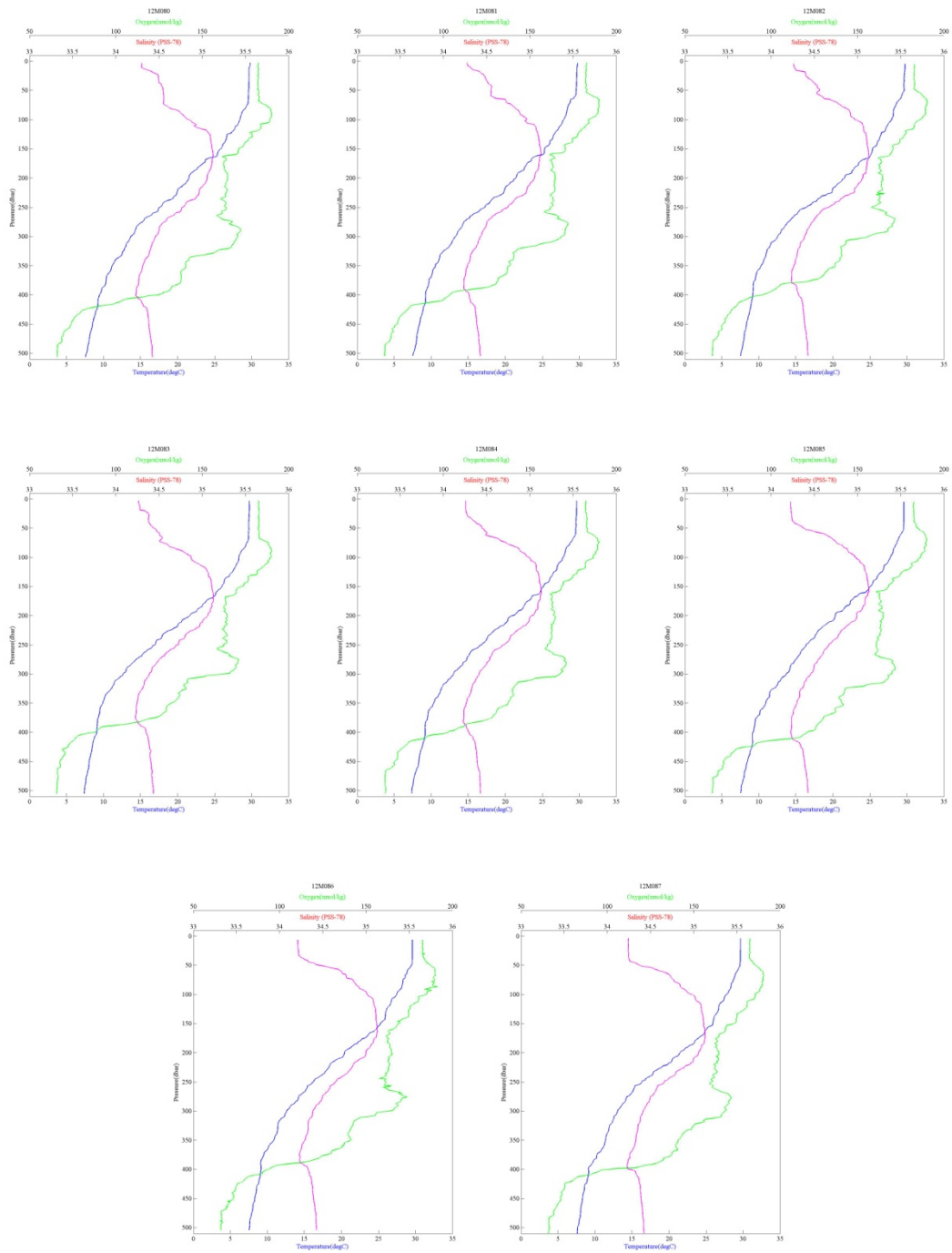
CTD profile (20 Jun 2013 casts)



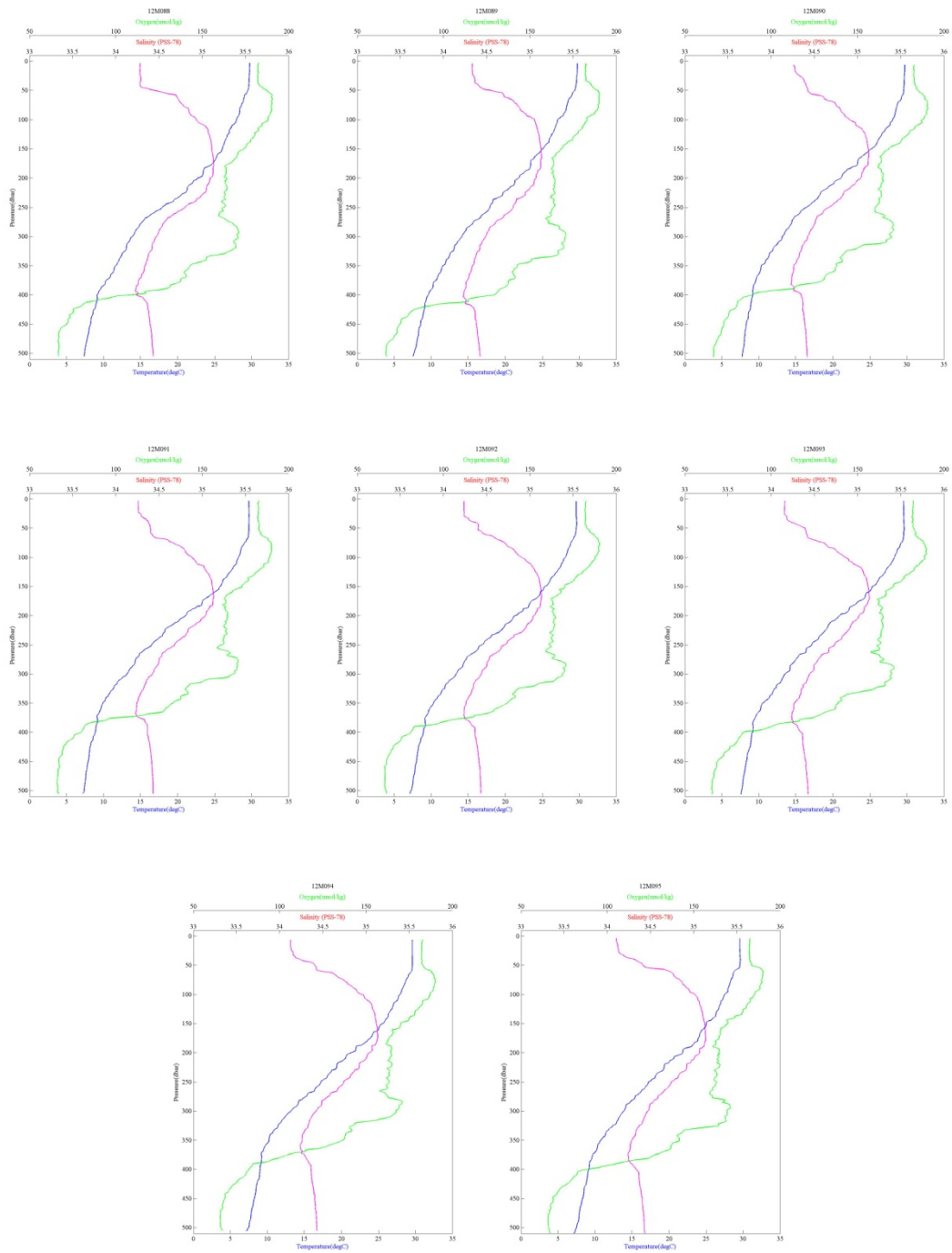
CTD profile (21 Jun 2013 casts)



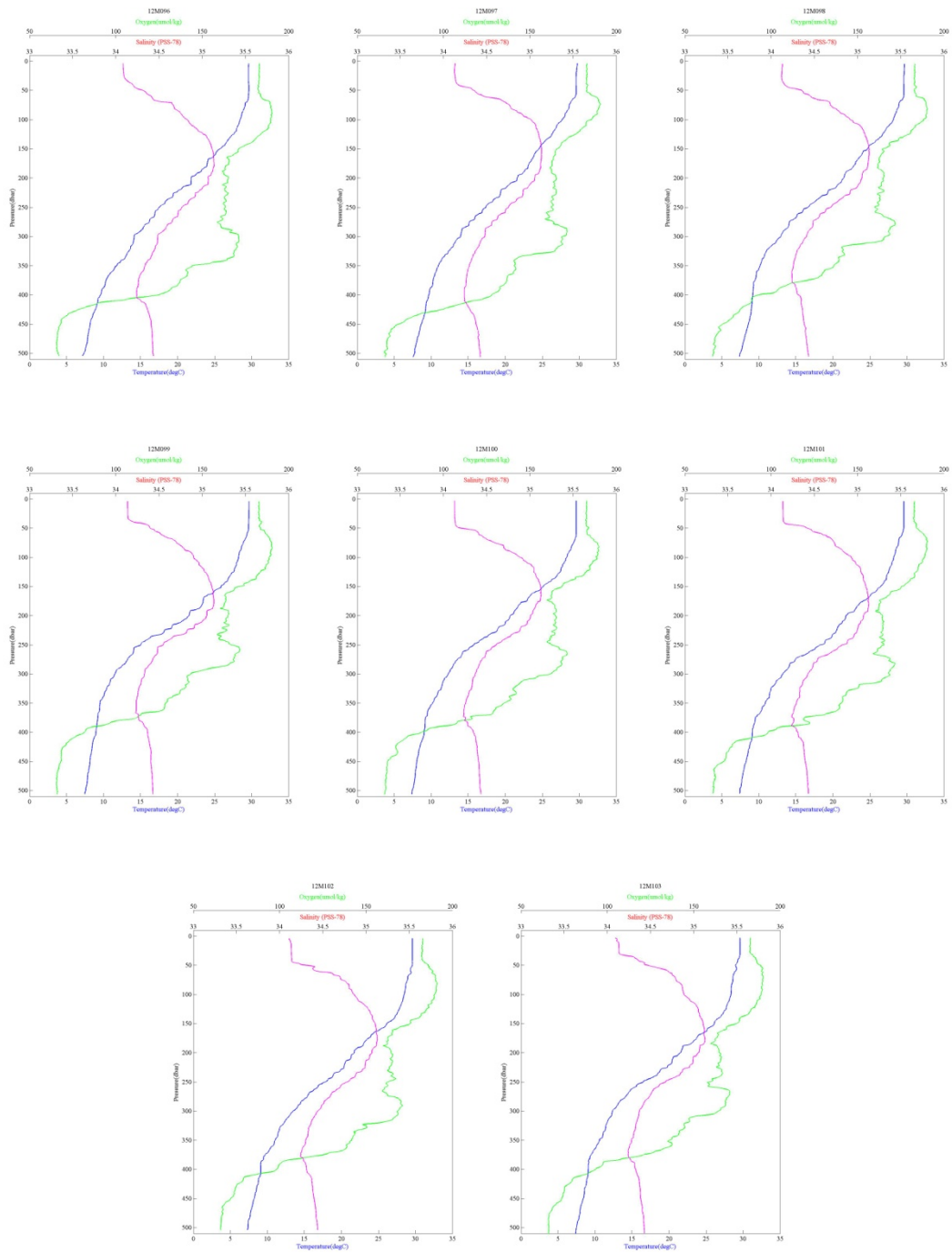
CTD profile (22 Jun 2013 casts)



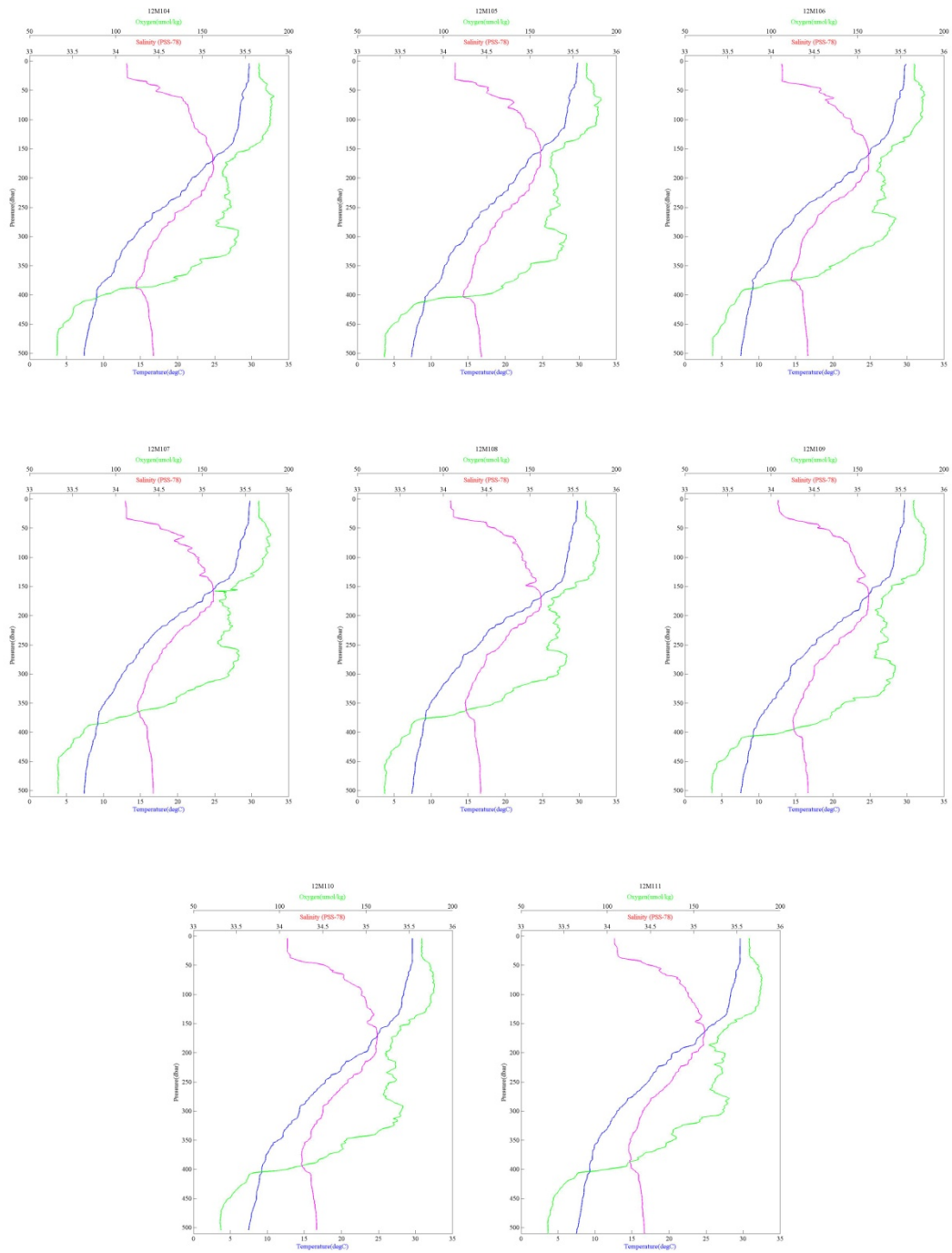
CTD profile (23 Jun 2013 casts)



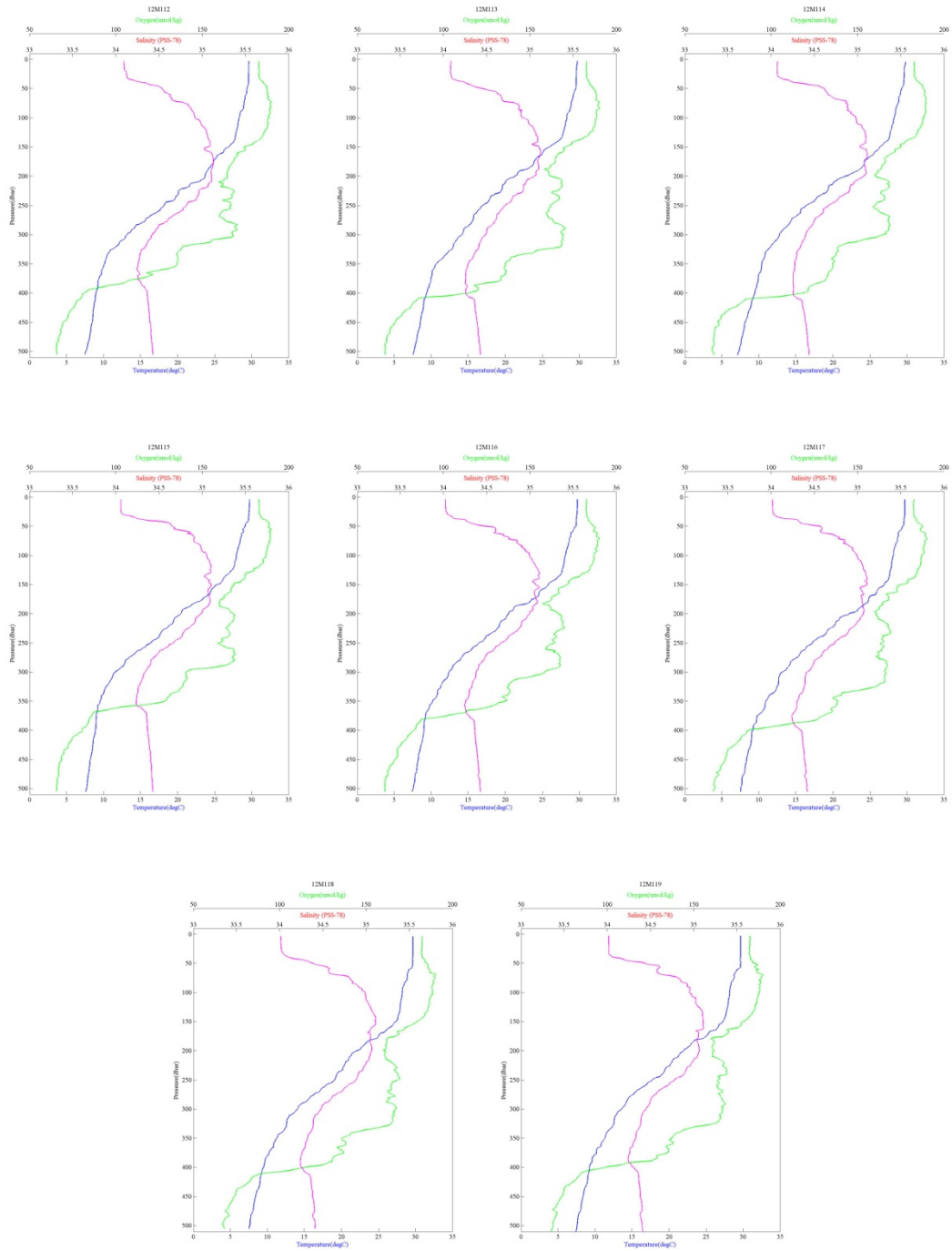
CTD profile (24 Jun 2013 casts)



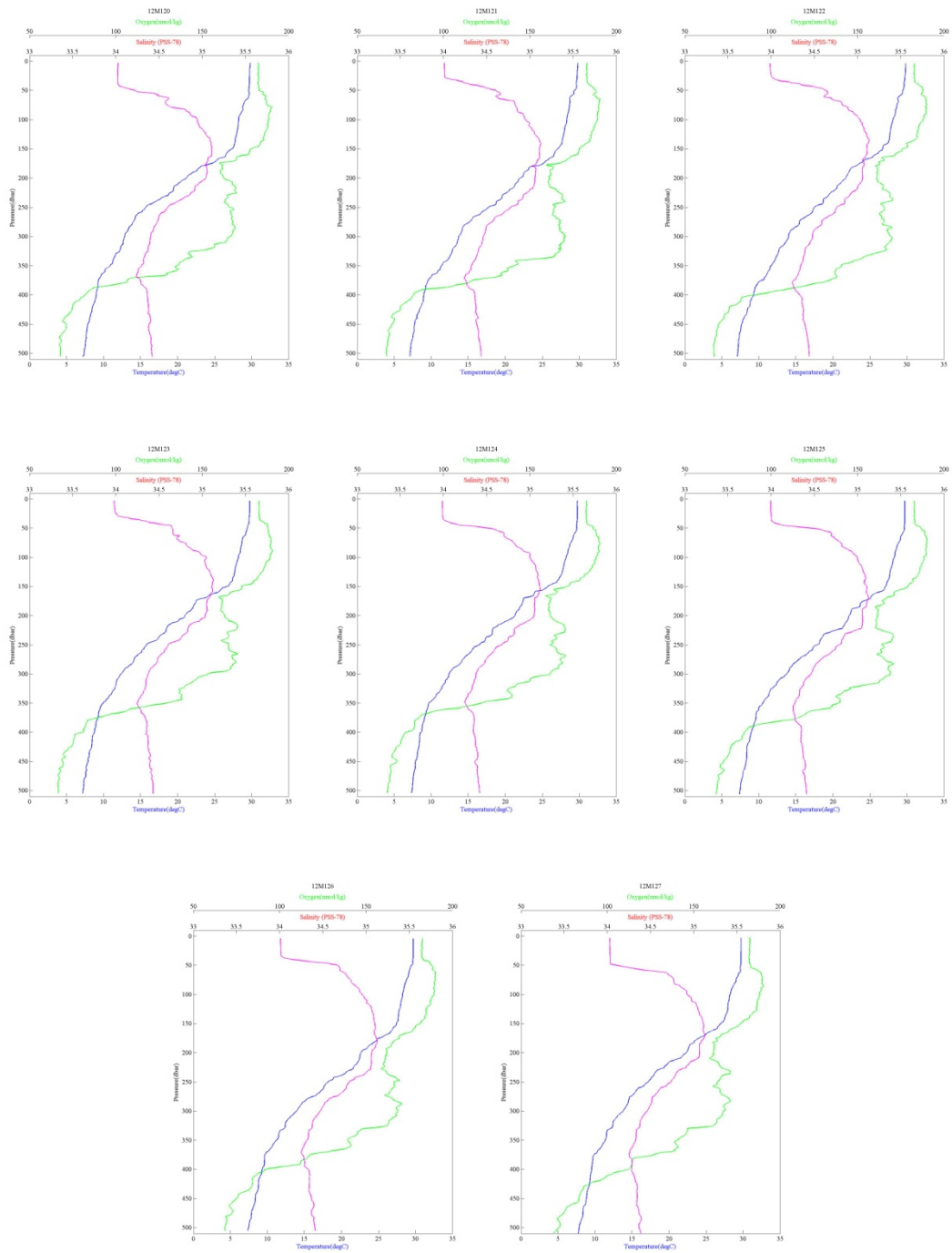
CTD profile (25 Jun 2013 casts)



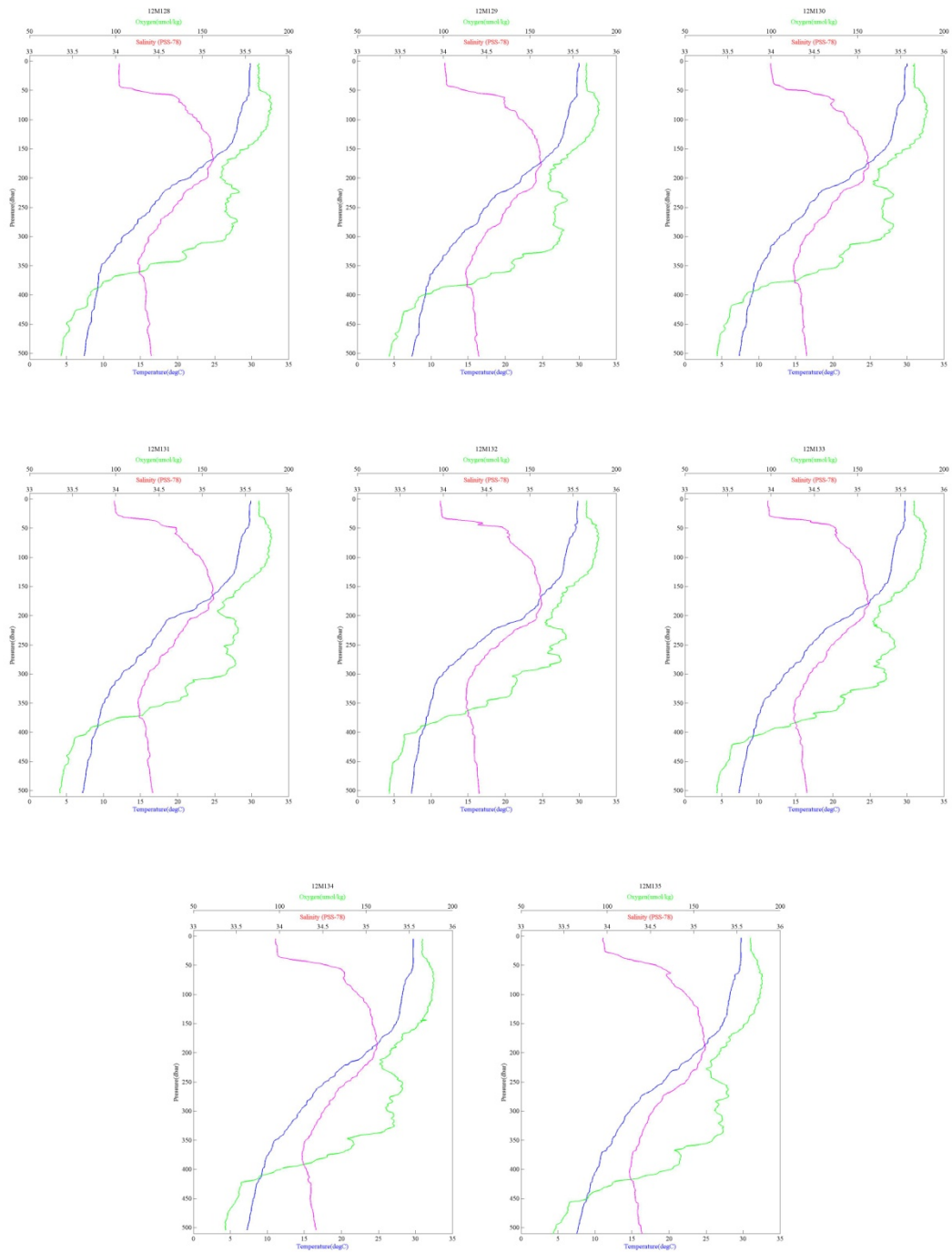
CTD profile (26 Jun 2013 casts)



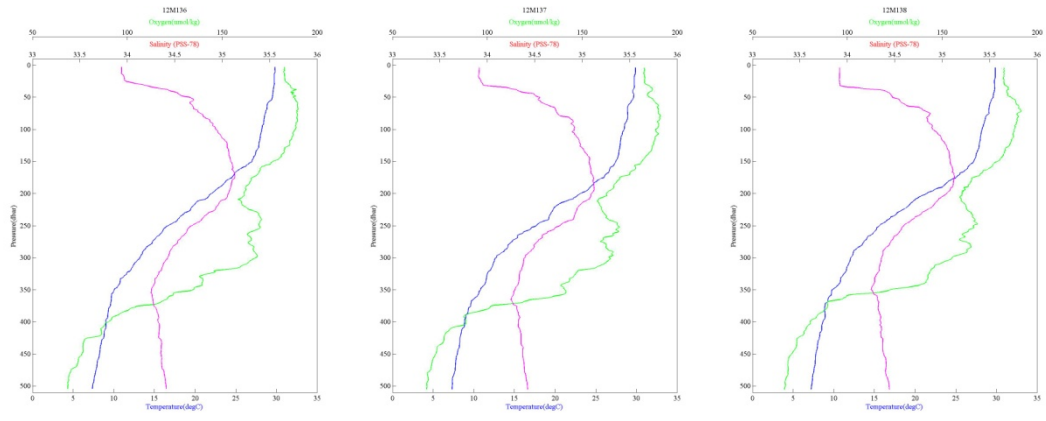
CTD profile (27 Jun 2013 casts)



CTD profile (28 Jun 2013 casts)



CTD profile (29 Jun 2013 casts)



CTD profile (30 Jun 2013 casts)